/

BNWL-2100 PT1
UC-48

Pacific Northwest Laboratory Annual Report for 1976 to the ERDA Assistant Administrator for Environment and Safety

Part 1 Biomedical Sciences

May 1977

Prepared for the Energy Research and Development Administration under Contract EY-76-C-06-1830

Battelle
Pacific Northwest Laboratories

BNWL-2100 PT1

NOTICE

PACIFIC NORTHWEST LABORATORY
operated by
BATTELLE
for the
ENERGY RESEARCH AND DEVELOPMENT ADMINISTRATION
Under Contract EY-76-C-06-1830

Printed in the United States of America
Available from
National Technical Information Service
U.S. Department of Commerce
5285 Port Royal Road
Springfield, Virginia 22151
Price: Printed Copy $_____*; Microfiche $3.00

*Pages	NTIS Selling Price
001-025	$4.50
026-050	$5.00
051-075	$5.50
076-100	$6.00
101-125	$6.50
126-150	$7.00
151-175	$7.75
176-200	$8.50
201-225	$8.75
226-250	$9.00
251-275	$10.00
276-300	$10.25

ERDA-RL RICHLAND, WA

BNWL-2100 PT1
UC-48

Pacific Northwest Laboratory Annual Report for 1976 to the ERDA Assistant Administrator for Environment and Safety

Part 1 Biomedical Sciences

by
R. C. Thompson and Staff Members
of Pacific Northwest Laboratory

May 1977

Battelle
Pacific Northwest Laboratories
Richland, Washington 99352

PREFACE

Pacific Northwest Laboratory's 1976 Annual Report to the ERDA Assistant Administrator for Environment and Safety is organized by major program categories into five Volumes, or Parts. Parts 1-4 are oriented to particular segments of the program supported by the Division of Biomedical and Environmental Research. Part 5 includes reports on projects supported by the Division of Safety, Standards and Compliance; Division of Technology Overview; Division of Environmental Control Technology; and the Office of Environmental Policy Analysis. Each Part consists of project reports authored by scientists from several PNL research departments, reflecting the interdisciplinary nature of the research effort. The Parts of the 1976 Annual Report are:

Part 1	Biomedical Sciences Program Manager - W. R. Wiley	R. C. Thompson, Report Coordinator D. L. Felton, Editor
Part 2	Ecological Sciences Program Manager - B. E. Vaughan	B. E. Vaughan, Report Coordinator J. L. Helbling, Editor
Part 3	Atmospheric Sciences Program Manager - C. L. Simpson	J. M. Hales, Report Coordinator E. L. Owzarski, Editor
Part 4	Physical and Technological Programs Program Manager - J. M. Nielsen	J. M. Nielsen, Report Coordinator G. M. Garnant, Editor
Part 5	Control Technology, Overview, Safety, and Policy Analysis Program Managers - N. E. Carter D. B. Cearlock J. C. Fox D. L. Hessel H. V. Larson	W. J. Bair, Report Coordinator L. C. Counts/R. W. Baalman, Editors

Activities of the Environmental and Safety Research Program at PNL are broader in scope than the articles in this report indicate. PNL staff members participate throughout the year in many projects not funded through specific 189s. These efforts include overall program planning, response to requests for information from the ERDA Assistant Administrator for Environment and Safety and other officials, participation on national and international standard-setting committees, and public education. During 1976, staff of PNL's Environmental and Safety Research Program:

- prepared two volumes (Fission and Fusion) of ERDA's Balanced Program Plan for Biomedical and Environmental Research;
- contributed to a number of environmental assessments and impact statements, including the Generic Environmental Statement for Mixed Oxide Fuels and the Clinch River Breeder Reactor Statement, and participated in hearings on nuclear issues;
- sat on National Academy of Sciences/National Research Council Committees, the National Council on Radiation Protection and Measurements, and the International Commission on Radiological Protection;
- compiled and prepared the final reports for two of these committee efforts; and
- provided, in response to requests from the Assistant Administrator for Environment and Safety, interpretations of research results to clarify information given to the public on a number of issues. These included the Hanford Mortality Study findings, faulty published interpretations of data on mortality in plutonium workers, and several other issues concerned with nuclear power.

W. J. Bair, Manager
S. Marks, Associate Manager
Environmental and Safety Prsearch Program

Previous Reports in this Series:

Annual Report for

1951	HW-25021, HW-25709
1952	HW-27814, HW-28636
1953	HW-30437, HW-30464
1954	HW-30306, HW-33128, HW-35905, HW-35917
1955	HW-39558, HW-41315, HW-41500
1956	HW-47500
1957	HW-53500
1958	HW-59500
1959	HW-63824, HW-65500
1960	HW-69500, HW-70050
1961	HW-72500, HW-73337
1962	HW-76000, HW-77609
1963	HW-80500, HW-81746
1964	BNWL-122
1965	BNWL-280, BNWL-235, Vol. 1-4
1966	BNWL-480, Vol. 1, BNWL-481, Vol. 2, Pt. 1-4
1967	BNWL-714, Vol. 1, BNWL-715, Vol. 2, Pt. 1-4
1968	BNWL-1050, Vol. 1, Pt. 1-2, BNWL-1051, Vol. 2, Pt. 1-3
1969	BNWL-1306, Vol. 1, Pt. 1-2, BNWL-1307, Vol. 2, Pt. 1-3
1970	BNWL-1550, Vol. 1, Pt. 1-2, BNWL-1551, Vol. 2, Pt. 1-2
1971	BNWL-1650, Vol. 1, Pt. 1-2, BNWL-1651, Vol. 2, Pt. 1-2
1972	BNWL-1750, Vol. 1, Pt. 1-2, BNWL-1751, Vol. 2, Pt. 1-2
1973	BNWL-1850, Pt. 1-4
1974	BNWL-1950, Pt. 1-4
1975	BNWL-2000, Pt. 1-4

FOREWORD

This volume describes progress on biomedical and health effects research conducted at PNL in 1976. The contents of the volume are a reflection of our continuing emphasis on the evaluation of risk to man from existing and/or developing energy-related technologies. The emphasis of the PNL program is consistent with the ERDA goal of increasing and diversifying national energy resources without increasing risks to human health.

Most of the studies described in this report relate to process-specific activities for four major energy technologies: nuclear fuel cycle; fossil fuel cycle (oil, gas, and coal processing, mining, and utilization); shale oil processing; and electrical systems (high-voltage DC fields). In addition, research reports are included on the application of nuclear energy to biomedical problems.

Technically, the energy-related projects presented here all center around a common research format involving multitiered toxicologic evaluation of potentially hazardous by-products, fugitive gases and effluents from process-specific energy activities. The shale oil projects, for example, are illustrative of the multitiered toxicologic concept. By-products and fugitive effluents are examined by an inexpensive microbial mutagenesis assay. The results of these investigations are used to set priorities for materials to be used in the more expensive animal carcinogenicity and teratogenicity test systems. The initial acute animal studies, in turn, are used to identify the need for examining non-carcinogenic effects, such as damage to respiratory, neurologic, and immunologic systems.

The validity of applying results from animal experimentation to man is firmly based on empirical observations. However, as indicated in reports on animal life-span studies associated with nuclear fuel cycles, some progress is being made in obtaining data which will provide a more quantitative basis for the extrapolation of animal data to man.

Major milestones have been achieved in a project designed to develop a wearable blood irradiator. It is anticipated that the device will be available for clinical trials within the next two to three years.

The biomedical and health effects program at PNL is an interdisciplinary effort requiring scientific contributions from practically all research departments at PNL. The personnel in the Biology Department, the principal contributors to the volume, are listed on pages 299 through 308. Requests for reprints from the list of publications and presentations for 1976 on pages 289 to 293 will be honored, except as noted.

CONTENTS

• AEROSOL AND ANALYTICAL TECHNOLOGY

Person in Charge: W. C. Cannon

This project is concerned with technological development of aerosol exposure systems and radiochemical analysis, as well as the maintenance of facilities for acute inhalation exposure of experimental animals to nuclear materials.

Current research and development in aerosol technology seeks to improve the ability to deliver prescribed inhalation doses to experimental animals for toxicologic studies. To this end, inhaled aerosol deposition studies are being carried out and instruments for aerosol measurement and aerosol generation control are being developed.

Current research in radiochemical analytical techniques seeks improved efficiency in the areas of biologic sample bulk reduction and in low-level radionuclide extraction. Development of techniques for analysis of biologic samples for some non-nuclear toxicants has also been carried out.

• Denotes 189 Title

DEPOSITION OF INHALED AEROSOLS IN BEAGLE DOGS

Investigators:

W. C. Cannon, D. K. Craig, J. P. Herring and G. J. Powers

Technical Assistance:

E. F. Blanton and M. F. England

Additional measurements have been made of deposition and retention of inhaled radioactively labeled iron oxide aerosols generated by a spinning top aerosol generator.

This is a continuation of the study described in the 1975 Annual Report. The same five beagle dogs were exposed to five aerosols of iron oxide labeled with ^{198}Au. The aerosol particle sizes ranged from 1.6 to 4.5 μm aerodynamic equivalent diameter (AED). These aerosols differed from those previously used in that they were generated by a spinning top generator instead of a Lovelace nebulizer, and thus had a much narrower size distribution. Also, the colloidal iron suspension was spiked with ^{198}Au-labeled colloidal gold rather than the $^{198}AuCl_3$ used previously.

The total initial deposition (TID) of aerosol was measured as the sum of the activity excreted during the first seven days postexposure plus the seventh-day whole-body count. Semilog plots (see Figure 1.1) of retained activity, expressed as a percentage of TID for a 14-day period, display the characteristic rapid upper respiratory clearance and slow alveolar clearance curves. Extrapolation of the latter to time zero gives the percent of TID initially deposited in the alveolar region. In Figure 1.2, data points represent percent initial alveolar deposition versus activity median aerodynamic diameter (AMAD) of the aerosols. AMADs were calculated from cascade impactor data using the NEWCAS computer program. This program is not particularly well suited to analysis of

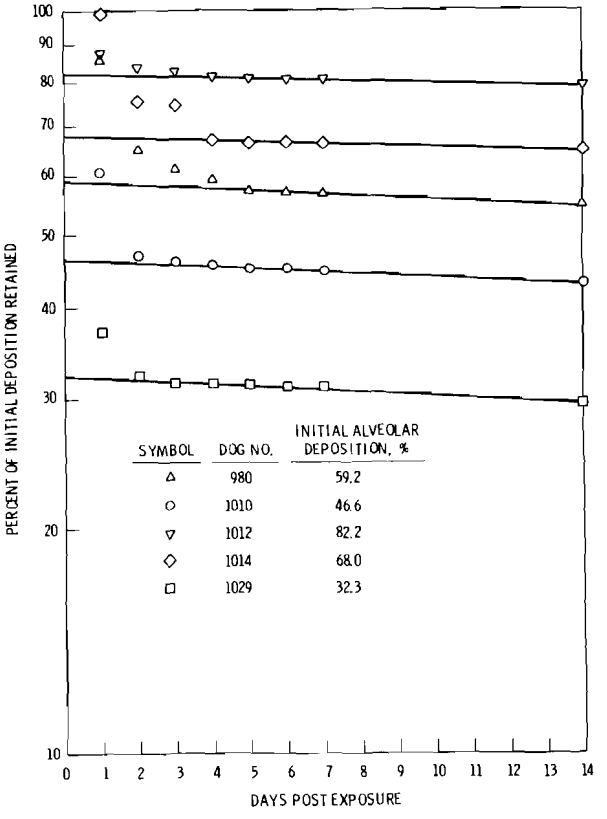

FIGURE 1.1. Typical Aerosol Deposition Clearance Curves

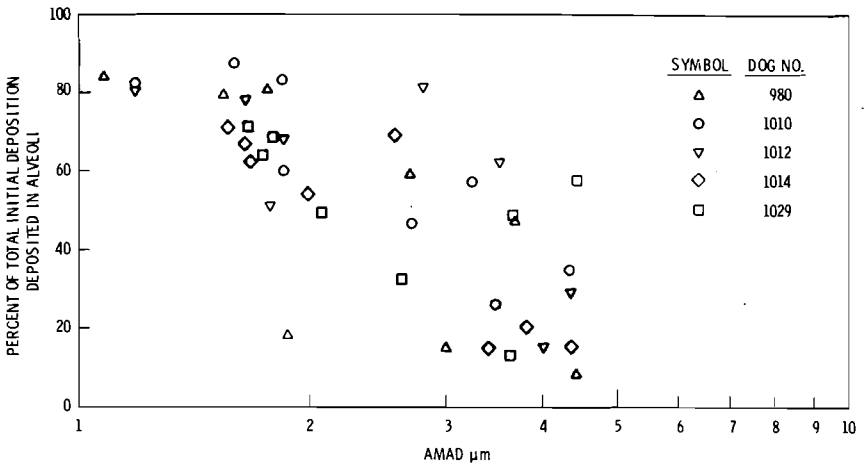

FIGURE 1.2. Variation of Alveolar Deposition with Aerosol Particle Size

the narrow size distributions generated by the spinning top generator, and an improved data reduction method will be sought for these aerosols.

In Figure 1.2 the percent of total initial depositions in the alveoli are plotted against the AMAD of the aerosol. The shaded area includes 35 of 40 data points and may represent reasonable limits for expected alveolar depositions.

Future work in this study will seek ways to generate submicron aerosols by such schemes as the use of the small satellite particles generated by the spinning top generator but usually discarded with the exhaust air. Improvements of the spinning top generator system may include a better liquid feed system, plus a particle drier and charge neutralizer.

CONTROLLED OUTPUT AEROSOL GENERATORS

Investigators:

W. C. Cannon and J. R. Decker

Technical Assistance:

J. M. Sloot, M. F. England, E. G. Kuffel and F. M. Cuta

Techniques were investigated for controlling the aerosol generation rates of liquid nebulizers.

Changes in aerosol concentration due to variations in aerosol generator output rates cause problems in achieving desired aerosol inhalation dosage. Possible methods of instituting automatic feedback control of nebulizer-type generators are being investigated. Among the possible generator output control methods being considered are air pressure control for nebulizers having liquid reservoirs and use of controlled liquid feed devices, such as syringe pumps, for specially designed nebulizers.

A continuous indicator of output rate is necessary for automatic feedback control of generator output. Measurement of intensity of light reflected from the liquid aerosol before drying shows promise as the needed indicator of generator output.

A Model RP-800 reflectance photometer, (PBL Electrooptics, Inc., West Newbury, MA), in which a light source and a photometer are connected to a single reflectance probe via a bifurcated fiber optics light pipe, is undergoing evaluation as an instrument for measurement of generator output. Figure 1.3 is a plot of photometer reading versus generator output in microliters of liquid per minute for a Lovelace (Sandia Research and Development Corp., Albuquerque, NM), and a Retec N-301PPB nebulizer (Retec Development Laboratory, Portland, OR).

The upper scale refers to the Lovelace nebulizer and the lower to the Retec. The difference in sensitivity of the photometer to the generator output rates is only partially explained by the greater airflow rate of the Retec, which reduces the droplet aerosol density. Differences in droplet size distribution may also reflect sensitivity.

The reflectance photometer will be further tested by instituting manual air pressure control to maintain a constant

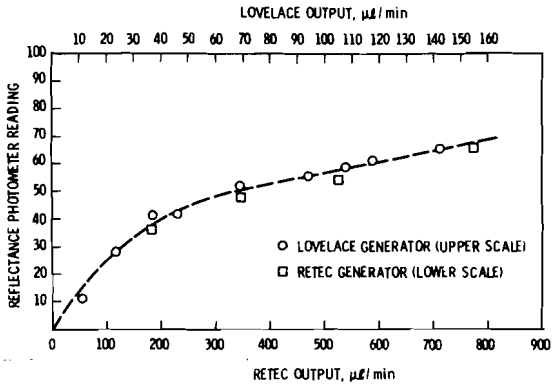

FIGURE 1.3. Measurement of Light Reflected by a Liquid Droplet Aerosol

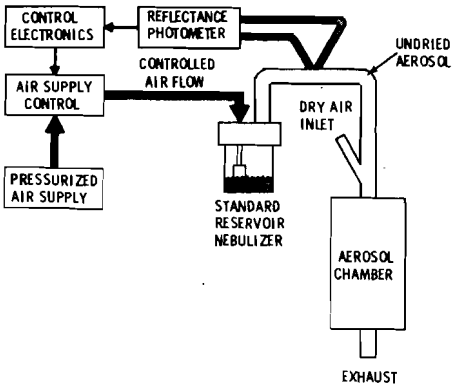

FIGURE 1.4. Automatic Aerosol Concentration Controller for Standard Reservoir Nebulizer

photometer reading while monitoring aerosol concentration and particle size. If effective, this arrangement may be used as an interim generation control system for animal exposures.

Figures 1.4 and 1.5 are diagrams of proposed automatic control systems for a standard reservoir type nebulizer and a special pump-fed nebulizer, respectively. A prototype unit of the pump-fed nebulizer has been built and is undergoing testing.

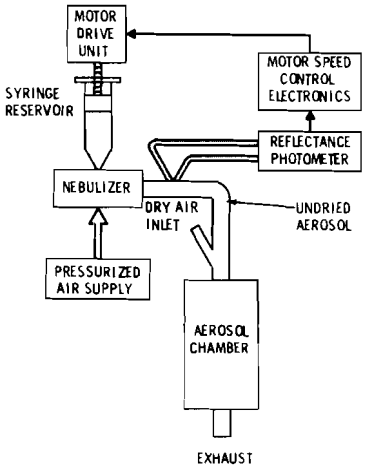

FIGURE 1.5. Automatic Aerosol Concentration Controller for Special Pump-Fed Nebulizer

• TOXICOLOGY OF PLUTONIUM-SODIUM

Person in Charge: D. D. Mahlum

One hypothetical liquid metal fast breeder reactor (LMFBR) accident postulates the formation of sodium vapor, through which plutonium and uranium oxide particles would pass enroute to release, resulting in a mixed plutonium-uranium-sodium aerosol. Studies in England with aerosols generated by an exploding wire technique, in which the plutonium and sodium are in intimate contact, suggest that the resulting aerosol is more soluble and more easily translocated from the lung than are aerosols of plutonium alone. It is not known, however, whether mixed aerosols formed by other means, which may more closely simulate a core disruptive accident, would have similar properties.

This project seeks to (1) devise methodology for the continuous generation of condensation aerosols from vaporization of LMFBR-type fuels, (2) devise methods for producing mixed aerosols of fuel and sodium under several conditions, including passage of the fuel aerosols through sodium vapor; (3) determine the physical characteristics of the aerosols prepared in (1) and (2); (4) determine the biological characteristics of such aerosols; and (5) evaluate the biological effects of mixed fuel-sodium aerosols prepared under differing conditions.

Efforts during FY 1976 have focused on the development of methodology for aerosol generation. After a number of possibilities for producing condensation aerosols were evaluated, it was decided that a laser method offered the most promise for continuous generation of the requisite plutonium-uranium aerosol. One of the following reports describes experiments performed to show the feasibility of using laser vaporization of UO_2-PuO_2 fast reactor fuels to generate condensation aerosols. The other report describes the method devised for generation of sodium aerosols.

In FY 1977 rats will be exposed to aerosols of various concentrations of Na only and various ratios of Na to Pu, using nose-only exposures. Rats will be sacrificed at intervals extending to 1 yr postexposure to follow the translocation of material from the lungs to other tissues. These data will be evaluated to determine the need for long-term toxicologic studies.

SODIUM AEROSOL GENERATION

Investigators:

M. D. Allen, W. T. Kaune, and D. K. Craig

Technical Assistance:

J. K. Briant

A method has been developed for generating sodium condensation aerosols for rodent inhalation studies. Sodium is vaporized into an argon sweep gas using a resistance furnace. The sodium metal condensate is mixed with air in an aging chamber and is then passed into a rodent exposure chamber.

Liquid sodium is used as the heat transfer medium in Liquid Metal Fast Breeder Reactors (LMFBRs). In a hypothetical LMFBR accident in which the reactor core vaporizes while under liquid sodium, the PuO_2-UO_2 condensation aerosol formed may be expected to mix violently with sodium aerosol. This project will eventually investigate the physical, chemical and biological behavior of mixed PuO_2-UO_2-Na aerosols; however, it was first necessary to develop a method for generating a respirable sodium aerosol at a constant rate.

The apparatus used to generate sodium aerosol is shown schematically in Figure 2.1. The argon sweep gas is introduced at a rate of 0.5 ℓ/min, passing through a quartz tube packed with anhydrous $CaSO_4$ to remove water vapor, and through copper turnings heated to 700°C to remove oxygen. The argon gas then sweeps sodium vapor from a stainless steel boat, which has a lip to prevent sodium from creeping over the edge. The sodium vapor is first mixed with dry air to prevent H_2 formation. The oxide aerosol is then diluted with air controlled at 50±2% relative humidity; the particle size and final chemical form depend on relative humidity.

The logarithm of the sodium aerosol concentration in the exposure chamber versus the reciprocal of the furnace temperature is plotted in Figure 2.2. The best fit through the data points is a straight line:

$$\log_{10} C \left(\frac{\mu g}{\ell}\right) = - \frac{4,790}{T(°K)} + 8.0 \qquad (1)$$

The concentration measurements were obtained by collecting the sodium aerosol in the exhaust from the exposure chamber on 47-mm dia membrane filter paper with a mean pore size of 0.45 μm. Sodium aerosol was collected on each filter for 5 min at a flow rate of 10 ℓ/min. The increase in mass on the filter was measured gravimetrically.

The aerosol concentration should increase with temperature in the same way as the vapor pressure. The effect of temperature (T) on the vapor pressure of sodium (p) is given by the equation:

$$\log_{10} P \text{ (mm of Hg)} = - \frac{5,400}{T(°K)} + 7.551 \qquad (2)$$

In our experiments there was less than 13% difference between the slopes of the curves

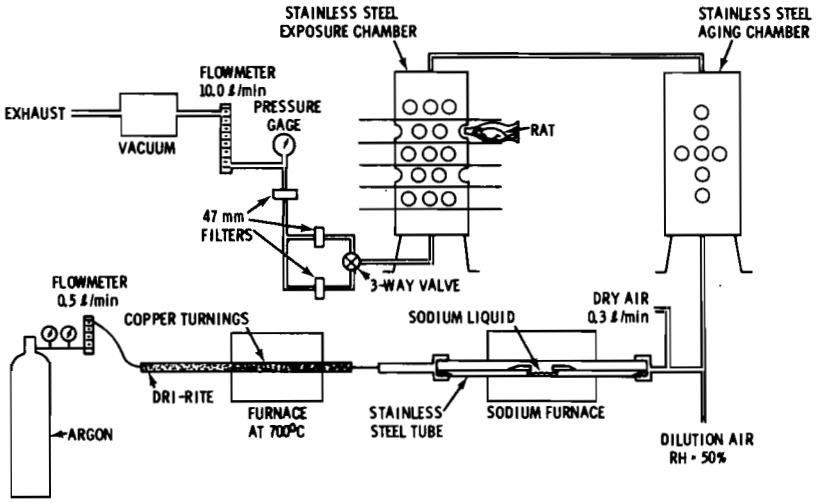

FIGURE 2.1. Sodium Aerosol Generator and Rat Exposure Chamber

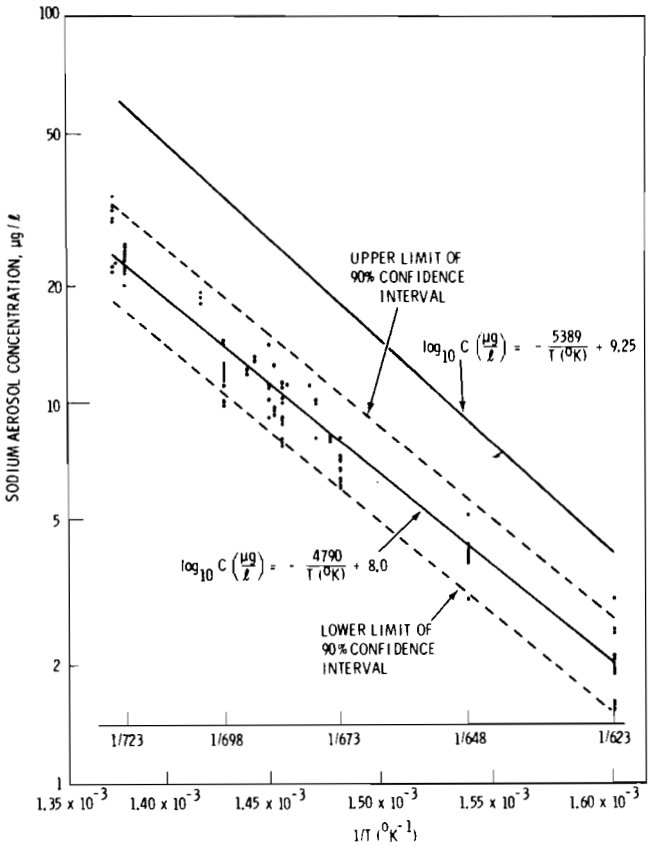

FIGURE 2.2. Sodium Aerosol Concentration in the Exposure Chamber Versus the Reciprocal of the Furnace Temperature

for equations 1 and 2. The straight line through the measured points has a smaller slope than the theoretical curve. This may be because more aerosol is lost to the walls of the system at higher concentrations.

Figure 2.3 shows a transmission electron micrograph of sodium aerosol deposited on a carbon-coated copper grid by a point-to-plane electrostatic precipitator. The physical sizes of the particles, which are approximately equal to the aerodynamic sizes (since the density of sodium is 0.97 g/cm^3 and the particles are nearly spherical), range between 0.1 and 1.5 μm. Since the sodium aerosol was diluted with air at 50% relative humidity, the aerosol in the exposure chamber was probably a mixture of sodium monoxide, peroxide, hydroxide, and small amounts of sodium carbonate.

The aerodynamic size distribution of the sodium aerosol was investigated with Mercer cascade impactors and a laboratory aerosol particle spectrometer (LAPS) spiral centrifuge. An atomic absorption spectrophotometer was used to measure the mass of sodium deposited on each stage of the cascade impactor and on each section of the stainless steel strip used in the spiral centrifuge. Both methods indicated that the aerosol particle diameters are distributed normally with respect to the logarithm of particle size. However, because of losses of large particles in the entrance of the spiral centrifuge, the mass median diameter and the geometric standard deviation determined with the LAPS tended to be smaller than for the cascade impactors. For the seven-stage cascade impactors, the mass median diameter was 1.3 μm and the geometric standard deviation was 1.8.

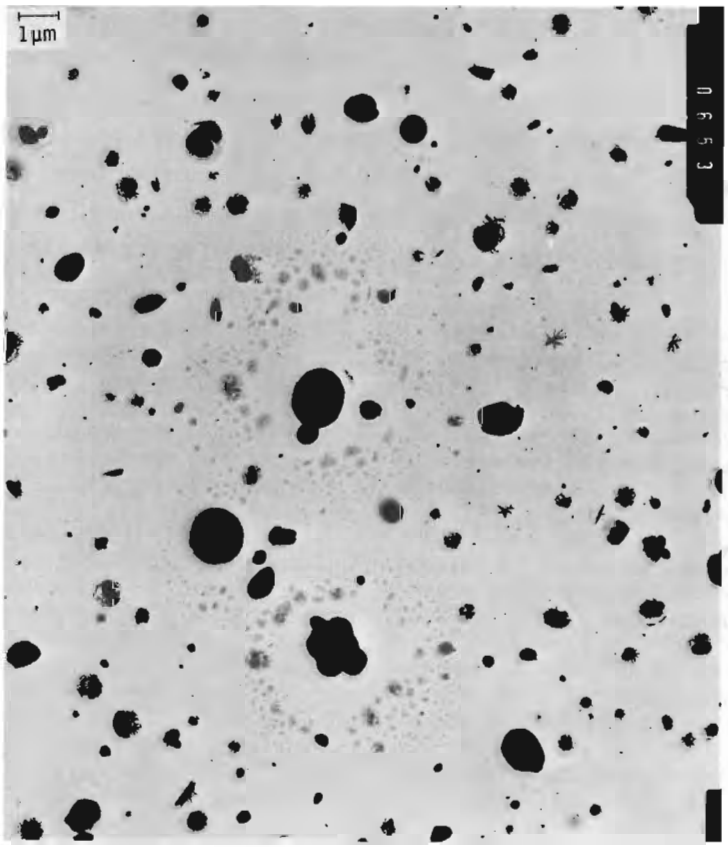

FIGURE 2.3. Transmission Electron Micrograph of Polydispersed Sodium Condensation Aerosol

LASER-GENERATED PuO_2-UO_2 CONDENSATION AEROSOLS

Investigators:

M. D. Allen, W. T. Kaune, and D. K. Craig

Technical Assistance:

J. K. Briant and J. P. Herring

A 340-watt CO_2 laser is being used to generate PuO_2-UO_2 condensation aerosol from the surface of a Liquid Metal Fast Breeder Reactor (LMFBR) fuel pellet. A wide range of concentrations is achieved by varying the laser power, pulse width, and/or pulse period. The resulting aerosol is composed of branched chain-like aggregates, with the primary particle size ranging between 0.005 and 0.15 μm. X-ray diffraction analyses show that these aerosols condense into a face-centered cubic crystal structure. The activity mean aerodynamic diameter (AMAD), for most power levels, is approximately 0.85 μm with a geometric standard deviation of 1.5.

The aerosol which may be produced by a major reactor accident will be composed of small primary particles condensed from the vapor state and subsequently coagulated into long, branched, chain-like aggregates. To vaporize mixed-oxide fast reactor fuels, which are typically 22% PuO_2 and 78% UO_2, temperatures over 3000°C are required. After considering a number of methods for vaporizing refractory materials, a pulsed 340-watt CO_2 laser was selected. A one-millisecond pulse will generate a surface temperature of 10,000°C in a very localized area on the surface of an LMFBR fuel pellet. Each pulse will produce a small vapor plume, which rapidly condenses and coagulates into chain aggregates (Figure 2.4). A PuO_2-UO_2 aerosol can be generated at a constant rate by repeatedly pulsing the laser onto the surface of a rotating fuel pellet.

During each 30-min experiment, six concentration measurements were taken from the top row of sampling ports in the exposure chamber (described elsewhere in this Annual Report) and six from the bottom row. Typical values are given in Table 2.1. Data from the top and bottom ports show no significant variation in concentration with height in the exposure chamber; and also show that the aerosol concentration is reasonably constant with time.

Table 2.2 lists aerosol concentration and activity median aerodynamic diameters (AMAD) as a function of laser power, pulse width, and pulse period. These three variables give a wide range of adjustments which can be made to attain a certain concentration. The laser power can be varied between 50 and 340 watts, the pulse width can be varied between 1 msec and 10 sec (or longer, manually), and the pulse period can be varied between 10 msec and 40 sec (or longer, manually). In general, the aerosol generation rate increases with increasing power and pulse width, and is inversely proportional to the pulse period. The AMAD tends to increase with decreasing aerosol concentration.

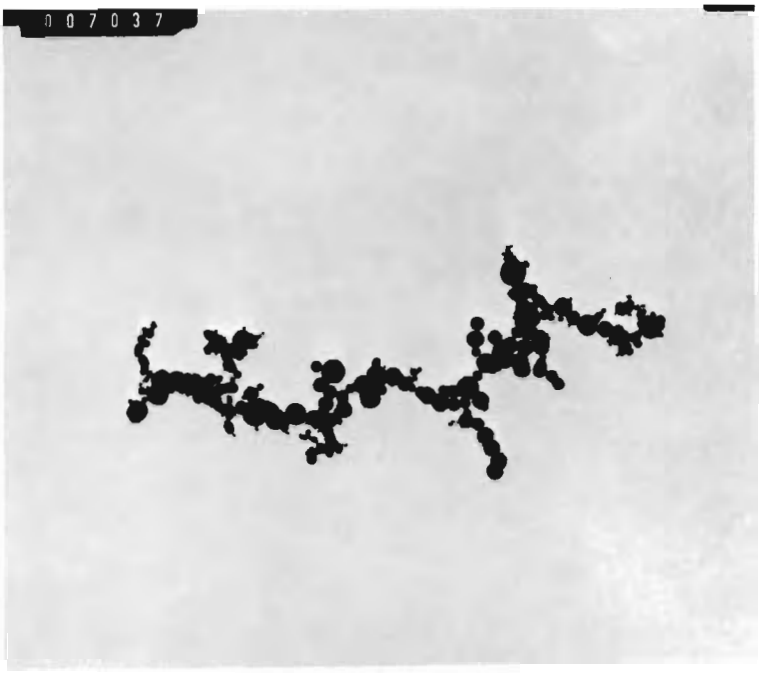

FIGURE 2.4. Transmission Electron Micrograph Showing the Structure of a PuO_2-UO_2 Aggregate Which has been Deposited on a Carbon-Coated Copper Grid by a Point-to-Plane Electrostatic Precipitator. The chain-like structure is typical of the condensation aerosols of metal oxides.

TABLE 2.1. PuO_2-UO_2 Aerosol Concentration Measurements

SAMPLED FROM TOP PORTS		SAMPLED FROM BOTTOM PORTS	
TIME (min)	CONCENTRATION (nCi/ℓ)	TIME (min)	CONCENTRATION (nCi/ℓ)
0 - 5	62.2	1 - 6	63.8
5 - 10	64.1	6 - 11	63.0
10 - 15	62.2	11 - 16	61.3
15 - 20	62.3	16 - 21	62.7
20 - 25	62.8	21 - 26	58.8
25 - 30	60.0	26 - 31	56.7

TABLE 2.2. Laser Parameters vs PuO_2-UO_2 Aerosol Characteristics

POWER (watts)	PULSE WIDTH (msec)	PULSE PERIOD (sec)	AVERAGE CONCENTRATION (nCi/ℓ)	AVERAGE AMAD ± SD[a] (μm)	AVERAGE GSD
340	10	2.2	528.4	0.928 ± 0.018	1.52
340	1	1	61.65	0.870 ± 0.061	1.64
112	3	2	3.82	1.284 ± 0.015	1.55
105	3	10	~ 0.05	1.456 ± 0.197	2.10
220	5	2.2	84.44	0.899 ± 0.046	1.50
220	5	4	49.79	0.804 ± 0.049	1.52
220	5	4	41.43	0.865 ± 0.020	1.45

[a] SD = STANDARD DEVIATION

X-ray diffraction analyses on laser-generated aerosols show that the crystal structure is a fluorite-type, face-centered cubic. The dependence of the lattice parameter on pulse width and on laser power is reported in Table 2.3. There seems to be no dependence on either pulse width or power; however, the lattice parameters measured from aerosol samples are significantly lower than the value of 5.4589 Å measured from an LMFBR fuel pellet, which may indicate a change in the oxygen-to-metal ratio.

TABLE 2.3. Lattice Parameters of PuO_2-UO_2 Aerosols

POWER (watts)	PULSE WIDTH (msec)	LATTICE PARAMETER ± THE ACCURACY OF THE MEASUREMENT (Å)
220	2	5.434 ± 0.01
220	5	5.432 ± 0.003
220	10	5.433 ± 0.003
110	5	5.442 ± 0.01
220	5	5.432 ± 0.003
330	5	5.441 ± 0.003

• INHALED PLUTONIUM OXIDE IN DOGS

Person in Charge: J. F. Park

This project is concerned with long-term experiments to determine the dose-effect relationships of inhaled plutonium oxide in beagle dogs.

The major life-span study involving about 350 beagles is currently in progress. These animals received a single 5- to 30-minute exposure to a PuO_2 aerosol as shown below:

Alveolar Deposition (μCi)	Number of Animals	
	$^{239}PuO_2$	$^{238}PuO_2$
3	10	10
1.25	20	20
0.25	20	20
0.05	20	20
0.01	20	20
0.002	20	20
Controls	40	

The ^{239}Pu dogs were exposed in FY 1971 and FY 1972; the $^{238}PuO_2$ dogs, in FY 1973 and FY 1974. The three highest deposition levels overlap those employed in previously completed studies, and should predictably lead to a high incidence of lung and/or bone tumors. The lowest level corresponds to the presently established permissible human lung burden, i.e., it will result in an estimated average dose of 15 rem/yr to the lung. In addition to the dogs maintained for life-span observations, 50 dogs were exposed for periodic sacrifice to obtain information on deposition, retention, translocation, and excretion of inhaled plutonium, and on the pathogenesis of dose-related effects.

Data from these experiments will be used for estimating the health effects of these alpha-emitting radionuclides, which are prominent components of nuclear fuel cycle effluents.

DOSE-EFFECT STUDIES WITH INHALED PLUTONIUM OXIDE IN BEAGLES

Investigators:

J. F. Park, R. L. Buschbom, A. C. Case, D. L. Catt, D. K. Craig, G. E. Dagle, J. E. Lund, R. M. Madison, G. J. Powers, H. A. Ragan, S. E. Rowe, D. L. Stevens, C. R. Watson and E. L. Wierman

Technical Assistance:

J. S. Barnett, E. F. Edmerson, S. L. English, V. T. Faubert, R. E. Flores, G. D. Erwin, D. M. Jeske, S. L. Krum, L. L. Lang, S. J. Lepka, B. G. Moore, M. C. Perkins, M. J. Pipes, L. R. Peters, P. J. Raney and B. B. Thompson

Beagle dogs given a single exposure to $^{239}PuO_2$ or $^{238}PuO_2$ aerosols are being observed for life-span dose-effect relationships. The ^{239}Pu body burden of the nine dogs that died of pulmonary fibrosis-induced respiratory insufficiency during the first 3 yr after exposure was 1 to 12 μCi. One of these dogs had a pulmonary tumor. Five additional dogs with body burdens of 0.7 to 1.8 μCi died due to pulmonary neoplasia 3 to 5 yr after exposure. None of the dogs exposed to ^{238}Pu have died during the first 3 postexposure yr. Lymphocytopenia was the earliest observed effect after inhalation of $^{239}PuO_2$ or $^{238}PuO_2$, occurring 0.5 to 2 yr after deposition of $\geq$ 80 nCi plutonium in the lungs.

To determine the life-span dose-effect relationships of inhaled plutonium, 18-month-old beagle dogs were exposed to aerosols of $^{239}PuO_2$ (mean AMAD 2.3 μm, mean GSD 1.9), prepared by calcining the oxalate at 750°C for 2 hr; or to $^{238}PuO_2$ (mean AMAD 1.8 μm, mean GSD 1.9), prepared by calcining the oxalate at 700°C and subjecting the product to $H_2{}^{16}O$ steam in argon exchange at 800°C for 96 hr. This material, referred to as pure plutonium oxide, is used as fuel in space-nuclear power systems.

One hundred thirty dogs exposed to $^{239}PuO_2$ in 1970 and 1971 were selected for long-term studies; 22 will be sacrificed to obtain plutonium distribution and pathology data, and 108 were assigned to life-span dose-effect studies (Table 3.1).

One hundred thirteen dogs exposed to $^{238}PuO_2$ in 1973 and 1974 were selected for life-span dose-effect studies (Table 3.2). Twenty-four additional dogs were exposed for periodic sacrifice. The appendix (following the entire report) shows the status of the dogs on these experiments.

During the first 5 yr following exposure to $^{239}PuO_2$, seven dogs in the highest-level dose group and seven dogs in Dose Level Group 5 were euthanized when death was imminent. Thirteen dogs were sacrificed for comparison of plutonium tissue distribution. Table 3.3 shows the causes of death and the distribution of ^{239}Pu in the tissues of these animals. One 80-month-old control dog was euthanized because of an oral tumor.

TABLE 3.1. Dose-Effect Studies with Inhaled $^{239}PuO_2$ in Beagles.

DOSE LEVEL GROUP	NUMBER OF DOGS		INITIAL ALVEOLAR DEPOSITION[a]	
	MALE	FEMALE	nCi[b]	nCi/g LUNG[b]
0	10	10	0	
1	10	10	3.5± 1.3	0.029 ± 0.011
2	10	10	22 ± 4	0.18 ± 0.035
3	10	10	79 ± 14	0.66 ± 0.13
4	10	10	300 ± 62	2.4 ± 0.39
5	10	10	1100 ± 170	9.3 ± 1.4
6	3/63	5/65	5800 ± 3300	50 ± 22

[a] ESTIMATED FROM EXTERNAL THORAX COUNTS AT 14 AND 30 DAYS POSTEXPOSURE AND ESTIMATED LUNG WEIGHTS (0.011 x BODY WEIGHT)

[b] MEAN ± 95% CONFIDENCE INTERVALS AROUND THE MEANS

TABLE 3.2. Dose-Effect Studies with Inhaled $^{238}PuO_2$ in Beagles.

DOSE LEVEL GROUP	NUMBER OF DOGS		INITIAL ALVEOLAR DEPOSITION[a]	
	MALE	FEMALE	nCi[b]	nCi/g LUNG[b]
0	10	10	0	
1	10	10	2.3± 0.8	0.016 ± 0.0073
2	10	10	18 ± 3	0.15 ± 0.029
3	10	10	77 ± 11	0.56 ± 0.07
4	10	10	350 ± 81	2.6 ± 0.47
5	10	10	1300 ± 270	10 ± 1.9
6	7/67	6/66	5200 ± 1400	43 ± 12

[a] ESTIMATED FROM EXTERNAL THORAX COUNTS AT 14 AND 30 DAYS POSTEXPOSURE AND ESTIMATED LUNG WEIGHTS (0.011 x BODY WEIGHT)

[b] MEAN ± 95% CONFIDENCE INTERVALS AROUND THE MEANS

TABLE 3.3. Tissue Distribution of Plutonium in Beagles After Inhalation of $^{239}PuO_2$.

DOG NUMBER	TIME AFTER EXPOSURE, MONTHS	FINAL BODY BURDEN, µCi	PERCENT OF FINAL BODY BURDEN					CAUSE OF DEATH
			LUNGS	THORACIC LYMPH NODES[a]	ABDOMINAL LYMPH NODES[b]	LIVER	SKELETON	
478 M	0.25	0.29	98	0.15	0.017	0.24	0.08	SACRIFICE
435 F	0.25	3.8	99	0.10	0.006	0.00	0.03	SACRIFICE
816 M	0.50	0.40	99	0.12	0.010	0.00	0.03	SACRIFICE
918 M	1	0.074	99	0.82	0.014	0.11	0.08	SACRIFICE
920 F	1	0.011	94	0.47	0.029	0.08	0.61	SACRIFICE
913 M	1	4.8	98	1.1	0.002	0.03	0.05	SACRIFICE
702 F	5	1.7	94	5.7	0.0004	0.01	0.09	SACRIFICE
709 M	5	1.7	97	2.2	0.003	0.00	0.05	SACRIFICE
734 M	5	0.91	96	3.4	0.0002	0.01	0.05	SACRIFICE
739 F	5	1.5	95	4.7	0.003	0.001	0.00	SACRIFICE
910 M	11	12.3	84	15	----	0.06	0.04	RESPIRATORY INSUFFICIENCY
747 F	12	5.4	71	29	0.026	0.07	0.07	RESPIRATORY INSUFFICIENCY
906 F	12	6.2	88	12	0.001	0.03	0.05	RESPIRATORY INSUFFICIENCY
849 F	13	0.0007	80	15	0.20	0.04	1.6	SACRIFICE
896 F	15	4.1	81	15	0.92	0.23	0.12	RESPIRATORY INSUFFICIENCY
817 M	21	3.8	64	34	0.13	1.4	0.19	RESPIRATORY INSUFFICIENCY
815 M	25	0.074	64	32	----	0.08	0.10	SACRIFICE
829 M	26	3.2	75	19	0.79	4.2	0.45	RESPIRATORY INSUFFICIENCY
760 M	31	0.98	71	23	0.57	3.7	0.28	RESPIRATORY INSUFFICIENCY
890 F	31	2.0	55	28	2.2	13.0	0.26	RESPIRATORY INSUFFICIENCY
804 M	37	1.1	62	29	0.19	7.9	0.36	RESPIRATORY INSUFFICIENCY AND LUNG TUMOR
798 F	43	0.0056	55	44	0.02	0.17	0.43	SACRIFICE
772 M	53	1.8	42	22	0.88	29	0.69	LUNG TUMOR
759 M	53	0.71	43	27	12.3	15	0.65	LUNG TUMOR
796 F	55	0.67	40	31	4.1	21	1.04	LUNG TUMOR
783 M	59	1.4	59	11	1.8	26	0.67	LUNG TUMOR
873 M	62	1.8	45	27	6.4	16	0.74	LUNG TUMOR

[a] INCLUDES TRACHEOBRONCHIAL, MEDIASTINAL AND STERNAL LYMPH NODES

[b] INCLUDES HEPATIC, SPLENIC AND MESENTERIC LYMPH NODES

As survival time increased, the fraction of plutonium in the lung decreased. During the first postexposure year, plutonium was translocated primarily to the thoracic lymph nodes, with little plutonium translocated to other tissues. Later, plutonium was also found in abdominal lymph nodes, principally the hepatic lymph nodes. The fraction of plutonium in liver increased, accounting for 15 to 29% of final body burden 4 to 5 yr after exposure. The organ distribution of plutonium in the periodically sacrificed dogs was generally similar to that of the high-dose-level dogs euthanized when death was imminent. The two exceptions were the larger fraction of plutonium in the skeleton of dog 849 F, and a smaller fraction in the liver of the low-level dogs sacrificed during the second and fourth postexposure years. Dog 798, sacrificed 3-1/2 yr postexposure had a larger fraction of plutonium in the thoracic lymph nodes than the dogs that died during the 3- to 5-yr postexposure period.

The dogs euthanized because of respiratory insufficiency during the 3-yr postexposure period had increased respiration rates, hypercapnia and hypoxemia associated with lesions in the lungs. Intermittent anorexia and body weight loss accompanied the respiratory insufficiency. Histopathologic examination of the lungs showed radiation pneumonitis characterized by interstitial and subpleural fibrosis, increased numbers of alveolar macrophages, alveolar epithelial hyperplasia, and foci of squamous metaplasia. Autoradiographs showed activity primarily composed of large stars, more numerous in areas of interstitial and subpleural fibrosis. Dog 804 M also had a pulmonary tumor classified as a bronchiolar-alveolar carcinoma.

The five dogs euthanized 3 to 5 yr after exposure showed radiographic evidence of pulmonary neoplasia before respiratory insufficiency was observed. However, respiratory insufficiency was observed prior to euthanasia, probably due, primarily, to neoplasia in the lung. In three of the dogs the lung tumors were classified as bronchiolar-alveolar carcinoma; in one dog as adenosquamous carcinoma; and in the other dog as epidermoid carcinoma. The epidermoid carcinoma metastasized to the skeleton; the bronchiolar-alveolar carcinomas metastasized to the thoracic lymph nodes in one dog, heart and thoracic lymph nodes in one dog, and to the thoracic lymph nodes, mediastinum, kidney, skeleton and axillary lymph node in the other dog. Two of the dogs had lesions of secondary hypertrophic osteoarthropathy. Sclerosing lymphadenitis was associated with the high concentration of plutonium in the thoracic and hepatic lymph nodes. There was also a generalized lymphoid atrophy which may be related to the debilitation in the dogs with respiratory insufficiency, or to lymphocytopenia. The liver of the dogs euthanized during the 4- to 5-yr postexposure period showed moderate diffuse centrilobular congestion. The liver cells in these areas contained fine granular yellow pigment resembling lipofuscin and were frequently vacuolated. Focal aggregation of vacuolated lipofuscin-containing cells in the sinusoids was associated with alpha stars on autoradiographs.

The lungs and tracheobronchial lymph nodes of the dogs sacrified 1 mo postexposure were normal with the exception of dog 913M (4.8 μCi final body burden), which had slight lymphoid atrophy of tracheobronchial lymph nodes, characterized by increased amounts of phagocytized pigment in the medulla, reduced numbers of mature lymphocytes and an apparent unmasking of the reticular cells in the outer area of the cortex. The lungs of dog 913 M had focal areas of interstitial pneumonitis consisting of alveolar interstitial fibrosis, increased numbers of alveolar macrophages, alveolar epithelial hyperplasia and a few mononuclear inflammatory cells. In the dogs sacrificed 5 mo postexposure (0.9 to 1.7 μCi final body burden), the tracheobronchial lymph nodes were essentially normal, with increased numbers of hemosiderin-laden macrophages in the medullary sinuses. They had a few foci of interstitial pneumonitis, characterized primarily by increased numbers of alveolar macrophages. No plutonium-related lesions were observed in dog 849 F (0.7 nCi final body burden) at 13 mo postexposure. Dog 798 F (5.6 nCi final body burden), at 43 mo postexposure, had slight lymphoid atrophy in the tracheobronchial lymph nodes, similar to dog 913 M. The tracheobronchial lymph nodes of dog 815 M (74 nCi final body burden), at 25 mo postexposure, had moderate lymphoid atrophy of the tracheobronchial lymph nodes, characterized by decreased lymphoid follicles in the cortex, increased amounts of phagocytized pigment in the medulla, poorly defined medullary cords and increased fibrous connective tissue. The lungs of dog 798 F and 815 M were essentially normal, with the exception of an occasional focal area of pleural or subpleural fibrosis, associated with alpha stars on the autoradiographs.

Lymphocytopenia developed after inhalation of $^{239}PuO_2$ in the dose level groups with mean initial alveolar depositions of 79 nCi and greater. The reduction in lymphocytes was dose-related, both in time of appearance and magnitude. At mean alveolar depositions of 3.5 and 22 nCi, lymphocyte values were within ranges observed in control dogs. These dose-effect relationships have remained essentially unchanged through 5 yr postexposure

(Figure 3.1). A reduction in total leukocytes (Figure 3.1) was evident in the higher dose groups that were also lymphocytopenic. This decrease, with the exception of the highest-level groups, was due to the reduction in lymphocytes, since no reduction was evident in neutrophils, (Figure 3.1), eosinophils, or monocytes. No effects have been observed on red cell parameters following $^{239}PuO_2$ inhalation.

None of the dogs in the $^{238}PuO_2$ life-span dose-effect study died during the 3 yr post-exposure. Dose-related lymphocytopenia was observed in groups with mean alveolar deposition of 77 to 5200 nCi, similarly to the dogs exposed to $^{239}PuO_2$. The lymphocyte depression was, however, more pronounced both as to time and magnitude following ^{238}Pu exposure.

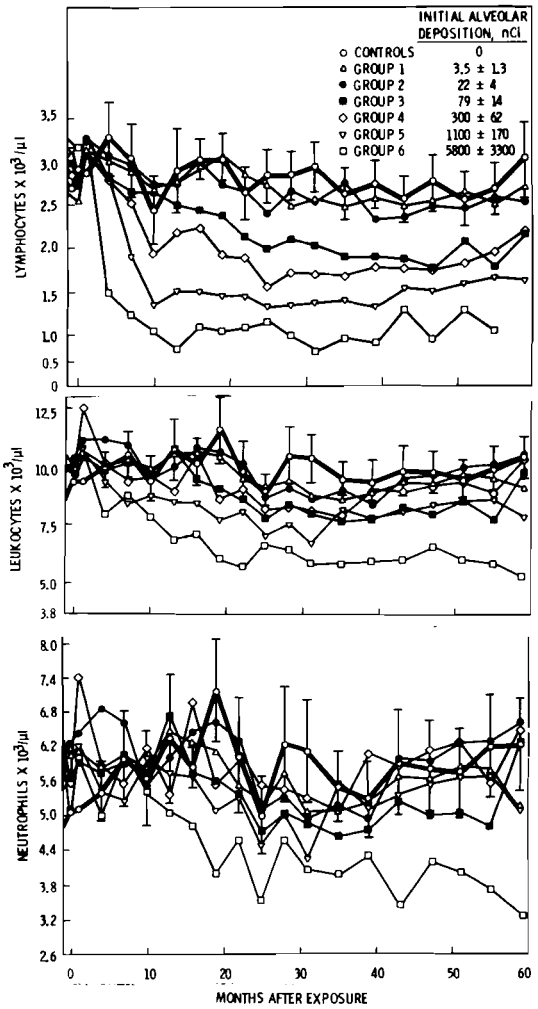

FIGURE 3.1. Mean Lymphocyte, Leukocyte, and Neutrophil Values from Dogs After Inhalation of $^{239}PuO_2$. Mean values from age-related control dogs are shown with the 95% confidence interval.

This effect was particularly evident in the 3-, 4-, and 5-dose level groups. As was found with ^{239}Pu, lymphocyte values in the two lowest exposure groups, i.e., 2.3 and 18 nCi, were not different from control values. A dose-related reduction in total leukocytes was evident, primarly due to the lymphocytopenia (Figure 3.2). However, in groups 5 and 6 a time-related neutropenia was obvious, with an apparent trend to reduced neutrophil values in Group 4 (Figure 3.2). No difference in monocyte values was seen in relation to dose levels. A significant and progressive reduction in eosinophils was evident only in Group 6 dogs following ^{238}Pu inhalation. No chronic effects have been observed in the red cell parameters.

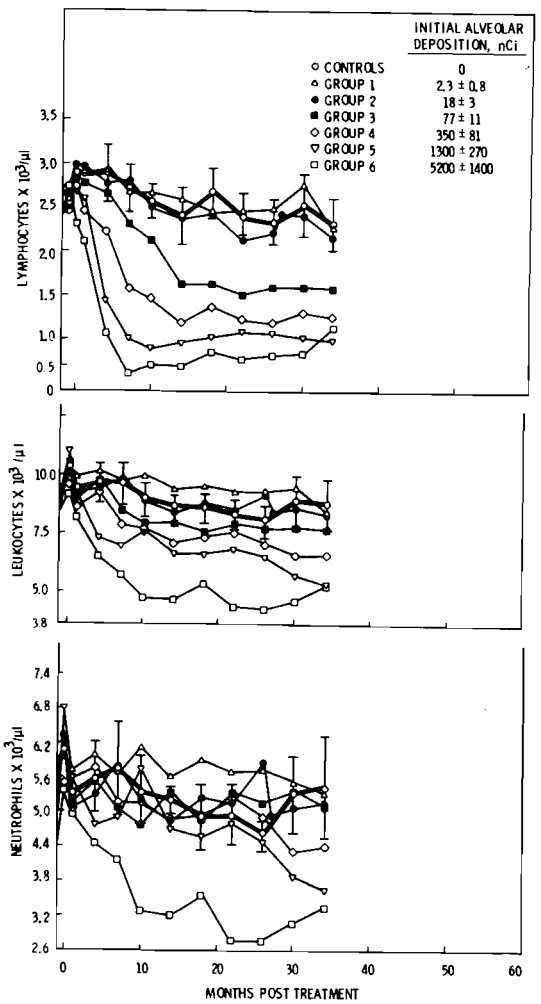

FIGURE 3.2. Mean Lymphocyte, Leukocyte, and Neutrophil Values from Dogs After Inhalation of $^{238}PuO_2$. Mean values from age-related control dogs are shown with the 95% confidence interval.

Table 3.4 shows the distribution of ^{238}Pu in dogs sacrificed periodically during the first postexposure year. The fraction of the final body burden in the lungs of the ^{238}Pu-exposed dogs 1 yr postexposure was about 50% compared to 80% in the ^{239}Pu-exposed dogs. About 17% of the plutonium was found in the thoracic lymph nodes 1 yr after exposure for both ^{239}Pu and ^{238}Pu. About 10% of the final body burden was found in the liver and 18% in the skeleton of the ^{238}Pu-exposed dogs 1 yr postexposure, compared to less than 1% in these organs in the ^{239}Pu-exposed dogs.

After inhalation of $^{239}PuO_2$ or $^{238}PuO_2$, lymphocytopenia was the earliest observed effect, occurring after deposition of $\geq$80 nCi plutonium in the lungs. On a concentration basis, the 80-nCi dose level is about 40 times the 16-nCi maximum permissible human lung deposition, based on 0.3 rem/week to the lung.

TABLE 3.4. Tissue Distribution of Plutonium in Beagles After Inhalation of $^{238}PuO_2$

DOG NUMBER	TIME AFTER EXPOSURE, MONTHS	FINAL BODY BURDEN, μCi	PERCENT OF FINAL BODY BURDEN					
			LUNGS	THORACIC LYMPH NODES[a]	ABDOMINAL LYMPH NODES[b]	LIVER	SKELETON	CAUSE OF DEATH
1032 M	0.25	0.15	97	0.03	0.2	1.7	0.16	SACRIFICE
921 F	1	0.0044	93	0.12	0.04	0.38	2.1	SACRIFICE
930 F	1	0.052	99	0.52	0.009	0.75	0.35	SACRIFICE
931 F	1	0.35	96	1.6	0.009	0.05	0.03	SACRIFICE
929 F	2	0.022	89	7.5	0.002	0.26	0.58	SACRIFICE
932 F	2	0.38	95	2.5	0.004	0.18	0.35	SACRIFICE
923 F	2	0.0023	85	9.4	0.03	0.09	0.44	SACRIFICE
925 M	3	0.0064	91	3.7	0.04	0.04	0.96	SACRIFICE
926 M	3	0.078	86	10	0.22	0.65	1.1	SACRIFICE
934 M	3	0.90	91	4.7	1.7	0.45	0.93	SACRIFICE
1318 M	12	0.030	45	27	0.07	11	15	SACRIFICE
1319 M	12	0.065	49	12	0.02	13	24	SACRIFICE
1214 M	13	0.012	60	10	0.36	7.2	14	SACRIFICE

[a] INCLUDES TRACHEOBRONCHIAL, STERNAL AND MEDIASTINAL LYMPH NODES

[b] INCLUDES HEPATIC, SPLENIC AND MESENTERIC LYMPH NODES

• LOW LEVEL PLUTONIUM NITRATE INHALATION STUDIES IN BEAGLES

Person in Charge: G. E. Dagle

The objective of this study, first funded in FY 1976, is to determine the dose-effect relationships of inhaled plutonium nitrate in life-span studies in beagle dogs. The critical tissue after inhalation of "soluble" plutonium (such as plutonium nitrate) is generally considered to be the skeleton or liver, on the assumption that such plutonium will be rapidly translocated from the lung to skeleton and liver. In several rodent studies, however, inhalation of "soluble" plutonium has resulted in lung tumors as well as skeletal tumors.

Over half of the dogs on the life-span study with $^{239}Pu(NO_3)_4$ were exposed during FY 1976 and the remainder will be exposed during FY 1977 and early FY 1978. Dogs will be placed in the $^{238}Pu(NO_3)_4$ life-span studies during FY 1978 and FY 1979. Additional dogs will be exposed and periodically sacrificed to provide information on deposition and translocation of plutonium nitrate and to study the pathogenesis of dose-related effects.

INHALED PLUTONIUM NITRATE IN DOGS

Investigators:

G. E. Dagle, W. C. Cannon, H. A. Ragan, C. R. Watson

D. L. Stevens, F. T. Cross, P. J. Dionne, and

T. P. Harrington

Technical Assistance:

R. B. Samples and S. L. Owzarski

Beagle dogs given a single inhalation exposure to $^{239}Pu(NO_3)_4$ are being observed for life-span dose-effect relationships. Over half of the dogs planned for $^{239}Pu(NO_3)_4$ exposure have been exposed and the remaining dogs will be exposed as they reach adult age.

The primary objective of this project is to determine dose-effect relationships of inhaled plutonium nitrate in life-span studies with beagle dogs. Included are low dose levels which are not expected to elicit effects but which are needed, not only to determine the level at or below which no effect is observed, but also to evaluate the retention and translocation of the materials at levels to which humans may be exposed.

Sixty-one dogs were exposed to aerosols of $^{239}Pu(NO_3)_4$ during 1976 for planned life-span observation (Table 4.1). In addition, 18 dogs were exposed and sacrificed for metabolism studies, 13 dogs were exposed to nitric acid aerosols as vehicle controls, 14 dogs were selected as untreated controls for life-span observation, and 4 dogs were selected as controls for periodic sacrifice. The dogs were exposed in aerosol chambers using techniques described in previous Annual Reports for inhaled plutonium oxide studies in beagles.

Solutions of $^{239}Pu(NO_3)_4$ in 0.27 N HNO_3 were nebulized to produce the aerosols. The mist was introduced into the 10-ℓ/min air flow through an 18-ℓ aerosol chamber. Changes in aerosol concentration to achieve the various exposure levels were effected by varying the $^{239}Pu(NO_3)_4$ solution concentration.

TABLE 4.1. Inhaled Plutonium Nitrate in Dogs: Exposures in 1976 for Life-span Observations

NUMBER OF DOGS	INITIAL ALVEOLAR DEPOSITION (nCi) TARGET DOSAGE	ESTIMATE FROM THORAX COUNT, 2 wk POST EXPOSURE	AEROSOL PARAMETERS AMAD (μm)	GSD	CONCENTRATION (nCi/ℓ)
5	3000	5445 ± 1841	0.95	2.12	534 ± 118
10	1250	2293 ± 506	1.01	2.00	322 ± 66
13	250	312 ± 68	0.88	1.83	99 ± 20
13	50	59 ± 18	0.80	1.90	21 ± 7
10	10	8 ± 5	0.75	1.88	3.2 ± 0.5
10	2	--	0.70	2.37	0.83 ± 0.3
13	VEHICLE	--	--	--	--
14	CONTROL	--	--	--	--

AMAD = ACTIVITY MEDIAN AERODYNAMIC DIAMETER (μm)

GSD = GEOMETRIC STANDARD DEVIATION OF DISTRIBUTION

Aerosol concentrations were determined by measuring samples of aerosol collected on a

membrane filter prior to exposing each animal, and were counted by a special alpha counting system. Respiration measurements provided an indication of the volume inhaled as the exposure proceeded. When the product of inhaled volume and aerosol concentration reached a value predetermined by the particle size in a pre-exposure aerosol test, the exposure was terminated. During exposure, filter paper samples and cascade impactor samples were taken for postexposure analysis to determine concentration and particle size of the inhaled aerosol. The higher exposure levels had larger median diameter aerosols since the higher exposure levels required greater aerosol and solution concentrations.

The aerosol solutions were evaluated for polymerization and disproportionation of the $^{239}Pu(NO_3)_4$. Ultrafiltration studies demonstrated that the solutions were 97 to 100% ultrafilterable up to 24 hr postexposure, suggesting that polymerization did not occur to any significant degree. Disproportionation studies showed that the disproportion rate became faster as total ^{239}Pu concentration was increased in the 0.27 N HNO_3 solutions used. Disproportionation was of no concern with the exposure times used for solutions containing <20 μCi/ml in 0.27 N HNO_3; this was the highest concentration used for the 4 lower dose levels. Disproportionation could be of some significance in the solution concentration used at the two highest dose levels (target depositions of 1250 nCi and 3000 nCi). Only 7% Pu(VI) was present after 2 hr in the solution of highest concentration (150 μCi/ml); this would probably not have any measurable biological effect in the long-term studies.

After exposure to aerosols, fecal and urine samples were collected for radiochemical analysis for 1 mo, and whole-body counts were made at 2 and 4 wk postexposure. Blood samples were taken for hematologic and clinical chemical evaluation at 1 mo postexposure and at 4-mo intervals thereafter. Body burdens of plutonium will be estimated at yearly intervals by urine and fecal radioanalysis and external body counting. The occurrence of tumors will be monitored by periodic physical examinations and annual thoracic radiographs.

A dynamic model describing the translocation of plutonium nitrate in the beagle is being developed. The model will use procedures developed by Dionne and Stuart with the BNW hybrid computer to study the translocation of $^{239}PuO_2$. Their model has been modified to operate in an interactive mode on BNW's digital computer system MINERVA, which consists of a PDP 11/35 and a Vector General graphics display CRT. The model prediction for each of the compartments is compared with the corresponding data and the model parameters are adjusted until a "best fit" is obtained for all compartments. The model fitting process is by necessity an iterative procedure since adjustments to one of the compartments will affect others. As new data becomes available, the model must be re-evaluated to determine if the compartments and pathways in the model as well as the parameters still give the "best fit". An additional computer model is being developed to estimate initial alveolar burden and organ dose from cumulative excretion data.

Hematologic effects of $^{239}Pu(NO_3)_4$ inhalation through 4 mo postexposure are shown in Table 4.2. At this time statistical evaluations are based on Student's 't' test, comparing each group only with the control animals, rather than multiple range statistical comparisons between groups.

By 1 mo postexposure a significant lymphopenia was present in Groups 5 and 6. Mean neutrophil values in these groups were reduced, but the differences at that time were not significantly different from control values.

By 4 mo postexposure, significant reductions in leukocyte values were evident in Groups 4, 5, and 6. In Group 4 the leukopenia was due to a decrease in neutrophils with no effect noted on other leukocytes, including lymphocytes. Highly significant and apparently dose-related reductions in total leukocytes, neutrophils, and lymphocytes were obvious in Groups 5 and 6.

Although this study is in a very early stage, the hematologic effects of $^{239}Pu(NO_3)_4$ are already strikingly different from those observed following $^{239}PuO_2$ inhalation (this and previous Annual Reports). With $^{239}PuO_2$, even at the highest alveolar depositions of ∿ 5000 nCi, no effect was evident at 1 mo postexposure and subsequently only a dose-related lymphopenia developed. The significant reduction in circulating lymphocytes at 1 mo following $^{239}Pu(NO_3)_4$ inhalation is probably due to the more rapid and widespread translocation of this form of plutonium, with involvement of more lymphoid tissue and constant irradiation of circulating lymphocytes traversing hepatic and splenic vessels. Neutropenia present by 4 mo after exposure may be the result of plutonium deposition in bone, especially at the osteomyeloid interfaces.

TABLE 4.2. Hematologic Effects of Plutonium Nitrate Inhalation in Beagles (Mean ± 1)

TREATMENT GROUP (MEAN nCi)	n	POST EXPOSURE (mo)	LEUKOCYTES ($x10^3/mm^3$)	NEUTROPHILS ($x10^3/mm^3$)	LYMPHOCYTES ($x10^3/mm^3$)
CONTROL	15	0	10.4 ± 3.2	5.33 ± 1.28	2.75 ± 0.55
VEHICLE ONLY	13		9.8 ± 1.6	5.60 ± 1.10	2.86 ± 0.65
1	13		8.7 ± 1.5	4.97 ± 0.98	2.65 ± 0.63
2 (8)	10		10.7 ± 2.5	6.51 ± 2.23	2.84 ± 0.57
3 (59)	19		9.3 ± 2.2	5.19 ± 1.30	2.75 ± 0.70
4 (312)	10		10.4 ± 2.9	5.93 ± 2.30	2.99 ± 0.83
5 (2293)	13		8.9 ± 2.0	5.22 ± 1.78	2.62 ± 0.46
6 (5445)	5		8.9 ± 2.3	5.63 ± 2.01	2.17 ± 0.45
CONTROL	18	1	9.3 ± 1.2	5.21 ± 0.92	2.54 ± 0.37
VEHICLE ONLY	10		8.9 ± 1.1	5.14 ± 0.99	2.53 ± 0.49
1	12		9.8 ± 3.8	6.22 ± 3.45	2.27 ± 0.45
2 (8)	10		8.9 ± 1.6	5.02 ± 1.31	2.85 ± 0.55
3 (59)	19		9.2 ± 1.8	5.19 ± 1.25	2.80 ± 0.92
4 (312)	13		9.8 ± 2.0	5.68 ± 1.84	2.69 ± 0.43
5 (2293)	13		7.6 ± 1.1[a]	4.72 ± 1.26	1.87 ± 0.53[a]
6 (5445)	5		7.0 ± 1.0[a]	4.56 ± 0.98	1.54 ± 0.44[a]
CONTROL	9	4	9.8 ± 1.1	5.91 ± 0.93	2.43 ± 0.46
VEHICLE ONLY	3		8.5 ± 2.4	5.01 ± 1.82	2.36 ± 0.59
1	10		8.9 ± 1.2	5.30 ± 1.21	2.45 ± 0.38
2 (8)	10		8.9 ± 1.6	5.20 ± 1.17	2.73 ± 0.71
3 (59)	10		8.9 ± 1.4	5.62 ± 1.25	2.53 ± 0.66
4 (312)	10		8.4 ± 1.0[b]	4.83 ± 0.76[c]	2.61 ± 0.57
5 (2293)	10		5.7 ± 1.5[a]	3.78 ± 1.77[b]	1.35 ± 0.62[a]
6 (5445)	5		4.1 ± 1.1[a]	2.70 ± 0.78[a]	0.96 ± 0.31[a]

[a] $P<0.001$; [b] $P<0.01$; [c] $P<0.02$

• INHALED TRANSURANICS IN RODENTS

Person in Charge: C. L. Sanders

This project is concerned with the fate and carcinogenic effects of inhaled transuranic compounds in rodents, specifically the role of dose and dose-distribution in space and time upon the pathogenesis of lung tumors. Completed life-span studies include groups of rats exposed at several dose levels to high-fired $^{238}PuO_2$, $^{239}PuO_2$, and $^{244}CmO_2$, $^{238}PuO_2$ suspended in water prior to aerosolization, air-oxidized $^{239}PuO_2$, $^{238}Pu(NO_3)_4$, $^{239}Pu(NO_3)_4$ and $^{253}Es(NO_3)_3$. Another life-span study involving the cocarcinogenesis of beryllium oxide and $^{239}PuO_2$ has also been completed.

Emphasis in the project is placed upon analyses of data from completed life-span studies, on the microdosimetry of alpha-emitters in the lung using morphometric and quantitative autoradiographic techniques, on studies into the cellular origin of carcinomas using electron microscopy and cellular kinetics studies with tritiated thymidine, and on transplantation studies of lung tumors in rat and hamster to determine the time sequence and degree of malignancy of tumors. We hope to accurately determine the radiation dose delivered to target epithelial cells in the lung from transuranics which give a wide variety of dose-distributions, and to describe how these cells evolve into carcinomas. In addition, two life-span studies, one with inhaled $^{241}AmO_2$ and the other looking into the role of dose protraction with inhaled $^{239}PuO_2$, are being carried out. Such studies are critical for describing the health hazards to man from inhaled transuranic compounds.

ROLE OF PROTRACTED EXPOSURE ON THE TOXICOLOGY OF INHALED $^{239}PuO_2$

Investigators:

C. L. Sanders

Technical Assistance:

J. Baker and G. J. Powers

Studies were initiated to examine in rats the effects of a protracted exposure to inhaled $^{239}PuO_2$.

Female Wistar SPF rats were exposed for 30 min to an aerosol of $^{239}PuO_2$ calcined at 700°C. The rats were about 70 days of age when first exposed. Four groups of 70 rats each were treated as follows: (1) unexposed controls; (2) one exposure to $^{239}PuO_2$ at 70 days of age; (3) nine exposures to $^{239}PuO_2$ at 70, 77, 84, 91, 98, 105, 112, 119, and 126 days of age; and (4) three exposures to $^{239}PuO_2$ at 70, 98, and 126 days of age. Groups of five rats from each plutonium-exposed group were placed in individual metabolism cages and excreta were collected for ^{239}Pu analysis. These rats were killed at 64 to 89 days after the first exposure and their tissues analyzed for ^{239}Pu contents. The remaining 65 rats from each of the plutonium-exposed groups and the 70 unexposed controls will be held for life-span observation.

Upper respiratory tract deposition was measured as the amount of ^{239}Pu present in excreta from 0-3 days after each exposure. A small amount of this Pu will be from particles deposited and cleared from the alveoli. Alveolar deposition was measured as the amount of ^{239}Pu present in excreta at 4-7 days after each weekly exposure, 4-28 days after each monthly exposure or 4-71 days after a single exposure to PuO_2 plus the amount of Pu present in the body at death. Early alveolar clearance during the first 3 days after each inhalation was not measured. Thus the estimate of alveolar clearance may be significantly underestimated in the group receiving weekly exposures.

Particle size characteristics of the PuO_2 aerosols did not vary either within or among the various exposures. The activity median aerodynamic diameter of the PuO_2 aerosols averaged 1.51 μm with an average geometric standard deviation of 1.76 and a calculated count median diameter of 0.17 μm. Total alveolar deposition of ^{239}Pu was estimated as 240 nCi given in one exposure, 30 nCi given as 3 monthly exposures and 97 nCi given as 9 weekly exposures. The terminal body burdens for each group were 68 nCi ^{239}Pu at 71 days after a single exposure, 10 nCi at 89 days after the first of 3 monthly exposures and 50 nCi at 64 days after the first of 9 weekly exposures. The distribution of ^{239}Pu among the tissues of the body was not changed by multiple exposures to PuO_2. About 95% of the terminal body burdens were found in the lung, 1% in the thoracic lymph nodes, 0.2% in the skeleton, 0.5% in the liver and 2-5% in the remaining tissues.

The rates at which plutonium was cleared from the lung following exposures are plotted in Figure 5.1, which shows the total alveolar deposition of ^{239}Pu based on the summation of terminal depositions and measurements of ^{239}Pu in excreta at times of

greater than 3 days after each exposure. Multiple exposures to Pu did appear to decrease the rate at which Pu was cleared from the alveoli. The amount of Pu cleared from the alveoli appeared to be less following each successive exposure, with this effect appearing more pronounced after weekly exposures than after monthly exposures. Previous studies have shown that cumulative damage to alveolar macrophages from phagocytized $^{239}PuO_2$ particles will inhibit the alveolar clearance of particles. Thus protraction of exposures may result in an overall greater retention time for ^{239}Pu in the lung than following a single exposure.

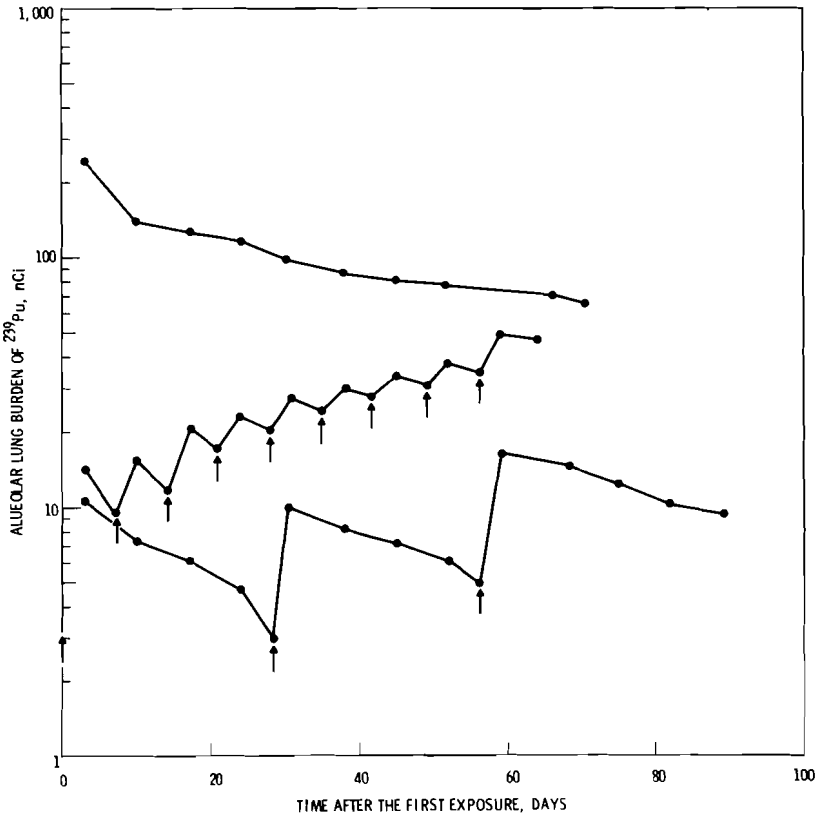

FIGURE 5.1. Effect of Multiple Exposures to $^{239}PuO_2$ Upon the Deposition and Clearance of ^{239}Pu in the Alveoli. Each group received an exposure at 0 time. Each point represents a mean from five rats per group. Arrows mark exposure times.

COCARCINOGENESIS OF INHALED PLUTONIUM DIOXIDE AND BERYLLIUM OXIDE

Investigators:

C. L. Sanders and G. J. Powers

Inhaled beryllium oxide results in impaired alveolar clearance of inhaled $^{239}PuO_2$ and induces an inflammatory reaction in the lung. However, only one of 184 rats exposed to beryllium developed a lung tumor; none of 128 unexposed rats developed a lung tumor. Fifty-six lung tumors were induced in 181 rats exposed to plutonium. A total of 37 lung tumors were found in 119 rats given combined exposures to beryllium and plutonium. Only in rats given the highest levels of both beryllium and plutonium was there an incidence of lung tumors greater than that seen with exposure to plutonium only.

Previous studies have demonstrated an impairment of alveolar clearance by inhaled beryllium oxide in the lungs of rats. Soluble chemical forms of beryllium compounds deposited in the lungs of rodents are potent carcinogens, as are all compounds of ^{239}Pu. Insoluble beryllium oxide is, however, a comparatively weak pulmonary carcinogen, despite the fact that it impairs alveolar clearance of other particles less toxic to alveolar macrophages. This report demonstrates the influence of prior exposure to beryllium oxide upon the alveolar clearance and pulmonary carcinogenicity of a subsequent exposure to $^{239}PuO_2$ particles.

Groups of female rats were given inhalation exposures to aerosols of either high-fired (1000°C) beryllium oxide or high-fired (750°C) $^{239}PuO_2$, and examined for distribution of metal in tissues, and pathologic effects over their life span. The mass median aerodynamic diameter of beryllium oxide for all exposures was 1.10 μm ± 0.17 μm and for $^{239}PuO_2$, the activity median aerodynamic diameter was 2.20 ± 0.14 μm for all exposures. $^{239}PuO_2$ was generated in water suspension and beryllium oxide was generated as a dry dust, using a Wright Dust Feed Mechanism. In rats given both metals, exposure to beryllium occurred three days prior to exposure to plutonium.

A total of 612 rats were used in the life-span portion of the study: 128 unexposed controls, 184 rats given only beryllium, 181 rats given only plutonium, and 119 rats given both beryllium and plutonium. The exposure levels and number of rats in each group are shown in Table 5.1.

The alveolar clearance of ^{239}Pu is faster than the alveolar clearance of beryllium (Figure 5.2). About 50% of the initial alveolar deposition of ^{239}Pu was cleared during the first 30 days after exposure, compared to only about 35% of deposited beryllium. At 1 yr after exposure, about 6% of deposited ^{239}Pu remained in the lung, compared to 25% of deposited beryllium. The clearance of ^{239}Pu in rats previously exposed to beryllium was similar to the beryllium clearance kinetics. About 10-15% of the initial alveolar deposition of ^{239}Pu remained in the lung at about 600 days after exposure, compared to only 2-3% of ^{239}Pu deposition in rats given only ^{239}Pu (Figure 5.2). At 1-2 yr after exposure, about 1-2% of alveoli-deposited ^{239}Pu was translocated to pulmonary lymph nodes

TABLE 5.1. Protocol for Inhalation Exposure of Rats to BeO and/or $^{239}PuO_2$ and Resulting Pulmonary Pathology

INITIAL ALVEOLAR DEPOSITION[a]		NUMBER OF RATS	INCIDENCE OF PULMONARY PATHOLOGY, %						
			NEOPLASIA					METAPLASIA	
PLUTONIUM, nCi	BERYLLIUM, µg		TOTAL	ADENOCARCINOMA	ADENOSQUAMOUS	SQUAMOUS CELL	OTHER[b]	ADENOMATOUS	SQUAMOUS
0	0	80	0	0	0	0	0	0	0
0	0	48	0	0	0	0	0	2.1	0
5.0 ± 2.2	0	60	10	5.0	0	1.7	3.3[c]	3.3	0
45 ± 22	0	91	37	30	0	5.5	2.2	15	0
180 ± 54	0	30	53	20	0	23	10	27	10
0	0.9 ± 0.3	61	0	0	0	0	0	0	0
0	16 ± 15	65	0	0	0	0	0	0	0
0	57 ± 17	58	1.7	1.7	0	0	0	0	0
7.6 ± 5.5	14 ± 4.8	26	15	15	0	0	0	3.8	0
76 ± 21	14 ± 4.8	29	38	31	6.9	0	0	3.4	3.4
3.8 ± 1.5	91 ± 8.1	33	12	9.1	0	0	3.0[d]	18	0
59 ± 7.6	91 ± 8.1	31	58	39	6.5	6.5	6.5[e]	23	6.5

[a] MEAN ± STANDARD DEVIATION (n, 3-5)

[b] HEMANGIOSARCOMA EXCEPT WHERE SHOWN OTHERWISE.

[c] ONE FIBROSARCOMA

[d] ONE FIBROSARCOMA

[e] ONE MESOTHELIOMA AND ONE LEIOMYOSARCOMA

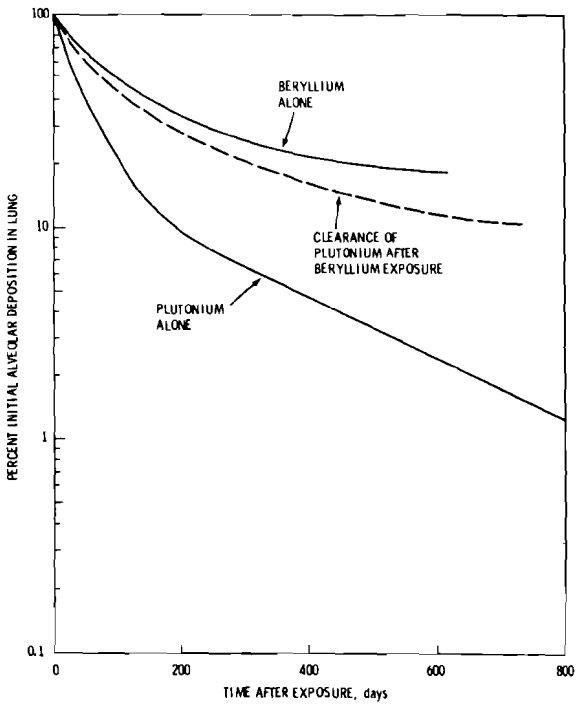

FIGURE 5.2. Alveolar Clearance of Inhaled Beryllium Following Inhalation of Beryllium Oxide and of ^{239}Pu Following Inhalation of $^{239}PuO_2$ by Itself or of $^{239}PuO_2$ Preceded by an Inhalation Exposure to High Dose of Beryllium Oxide. (Curves were drawn by eye from the individual data points.)

in rats exposed only to $^{239}PuO_2$, compared to about 10% of deposited beryllium being translocated to pulmonary lymph nodes. Rats given both beryllium and plutonium showed an increased translocation of ^{239}Pu to lymph nodes compared to rats given only plutonium.

None of the unexposed rats developed a lung tumor. One of the unexposed rats did develop an early stage of adenomatous metaplasia, which may be a premalignant stage preceding the development of carcinoma in the lung (Table 5.1). Only one of the rats exposed to beryllium only, developed a lung tumor: an adenocarcinoma found in a rat given the largest dose of beryllium. No rats given beryllium only developed metaplasia.

There was good correlation between the amount of deposited plutonium and the induction of lung tumors (Table 5.1). Most of the lung tumors were adenocarcinomas except at the highest deposition (180 nCi), where over half the lung tumors were squamous cell carcinomas and hemangiosarcomas. Adenomatous metaplasia increased in incidence with increasing deposition of plutonium. Squamous cell metaplasia was found only at the highest deposition level (Table 5.1).

In groups of rats given either 7.6 nCi or 76 nCi of ^{239}Pu and 14 μg beryllium a 15% incidence of lung tumors with 7.6 nCi and a 38% incidence with 76 nCi was observed. All but two of the tumors were adenocarcinomas. In groups given either 3.8 nCi or 59 nCi of ^{239}Pu and 91 μg beryllium there was a 12% incidence of lung tumors with 3.8 nCi and a 58% incidence with 59 nCi. Most tumors were adenocarcinomas except for six in the group given 59 nCi, which were equally mixed among squamous cell carcinomas, adenosquamous carcinomas, mesothelioma and leiomyosarcoma (Table 5.1).

The incidence of lung tumors in rats given plutonium and 14 μg beryllium was about what would be expected in rats given only plutonium. The incidence of lung tumors in rats given plutonium and 91 μg beryllium was greater, particularly at the highest deposition of plutonium, than that which would be expected for plutonium alone. This difference, although not statistically significant, may be due to the greater radiation dose delivered to the lungs of rats given both metals as compared to animals given only plutonium, since the high dose level of beryllium impairs the alveolar clearance of plutonium.

LATE EFFECTS OF INHALED $Pu(NO_3)_4$ IN RATS

Investigators:

J. E. Ballou, G. E. Dagle and K. E. McDonald

Rats that inhaled $^{239}Pu(NO_3)_4$ or $^{238}Pu(NO_3)_4$ developed lung tumors and bone tumors. Lung tumors were clearly associated with Pu inhalation (accumulated dose to lung, 1 rad to 5000 rads); bone tumors could not be unequivocally related to the radiation insult.

Male Wistar rats exposed at 60 days of age to graded doses of inhaled $^{239}Pu(NO_3)_4$ or $^{238}Pu(NO_3)_4$ have all died during the ensuing 3-yr postexposure period. The experimental protocol and interim progress reports were presented in earlier Annual Reports. This report describes the completed pathologic findings. Radioanalyses have not been completed for samples containing low levels of plutonium deposition.

The malignant lung and bone tumors found at death in plutonium-treated and control

rats are shown in Table 5.2. Tumors of the lung were confined to those animals exposed to plutonium aerosols. Osteosarcomas were observed in 6 of 11 groups administered plutonium as well as in the treated control group which was exposed to the aerosol vehicle (0.27N nitric acid). The latter finding is the subject of a separate research program discussed elsewhere in this Annual Report. A more detailed tabulation of all malignant tumors is presented in Table 5.3.

It can be assumed that alpha radiation from inhaled plutonium is the causative agent in the induction of the lung tumors, however a clear dose-response relationship is not evident from these data. This may be due to the method of assigning animals to dose groups based on average initial lung burden, rather than on the basis of the radiation dose accumulated by each animal. In our experience, a variation of 2- to 5-fold in initial lung burden is typical of animals exposed to the same aerosol, a 3-fold difference in postexposure survival time is a common observation. Since the accumulated radiation dose is a function of the initial lung burden and the length of survival after plutonium administration, it is expected that there would be an overlap in accumulated dose among animals in the various exposure levels. The overall effect is to produce a continuum of radiation dose levels rather than the discrete dose groups implied by the average initial lung burdens listed in Table 5.2. Radiation dose will eventually be calculated for each animal, based on plutonium analyses, when these results are available. A comparison of accumulated radiation dose, tumor incidence and survival time will then be possible.

The bone tumors cannot be unequivocally related to plutonium nitrate inhalation because of the unexpected finding of osteosarcomas in control animals treated with the 0.27N nitric acid vehicle. The data clearly indicate, however, that inhaled plutonium nitrate in the rat is a more effective inducer of lung tumors than of tumors of the skeleton. It seems further indicated that $^{238}Pu(NO_3)_4$ may be a more effective bone tumor inducer than $^{239}Pu(NO_3)_4$. The reason for this effect is not readily apparent from these data since the estimated accumulated radiation dose to skeleton is quite comparable for the two isotopes.

TABLE 5.2. Malignant Lung and Bone Tumors in Rats Exposed to Plutonium Nitrate Aerosols

TREATMENT[a]	INITIAL LUNG BURDEN (nCi ± SD)	AVERAGE SURVIVAL TIME, (days)	NUMBER OF RATS	ESTIMATED 500-DAY ACCUMULATED DOSE, rads		RATS WITH MALIGNANT TUMORS[b]	
				SKELETON	LUNG	SKELETON	LUNG
$^{239}Pu(NO_3)_4$	0.06 ± 0.02	687	64	0.02	0.2	0	2
	1.25 ± 0.30	642	61	0.5	5	1	0
	2.17 ± 1.2	645	63	0.9	10	0	1
	2.43 ± 1.8	662	65	0.9	10	1	1
	142 ± 47	608	60	50	600	0	34
	919 ± 359	175	65	350	4000	1	6
$^{238}Pu(NO_3)_4$	0.02 ± 0.01	686	58	--	0.08	0	0
	0.52 ± 0.16	677	60	--	2	1	0
	3.38 ± 0.76	661	59	2	11	0	2
	70 ± 27	599	52	66	225	5	24
	1514 ± 782	265	72	500	5000	7	14
NONTREATED CONTROLS	NONE	685	98	0	0	0	0
HNO_3 TREATED CONTROLS	NONE	738	97	0	0	5	0

[a] ANIMALS WERE EXPOSED FOR 30 MINUTES TO AEROSOLS

[b] OSTEOSARCOMAS OF SKELETON: ADENOCARCINOMAS, HEMANGIOSARCOMAS, SQUAMOUS CELL CARCINOMAS AND MALIGNANT MESOTHELIOMAS OF THE LUNG AND MEDIASTINUM.

TABLE 5.3. Malignant Tumors Following Inhalation of $^{239}Pu(NO_3)_4$ or $^{238}Pu(NO_3)_4$

			INITIAL LUNG BURDEN (nCi ± SD)										
			^{239}Pu						^{238}Pu				
LESION	NON-TREATED CONTROL	NON-TREATED CONTROL	0.058 ± 0.016	1.25 ± 0.3	2.17 ± 1.2	2.43 ± 1.8	142 ± 47	919 ± 360	0.02 ± 0.01	0.52 ± 0.16	3.38 ± 0.8	70 ± 27	1513 ± 782
OSTEOSARCOMA		5		1		1		1		1		5	7
ADENOCARCINOMA-LUNG			1				30	3			1	19	12
SQUAMOUS CELL CARCINOMA-LUNG			1			1	5	4			1	3	2
ADENOSQUAMOUS CARCINOMA-LUNG													1
HEMANGIOSARCOMA-LUNG			1					1					1
SARCOMA-LUNG												1	
MALIGNANT MESOTHELIOMA-LUNG					1		2				1	2	
LEUKEMIA-GRANULOCYTIC	2	2		1	2		1		2	1	2	3	2
LEUKEMIA-LYMPHOCYTIC	1	3		1		1				3	2	1	1
MALIGNANT LYMPHOMA[a]	3	3	1	2	2		2		1	3	4	7	2
MALIGNANT THYMOMA	1						1						
LYMPHOSARCOMA[b]	1			1		1		1	1				
RETICULUM CELL SARCOMA[c]		1	1		1				1	1	1		
FIBROSARCOMA[d]	9	7	4	8	4	7	6		7	3	4	3	
NEUROFIBROSARCOMA[e]	4	4				2			1	3	1		
LEIOMYOSARCOMA[f]	1	1			1						1		
RHABDOMYOSARCOMA						1							
MYXOSARCOMA											1		
SQUAMOUS CARCINOMA[g]	2					1	1			1	2		
MEGAKARYOCYTIC MYELOSIS					1								
MYELOSARCOMA-LIVER, SPLEEN					1					1			
HEPATOMA	1						1		1				
HEMANGIOSARCOMA-SPLEEN	1	1				1	1						
PHEOCHROMOBLASTOMA	1	2				2	2		1	1	1	1	
CARCINOMA-ADRENAL	1				2		1			1	1	1	1
CARCINOMA-THYMUS	1												
CARCINOMA-PITUITARY											1		
LIPOSARCOMA	1	1							1				
ADENOCARCINOMA-THYROID		1	1				1						
ADENOCARCINOMA-BREAST		1		1			1						2
ADENOCARCINOMA-VISCERA			1				1						
ADENOCARCINOMA-PANCREAS		1									1		
CARCINOMA-BASAL CELL					1								
MALIGNANT MESOTHELIOMA-ABDOMEN				1									
ASTROCYTOMA-BRAIN			1				1		1	1			
DYSGERMINOMA-TESTES		1							1				
#TUMORS/#RATS WITH TUMORS/ #RATS	30/27 98	34/30 97	12/11 64	16/16 61	16/16 63	18/18 65	57/45 60	10/8 65	18/17 58	20/19 60	25/24 59	46/37 52	31/21 72

[a] INCLUDES MALIGNANT LYMPHOMA PRIMARY TO SPLEEN, THYMUS, LYMPH NODES AND INTESTINES.

[b] LYMPHOSARCOMA OF LYMPH NODES, THYMUS AND NO PRIMARY SITE IDENTIFIED.

[c] LESIONS OF LYMPH NODES AND OTHER TISSUES OF THE RETICULOENDOTHELIAL SYSTEM.

[d] FIBROSARCOMA OF HEART, EXTREMITIES, SPLEEN AND SUBCUTANEOUS TISSUES.

[e] NEUROFIBROSARCOMA OF SKIN, ABDOMEN, EYE, MEDIASTINUM AND SUBCUTANEOUS TISSUE.

[f] LEIOMYOSARCOMA OF INTESTINE, VASCULATURE, STOMACH AND PANCREAS.

[g] LESIONS PRIMARY TO SKIN, MANDIBLE, EYE AND SUBCUTANEOUS TISSUES.

EARLY FATE OF INHALED CRYSTALLINE $^{239}Pu(NO_3)_4$ IN RATS

Investigators:

J. E. Ballou, R. A. Gies, and J. L. Ryan[a]

Technical Assistance:

R. L. Music

Preliminary results suggest that $Pu(NO_3)_4$ inhaled as crystalline solid aerosol is retained more tenaciously in the lung and excreted less in urine than inhaled $Pu(NO_3)_4$ aerosols generated from a nitric acid solution.

Vacuum-dried salts of plutonium nitrate have been suggested as more acceptable compounds for mass transport of reprocessed reactor fuel materials than the previously employed highly acid solutions of plutonium. The dehydrated compound is considered to be less hazardous for shipping purposes and can be readily reconstituted to form the acid solutions required in fuel fabrication. When dried under vacuum conditions, plutonium nitrate forms a neutral, hygroscopic salt, with density 2.9 g/cm^3 and the chemical formula $Pu(NO_3)_4 \cdot 5H_2O$. The compound hydrolyzes to form plutonium hydroxide and nitric acid.

Under physiological conditions, e.g., in the lung after inhalation of the aerosolized material, dry plutonium nitrate is expected to hydrolyze and polymerize as aggregates of plutonium hydroxide. The potential chemical-biological reactivity would presumably be short-lived, perhaps limited to the time of initial contact with vapor-saturated air in the respiratory tract or to the time of contact with pulmonary tissues. Similar reactions are predicted for inhaled aerosols of acid plutonium solutions.

The present study was initiated to investigate the metabolism of inhaled crystalline plutonium nitrate for comparison with the results of ongoing studies with plutonium nitrate solutions. The relative hazard of the two forms of plutonium will be evaluated on the basis of pulmonary retention and distribution in tissues.

Aerosols of crystalline $Pu(NO_3)_4 \cdot 5H_2O$ were generated, using a Lovelace nebulizer and a perfluorinated compound (trifluorobutylamine) as the suspending medium. The generator contents were agitated by ultrasonic stirring during the exposure period. The suspension was 0.015% ultrafilterable through Visking tubing, indicating essentially no solubilization of $Pu(NO_3)_4$ by the fluorocarbon. Thirty-five male Wistar rats were administered aerosols during a 75-min nose-only exposure, and sacrificed in groups of five immediately after exposure and after 7, 30, 60, 100, 150, and 200 days. Excreta were collected daily for the five rats sacrificed after 7 days. This study is still in progress so only partial results are available.

The distribution of plutonium, immediately after exposure to the aerosol, is shown in Table 5.4. The data are compared with

---

[a] Chemical Technology, Department, BNW

TABLE 5.4. Initial Disposition of $^{239}Pu(NO_3)_4$ Inhaled as a Solution in 0.27N HNO_3 and as a Crystalline Solid Suspended in Fluorocarbon

	$^{239}Pu(NO_3)_4$	
	SOLUTION	CRYSTALLINE SOLID
EXPOSURE CHARACTERISTICS[a]		
TIME DURATION (min)	30	75
AMAD (μm)	0.602	1.277
GSD[b]	2.369	2.003
INITIAL LUNG BURDEN (nCi)	2.4 ± 1.8	3.9 ± 1.3
PERCENTAGE DISTRIBUTION OF DEPOSITED PLUTONIUM		
UPPER RESPIRATORY TRACT		
TRACHEA	2.1	0.8
NOSE	5.8	4.8
TONGUE AND ESOPHAGUS	12.7	3.0
HEAD	8.1	2.0
STOMACH AND JEJUNUM	33.7	28.4
TOTAL	62.4	39.0
TRANSLOCATED TO TISSUE		
LIVER	0.04	0.06
RESIDUAL CARCASS	3.5	1.1
TOTAL	3.54	1.16
RETAINED IN LUNG	9.1	15.2
RETAINED IN PELT	25.0	44.6

[a] AMAD = ACTIVITY MEDIAN AERODYNAMIC DIAMETER (μm)
[b] GSD = GEOMETRIC STANDARD DEVIATION

the distribution of a comparable amount of plutonium deposited from an aerosolized solution of plutonium in nitric acid. The percent deposited in the lung appears to be greater for the crystalline material, although the larger particle size might have been expected to favor deposition in the upper respiratory tract. The longer exposure time for the rats administered the crystalline aerosol (75 min versus 30 min) may also influence the comparability of the two sets of data.

The daily urinary excretion of inhaled $Pu(NO_3)_4$ (crystalline versus solution forms) is compared in Figure 5.3. Excretion of the inhaled solubilized material is most often higher, perhaps indicative of a greater mobility of the acid solutions. The more rapid translocation of inhaled $Pu(NO_3)_4$ solution is further suggested in Figure 5.4, which shows the limited data now available for pulmonary retention of the crystalline compound.

The influence of the fluorocarbon aerosol vehicle on plutonium metabolism is as yet unknown, however the effect is expected to be minimal. Similar fluorocarbon compounds are notably nontoxic when used in pulmonary ventilation studies, e.g., involving lavage or immersion for extended time periods. These fluorocarbons are, however, well-retained in the lung and are translocated to the pulmonary lymph nodes, where they might conceivably influence the retention and translocation of inhaled plutonium.

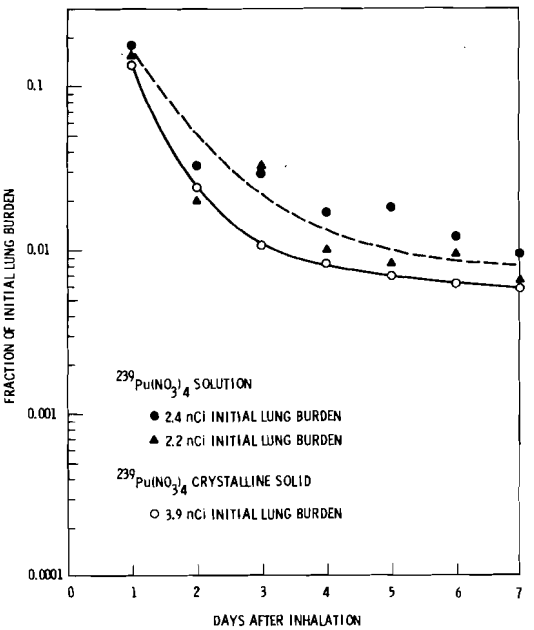

FIGURE 5.3. Urinary Excretion of Inhaled Plutonium Nitrate

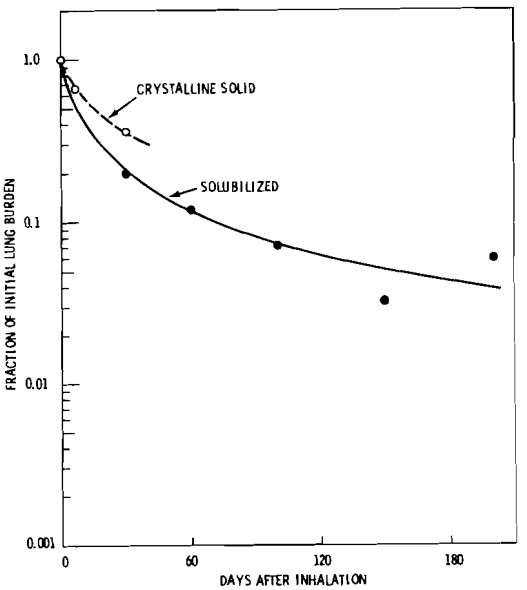

FIGURE 5.4. Retention of Inhaled Crystalline and Solubilized Plutonium Nitrate in the Lung. (Initial lung burdens were 3.9 nCi and 2.4 nCi, respectively).

QUANTITATIVE AUTORADIOGRAPHY OF INHALED $^{239}PuO_2$ IN THE LUNG

Investigators:

K. Rhoads, D. Moon and C. L. Sanders

PuO_2 particles behaved similarly in the lungs of rat and hamster. The relative concentrations of PuO_2 up to 1-yr postexposure were 1.0 for lung parenchyma, 1.3 for subpleural areas, 0.5 for peribronchiolar regions and 0.2 for perivascular regions in the lungs.

Two observations from life-span studies of inhaled $^{239}PuO_2$ in rats and hamsters have provided the impetus for further investigation of plutonium particle distribution in lung. The first was a qualitative observation that particles were translocated within the lung following exposure and concentrated in the subpleural regions. This translocation appeared to be dose- and time-dependent, occurring to a greater extent in animals with larger Pu lung burdens. The second finding was that there is a difference between the rat and hamster in pathologic response to $^{239}PuO_2$, with rats developing a high incidence of malignant lung tumors while hamsters developed very few such tumors (Annual Report, 1975).

A quantitative study of $^{239}PuO_2$ particle distribution was performed to determine the role of time, dose, and species on particle fate, in an attempt to explain the difference in tumor response between the two species. Previous studies have shown no difference between the rat and hamster in lung clearance or translocation to extrapulmonary tissues (Annual Reports 1974, 1975).

Twenty-four Wistar SPF female rats and 20 female Syrian golden hamsters were exposed to an aerosol of $^{239}PuO_2$ particles at 70 days of age. Exposures were nose-only for 45 and 30 min, for rats and hamsters respectively. The particle size distribution was considered log-normal for both exposures. The activity median aerodynamic diameter/geometric standard deviation (AMAD/GSD) for the particles in these exposures were 3.8 μ/2.5 for rats and 3.4 μ/2.4 for hamsters. Animals were necropsied at intervals up to 1 yr after exposure. Following tracheal cannulation, the lungs were fixed with glutaraldehyde at 20 cm H_2O pressure. Photomicrograph montages were prepared from autoradiographs (2-wk exposure) of cross sections of the top half of the left lung lobe.

For purposes of analysis, the lung tissue was divided into 6 components, which are illustrated in Figure 5.5. Peribronchial-bronchiolar (PB) and perivascular (PV) were defined as the entire wall of the airway or blood vessel, including lining cells, connective tissue and spaces. Bronchial-bronchiolar (B) and vascular (V) included only the lumen of the airway or vessel. Subpleural (SP) was defined as the area within 1 cm of the pleural surface on photomontages, which corresponds to a distance of 0.33 cm from the pleural surface of the fixed lungs. Parenchymal (P) included all alveolar lung except that designated as subpleural.

Morphometric estimation of the volume fraction occupied by each component was performed by point-counting volumetry. The alpha particle stars were then counted and

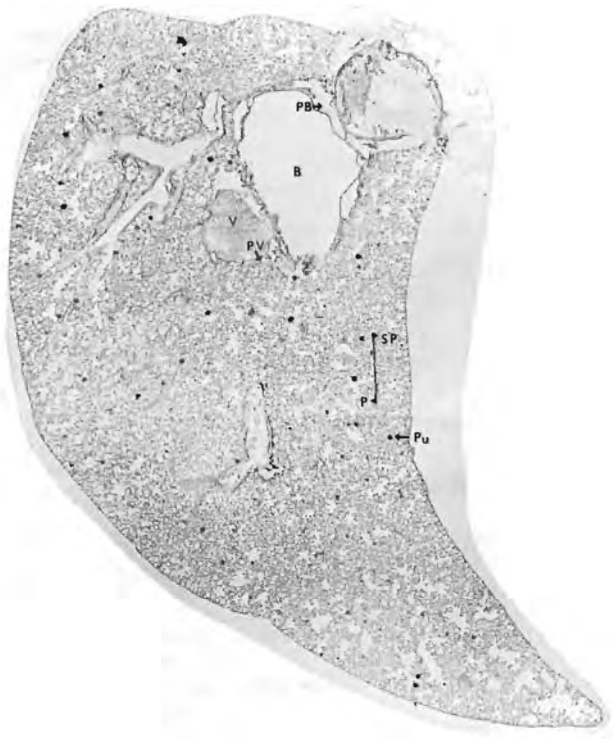

FIGURE 5.5. Photomicrograph Montage Prepared from an Autoradiograph of a Cross-Section of the Left Lobe of a Hamster Lung. The animal had a terminal Pu lung burden of 82 nCi at the time of sacrifice 14 days after exposure. The autoradiograms were prepared on NTA plates and exposed for 2 wk. B = bronchial-bronchiolar, PB = peribronchial-bronchiolar, V = vascular, PV = perivascular, SP = subpleural, P = parenchymal, PU = alpha star produced by a $^{239}PuO_2$ particle.

the location of each was recorded in one of the six tissue categories. The smallest stars included in this analysis contained about 20 tracks, which correspond to a minimum particle diameter of about 0.15 μ. The volume fractions and the particle distribution thus obtained were then used to define a relative particle concentration for each tissue component (definition in Table 5.5). The data were grouped according to initial alveolar deposition and time after exposure. The mean lung burden and number of animals in each group are shown in Table 5.5, as are the tissue volume fractions and the relative particle concentrations.

There was no difference between rat and hamster in the volume distribution of the lung tissue components. Parenchymal lung occupied about 55% of the total volume, with subpleural accounting for 30%, and blood vessels and airways, 15%.

No particles were seen in vascular areas of the lung. In general, the PuO_2 particle concentration was lower in the bronchial, peribronchial, and perivascular regions of the lung than in the parenchymal or subpleural. At times >120 days, there was an indication of particle concentration in subpleural regions for both rat and hamster.

Because the PuO_2 particle distribution is not uniform in all components of the lung, a correction must be applied in order to estimate the dose received by any particular component. In order to obtain doses for specific components, the average lung dose should be multiplied by a factor of 1.0 for parenchyma, 1.3 for subpleural, 0.5 for peribronchial-bronchiolar, and 0.2 for perivascular. These values are similar for rats and hamsters and are applicable at relatively long periods postexposure (120-350 days).

The practical application of this data lies in two areas. Alveolar and bronchiolar epithelia, which have been implicated as cells of origin for Pu-induced lung tumors, receive very different levels of exposure to inhaled PuO_2 particles, based on the

relative particle concentrations in parenchymal and bronchiolar tissue. This may imply that bronchiolar epithelial cells are more sensitive to neoplastic transformation than alveolar epithelial cells. With respect to the species difference in tumor response, it does not appear from this data that differences in PuO_2 particle distribution can account for the difference in tumor formation observed between rats and hamsters in life-span studies.

TABLE 5.5. Distribution of Inhaled $^{239}PuO_2$ Particles in Lung

LUNG TISSUE COMPONENTS	RATS					HAMSTERS				
	VOLUME FRACTION $\bar{x} \pm SD$	RELATIVE PARTICLE DENSITIES[a] LOW DOSES <90 days	LOW DOSES >120 days	HIGH DOSES <90 days	HIGH DOSES >120 days	RELATIVE PARTICLE DENSITIES[a] LOW DOSES <90 days	LOW DOSES >120 days	HIGH DOSES <90 days	HIGH DOSES >120 days	VOLUME FRACTION
TOTAL SUBPLEURAL	28 ± 5	1.26 ± 0.26	1.29 ± 0.50	1.08 ± 0.27	1.76 ± 0.35	1.05 ± 0.26	1.73 ± 0.57	0.94 ± 0.21	1.35 ± 0.20	34 ± 7
PARENCHYMAL	57 ± 6	1.12 ± 0.19	1.02 ± 0.27	1.18 ± 0.12	1.83 ± 0.14	1.06 ± 0.29	0.76 ± 0.25	1.34 ± 0.28	0.98 ± 0.18	55 ± 7
BRONCHIAL-BRONCHIOLAR	4 ± 2	0.66 ± 0.57	0.06 ± 0.13	0.12 ± 0.20	0.26 ± 0.44	2.20 ± 4.40	0	0.15 ± 0.30	0	3 ± 2
VASCULAR	4 ± 1	0	0	0	0	0	0	0	0	3 ± 1
PERIBRONCHIAL-BRONCHIOLAR	3 ± 1	0.36 ± 0.17	1.81 ± 2.81	0.10 ± 0.13	0.29 ± 0.31	1.54 ± 2.32	0.30 ± 0.67	0.32 ± 0.37	0.40 ± 0.89	2 ± 1
PERIVASCULAR	4 ± 1	0.05 ± 0.06	0.46 ± 0.64	0.07 ± 0.09	0.55 ± 1.05	0.05 ± 0.11	0	0.54 ± 0.97	0	3 ± 1
NUMBER OF ANIMALS IN GROUP	24	4	6	6	8	6	5	4	5	20

[a] RELATIVE PARTICLE DENSITY = $\frac{\text{FRACTION OF STARS OBSERVED IN TISSUE COMPONENT x}}{\text{VOLUME FRACTION OF TISSUE COMPONENT x}}$

• INHALED PLUTONIUM IN SWINE

Person in Charge: M. T. Karagianes

Preliminary experiments, using discretionary funds, have been performed for this proposed project. Estimates of the possible effects of inhaled plutonium in man are based largely on data from studies with rodents and dogs. Data from a larger species would be useful in extrapolation of this animal data to man. The miniature swine has served as a useful experimental model for man in many biomedical investigations because of physiologic and anatomic similarities.

It is proposed to expose swine to $^{239}PuO_2$ aerosols, by inhalation, to determine short- and long-term effects. Short-term studies (up to 1 yr) would investigate plutonium deposition, distribution and excretion, providing information necessary to the design and interpretation of long-term studies. Long-term experiments would be primarily concerned with evaluating carcinogenic effects, but would also provide material for the study of other possible effects and the mechanisms responsible for these effects. The results obtained from all studies would be compared with other animal and human data and would be used to assess the swine as a model for predicting effects in humans.

$^{239}PuO_2$ AEROSOL EXPOSURE OF MINIATURE SWINE

Investigators:

M. T. Karagianes, J. L. Beamer, D. K. Craig,
W. T. Kaune, J. R. Decker, and W. C. Cannon

Technical Assistance:

A. J. Clary, J. P. Herring, E. L. Blanton,
M. C. Miller, and E. G. Kuffel

Techniques were developed for intranasal exposure of miniature swine to radioactive aerosols. Distribution, retention and excretion data are reported for four swine exposed to inhaled $^{239}PuO_2$.

Initial work on this project was directed at modifying existing aerosol equipment and establishing proper techniques for the inhalation exposure of miniature swine. Swine aerosol chamber design, face masks for intranasal exposure and the methods used to expose the animals to $^{239}PuO_2$ were described in the 1975 Annual Report.

Four young adult ($\sim$ 2 years) female Hanford Miniature swine, weighing approximately 70 kg, were killed at 10, 13, 30, and 90 days following intranasal exposure to $^{239}PuO_2$. Two of these swine were exposed to $^{239}PuO_2$ aerosols having an AMAD of 3.0 μm and a GSD of 2.1. Two others were exposed to similar aerosols having an AMAD of 2.0 μm and a GSD of 1.8. Plutonium analyses were performed by liquid scintillation counting. All postexposure excreta were analyzed for Pu and representative lung and lymph node samples were examined by microscopic and autoradiographic techniques.

The distribution data in Table 6.1 are particularly notable for the large amount of ^{239}Pu retained in the gastrointestinal tract. Whether this is related to fecal retention or to unusual retention properties of the epithelium is unknown. Since dose to the gastrointestinal tract is a significant factor in the estimated human exposure to many inhaled radionuclides, the observations in swine may be of considerable significance if human retention is similar to that observed in these swine.

Table 6.1 also shows urinary excretion levels that would suggest considerable absorption to the systemic circulation; however, separation of urine and feces was difficult and most of the activity measured in the urine was probably leached from the feces.

The whole-body clearance curves shown in Figure 6.1 were constructed by subtracting the cumulative fecal and urinary excretion data from the total initial deposition. Curves shown in Figure 6.1 are for pigs that survived 30 and 90 days postexposure. The data points were fitted by a computer model that assumed two exponential components. The retention equations that best fit the data are also shown in Figure 6.1.

While the data seem to be reasonably well represented by the double exponential

TABLE 6.1. Distribution of Inhaled $^{239}PuO_2$ Aerosols in Swine

PIG NUMBER	5351	5350	5362	5355
AMAD OF EXPOSURE AEROSOL, μm	3.0	3.0	2.0	2.0
DAYS POST EXPOSURE	10	13	30	90
INITIAL BODY BURDEN, nCi[a]	1856	6621	2521	2871
	% OF INITIAL BODY BURDEN			
BODY TOTAL	74.7	53.0	18.0	3.0
LUNG	70.7	46.2	16.8	2.2
PULMONARY LYMPH NODES	0.5	2.0	0.2	0.3
ALL REMAINING TISSUE[b]	3.5	4.8	1.0	0.5
EXCRETA TOTAL	25.3	47.0	82.0	97.0
FECES	21.9	46.0	80.0	92.5
URINE	3.4	1.0	2.0	4.5
FINAL BODY BURDEN, nCi	1385	3490	457	87
	% OF FINAL BODY BURDEN			
LUNG, TOTAL	94.65	87.09	92.65	72.59
PULMONARY LYMPH NODES	0.02	0.05	0.31	8.80
THORACIC TISSUE	0.60	3.70	0.72	1.92
SYSTEMIC DISPOSITION[c]	4.71	9.15	6.30	16.68
(GASTROINTESTINAL TRACT AND CONTENTS)	(4.62)	(9.15)	(6.26)	(1.78)

(a) SUM OF ESTIMATED TOTAL BODY BURDEN AT NECROPSY AND TOTAL Pu EXCRETED
(b) INCLUDES REMAINING THORACIC ORGANS, TRACHEA AND TRACHEAL BIFURCATION
(c) INCLUDES ABDOMINAL ORGANS, MUSCLES, SKIN AND BONE

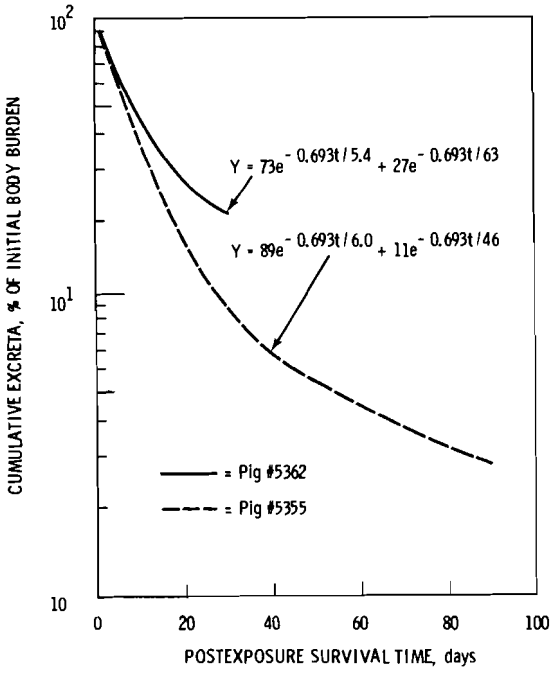

FIGURE 6.1. Whole-Body Clearance Curves for Miniature Swine Exposed Intranasally to $^{239}Pu_2$ Aerosols

model, certain quantitative limitations must be stressed. Evaluation of the short-term component is complicated by the fact that fecal elimination did not occur until the third day postexposure, which may have obscured an even shorter-term initial component, particularly in the data from the 90-day pig. It is also apparent that a much longer half-life might have been obtained for most of the longer-lived component if data had been obtained over a longer time period. It can be stated, however, that about 90% of initially inhaled Pu is lost with half-lives on the order of a few days or less, and that ∿ 10% is retained with half-lives on the order of 50 days or longer--possibly much longer.

Complete blood counts of samples taken from the swine before and after exposure, as well as from caged controls, showed all hematologic parameters to be within normal limits.

Microscopic and autoradiographic examination of lung tissue specimens showed no pathologic lesions other than a mild pulmonary congestion and edema. Generally the retained Pu particles were found in the alveolar walls with a few present in the subpleura and around the terminal bronchioles of the lungs.

• INHALATION HAZARDS TO URANIUM MINERS

Person in Charge: B. O. Stuart

The objective of this project is to identify the specific uranium mine air contaminants, and the levels of these contaminants, that initiate or promote the development of respiratory tract pathology. The 6X higher than normal incidence of lung cancer and the 5.3X higher than normal mortality from pulmonary fibrosis and emphysema among uranium miners of the Colorado plateau, in a period of increasing demand for uranium ore, is a matter of both national and international concern. Epidemiologic studies among uranium miners have been based on very uncertain exposure histories. Studies with experimental animals offer the only hope of unraveling the complex etiology of observed effects. The drastically increased mine ventilation rates demanded by new regulations will markedly change radon daughter attachment ratios and radon:radon daughter ratios and will create new patterns of radiation dose, possibly altering the tissue at risk.

Under this project, large and small laboratory animals have received daily, life-span exposures, by realistic inhalation techniques, at levels and ratios of mine air contaminants that have been correlated with actual human exposure conditions. Massive fibrosis, bullous emphysema and respiratory tract neoplasia have been produced in beagle dogs after 4 to 5-1/2 yr of daily exposures to radon daughters with uranium ore dust, with and without concurrent cigarette smoking.

Current research efforts include studies of pulmonary pathogenesis with chronically inhaled radon daughters, uranium ore dust, and cigarette smoke in beagle dogs, together with interspecies comparisons in simultaneously exposed hamsters and rats. Data from these comparative studies should aid in the extrapolation of the dose-effect relationships to man. Also in progress are studies of the biological consequences of varying the ratios of attached versus unattached radon daughter radionuclides. These studies will provide data to evaluate the relative hazards of dusty versus minimal-dust conditions in uranium mine operations. Studies to assess the relative hazards of Rn, RaA, and RaC' will provide data essential to the evaluation of inhalation hazards in future, well-ventilated, uranium mines as compared to conditions prevalent in the early 1950s.

CARCINOGENESIS OF INHALED RADON DAUGHTERS WITH URANIUM ORE DUST IN BEAGLE DOGS

Investigators:

R. E. Filipy, G. E. Dagle, R. F. Palmer, and B. O. Stuart

Technical Assistance:

W. Skinner, C. R. Petty, and K. C. Upton

Daily exposures of adult beagle dogs to inhaled radon daughters and to uranium ore dust for 4-1/2 to 6 yr have produced respiratory tract carcinomas, at similar cumulative working level months (WLM) of exposures to those which induced carcinomas in uranium miners. Biological data from the beagle-dog experiments can therefore be used for prediction of carcinogenic risk under changing exposure conditions in future uranium miners.

The continuing experiments described in this report were designed to study the cause and effect relationships in the development of pulmonary neoplasia from daily inhalation exposures of dogs to the uranium mine air contaminants of radon daughters with uranium ore dust and cigarette smoke, both combined and separately, under carefully controlled conditions, over the lifespan of the animals. Sixty-nine beagle dogs raised in our laboratory were trained and placed on exposure regimens outlined in Table 7.1.

TABLE 7.1. Experimental Design for Beagle Dog Studies

GROUP[a]	NUMBER OF ANIMALS	EXPOSURE
1	20	600 WL RADON DAUGHTERS WITH URANIUM ORE DUST (15 mg/m^3)
2	20	CIGARETTE SMOKE PLUS 600 WL RADON DAUGHTERS WITH URANIUM ORE DUST
3	20	CIGARETTE SMOKE
4	9	CONTROLS

[a] GROUPS 1 AND 4 UNDERWENT PERIODS OF SHAM SMOKING IDENTICAL TO CIGARETTE SMOKE EXPOSURE OF GROUPS 2 AND 3.

Alveolar epithelial changes were prominent in the lungs of dogs from Groups 1 and 2 that had exposures longer than 30 months. The least severe form of these changes consisted of small foci of cuboidal metaplasia (adenomatosis) adjacent to the bronchioles and alveolar ducts. In dogs with longer exposure histories (40 months or more), large areas of adenomatosis were present, occasionally involving the major portion of a section through a lung lobe. Frequently, the lesion had progressed to squamous metaplasia of the alveolar epithelium in which atypical cells were present. These cells were characterized by marginated nuclear chromatin, irregularly shaped nuclei, and decreased nuclear-to-cytoplasmic ratio.

In two of the dogs exposed for 48 and 54 mo, there were epidermoid carcinomas associated with emphysemic bullae. The tumors were solitary masses in peripheral areas of single lobes and consisted of irregularly shaped lobules of nonkeratinizing stratified squamous epithelium with a scant amount of connective tissue stroma. They were locally invasive into adjacent alveoli. Another epidermoid carcinoma, in a dog exposed to radon daughters plus

uranium ore dust for 54 mo, appeared as a well-circumscribed mass composed of anaplastic cells with numerous mitotic figures (Figure 7.1).

Three other primary lung tumors (bronchioloalveolar carcinomas) were present in three dogs of Group 1 exposed for 51, 54, and 54 mo. The tumors were solitary masses associated with distal bronchioles in single lobes, locally invasive into adjacent alveoli, and did not metastasize (Figure 7.2). A bronchioloalveolar adenoma, composed of a papillary proliferation of epithelium, was present in a dog that also had an epidermoid carcinoma. In addition, a fibrosarcoma was present in the anterior ventral portion of the right apical lobe of the lung from another Group 1 dog exposed for 54 mo. It consisted of a 3-cm dia, roughly spherical, well-circumscribed mass of low-grade malignancy.

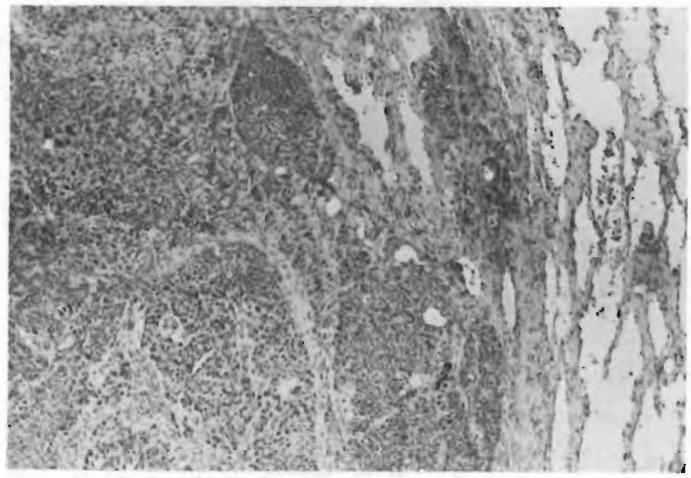

FIGURE 7.1. Epidermoid Carcinoma in the Lung of a Dog Exposed to Radon Daughters and Uranium Ore Dust for 54 Mo; 60X

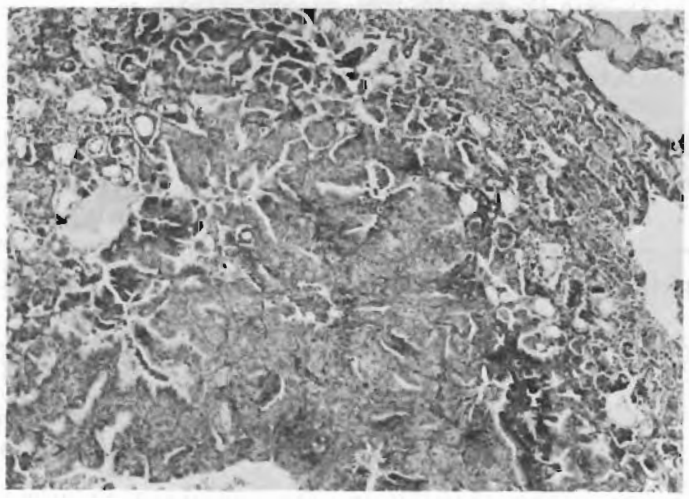

FIGURE 7.2. Bronchioloalveolar Carcinoma from a Dog Exposed for 54 Mo; 60X

Pathologic changes in upper respiratory air passages of the dogs from Groups 1 and 2 were primarily in the nasal mucosa. Squamous carcinomas arising from the epithelium of the nasal cavity occurred in three dogs after 46 to 51 mo of exposures (one from Group 2 and two from Group 1). In two of the dogs the tumors were visible as swellings on the outside of the nose. The largest tumor was composed of a tan, 4.5-cm dia mass arising from the area of the right maxilla and eroding into the oral cavity. These nasal carcinomas were composed of nonkeratinizing stratified squamous epithelium forming irregular cords infiltrating the submucosa and extending between spicules of bone (Figure 7.3). A large metastasis was present in the mandibular lymph node of one dog. The periods of daily exposures and the Cumulative Working Level Months (CWLM) associated with each respiratory tract carcinoma are given in Table 7.2.

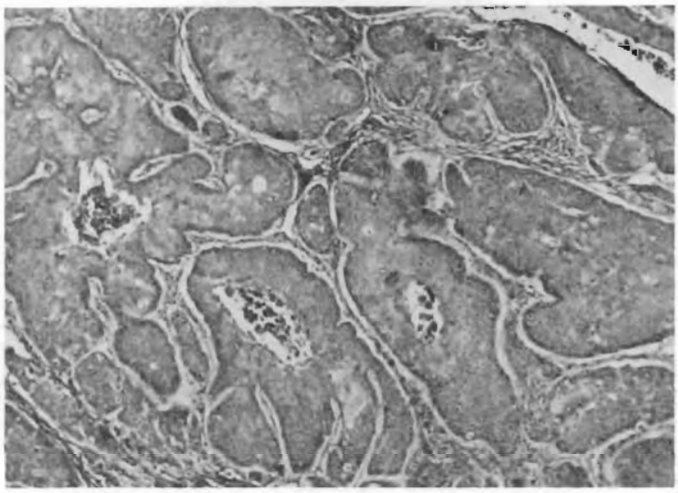

FIGURE 7.3. Squamous Carcinoma of the Nasal Epithelium of a Dog Exposed for 46 Mo; 70X

TABLE 7.2. Respiratory Tract Cancer in Beagle Dogs Exposed to Radon Daughters

DOG NO.	EXPOSURE TO RADON DAUGHTERS WITH URANIUM ORE DUST (mo)	TIME IN EXPOSURE CHAMBER (hr)	CUMULATIVE WORKING LEVEL MONTHS
BRONCHIOLOALVEOLAR CARCINOMA			
512	51	3997	11,900
525	54	4421	13,400
531	54	4417	13,400
EPIDERMOID CARCINOMA (PULMONARY)			
523	54	4289	13,000
541	54	4421	13,400
608	48	3941	12,500
NASAL CARCINOMA			
608	48	3941	12,500
615	46	3751	12,500
544	51	3867	11,700
FIBROSARCOMA (PULMONARY)			
540	54	4424	13,400

This research has demonstrated primary respiratory tract neoplasia, including bronchioloalveolar carcinoma, squamous carcinoma, epidermoid carcinoma, and pulmonary fibrosarcoma in 9 of 40 dogs that received 11,000 to 13,000 CWLM, which is similar to the higher exposure levels (6,000 to 8,435 CWLM) in cases of lung cancer in uranium miners. We are fortunate to have chosen levels that produced respiratory tract cancer in 4-1/2 yr (compared to 17 yr for man), demonstrating the suitability of the beagle dog as a large-animal model for lung cancer in uranium miners. The 600 WL used in the research is comparable to human exposure levels; many of the former uranium miners that are included in the epidemiological analyses upon which current limits are based received documented periods of exposure to concentrations in excess of 100 WL, with several cases as high as 230 WL. Earlier undocumented mine exposures undoubtedly reached considerably higher levels. Therefore, these experimental findings of primary neoplasia using a large-animal model correlate within factors of 3- to 6-fold with actual human exposure experience.

NON-NEOPLASTIC PULMONARY DISEASE FROM INHALED RADON DAUGHTERS WITH URANIUM ORE DUST IN BEAGLE DOGS

Investigators:

R. E. Filipy, R. F. Palmer, and B. O. Stuart

Technical Assistance:

W. Skinner, C. R. Petty, and K. C. Upton

Daily exposures of adult beagle dogs to inhaled radon daughters plus uranium ore dust, with and without concurrent cigarette smoking, for 2 to 5-1/2 yr have produced massive pulmonary fibrosis and severe emphysema. The cumulative exposure doses are similar to those associated with a 5-fold or greater increase in death rate of uranium miners due to chronic respiratory insufficiency, including pneumoconiosis, pulmonary fibrosis, and emphysema.

In addition to the markedly increased risk of lung cancer (6-fold greater than normal incidence for age-correlated controls) in uranium miners, recent epidemiological analyses (May 1976) have shown a 5.3-fold increase in uranium miner deaths due to chronic respiratory insufficiency, including pneumoconiosis, pulmonary fibrosis, and emphysema. The high risk of respiratory disease appears to be related to concurrent inhalation exposure to radon daughters and silica-bearing uranium ore dust present in these mines, underscoring the critical need for carefully controlled cause and effect studies using appropriate large- and small-animal models to reliably assess the risk of fatal non-neoplastic pulmonary disease in present and future uranium miners. Our research program has produced massive pulmonary fibrosis and bullous emphysema, as well as respiratory tract neoplasia, in beagle dogs after 2 to 5-1/2 yr of daily exposures to radon daughters with uranium ore, with and without concurrent cigarette smoking, following the protocol given in Table 7.3. The pathogenesis of these lesions is described below.

Pulmonary macrophages containing a brown pigment, considered to be ore dust, were the earliest histologic manifestations

TABLE 7.3. Experimental Design for Beagle Dog Studies

GROUP[a]	NUMBER OF ANIMALS	EXPOSURE
1	20	600 WL RADON DAUGHTERS WITH URANIUM ORE DUST (15 mg/m^3)
2	20	CIGARETTE SMOKE PLUS 600 WL RADON DAUGHTERS WITH URANIUM ORE DUST
3	20	CIGARETTE SMOKE
4	9	CONTROLS

[a]GROUPS 1 AND 4 RECEIVED IDENTICAL PERIODS OF SHAM SMOKING.

of exposure of the dogs to radon daughters and uranium ore dust (Groups 1 and 2). The macrophages were accumulated in perivascular, peribronchiolar, and peribronchial areas that were frequently infiltrated with mononuclear inflammatory cells. Tracheobronchial lymph nodes of these dogs contained large amounts of uranium ore dust (Figure 7.4). After prolonged exposure to ore dust, these lymph nodes became markedly enlarged and dark in color. Microscopically, they contained large numbers of macrophages in the medullary cords and slight to moderate lymphoid follicular hyperplasia. Accumulations of macrophages bearing ore dust were evident in the lungs and lymph nodes of two dogs killed after only 6 mo of exposure to radon daughters and uranium ore dust, and in all dogs that died or were killed after longer exposures.

Pulmonary hyalinosis was a common microscopic change in dogs from Groups 1 and 2 that died or were killed after exposure of 27 mo or longer. The lesion was present in the lungs of 17 of the 20 Group 1 dogs and all 19 dogs from Group 2. The least severe form of the lesion consisted of individual alveolar macrophages containing the hyaline material. In the lungs of dogs with long exposure histories, large areas of some lung lobes were affected (Figure 7.5), frequently associated with a granulomatous reaction. Frequently, masses of the hyaline material were encapsulated by fibrous connective tissue. The hyaline material was characterized on the basis of histochemical reactions as a calcium-lipid-mucopolysaccharide complex. Ultrastructural studies suggest that the lesion may be a result of cellular degradation

Vesicular emphysema was present in the lungs of all dogs from Groups 1 and 2. In dogs that died or were killed early in the experiment (<2-1/2 yr), the lesions were less severe; however, alveolar septa were interrupted, especially in the subpleural parenchyma. The lesions were more severe in dogs which had been exposed to radon daughters and uranium ore dust for 30 to 45 mo; in dogs with exposure histories longer than 45 mo, bullous emphysema was common. Subpleural cavities were visible on gross examination and they occasionally had dimensions exceeding 1 cm (Figure 7.6). Bullous emphysema was present in the lungs of 11 of 20 dogs from Group 1, and in 13 of 19 dogs from Group 2.

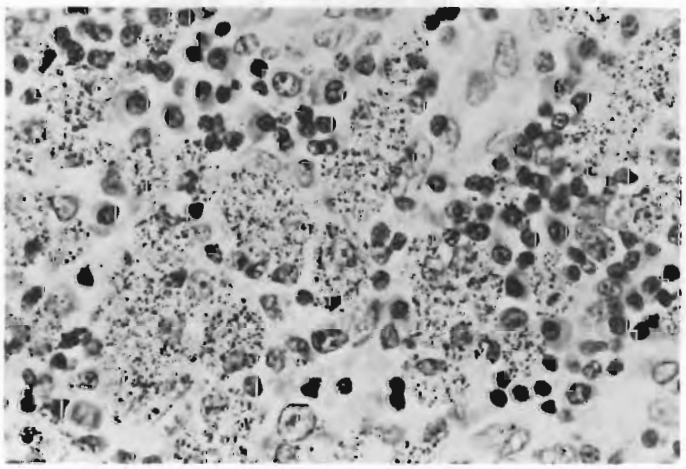

FIGURE 7.4. Tracheobronchial Lymph Node Containing Uranium Ore Dust; Exposure to Radon Daughters and Uranium Ore Dust for 52 Mo, to Cigarette Smoke for 61 Mo; 3 Mo Elapsed Between Cessation of Exposures and Death. H&E. 700X.

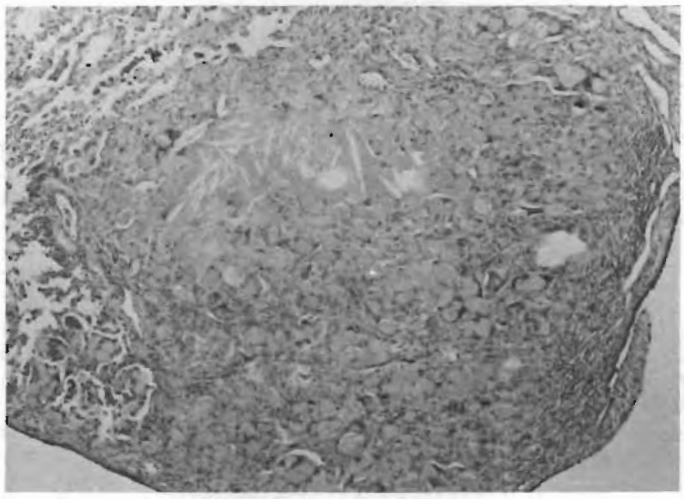

FIGURE 7.5. Dense Accumulation of Hyaline Structures With Associated Granulomatous Response; Exposure to Radon Daughters and Uranium Ore Dust for 43 Mo. H&E. 90X.

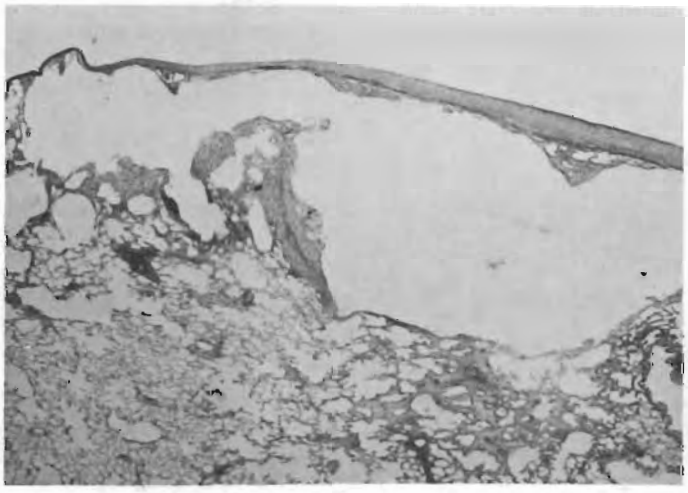

FIGURE 7.6. Bullous Emphysema in a Lung Section from a Dog Exposed for 48 Mo to Radon Daughters and Uranium Ore Dust. H&E. 21X.

Pulmonary fibrosis was present in all dogs from Groups 1 and 2 of this experiment. Alveolar septal fibrosis was apparent to a slight degree in the two dogs killed after 6 mo exposure and was progressively worse after longer exposure. The condition was characterized by large fibrotic areas in the parenchyma (Figure 7.7), which occasionally involved the major portion of some lung lobes. Pleural thickening due to fibrosis was consistently severe in dogs exposed to radon daughters and uranium ore dust. It was visible at gross examination as gray-white "scars," many of which appeared to be umbilicated and were depressed. Small subpleural pulmonary arteries, especially in the areas of marked pleural and septal fibrosis, were frequently partially or completely occluded. The occlusion was considered a result of fibrosis of arterial walls and intimal hyperplasia. The arterial lesion was present, to a greater or lesser degree, in nearly all dogs of the two groups that were exposed to radon daughters and uranium ore dust for periods longer than 40 mo.

Further detailed histopathologic and ultrastructural studies are in progress to determine the pathogenesis of these lethal degenerative pulmonary diseases and to correlate pathologic changes with altered respiratory patterns. This research will provide cause-and-effect data upon which to base realistic exposure standards for uranium mine air contaminants.

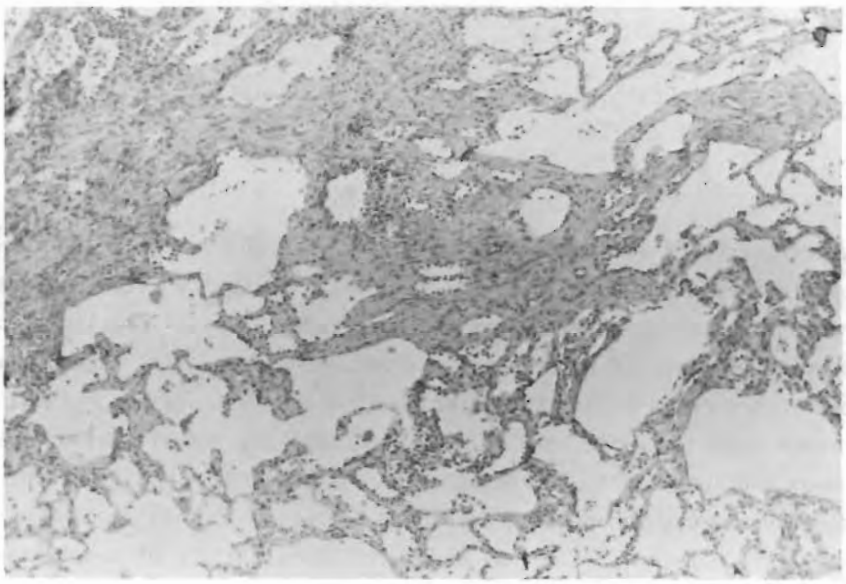

FIGURE 7.7. Example of Alveolar Septal Fibrosis Found in Dogs of Groups 1 and 2. H&E. 60X.

COMPARATIVE TOXICITY IN RATS VS. HAMSTERS OF INHALED RADON DAUGHTERS WITH AND WITHOUT URANIUM ORE DUST

Investigators:

J. C. Gaven, R. F. Palmer, K. E. McDonald, J. E. Lund and B. O. Stuart

Technical Assistance:

H. D. Steele

Simultaneous exposures of rats and hamsters to inhaled radon daughters, with and without uranium ore dust, were performed daily for five months. Pulmonary pathology developing in 6 to 13 mo after cessation of daily exposures included interstitial fibrosis, emphysema, epithelial hyperplasia, squamous metaplasia, and malignant neoplasia. Rats showed a greater variety and more severe response to these uranium mine inhalation exposures than did hamsters. Inhalation of radon daughters with uranium ore dust displayed the site of greatest damage, including squamous carcinoma, from the nasopharynx to the lungs. Sixty percent of the rats exposed to radon daughters with ore dust developed primary pulmonary carcinomas, providing an appropriate short-term experimental animal model for investigation of respiratory tract carcinogenesis in uranium miners.

Groups of 32 rats and 34 hamsters were exposed simultaneously in spherical chambers for periods of 84 hr per week to aerosols consisting of radon daughters or radon daughters attached to uranium ore dust. Radon daughter concentrations were approximately 1200 Working Levels (WL) with and without 15 mg/m^3 of carnotite uranium ore dust. Parallel groups of control animals were housed in identical cages and chambers, and were exposed to room air only. Exposures were continued for 5 mo, after which all groups were held for life-span observation. Mortality and body weight were recorded periodically throughout the experiment. Figures 7.8 and 7.9 show the effects of the exposures on animal body weights for rats and hamsters, respectively. Body weight means for rats exposed to radon daughters alone compared to mean weights of rats exposed to radon daughters with uranium ore dust were not significantly different, but both were different from controls. Mean body weight values for control versus experimental groups of hamsters did not differ significantly throughout the course of the experiment.

Figures 7.10 and 7.11 show the mortality patterns for rats and hamsters, respectively. Paralleling the lack of effect of exposures upon body weights in hamsters, there is little effect of either exposure protocol upon mortality patterns in hamsters. However, in rats there were significantly reduced survival times in experimental groups compared to controls. Eleven rats in the control group remain alive at the present time.

Histopathologic studies of animals sacrificed when moribund have revealed differences in pathologic changes when comparing hamsters with rats exposed either

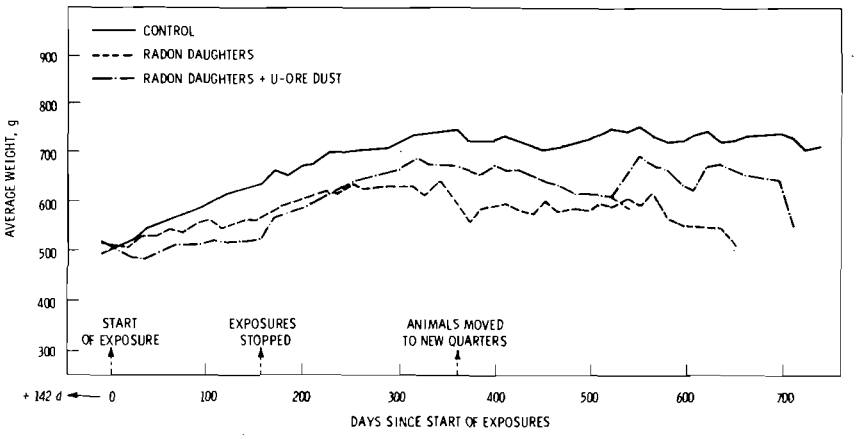

FIGURE 7.8. Weights of Rats Exposed to Radon Daughters With and Without Concomitant Uranium Ore Dust

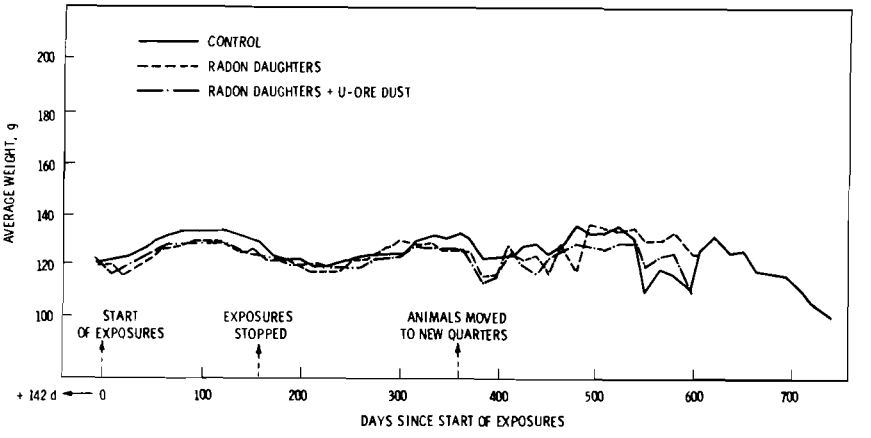

FIGURE 7.9. Weights of Hamsters Exposed to Radon Daughters With and Without Concomitant Uranium Ore Dust

to radon daughters alone or to radon daughters with uranium ore dust.

Hamsters exposed to radon daughters alone showed a variety of lesions in the nasal pharynx. They all showed some degree of squamous metaplasia of the epithelium, ranging from slight through moderate to severe progression with keratin formation. Several animals showed significant hyperplasia of the nasal epithelium. Eleven months after the cessation of daily exposures, one animal of the 34 developed squamous carcinoma of the nasal epithelium (Figure 7.12). Generally, the tracheal and laryngeal tissues of these animals appeared normal, with only one case of slight epithelial hyperplasia. The lungs showed slight to very slight bronchiolization of alveolar epithelium, and approximately 50% of the animals showed a slight degree of radiation pneumonitis.

Sprague-Dawley SPF rats exposed in the same chambers for the same period of time to radon daughters alone also showed a variety of lesions in the nasal passages. All animals showed some degree of squamous metaplasia in the nasal epithelium, generally to a greater degree of severity than seen in identically exposed hamsters. This metaplasia appeared in degrees varying from slight to severe in all of the rats so exposed. Many of the moderate or more severe cases also showed keratinization. Of the 32 rats exposed to radon daughters

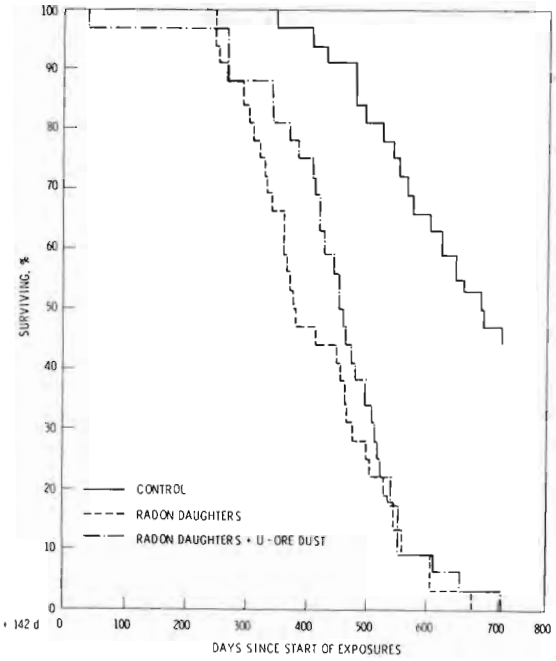

FIGURE 7.10. Mortality Patterns of Rats Exposed to Radon Daughters With and Without Concomitant Uranium Ore Dust

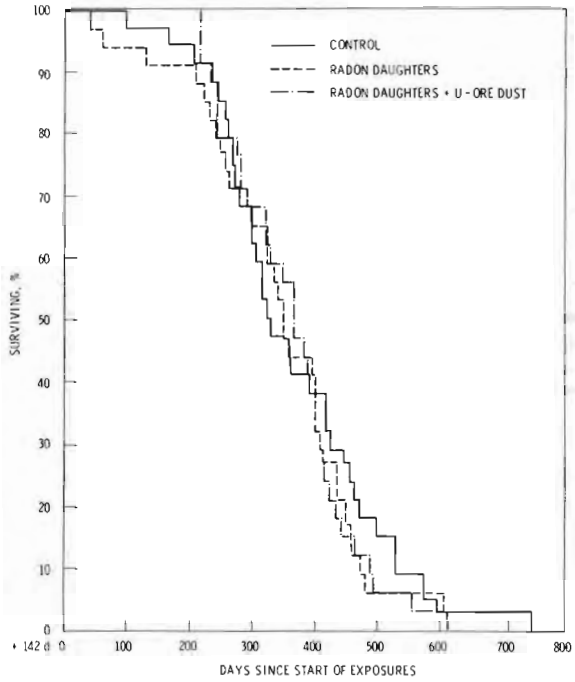

FIGURE 7.11. Mortality Patterns of Hamsters Exposed to Radon Daughters With and Without Concomitant Uranium Ore Dust

FIGURE 7.12. Squamous Carcinoma of the Nasal Epithelium of a Hamster Exposed to Radon Daughters Alone

alone, two developed squamous carcinoma of the nasal epithelium, with one appearing at 7 mo and the second appearing at 15 mo after cessation of the exposures. These animals also showed a greater degree of histopathologic change in the trachea than did hamsters, with five cases of very slight to moderate squamous metaplasia of tracheal epithelium. Two cases of marked squamous metaplasia with keratinization of the larynx were seen, and several cases of hyperplasia of the laryngeal epithelium appeared. The rats also showed a greater variety of changes in the lungs with a greater degree of severity, when compared to hamsters exposed in the same chamber. Slight to moderate radiation pneumonitis was present in approximately 50% of the animals. Almost all showed slight to moderate bronchiolization of alveolar epithelium. Approximately 30% showed a slight degree of adenomatosis with one case of marked adenomatosis and squamous metaplasia. Two cases of squamous carcinoma of the lung were observed at 7 mo after cessation of exposure and one case of bronchioloalveolar carcinoma plus squamous carcinoma appeared at 11 mo after exposure (Figure 7.13).

Both hamsters and rats exposed to radon daughters with uranium ore dust showed greater effects in the deep lung compared to their counterparts exposed to radon daughters alone. The nasopharyngeal epithelium of hamsters exposed to radon daughters with ore dust generally appeared normal, with perhaps 40% of the cases showing a very slight or slight degree of squamous metaplasia. All tracheal tissue appeared normal. The lungs of all hamsters exposed to radon daughters with uranium ore dust exhibited at least slight bronchiolization of alveolar epithelium, with moderate bronchiolization in 5 of the 34 animals in this group. Two cases of extensive fibrosis appeared, and there were several cases of emphysema and adenomatosis.

Rats exposed to radon daughters plus uranium ore dust showed nasal epithelial squamous metaplasia ranging from slight to moderate in all but six cases that appeared essentially normal. The tracheas of all animals showed essentially normal epithelium. However, 19 out of 32 rats exposed to radon daughters with ore dust developed frank carcinoma of the lungs, including 17 cases of squamous carcinoma (Figure 7.14), one adenocarcinoma (Figure 7.15) and one showing both squamous and adenocarcinomas. The majority of these appeared after 9 mo following the cessation of exposures.

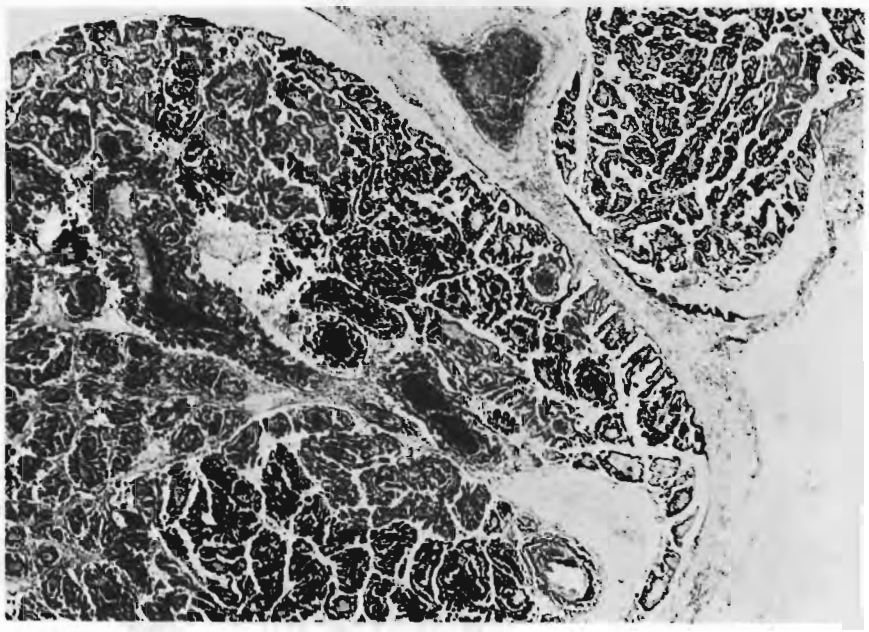

FIGURE 7.13. Bronchioloalveolar Carcinoma in a Rat Exposed to Radon Daughters Alone

Further experimental work in this study is designed to test the hypothesis that a shorter, more intense, exposure period to radon daughters with uranium ore dust may constitute a significantly greater risk of developing lung cancer than does a more protracted exposure at lower dose rates to accumulate the same total dose. If carcinogenic risk is related to dose rate, uranium miners who are currently exposed at lower dose rates under a fixed limit of total exposure dose will be subjected to a much different (and unknown) risk of developing lung cancer than were the early miners whose case histories were used to derive the present permissible air concentrations.

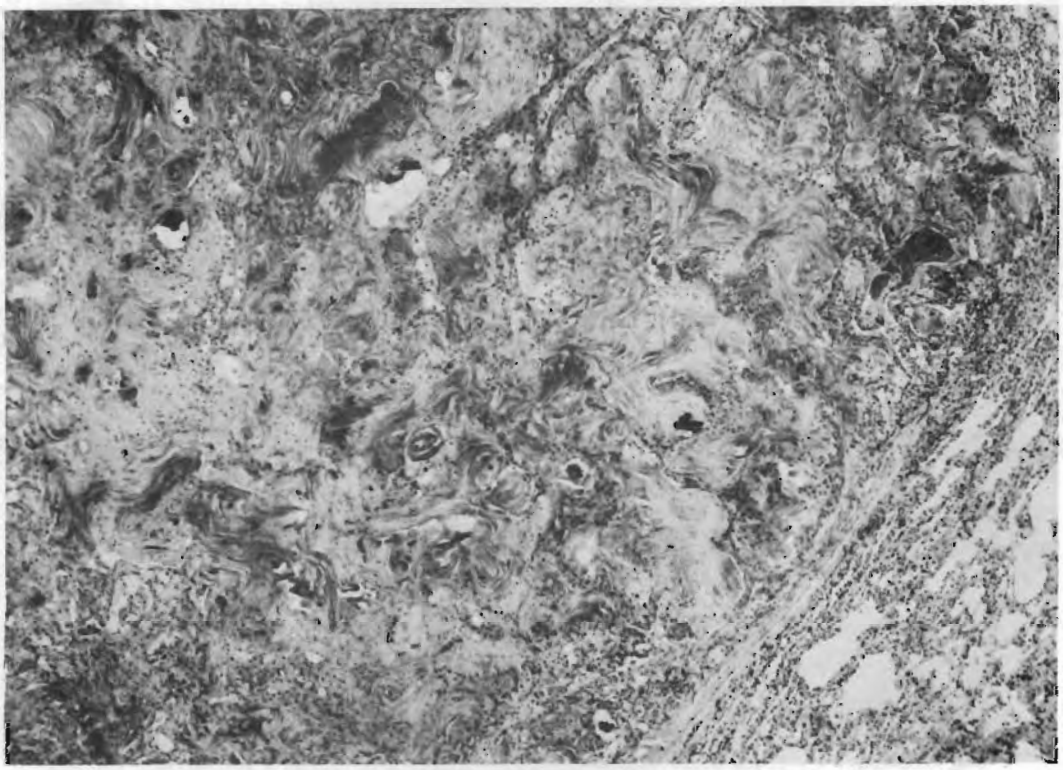

FIGURE 7.14. Squamous Carcinoma in the Lung of a Rat Exposed to Radon Daughters Plus Uranium Ore Dust

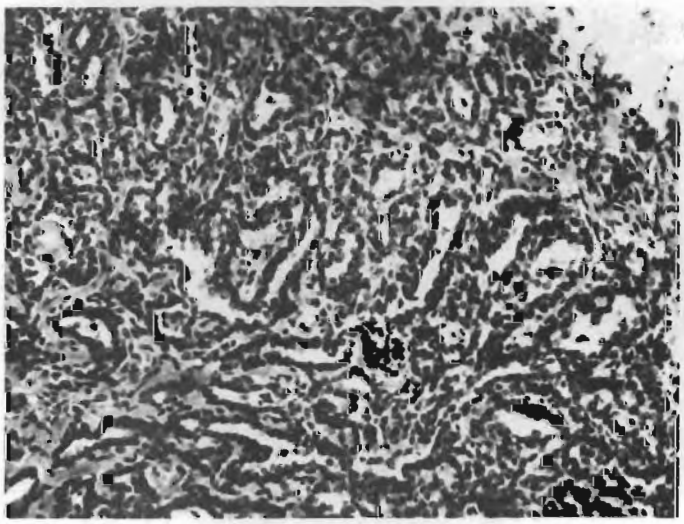

FIGURE 7.15. Adenocarcinoma in the Lung of a Rat Exposed to Radon Daughters Plus Uranium Ore Dust

EFFECTS OF CHRONIC CIGARETTE SMOKING ON PLATELET FUNCTIONS AND COAGULATION IN BEAGLE DOGS

Investigator:

H. A. Ragan

Technical Assistance:

M. J. Pipes, S. L. English, E. T. Edmerson, and M. C. Perkins

Coagulation and platelet function assays were performed in beagle dogs that had smoked ten cigarettes daily for 6 yr. There was no evidence of enhanced coagulation or detectable end-products of clotting in smoking dogs compared with age-related controls. Platelet reactivity was not increased, either as an acute or chronic effect of smoking, but rather a trend to reduced platelet activity was evident.

Previous Annual Reports have detailed the use of beagles to investigate the dose-effect and synergistic relationships which result in an increased incidence of lung tumors in uranium miners. A portion of the study included a group of dogs that had smoked ten cigarettes daily for 6 yr.

Studies in man have attempted to correlate changes in platelet function, coagulation, and serum lipids with the increased risk of ischemic heart disease in smokers. Results have, however, been inconsistent or conflicting. The present study was undertaken to determine if dogs maintained under strict housing and dietary control might manifest more consistent effects of smoking than those reported in humans.

For coagulation studies, a blood sample was collected in the morning after approximately 12 hr without smoking, and after fasting at least 8 hr. Each dog then smoked one cigarette, and 15 min later a second blood sample was obtained. Blood samples at times corresponding to those for the smokers were obtained from age-related control dogs.

Plasma nicotine levels 15 min after smoking one cigarette were 7.1 ± 3.8 µg/100 ml of plasma.

Results of adenosine diphosphate (ADP)-induced platelet aggregation are shown in Table 7.4. Using 2.0 µM ADP, there was a trend to increased slope and greater aggregation after one cigarette, but similar changes occurred in the control dogs. With 5.0 µM ADP, the slope and maximum aggregation were more pronounced in the smoking group before smoking than in the controls. Following one cigarette the slope tended to be flatter, but maximum response was greater than in the presmoking values. In the control dogs, the response slope was similar to the first sample, but a greater overall aggregation response was observed in the second sample. Changes in both groups with 10.0 µM ADP were similar to those obtained using 5.0 µM ADP.

Results of platelet adhesion assays indicate an effect similar to platelet aggregation studies (Table 7.5). The most pronounced differences were seen in Tube 1, in which there was greater mean adhesion in

TABLE 7.4. ADP-Induced Platelet Aggregation in Beagle Dogs (Mean ± SD)

	ADP (μM)	N	PRP PLATELETS x 10^3/mm^3 PRE-SMOKING	PRP PLATELETS x 10^3/mm^3 POST-SMOKING	SLOPE PRE-SMOKING	SLOPE POST-SMOKING	Δ OD PRE-SMOKING	Δ OD POST-SMOKING
	2.0							
SMOKERS		10	548 ± 80	545 ± 80	9.4 ± 4.4	11.5 ± 5.9	3.7 ± 2.9	4.9 ± 6.0
CONTROLS		10	426 ± 71	404 ± 68	9.7 ± 6.3	12.4 ± 3.9	3.9 ± 4.6	4.9 ± 4.9
	5.0							
SMOKERS		10	548 ± 80	545 ± 80	20.3 ± 7.1	17.3 ± 8.3	27.9 ±22.3	37.9 ± 29.0
CONTROLS		10	426 ± 71	404 ± 68	16.7 ± 4.1	17.8 ± 4.3	17.6 ± 7.3	24.6 ± 16.8
	10.0							
SMOKERS		10	548 ± 80	545 ± 80	30.1 ± 19.8	20.7 ± 7.4	50.5 ±26.0	56.7 ± 33.0
CONTROLS		10	426 ± 71	404 ± 68	20.9 ± 3.8	23.8 ± 4.2	50.3 ±21.8	53.9 ± 18.4

TABLE 7.5. Platelet Retention on Glass Beads in Beagle Dogs (%) (Mean ± 1 SD)

	N	TUBE 1 PRE-SMOKING	TUBE 1 POST-SMOKING	TUBE 2 PRE-SMOKING	TUBE 2 POST-SMOKING	TUBE 3 PRE-SMOKING	TUBE 3 POST-SMOKING
SMOKERS	10	81 ± 11	67 ± 23	91 ± 11	84 ± 24	97 ± 6	92 ± 19
CONTROLS	10	69 ± 15	57 ± 33	95 ± 4	85 ± 19	98 ± 2	92 ± 12

presmoking samples from the smoking group than from control dogs. After smoking one cigarette, there was a 17% decrease in platelet adhesiveness, but a comparable decrease occurred in the control dogs. Emotional stress is known to influence platelet function tests, and some of the effects observed on platelet aggregation and adhesion tests in these dogs may be attributed to this factor.

Russell's Viper Venom (Stypven) times with platelet-rich plasma were significantly longer ($P < 0.01$) after one cigarette than in the first sample (Table 7.6). However, no effect was seen on Stypven times when platelet-poor plasma was tested. This effect, again, is indicative of reduced platelet responsiveness after cigarette smoking.

No statistically significant differences between smokers and control dogs, or between the first and second samples of smokers, were evident on plasma prothrombin time, platelet count, euglobulin lysis time, ethanol gelation tests, fibrinogen concentration, or levels of fibrinogen degradation products (Table 7.7). The failure to find effects on these parameters is presumptive evidence that a hypercoagulable state has not been induced by smoking, and that intravascular clotting was not initiated.

Serum free fatty acid (FFA) levels before the start of daily smoking were significantly higher ($P < 0.01$) in the smoking group than in control dogs (Table 7.8). However, no additional effect was noted on FFA concentration after a single cigarette.

Serum glucose levels (Table 7.8) were not different between the two groups at the start of the day. However, there was a significant ($P < 0.05$) increase after one cigarette was smoked. A similar increase was present in a second sample from the control dogs, although it was not significantly different from the first sample. The change in glucose levels may be the result of stress.

From the results of these studies, it appears that in dogs there were no drastic changes attributable to cigarette smoking that could be detected by in vitro coagulation or platelet function assays. The minimal changes observed may be logically explained as being due to stress.

TABLE 7.6. Russell's Viper Venom Times in Beagle Dogs (Seconds) (Mean ± 1 SD)

	N	PLATELET-RICH PLASMA		PLATELET-POOR PLASMA	
		PRESMOKING	POSTSMOKING	PRESMOKING	POSTSMOKING
SMOKERS	10	10.0 ± 0.5	11.9 ± 0.8	11.1 ± 1.3	10.5 ± 1.0
CONTROLS	10	8.9 ± 1.1	10.9 ± 1.2	11.2 ± 1.5	11.4 ± 1.1

TABLE 7.7. Serum Free Fatty Acid and Glucose Levels in Beagle Dogs (Mean ± 1 SD)

	SMOKERS[a] N = 10		CONTROLS N = 10	
	PRESMOKING	POSTSMOKING	PRESMOKING	POSTSMOKING
PLATELET COUNT ($\times 10^3/mm^3$)	349 ± 59	293 ± 44	278 ± 87	249 ± 111
PROTHROMBIN TIME (sec)	7.7 ± 1.1	7.7 ± 1.1	8.0 ± 1.5	8.2 ± 1.4
EUGLOBULINLYSIS TIME (min)	40 ± 23	32 ± 16	45 ± 21	45 ± 20
FIBRINOGEN (mg/dl)	183 ± 89	195 ± 86	200 ± 47	283 ± 97
FDP (µg/ml)	< 2	< 2	< 2	< 2
ETHANOL GELATION (ppt)	--	--	--	--

[a] $P < 0.05$

TABLE 7.8. Some Coagulation Measurements in Beagle Dogs

	N	FREE FATTY ACID (mg/dl)		GLUCOSE (mg/dl)	
		PRESMOKING	POSTSMOKING	PRESMOKING	POSTSMOKING
SMOKERS	10	19.3 ± 5.8	17.6 ± 7.5	113.6 ± 11.1	125.8 ± 14.9
CONTROLS	10	12.1 ± 3.3	9.9 ± 3.4	110.5 ± 11.0	120.2 ± 11.4

• INHALATION HAZARDS TO COAL MINERS

Person in Charge: B. O. Stuart

This project provides data on the biologic behavior and effects of present and projected coal mine air contaminants, with particular emphasis on the etiology of the chronic respiratory disease, "coal workers' pneumoconiosis" (CWP). The use of diesel engines for coal handling in mines in order to avoid the disasters of fire, explosion and asphyxiation caused by arcing from the presently used electric engines is under intensive study. Our previous experiments have shown that chronic exposure of rodents to exhaust fumes from an inefficient, unscrubbed diesel engine can produce interstitial fibrosis, vesicular emphysema and bronchiolar epithelium. We are therefore studying the effects of such diesel exhaust in combination with other coal mine air contaminants.

The pathogenesis of CWP is being investigated in rats exposed 6 hr/day, 5 days/wk, for their lifetimes, to aerosols prepared from selected coals. Parallel groups are being similarly exposed to aerosols of coal dust plus diesel engine exhaust. Detailed organic and physicochemical analyses for specific gas-aerosol constituents (composition, particle size distribution, aerosol behavior) are carried out to correlate with the developing pathology, as observed in animals sacrificed at intervals during the course of the exposure. In the future we hope to initiate parallel studies using a representative well-tuned engine to assess comparative risks of respiratory disease under optimal conditions of future coal mine operation.

DAILY LIFE-SPAN EXPOSURE OF RODENTS TO COAL DUST AND DIESEL ENGINE EXHAUST

Investigators:

R. F. Palmer, B. O. Stuart and J. C. Gaven

Technical Assistance:

K. Mapstead

Four groups of rats are being exposed to high-CWP bituminous coal dust and/or diesel engine exhaust to study the pathogenesis of pneumoconiosis and pulmonary fibrosis and to correlate lung function changes with pulmonary pathology. The possibility of additional inhalation hazards associated with the proposed use of diesel engines in coal mines is being determined by daily exposure to exhaust from a diesel engine operating under appropriate load-cycling conditions.

This research will determine the biological behavior and effects of inhaled coal mine air contaminants, with particular emphasis on the pathology and changes in pulmonary function that may be related to the chronic respiratory disease known in man as "coal workers' pneumoconiosis" (CWP). This study will also investigate the possibility of increased risk of chronic respiratory diseases that may result from the proposed use of diesel engines in coal mines.

Bituminous coal mine dust, associated with high levels of CWP, is being tested via chronic inhalation exposures for its ability to induce pneumoconiosis, massive fibrosis and emphysema in the rat. Results of these studies will aid in determining the cause and progression of these diseases in coal mine workers, and will determine whether specific physiologic changes can be correlated with defined pulmonary pathology under carefully controlled exposure conditions. Pulmonary function tests in coal miners have shown reduced vital capacity, decreased dynamic compliance, and increased airway resistance. We have developed techniques for measuring respiration patterns, lung volume, dynamic and static compliance and airway resistance in large and small laboratory animals; these techniques will be used to compare functional changes with developing pathologic changes.

Two groups of 48 male rats are being exposed, 6 hr/day, 5 days/wk, to aerosols of high-CWP bituminous coal. Another group of 48 rats is similarly exposed to controlled levels of exhaust from an inefficiently operated diesel engine (simulating poor engine maintenance situations), in order to determine the risk associated with worst-case conditions of proposed coal haulage operations using diesel-powered equipment in mines. Another group of 48 rats is exposed to both diesel engine exhaust and coal dust, while a fifth group is exposed to room air only (Table 8.1).

The source of diesel engine exhaust is a 3-cylinder, 43-bhp engine driving a 15-kW generator connected to a series of resistance coils. To simulate typical operating

TABLE 8.1. Regimen for Rats Exposed to Coal Dust and Diesel Engine Exhaust

GROUP NO.	ANIMALS NO.	EXPOSURES (6hr/day, 5 days/wk)
1	48	DIESEL EXHAUST, 50 ± 5 ppm CO
2	48	DIESEL EXHAUST + 6 mg/m^3 COAL DUST
3	48	6 mg/m^3 COAL DUST
4	48	18 mg/m^3 COAL DUST
5	48	CONTROL

patterns of such engines in mines, a reversible motor is attached to the generator's voltage-controlling rheostat and a solenoid to the engine's governor, in order to vary both the load the engine is operating against and its speed. The control system is adjusted to provide the following speed-load cycle: The engine idles at 1300 rpm for 20 sec; accelerates to 1800 rpm with no load and holds for 20 sec; decelerates to 1500 rpm as a load of approximately 6 kW is applied, and holds there for 80 sec; accelerates to 1800 rpm as the load is removed; and then decelerates back to 1300 rpm to start the cycle again. During approximately half of each 4-min cycle the engine is accelerating or decelerating.

As shown schematically in Figure 8.1, a portion of the engine exhaust is diluted with compressed air, passed through a stainless-steel surge tank and an orifice meter, and is then divided into streams leading to the two exposure chambers. Just prior to entering the chambers, a controlled amount of compressed air is added to each exhaust stream through motorized needle valves. The level of "control air" for each

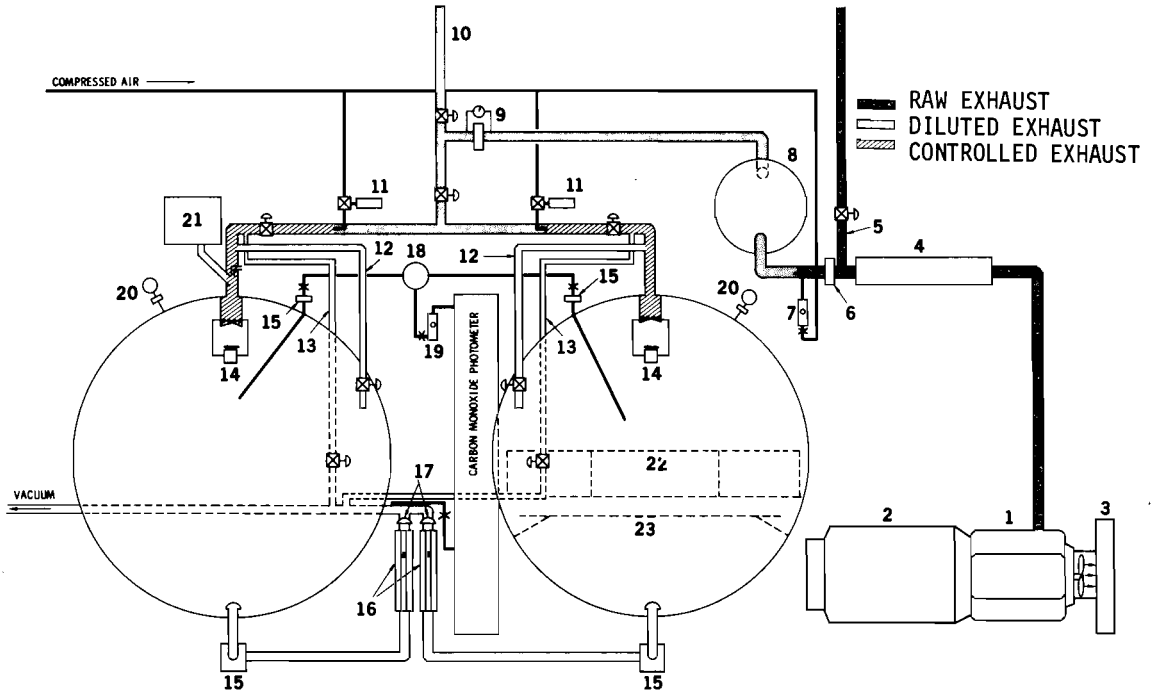

1 DIESEL ENGINE
2 25 kW GENERATOR
3 BANK OF RESISTANCE COILS
4 MUFFLER
5 PRIMARY EXHAUST OVERFLOW
6 ORIFICE
7 VALVED FLOW METER FOR PRIMARY DILUTION AIR
8 SURGE TANK
9 ORIFICE METER
10 SECONDARY EXHAUST OVERFLOW
11 MOTORIZED VALVES FOR CONTROL AIR (2)
12 PURGE LINES (2)
13 BYPASS LINES (2)
14 FANS (RHEOSTATED) (2)
15 FILTERS (4)
16 CHAMBER FLOW METERS (2)
17 VACUUM REGULATORS (2)
18 3-WAY SOLENOID VALVE
19 FLOW METER FOR CO PHOTOMETER
20 VACUUM GAUGES AND SWITCHES (2)
21 WRIGHT DUST MILL
22 SS WIRE MESH ANIMAL CAGES (6/CHAMBER)
23 SHELF FOR EXCRETION COLLECTION (2)

FIGURE 8.1. Diesel Exhaust Exposure System

exhaust stream is adjusted in response to the CO level in the chambers, as measured by an infrared photometer that samples each chamber during alternate 2-min periods.

The high-CWP bituminous coal dust used in these studies was obtained from an operating mine in Appalachia. It is introduced into the chambers via a Wright Dust Feed Mechanism, and has been shown to be 70-85% respirable under the exposure conditions that are maintained in the chambers.

Exposures were started in November of 1976, and no significant biological results have appeared to date.

• TOXICOLOGY OF TRITIUM AND KRYPTON

Person in Charge: J. E. Ballou

The scope of this project, first funded in FY 1976, has been revised to include only studies with krypton-85 gas, in response to recommendations by an ERDA Program Review Committee.

Krypton-85 is a major, long-lived ($T_{1/2}$ = 10.7 yr), radioactive gaseous effluent released during the dissolution of fuel elements in fuel reprocessing plants. The current practice of uncontrolled environmental release of megacurie amounts of krypton-85 is predicated on our understanding of the chemical and biological inertness of the noble gases and the magnitude of the dilution volume represented by the earth's atmosphere. The predicted contribution of the U.S. nuclear industry to the environmental level of krypton-85, although numerically large, is only a small fractional addition to the natural background radiation level. Although it seems clear that environmental krypton-85 will not constitute a radiation hazard of significance, this conclusion is largely based on physical rather than biological data. Studies with krypton-85 are, therefore, directed towards establishing the relative toxicity of the radionuclide, in animal experiments, in support of ERDA's desire to maintain credibility with a public that has emphasized its concern for a clean environment.

Two areas of research are included in this project: (1) studies involving the transfer kinetics and effect of krypton-85 in pregnant animals, and (2) studies involving chronic life-span exposure of rodents. These investigations are designed to provide information needed to estimate potential effects on the fetus (possibly the most sensitive part of the human population) and provide dose-effect data that can be compared with similar results from studies with other radionuclides, in order to establish the relative toxicity of krypton-85.

ACCUMULATION AND DISTRIBUTION OF ^{85}Kr IN RATS EXPOSED TO ^{85}Kr ATMOSPHERES

Investigators:

D. H. Willard and J. E. Ballou

Technical Assistance:

H. S. DeFord

Retention kinetics and tissue partition coefficients for ^{85}Kr were determined in rats exposed to known concentrations of ^{85}Kr gas. The tissue partition coefficients were used to calculate the relative tissue radiation dose, assuming exposure conditions equivalent to the maximum permissible concentration in air (MPC)a. The estimated radiation dose was highest in adrenals and body fat, about twice the dose estimated for the next highest tissue, ovaries. Saturation and desaturation curves show that the contents of the large intestines have a prolonged desaturation time compared to other samples analyzed.

Assessment of the hazard of radioactive gases has been based on radiation dose calulations, which were derived mostly from physical, rather than biological data. The present study is designed to obtain biological data needed to evaluate the hazard of ^{85}Kr in Wistar rats.

Male and female rats, weighing 400-500 g and 300-350 g, respectively, were exposed to ^{85}Kr atmospheres for 4 hr. Animals were sacrificed during and after exposure to determine the kinetics of saturation and desaturation with ^{85}Kr. Partition coefficients, defined as the ratio of ^{85}Kr activity per unit mass of tissue to the ^{85}Kr activity per unit volume of air (μCi/g:μCi/mℓ), were determined for 15 tissues and the intestinal contents. The values were used in estimating radiation dose at MPC exposure conditions.

The exposure chamber was an 18" x 19" x 20" plastic box designed to accommodate 12 to 24 rats housed in 7" x 9" x 5" stainless steel cages. The cages were constructed with expanded metal ends and bottoms to permit maximum contact with the gas atmosphere. Krypton-85 gas mixed with room air was pumped through the box and vented, along with diluting air, into the building exhaust stream before release to the environment. The chamber concentration ranged from 6 to 47 μCi ^{85}Kr/ℓ with 9 of the 13 exposures controlled at 17 μCi/ℓ.

Typical saturation-desaturation curves for several rat tissues are shown in Figure 9.1. The majority of tissues equilibrated quickly (within 2-3 hr) with the ^{85}Kr atmosphere. Body fat and the gastrointestinal tract were exceptions, requiring nearly 4 hr before equilibrium was attained. The desaturation curves (^{85}Kr concentration after exposure ceased) are somewhat surprising, since tissues such as the GI tract, which equilibrated slowly, desaturated quite rapidly. The adrenals, on the other hand, became saturated fairly quickly with ^{85}Kr but retained the radionuclide for relatively long periods

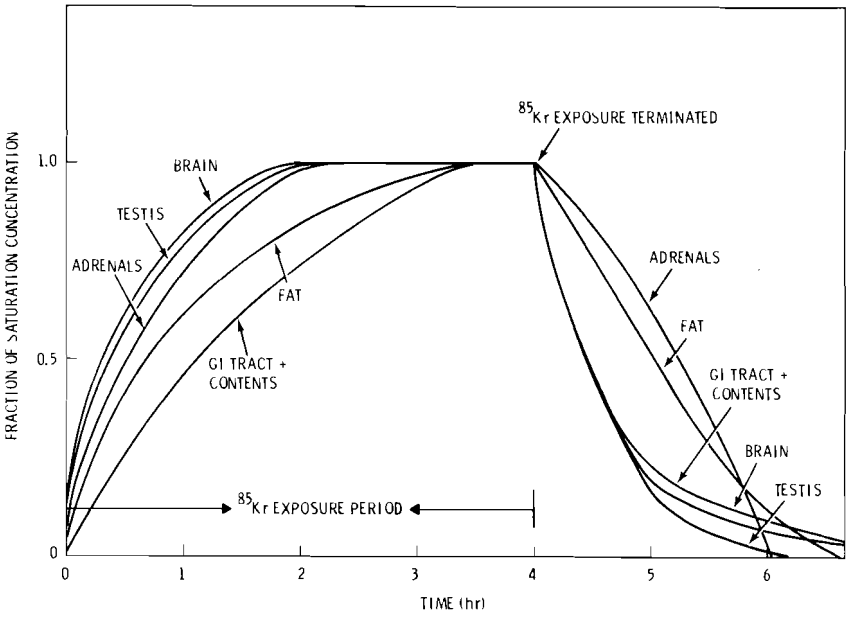

FIGURE 9.1. Tissue Saturation-Desaturation Curves for ^{85}Kr Exposure

of time. The retention of ^{85}Kr in adrenals appears to be related to their high fat content as has been suggested by others. Retention of ^{85}Kr in the gastrointestinal tract was found to vary widely for no apparent reason. Examination of individual gut segments and their contents (Figure 9.2) showed that the contents of the large intestine contained uniquely large amounts of ^{85}Kr, and retained ^{85}Kr at least as well as did fat. The amount of ^{85}Kr in large-intestine contents appeared to be related to the amount of food present, and was particularly elevated when gas bubbles were present in the intestine. Starvation for 48 hr before exposure did not affect the ^{85}Kr concentration in gut tissues. Sterilization of the intestine with antibiotic drugs did not affect the amount of ^{85}Kr associated with tissues or contents of the large intestine. It was concluded that this affinity for ^{85}Kr was not related to the action of the intestinal flora nor associated with the intestinal mucosal layer that was at least partially removed on stripping the gut to obtain the contents. The ^{85}Kr level in the gut could be markedly increased by injecting air into the gut lumen; air blebs injected subcutaneously were observed to concentrate the gas in a similar manner. Corn oil, glycerine and 0.9% saline injected into the gut lumen concentrated ^{85}Kr to a lesser extent than did a bolus of air. The affinity of ^{85}Kr for air spaces in the gut is apparently related to the relatively low solubility of the gas in tissues as compared to an essentially infinite solubility in air.

The equilibration curves shown in Figure 9.3 were obtained by sacrificing rats during the course of exposure. Tissue and gas samples were analyzed by scintillation counting techniques. The equilibrium concentration was taken as the peak concentration attained during the 4-hr exposure to ^{85}Kr. Radiation dose was calculated for (MPC)a conditions (3×10^{-7} μCi ^{85}Kr/ml), assuming the partition coefficients determined experimentally were valid for the much lower MPC concentrations. Thus the tissue concentration expressed as μCi/g at MPC conditions was just the partition coefficient multiplied by 3×10^{-7}. The radiation dose calculation was further simplified by assuming the significant tissue dose was due to beta radiation with $\bar{E}$ = 0.224 MeV. The tissue partition coefficients and estimated accumulated radiation dose after 1-yr exposure to MPC conditions are listed in Table 9.1. The results are in agreement with other published data for other species. The values are averages for both male and female rats since no sex differences were noted. Tissues with high fat content received the highest radiation dose as would be predicted from other studies. The value for ovaries is among the highest; however, only a iimited number of animals were analyzed; we are

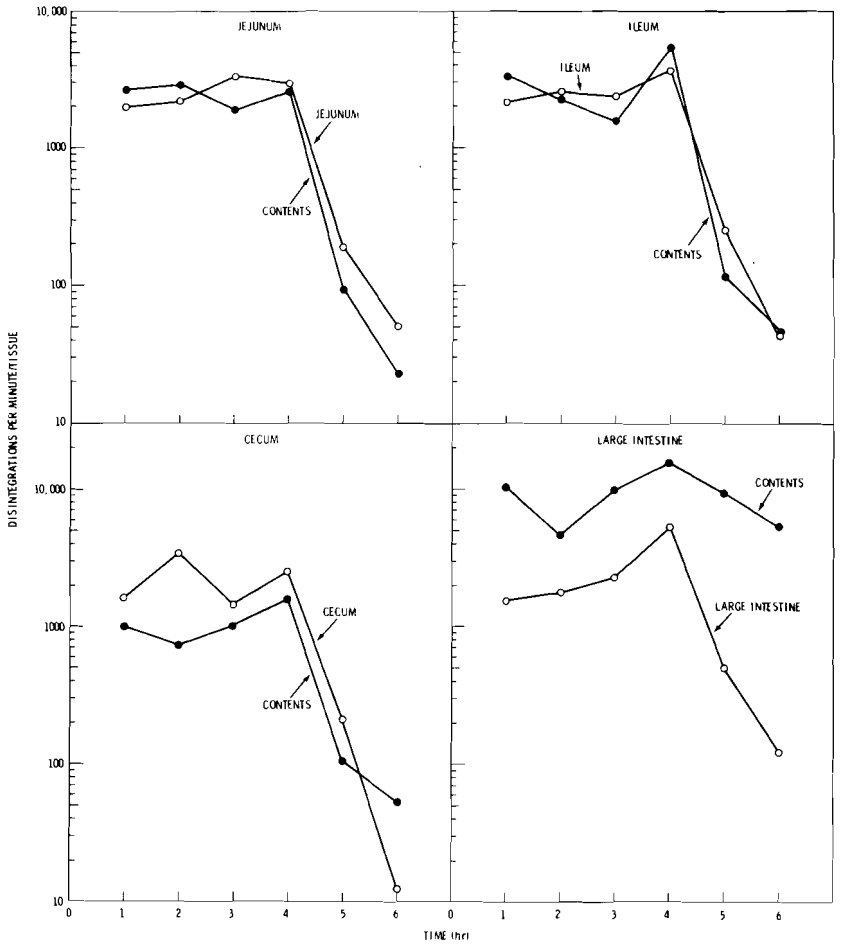

FIGURE 9.2. Saturation-Desaturation Curves for ^{85}Kr in Intestinal Tissues and Contents

investigating this further. The tendency for ^{85}Kr to accumulate in the contents of the large intestine results in a nearly two-times larger radiation dose to the contents than to the intestinal tissue per se. Approximately one-fourth the radiation dose to gut contents will reach the lining cells of the intestinal lumen, thus contributing significantly to the estimated dose to intestine.

Partition coefficients for major organs in juvenile rats (1 to 21 days of age) were not significantly different from the adult.

It is noteworthy that the predicted radiation doses (assuming exposure to MPC concentration) are negligibly small when one considers only the tissue content of ^{85}Kr. The dose to lung is misleading, in this case, since only 7% of the estimated total dose is derived from ^{85}Kr "bound" in tissue, while the remainder is delivered by ^{85}Kr in the lung air. A similar situation holds for pelt: if one assumes infinite beta geometry, the internal dose is a negligible fraction of the dose estimated for skin surfaces. The biological significance of the estimated skin dose is subject to question because of the limited range of the beta radiation, the shielding influence of hair and of cages, and the lack of conformity to the requirements of infinite beta geometry.

The data in Table 9.1 are useful in suggesting dose levels for long-term chronic exposure studies with ^{85}Kr. Assuming these dose estimates are predictive of biological effectiveness, a reasonable tumorigenic dose to lung would require exposure concentrations on the order of 10^4 to 10^5 times the MPC. A skin surface dose of 16.5 to 165 rads per day would be predicted for these exposure levels.

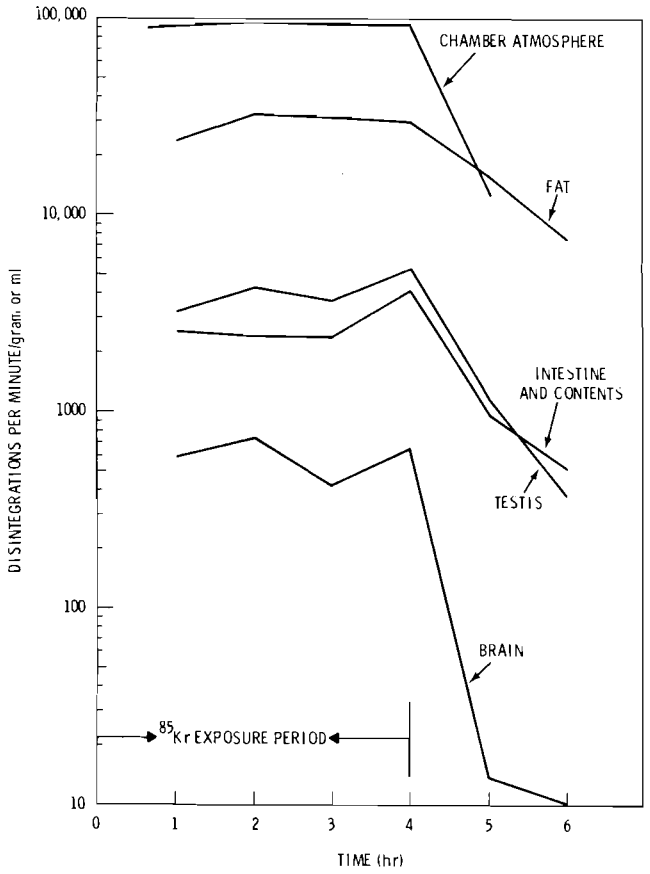

FIGURE 9.3. Saturation-Desaturation Curves for Rats Exposed to ^{85}Kr Atmospheres

TABLE 9.1. Partition Coefficients and Dose Estimates for Rats Exposed to ^{85}Kr Atmospheres

	NUMBER OF RATS	PARTITION COEFFICIENT ± SD	DOSE AT MPCa (UNRESTRICTED) (μ rad/year)
ADRENALS	12	0.372 ± 0.269	467
FAT	17	0.346 ± 0.046	434
OVARIES	4	0.176 ± 0.078	221
PELT	17	0.154 ± 0.034	193
LUNGS	15	0.074 ± 0.027	93
TESTIS	8	0.050 ± 0.007	62
MUSCLE	11	0.046 ± 0.016	58
KIDNEYS	13	0.042 ± 0.008	58
SPLEEN	11	0.034 ± 0.009	43
LIVER	15	0.022 ± 0.004	28
BONE	11	0.015 ± 0.004	19
HEART	13	0.012 ± 0.007	15
BRAIN	12	0.007 ± 0.002	9
LARGE INTESTINE CONTENTS	12	0.138 ± 0.032	173
JEJUNUM CONTENTS	12	0.085 ± 0.068	107
LARGE INTESTINE	17	0.081 ± 0.042	102
CECUM	15	0.058 ± 0.033	73
STOMACH CONTENTS	12	0.054 ± 0.018	68
ILEUM	17	0.050 ± 0.023	63
ILEUM CONTENTS	12	0.050 ± 0.030	63
JEJUNUM	17	0.047 ± 0.014	59
STOMACH	15	0.038 ± 0.009	48
DUODENUM	17	0.036 ± 0.031	45
DUODENUM CONTENTS	10	0.030 ± 0.015	38
CECUM CONTENTS	12	0.028 ± 0.017	35

RETENTION OF ^{85}Kr IN THE RAT AND BEAGLE DOG

Investigators:

D. H. Willard and J. E. Ballou

Technical Assistance:

H. S. DeFord

Rats and dogs exposed to ^{85}Kr atmospheres retained ^{85}Kr with similar retention kinetics. Retention in both species could be described by two exponential functions: a short-lived component with half-life of 5-7 min, accounting for 40-45% of the activity; and a longer-lived component with half-life of 40-60 min, accounting for 55-60%. Administration of a tranquilizing drug, acetylpromazine, did not alter relative ^{85}Kr retention as a function of time in the beagle dog; however, total retention was decreased to about 1/20th the expected value, probably because of depressed respiratory function.

Preliminary studies (Annual Report, 1973) in rats and dogs exposed "nose-only" to ^{85}Kr-contaminated atmospheres showed retention half-times in general agreement with values reported by others for man and animals. Retention values for dogs treated with a tranquilizing drug (acetylpromazine) were approximately four times longer than normal. To confirm these findings, additional animals were exposed to ^{85}Kr and the retention of the radionuclide was measured by external counting techniques.

Rats were exposed in a plastic chamber, 18" x 19" x 20", through which the ^{85}Kr-contaminated atmosphere was passed before being exhausted to a laboratory hood. The rats were exposed for 2 to 4 hr to atmospheres containing 12 to 47 μCi ^{85}Kr/ℓ.

A recirculating system employing a mask and "nose-only" exposure was used for the dogs. The recirculating system was adjusted to maintain physiological conditions, i.e., oxygen was supplemented and respiratory moisture and carbon dioxide were removed by chemical adsorbents. The dogs were exposed to atmospheres containing 50 to 100 μCi/ℓ ^{85}Kr. Whole-body counting was carried out with four 6" NaI crystals assembled in an array that minimized the effect of animal position on the resultant count. In vivo counting was carried out with the dog placed inside a plastic tube (1/4" thick by 8" dia) which fit inside a 9" plastic tube that was interfaced with the four gamma detectors. The dog was first exposed for 1 hr to an atmosphere containing 50 μCi ^{85}Kr/ℓ. External counts were made as soon as possible and continued for 140 min. On the following day the same dog was administered 0.7 mg of acetylpromazine intravenously, 5 min before exposure to ^{85}Kr (1-hr exposure to 100 μCi/ℓ) and external counts were repeated.

Retention curves for ^{85}Kr in the rats and the young adult dogs are shown in Figure 9.4. Whole-body retention for these species was quite similar and could be described as the sum of two exponentials with half-lives of 5 to 7 min and 40 to 60 min, accounting for 40 to 45% and 55 to 60%, respectively, of the total ^{85}Kr activity.

Administration of the immobilizing drug, acetylpromazine, did not alter ^{85}Kr retention in the beagle dog as had been speculated in our earlier studies. The level of ^{85}Kr accumulated in the tranquilized dog was, however, a factor of 20 lower than expected based on results of the previous day's exposure of untranquilized dogs. It should be emphasized that the results for this exposure (Figure 9.4) have been adjusted to 1/10 the actual values for easier comparison of the retention curves. The ^{85}Kr exposure concentration was 1/2 that administered to the tranquilized animal. Severe respiratory distress, which followed drug treatment, and experimental difficulties with the comatose animal probably account for the lower deposition values. This study will be extended to include animals of more comparable age to the 11 year-old dog employed in earlier studies. Since body fat is a major reservoir of ^{85}Kr retention, it is conceivable that the tendency for older animals to be less active and accumulate more fat may account for the comparatively long (270-min half-life) retention of ^{85}Kr observed in the older dog.

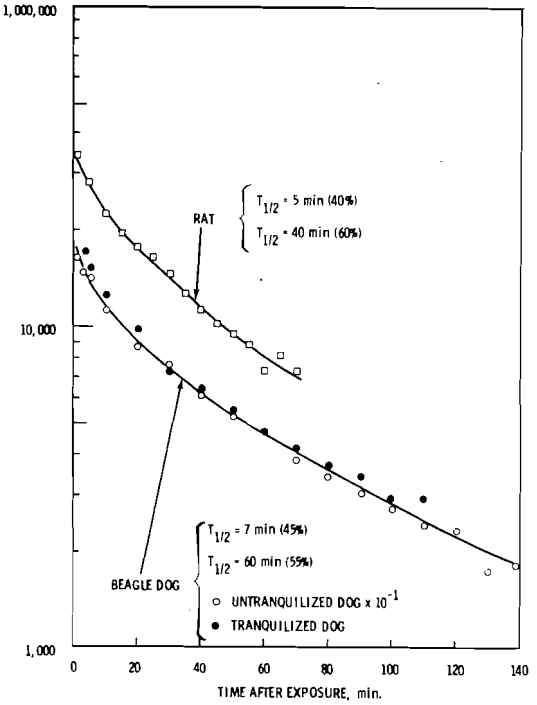

FIGURE 9.4. Total Body Retention of ^{85}Kr in Rats and Dogs

DISPOSITION OF ^{85}Kr IN GRAVID RATS

Investigators:

F. D. Andrew, M. R. Sikov, and D. H. Willard

Technical Assistance:

J. O. Hess, L. F. Haug, and H. S. DeFord

Pregnant rats were exposed to ^{85}Kr for 4-6 hr and sacrificed immediately thereafter. The ^{85}Kr concentration in the fetoplacental unit (FPU) was approximately the same at all gestation stages for intact FPU, isolated fetuses or fetal segments, as well as placentas and associated membranes. Maternal tissue concentrations varied over a wide range and only liver and intestine concentrations were relatively similar in both 20-day-gestation (dg) fetuses and adults.

There is concern about the effects on neonates of prolonged exposure to ^{85}Kr during pregnancy. Experiments with inhaled ^{85}Kr in gravid rats are in progress to establish dosimetry for design of effect studies.

In the initial experiment 12 pregnant Wistar rats at either 10, 15, or 20 dg were exposed to 37 $\mu Ci/\ell$ ^{85}Kr in air for 4-6 hr. They were killed by cervical dislocation and the trachea was clamped within 3 min after removal from the exposure chamber. A blood sample was collected from each animal immediately after sacrifice, and the gravid uterus was removed. Samples of uterus, intact FPU and isolated FPU components as well as several maternal tissues were removed and transferred immediately to prefilled and tared scintillation vials for beta counting and sample weight determination.

At 10 and 15 dg (four and five litters, respectively) intact FPUs and their associated uteri were analyzed separately (four each per litter) (Table 9.2). Two intact FPUs per litter, not separated from the surrounding uterus, were also measured at 10 dg. At 15 dg, four additional FPUs per litter were separated into two components for individual analysis: isolated fetuses and placentas plus adherent membranes. Two 20-dg fetuses from each of three litters were separated into four portions (head, thorax, abdomen and limbs) for analysis. The ^{85}Kr levels in representative organs from four additional fetuses per litter were also measured.

TABLE 9.2. ^{85}Kr Concentration in FPU [dpm/g x^{-10^3}, mean ± SD (N)].

ORGAN	DAY OF GESTATION WHEN ANALYZED		
	10	15	20
INTACT FPU	2.6 ± 0.9 (12)	2.3 ± 0.3 (11)	--
PLACENTA, ETC	--	1.8 ± 0.3 (16)	2.5 ± 0.6 (10)
ISOLATED FETUS-			
WHOLE	--	2.1 ± 0.2 (15)	--
HEAD	--	--	2.7 ± 0.6 (5)
THORAX	--	--	2.5 ± 0.6 (6)
ABDOMEN	--	--	2.7 ± 0.4 (3)
LIMBS	--	--	1.9 ± 0.6 (6)

The ^{85}Kr concentrations in the liver and intestine of 20-dg fetuses were similar to those in adults (Table 9.3). Values for fetal brown fat and thymus were much lower than for the same adult tissues. Blood values were much higher in fetuses than adults; the adult values are unexpectedly low, however. Concentrations in adult skeletal muscle taken from the suprascapular region were much greater than from the diaphragm, while suprascapular fetal muscle values were intermediate, lying between these extremes. Samples of suprascapular muscle in both fetuses and adults, however, may have been contaminated with brown fat. Adult fat levels from various regions had the highest ^{85}Kr levels while the lowest levels were seen in muscle, as has been reported for adult rats and guinea pigs. As seen in sheep studies presented elsewhere in this Annual Report, there were some marked variations in data for most sample types, presumably due to leaking scintillation vials or premature loss of ^{85}Kr from the tissues. Efforts are being made to alleviate this technical problem.

These results (Table 9.2 and 9.3) suggest that ^{85}Kr readily crosses the rat lung and equilibrates with maternal blood and tissues as well as with the FPU. The mean value for rat FPU of 2400 dpm/g, resulting from exposure of the dam to 37 $\mu Ci/\ell$, corresponds to levels of about 0.0011 $\mu Ci/g$. Future studies will investigate the limits of ^{85}Kr disposition of adult rats and their more radiosensitive FPU at different gestational stages. The present results and those from future studies should provide relevant radiation dose estimates for evaluating the effects of ^{85}Kr exposures during pregnancy.

TABLE 9.3. ^{85}Kr Concentration in Fetal and Adult Tissues [dpm/g $x\text{-}10^3$ mean ± SD (N)]

TISSUE	FETAL (DG 20)	ADULT
MESENTERIC FAT	--	26.0 ± 3.0 (8)
SUBCUTANEOUS FAT	--	25.2 ± 5.2 (5)
BROWN FAT[a]	3.3 ± 1.2 (12)	19.3 ± 5.4 (7)
SKELETAL MUSCLE[a]	1.4 ± 0.6 (11)	5.0 ± 3.1 (3)
SKELETAL MUSCLE	--	0.6 ± 0.1 (6)[f]
THYMUS	1.1 ± 0.8 (11)	2.5 ± 1.2 (10)
LIVER	2.6 ± 0.5 (7)	2.0 ± 0.4 (6)
INTESTINE	2.1 ± 0.3 (9)[b]	1.9 ± 1.6 (10)[c]
UTERUS	--	0.8 ± 0.2 (15)[d]
UTERUS	--	0.9 ± 0.3 (23)[e]
BLOOD	--	0.7 ± 0.2 (8)

[a] SUPRASCAPULAR
[b] ENTIRE
[c] LARGE
[d] DG 10
[e] DG 15
[f] DIAPHRAGMATIC

PRELIMINARY STUDIES IN SHEEP EXPOSED TO ^{85}Kr ATMOSPHERES

Investigators:

F. D. Andrew, D. H. Willard, J. E. Ballou, and M. R. Sikov

Technical Assistance:

J. O. Hess, R. F. Myers, and H. S. DeFord

Accumulation of ^{85}Kr in arterial blood of sheep occurs within 10 min of inhalation exposure initiation, and disappears by 30 min after exposure termination. As reported for other species, ^{85}Kr concentrations in fat were approximately 10 times those in other tissues.

Preliminary studies in nonpregnant adult ewes were performed to refine techniques and procedures for monitoring the tissue distribution and retention kinetics of ^{85}Kr. Following a 1- to 2-day postsurgical recuperation period, ewes were exposed to ^{85}Kr via a tracheostomy tube. Blood samples were collected for radioanalysis via arterial and/or venous catheters at intervals during the appropriate buildup, equilibration and clearance periods. In a subsequent exposure, animals were sacrificed under equilibrium conditions to provide tissue samples, which included major viscera and representative fat deposits. Krypton-85 concentrations in blood and other tissue samples were measured by liquid scintillation counting as soon as possible after removal from the animals.

Future studies will use pregnant animals at approximately 70, 95, or 120 days of gestation to evaluate the kinetics of ^{85}Kr exposure in the fetoplacental unit (FPU). At appropriate gestation stages calibrated catheters will be implanted in maternal and fetal blood vessels. Following a brief recovery period, pregnant ewes will be exposed to ^{85}Kr (25-50 μCi/ℓ) via a face mask or tracheostomy for 2-4 hr and blood samples will be obtained as before. Measurements will be made of the kinetics of cross-placental transfer of inhaled ^{85}Kr from initial exposure until equilibration, and of ^{85}Kr removal from blood after cessation of exposure. Maternal and fetal tissues will again be taken for radioanalysis following subsequent exposures.

Figure 9.5 presents data from five 4- or 5-hr exposures of three nonpregnant adult ewes, using 3-24 μCi/ℓ ^{85}Kr concentration. Arterial blood levels of ^{85}Kr reached about 90% of equilibrium levels within 30-60 min after initiation of exposure and arterial-venous equilibrium conditions were achieved within the first 60-90 min of inhalation, depending upon the exposure conditions. Following termination of ^{85}Kr exposure, arterial blood levels dropped to 4-17% of the final exposure value by 30 min, and venous levels were 7-10% of their final exposure level by 60 min. In these preliminary studies, arterial and venous levels varied considerably during the "equilibrium period" demonstrating both inter- and intra-animal variations. However, when the data were adjusted for exposure concentration, the mean arterial-venous differences were 8-16 dpm/ml. The question of whether variations in ^{85}Kr kinetics, respiratory physiology or sample processing may account for these differences is under consideration.

Tissue levels were measured in single animals after 4-hr exposures to ^{85}Kr levels of 16 or 24 μCi/ℓ. Concentrations in body fat samples from various locations were significantly higher than in any of the other tissues studied. At both exposure levels the order of ^{85}Kr concentration was: fat > adrenals > kidneys > intestine > muscle > liver > bone. Thus, the relative ^{85}Kr tissue concentrations in sheep are similar to those reported for rats and guinea pigs.

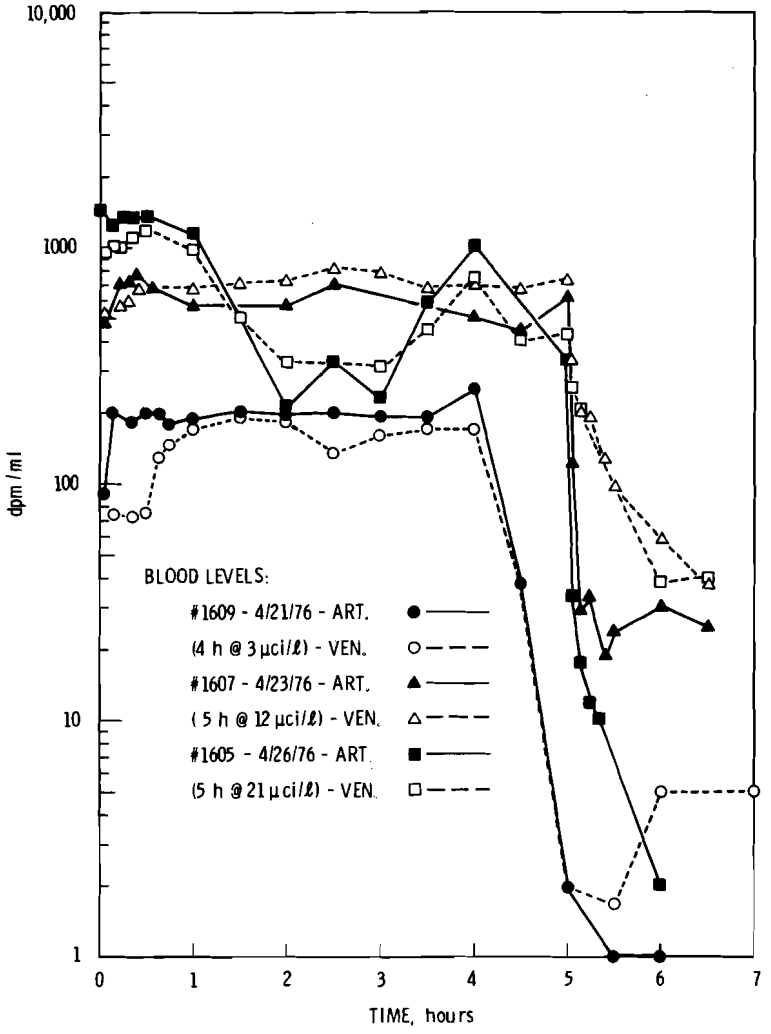

FIGURE 9.5. ^{85}Kr Blood Levels in Sheep

• TOXICOLOGY OF INHALED ACID AEROSOLS

Person in Charge: J. E. Ballou

This project was initiated in FY 1976. The major emphasis is two-fold: (1) to repeat earlier studies with inhaled 0.27 N HNO_3, which produced a 5% incidence of osteosarcomas in rats, and (2) to investigate the effects of multiple exposure to graded doses of common mineral acid aerosols (HNO_3, HCl and H_2SO_4) in the induction of latent biological effects. The dose ranges were established on the basis of short-term studies to determine the maximum tolerated dose, which was then employed as the highest of three dose levels for each acid aerosol. A clear dose-response relationship would establish acid aerosols as causative agents in the induction of bone tumors.

EXPOSURE OF RATS TO ACID AEROSOLS

Investigators:

J. E. Ballou, R. A. Gies, and F. G. Burton

Technical Assistance:

R. L. Music and D. H. Hunter

Rats were exposed to aerosols of nitric acid, hydrochloric acid, and sulfuric acid to determine the long-term biological effects. No effects other than the acutely toxic response to high levels of acid have been observed within 260 days postexposure.

Male Wistar rats, approximately 60 days of age, were administered aerosols of mineral acids (nitric, hydrochloric, and sulfuric) to determine long-term biological effects. The aerosols were generated with a nebulizer according to the protocol in Table 10.1. Unless otherwise indicated, the rats were exposed in individual cages in groups of 25 each, for 6 hr daily, on alternate weekdays, for a total of six exposures. Control rats were selected from each animal shipment and the treated controls were exposed in groups of five to a distilled water aerosol. One group of 62 rats was exposed to an aerosol generated from 0.27 N nitric acid using a Lovelace nebulizer. This was a repetition of an earlier study which showed a high incidence of bone tumors in rats exposed according to this protocol. Animal exposures are still in progress on this study. The rats will be held for life-span observation and histopathologic examination of late-developing lesions. The highest exposure levels in Table 10.1 approximate the maximum tolerated dose under our exposure conditions. The highest level of hydrochloric acid was acutely toxic (4% early mortality), producing skin lesions on the nose, ears and paws. The highest concentration of nitric acid (10 times TLV) produced transient respiratory distress after several exposures. Higher aerosol concentrations were lethal, causing swelling of laryngeal tissues and closure of the trachea. Sulfuric acid aerosols appeared to be well-tolerated even at concentrations three times higher than those of the other acids. This was observed even though the TLV for sulfuric acid is 5 to 7 times more restrictive.

The aerosol concentration and particle size distribution were determined by analyzing for acid anion in samples drawn from the chamber atmosphere. The analytical procedure employed specific ion electrodes which had a detection limit on the order of 0.1 μmole of the anion in 10 ml of solution. Chamber concentration was determined from the acid anion concentration in a series of three fritted glass bubbler traps filled with dilute sodium hydroxide or distilled water which scrubbed a known volume of chamber air. The aerosol particle size distribution was determined with a Mercer impactor using glass stages misted with sodium hydroxide to help prevent redistribution of the impacted acid aerosols. Values for particle size are of questionable accuracy because of the small amount of acid collected on the impactor stages and the limitations on the analytical technique mentioned earlier.

TABLE 10.1. Protocol for Acid Aerosol Exposures

AGENT	NUMBER OF RATS	CHAMBER CONCENTRATION		PARTICLE SIZE DISTRIBUTION[b]	
		mg/ℓ	FRACTION TLV[a]	MMAD, μm	GSD
NITRIC ACID	62[c]	0.034	7 ± 2	--	--
	50	0.049	10 ± 2	--	--
	50	0.018	3.5 ± 1.2	0.694	3.56
	50	0.013	2.6 ± 1.3	0.442	3.07
HYDROCHLORIC ACID	50	0.022	3 ± 1	1.808	3.89
	50	0.009	1.3 ± 0.6	1.361	4.06
	50	0.005	0.7 ± 0.4	1.132	4.09
SULFURIC ACID	50	0.156	156 ± 48	--	--
	50	0.023	22.6 ± 4	--	--
	50	IN PROGRESS		--	--
TREATED CONTROL	90				
NONTREATED CONTROL	45				

[a] TLV = THRESHOLD LIMIT VALUE, e.g. FOR NITRIC ACID IT IS 0.005 mg/ℓ, HYDROCHLORIC ACID, 0.007 mg/ℓ AND SULFURIC ACID, 0.001 mg/ℓ

[b] MMAD = MASS MEDIAN AERODYNAMIC DIAMETER; GSD = GEOMETRIC STANDARD DEVIATION

[c] THIS GROUP WAS EXPOSED (30 min, NOSE ONLY) TO 0.27N HNO_3 GENERATED WITH A LOVELACE NEBULIZER

This study has revealed a need for more sensitive analytical methods to detect low levels of acid aerosols simulating environmental contamination. Work is in progress to improve aerosol sampling techniques for particle size determination by modifying impactor collecting stages. The animals have not been on experiment long enough to exhibit the delayed effects of inhaled nitric acid (osteosarcomas) seen in an earlier study. The only overt effects of acid exposure seen to date have been acid burns on areas of exposed skin and two deaths due to hydrochloric acid inhalation.

• TOXICITY OF THORIUM CYCLE NUCLIDES

Person in Charge: J. E. Ballou

This project was first funded in FY 1976. The program was subsequently curtailed following recommendations of an ERDA Program Review Committee. Ongoing research is concentrated in two areas: (1) development of analytical techniques for ^{232}U decay product analyses, and (2) determination of the retention kinetics and long-term biological effects of inhaled ^{232}U and ^{233}U uranyl nitrate aerosols in rats. Studies with simulated thorium breeder fuel materials (mixed oxides of ^{232}Th, ^{233}U and ^{232}U) will be limited to short-term studies to characterize these materials prior to possible biological effects studies.

A principal objective of this research has been evaluation of the biological hazard of the high-specific-activity uranium isotopes. The studies have employed Wistar rats, an animal model used extensively in our laboratory in similar studies with a variety of radionuclides, including the transuranic elements. Comparative dose-response studies require accurate radioanalyses as a basis for radiation dose calculations. The determination of the ^{232}U decay series is a particularly challenging analytical problem since the series includes a dynamic system of several parent-daughter radionuclides, some with extremely short half-lives, several of which contribute significantly to the internal radiation dose. A knowledge of the steady state concentrations (not necessarily equilibrium concentrations) of decay products maintained in the living animal is required, since these concentrations may change after death as the decay series tends to establish parent-daughter equilibrium. Preliminary analytical results using Ge(Li) diode detectors have been encouraging since tissues can be analyzed directly without processing, and excellent resolution of low-energy (< 100 keV) X-rays and gamma photons is obtained. The number of samples that can be analyzed is limited, however, and only representative animals will be subjected to detailed analysis to establish and reconstruct the temporal relationship of the parent-daughter steady state concentrations. The radiation dose accumulated to the time of death will be estimated for each animal, based on an individual analysis of ^{232}U and ^{228}Th, and the reconstructed temporal relationship of the remaining members of the ^{232}U decay series during the animals' life spans. The dose-response relationship for inhaled ^{232}U will be compared with that of ^{233}U, and with similar results for ^{238}Pu, ^{239}Pu, and ^{253}Es, as a measure of the relative toxicity of high-specific-activity uranium.

EARLY DISPOSITION OF INHALED URANYL NITRATE (^{232}U and ^{233}U) IN RATS

Investigators:

J. E. Ballou and R. A. Gies

Technical Assistance:

R. L. Music

Uranyl nitrate (^{233}U) was retained mainly in lung, skeleton, pelt and kidney 60 days after inhalation exposure. The concentration in lung exceeded that in other tissues. Preliminary results with ^{232}U indicate retention in lung similar to that of ^{233}U, at total deposited mass levels of 0.1 μg or less.

Male Wistar rats, 60 days of age, were exposed to aerosols of ^{232}U and ^{233}U nitrate as shown in Table 11.1. Animals were sacrificed in groups of five immediately after exposure (to determine initial lung burden) and after 7, 30, 60, 100, 150, and 200 days to determine distribution and retention kinetics. Daily excreta were collected from the group sacrificed after 7 days. Rats were also held for life-span study of late-developing biological effects. The long-term animals are discussed in a separate report.

TABLE 11.1. Experimental Protocol and Aerosol Parameters

INITIAL LUNG BURDEN (nCi ± SD)		NUMBER OF RATS: PERIODIC SACRIFICE	NUMBER OF RATS: LATE EFFECTS STUDY	PARTICLE SIZE (μm)	GEOMETRIC SD	GENERATOR SOLUTION: CONC. (μCi / mℓ)	GENERATOR SOLUTION: % ULTRA FILTERABLE
$^{233}UO_2(NO_3)_2$	(ng)						
0.63 ± 0.2	66.2	35	65	0.48	1.71	0.80	94
10 ± 2	1050	35	65	0.99	1.95	7.65	95
36 ± 14	3759	35	65	2.12	2.19	84.4	98
$^{232}UO_2(NO_3)_2$							
0.74 ± 0.2	0.037	35	65	0.34	1.82	0.74	88[a]
5.85 ± 3	0.29	35	65	0.43	1.95	7.88	95
53 ± 14	2.5	35	65	0.36	2.24	71.0	94

[a] ULTRAFILTERABILITY DETERMINED 3 DAYS AFTER SAMPLE PREPARED; OTHER SAMPLES WERE ULTRAFILTERED WITHIN 4 HOURS OF PREPARATION.

The initial deposition and distribution of uranium following a 30-min, nose-only aerosol exposure is shown in Table 11.2. Results are shown only for ^{233}U; ^{232}U analyses are not yet completed. Initial deposition in the upper respiratory tract was significantly influenced by particle size, i.e., the larger particles were preferentially deposited in the upper airways and subsequently swallowed and transported to the stomach and jejunum. The percentage of the total amount deposited in other tissues, including the lung, was correspondingly less. The amount of ^{233}U translocated to tissues (liver and carcass) during the 30-min exposure was similar to that observed in rats exposed to nitrate solutions of the transuranic elements, including ^{241}Am, ^{253}Es, ^{239}Pu, and ^{238}Pu. The low value for translocation of ^{233}U after 0.63 nCi initial lung burden is thought to be an artifact related to the sensitivity of the analytical method rather than a true difference in metabolism.

Excretion of inhaled $^{233}UO_2(NO_3)_2$ is compared in Figure 11.1 with similar results for inhaled $^{239}Pu(NO_3)_4$. Fecal excretion is not noticeably different for the two radionuclides. This is to be expected since the major early clearance of inhaled materials involves physical processes, e.g., mucociliary clearance and ingestion, leading to clearance by way of the gastrointestinal tract. The large amounts of activity excreted during the early clearance phase would tend to obscure small differences in intestinal excretion, e.g., differences in biliary secretion that would be more readily observed at later times after exposure.

Urinary excretion of inhaled ^{233}U is clearly enhanced compared to ^{239}Pu. It does not follow, however, that the lung clearance of ^{233}U is greatly influenced by this excretory process, as will be discussed later. The excretion of ^{232}U, when data are available, will be of particular interest since the specific activity is orders-of-magnitude greater than either ^{233}U or ^{239}Pu.

The distribution and retention of ^{233}U in several tissues following initial deposition of from 2.86 to 510 nCi showed major sites of deposition in lung, skeleton, pelt, and kidney. After 60 days, retention in the lung and skeleton predominated, suggesting that the concentration in lung, and thus the accumulated radiation dose to lung, would exceed that in other tissues. The deposition in kidney, traditionally the organ of concern in uranium toxicity, does not appear to be the critical factor in the toxicity of high-specific-activity uranium.

The relative retention of inhaled uranium nitrate in major tissues is shown graphically in Figure 11.2. Uranium-233 retention is represented by results from the "medium" dose group (10 nCi ILB).

TABLE 11.2. Initial Disposition of $UO_2(NO_3)_2$ in the Rat.
(Values are average of five rats, expressed as % total deposition).

MEAN TOTAL INITIAL DEPOSITION (nCi)	2.86	71	510
UPPER RESPIRATORY TRACT			
TRACHEA	1.2	2.7	1.4
NOSE	2.6	2.6	5.4
TONGUE AND ESOPHAGUS	1.8	4.8	8.1
HEAD	6.8	9.8	8.6
STOMACH AND JEJUNUM	9.1	28.4	38.6
TOTAL	21.5	48.3	62.1
TRANSLOCATED TO TISSUES			
LIVER	0.11	0.59	0.24
RESIDUAL CARCASS	NONE DETECTED	3.9	3.2
TOTAL	0.11	4.49	3.44
RETAINED IN LUNG	22.2	14.1	7.0
RETAINED IN PELT	56.3	33.1	27.5

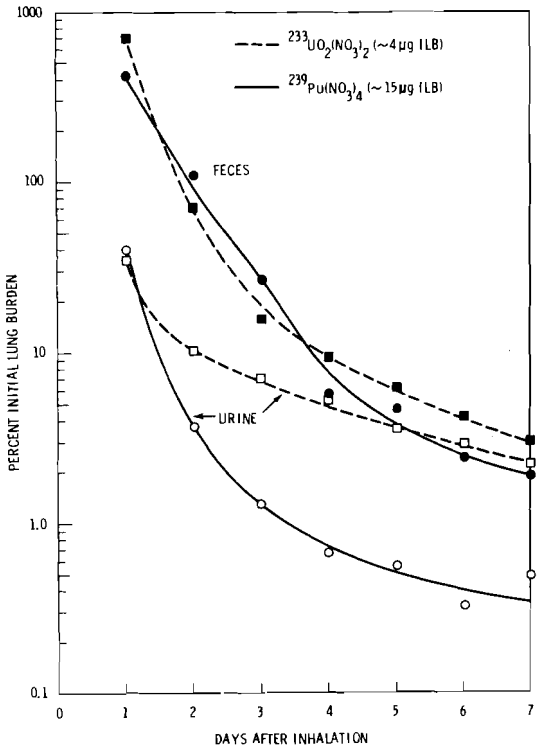

FIGURE 11.1. Daily Excretion of Uranium and Plutonium Inhaled as Nitrate Salts in 0.27 N Nitric Acid

Results for ^{232}U retention in the lung do not appear to differ greatly from those for ^{233}U. It is of further interest that pulmonary retention of ^{238}Pu and ^{239}Pu also agrees well with uranium retention at this early time after inhalation exposure. The results for lung retention are shown in more detail in Table 11.3. Uranium-232 clearance seems to agree reasonably well with the results for the lowest (0.63 nCi) lung burden of ^{233}U. This may indicate an influence of uranium mass on pulmonary clearance when >0.1 µg is deposited in the lung.

This study, which is still in progress, will elucidate the early clearance and disposition of ^{232}U and ^{233}U nitrate. This information, combined with radiochemical analyses of long-term animals, will permit the estimation of radiation dose accumulated in animals held for life-span study.

TABLE 11.3. Pulmonary Deposition and Retention of Inhaled Uranyl Nitrate

	INITIAL LUNG BURDEN (nCi)	% INITIAL LUNG BURDEN			
		7 DAYS	30 DAYS	60 DAYS	100 DAYS
$^{233}UO_2(NO_3)_2$	0.63	57	57	29	12
	10	40	27	15	8.5
	36	17	15	12	6.0
$^{232}UO_2(NO_3)_2$	0.74	45	37	--	--
	5.85	46	33	31	--
	53	64	58	--	18[a]

[a] VALUE FOR ONE RAT; OTHER VALUES ARE AVERAGE OF FIVE ANIMALS.

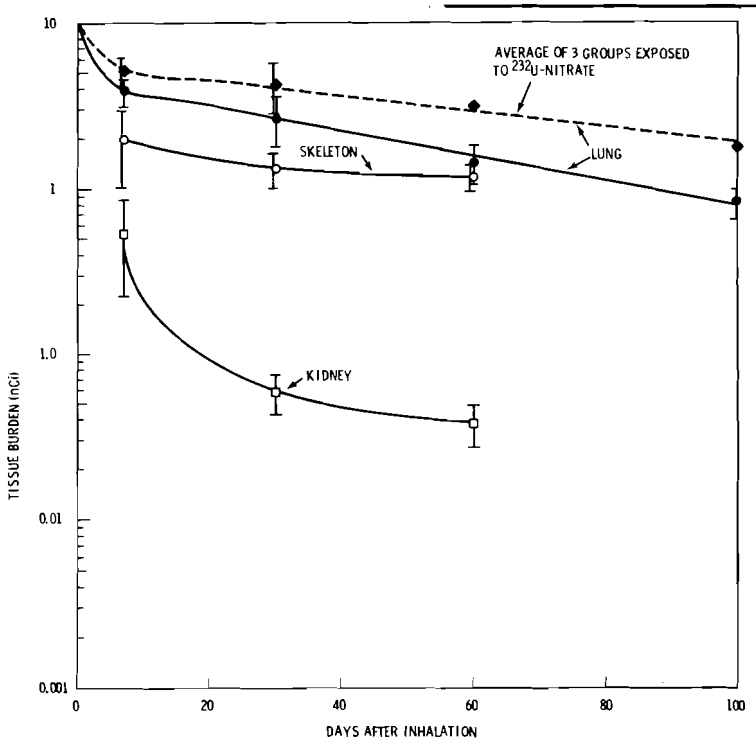

FIGURE 11.2. Retention of Inhaled ^{233}U-nitrate (10 nCi ILB) in Major Tissues

LONG-TERM EFFECTS OF INHALED URANYL NITRATE IN RATS

Investigators:

J. E. Ballou, R. A. Gies, and J. L. Ryan[(a)]

Technical Assistance:

R. L. Music

Rats were exposed to aerosols of ^{233}U and ^{232}U nitrate in a study of the long-term biological effects. Preliminary radiation dose estimates show lung > skeleton > kidney in each dose group.

Male Wistar rats were exposed to aerosols of $^{232}UO_2(NO_3)_2$ and $^{233}UO_2(NO_3)_2$ generated from 0.27 N nitric acid solution, using a Lovelace nebulizer. Animals were sacrificed to determine the early disposition of the radionuclides (reported elsewhere in this Annual Report) and the remaining rats will be held for life-observation of biologic effects. The animals are observed daily for signs of morbidity and are weighed at monthly intervals. Dead animals or animals sacrificed when moribund are radiographed and subjected to detailed necropsy and examination for pathologic lesions. Sections of eight tissues and all suspicious lesions are routinely sampled for histopathology. This is an ongoing study that has been in progress for 200 days and is expected to continue for approximately 3 yr.

The nitrate solutions of ^{232}U and ^{233}U were prepared for aerosolization by acid solubilization and purification on an ion exchange column. Special precautions were taken to prepare both isotopes in the same chemical and physical form. The metal oxides (3 mg ^{232}U and 1 g ^{233}U) were dissolved in a 95% concentrated HCl-5% concentrated HNO_3 mixture and the solution was passed through a Dowex 1X3 (50-100 mesh) resin column in Cl^- form, which absorbed the uranium. The column was washed with 12 M HCl until the gamma activity reached a very low level. The uranium was eluted as a bright yellow band with H_2O. The beta-gamma reading for the ^{232}U eluate was 1.5 mr/hr at the surface, compared to a prepurification reading of 4500 mr/hr at a distance of 1 in. The eluted uranium chloride was evaporated to dryness and resuspended in concentrated HNO_3 three times before final adjustment to volume in 2 M HNO_3. The final product is considered to be $UO_2(NO_3)_2$.

The exposure groups and estimated radiation dose to major tissues (based on preliminary distribution data) are listed in Table 11.4. The dose estimates for ^{232}U are minimum values since they do not include the contribution from the daughter products which will be born and decay in the animal during the life-span study. After 500 days, for example, the immediate product of ^{232}U decay (^{228}Th; $T_{1/2}$ = 1.91 yr; E_α = 5.4 MeV) will build up to 40% of the equilibrium level. The exact amount and retention kinetics of ^{228}Th in the animal will depend not only on the amount of parent ^{232}U present but also on the site of ^{232}U when ^{228}Th is produced. Thorium-228

(a) Chemical Technology Department

TABLE 11.4. Estimated Accumulated Radiation Dose to Rats Exposed to ^{232}U and ^{233}U Nitrate Aerosols

	INITIAL LUNG BURDEN (nCi)[a]	NO. RATS	ESTIMATED 500-DAY ACCUMULATED DOSE (rads) LUNG	SKELETON	KIDNEY
$^{233}UO_2(NO_3)_2$	0.63	65	2	0.5	0.1
	10	65	30	6	1.2
	36	65	100	20	4
$^{232}UO_2(NO_3)_2$	0.74	65	2	0.5	0.1
	5.85	65	18	4	1
	53	65	160	30	6
CONTROLS					
0.27N HNO_3		65			
NON-TREATED		45			

[a] DETERMINED AS THE AVERAGE OF 5 RAT LUNGS FROM ANIMALS SACRIFICED IMMEDIATELY AFTER THE 30-MIN NOSE-ONLY INHALATION EXPOSURE

produced in bone will be retained with different kinetics and exert a different biologic effect than ^{228}Th produced in the lung. A similar situation exists for the five alpha-emitting daughters produced by ^{228}Th decay, except that their short physical half-lives will assure equilibration during the long-term study. Again the amounts of individual decay products retained will be determined largely by metabolic factors. A detailed analysis of the individual radionuclides in representative animals will be obtained periodically during the course of the study. The pattern of distribution and retention of the daughter products will be used to refine the estimated dose calculations.

NONDESTRUCTIVE ANALYSIS FOR ^{232}U AND DECAY PROGENY IN ANIMAL TISSUES

Investigators:
J. E. Ballou and N. A. Wogman[a]
Technical Assistance:
R. A. Gies

Direct determination of ^{232}U and its decay products in animal tissues appears to be feasible using an intrinsic Ge(Li) diode detector (for energies of 5-100 keV) and a NaI(Tl) anticoincidence-shielded Ge(Li) diode for higher-energy gamma photons. The detection sensitivity for ^{232}U and ^{228}Th is 0.03 and 0.01 nCi, respectively, using a 300-min counting time.

A rapid, nondestructive, analytical technique is required to determine the mixed radionuclides in thorium fuel materials because of the probability of disequilibrium among the short-lived daughter products and the expense and time required for an exhaustive wet chemical analysis. Briefly, the mixture includes the decay series ^{232}U*, ^{228}Th*, ^{224}Ra*, ^{220}Rn*, ^{216}Po*, ^{212}Pb, ^{212}Bi*, ^{212}Po*, ^{208}Tl, and stable ^{208}Pb. The major

(a) Radiological Sciences

internal radiation dose is associated with the alpha-emitting radionuclides (indicated by asterisks), which should be determined quantitatively for accurate dosimetry. This paper reports preliminary results with two detector systems using germanium diodes: (1) an intrinsic germanium detector, employed to detect and differentiate low-energy X-rays and gamma photons, and (2) a NaI(Tl) anticoincidence-shielded germanium diode used to detect gamma photon energies > 100 keV. A typical spectrum for animal tissue analyzed by the intrinsic Ge(Li) detector is shown in Figure 11.3. Tissue samples were prepared by placing in the detector weighed amounts of raw tissue in screw-cap plastic counting vials. The detector system is a 400 mm^2 x 10 mm intrinsic germanium diode, having low background and high efficiency (10-30%) in the 5-100 keV energy range. Energy peaks below 20 keV in Figure 11.3 are a complex mixture of K and L X-rays from several radionuclides. Uranium-232 can be identified and quantitated (using a ^{232}U standard of the same geometry) by the photon peaks at 57.7 and 128.9 keV. Other energy peaks are identified with various daughter products as indicated. Higher-energy emissions (in excess of 100 keV) were detected with the NaI(Tl) anticoincidence-shielded germanium diode. This system permitted quantitation of ^{224}Ra, ^{220}Rn, and ^{208}Tl and verification of other analyses based on the low-energy emissions (^{212}Pb, ^{212}Bi, ^{228}Th). Energy peaks for the two Po isotopes (^{212}Po and ^{216}Po) have not yet been resolved; however, their short half-lives (fractions of seconds) make it possible to quantitate them on the assumption that they are in equilibrium with their immediate parents, ^{212}Bi and ^{220}Rn, respectively.

Table 11.5 shows results for ^{232}U analyses in lung tissue following inhalation of $^{232}UO_2(NO_3)_2$ aerosols. The animals were exposed to freshly separated ^{232}U, which then aged in the animal, i.e., the decay products of the ^{232}U series began to accumulate. Lungs containing freshly separated ^{232}U could be analyzed as accurately with a liquid scintillation system, which determined total alpha count, as with the intrinsic Ge(Li) diode, which determined ^{232}U specifically. With age and ingrowth of daughter activity, however, the two analyses were significantly different, illustrating the need for specificity in the analytical method. The apparent limit of 0.2 nCi for ^{232}U detection with the Ge(Li) diode shown in Table 11.5 is a relative number that can be improved by increasing the counting time.

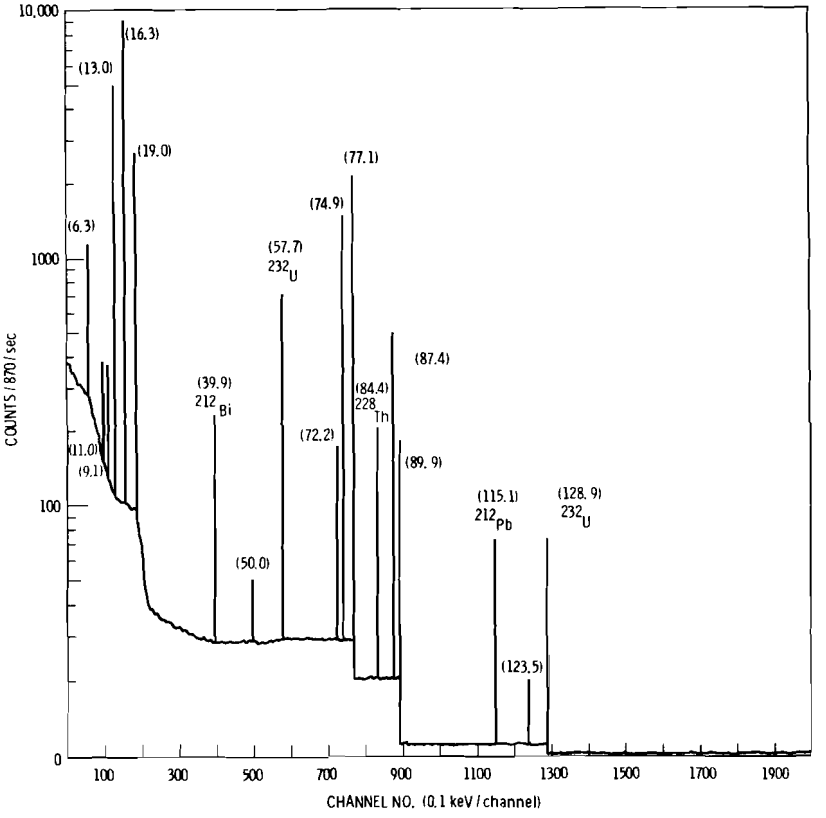

FIGURE 11.3. Energy Spectrum of ^{232}U and Decay Products (Intrinsic Ge(Li) Detector)

TABLE 11.5. Analysis of ^{232}U in Lung Using Scintillation Counting and an Intrinsic Ge(Li) Diode Detector. (Values are nCi ^{232}U)

	RAT LUNG	TOTAL ALPHA LIQUID SCINTILLATION	^{232}U PHOTON Ge(Li) DIODE
^{232}U FREE OF DECAY PRODUCTS	1	0.765	0.704
	2	0.740	0.690
	3	0.513	0.527
	4	1.036	1.004
	5	0.781	0.802
"AGED" ^{232}U	6	0.445	0.315
	7	0.423	0.216
	8	0.145	< 0.126
	9	0.172	0.158
	10	0.179	< 0.110

The most promising advantage of the Ge(Li) diode detector is its ability to detect and resolve the low-energy emissions from the ^{232}U decay series in a fresh tissue matrix. A preliminary evaluation of this technique is illustrated in Table 11.6. The values are for tissues from a single rat exposed to purified ^{232}U nitrate and sacrificed after 100 days. The tissue samples were subjected to a series of short counts starting within 3 min of sacrifice in an attempt to detect nonequilibrium amounts of the short-lived daughters, ^{212}Bi ($T_{1/2}$ = 60 min) and ^{208}Tl ($T_{1/2}$ = 3 min). These radionuclides were not present in sufficient amounts to be detected with short counting times; however, the probability of their detection will improve as the experiment progresses and the decay products grow back into equilibrium in the purified ^{232}U. Values for ^{232}U, ^{228}Th, ^{224}Ra and ^{212}Pb were obtained directly from either 100-min or 1000-min counts of the fresh tissue.

TABLE 11.6. Disposition of ^{232}U and Decay Products in Rat Tissues at Time of Death[a]

TISSUE	^{232}U	^{228}Th	^{224}Ra	^{212}Pb
LUNG	9.3 ± 0.9	2.6 ± 0.1	1.1 ± 0.04	0.44 ± 0.04
FEMUR	0.64 ± 0.07	0.12 ± 0.03	0.25 ± 0.04	0.77 ± 0.09
LIVER	< 0.2	< 0.1	0.006 ± 0.002	0.04 ± 0.01
KIDNEY	0.72 ± 0.1	0.1 ± 0.03	0.02 ± 0.004	0.09 ± 0.02

[a] DATA ARE FOR A SINGLE OBSERVATION EXPRESSED IN nCi ± SD

At the time the animal shown in Table 11.6 was sacrificed, the amount of ^{228}Th ingrowth into the purified ^{232}U should have been only 13% of the equilibrium level. The analysis for lung shows a value 30% of equilibrium for ^{228}Th. This "unsupported" excess of the daughter may indicate preferential translocation of the parent ^{232}U from lung, as has been shown by others, or, perhaps, the original ^{232}U was not as completely free of its decay products as had been indicated by alpha spectrometry and gamma analysis. The values for femur are surprising in that ^{224}Ra, which has an affinity for bone, is less abundant than its daughter product, ^{212}Pb. Further analysis of these results is probably not warranted, since they are very preliminary and may be adjusted as the procedure becomes more standardized and the counting data and spectra are subjected to more sophisticated computer analysis. At the present time, analyses for ^{232}U are thought to be valid in the range of 0.03-0.05 nCi using a counting time of 300 min. A detection limit for ^{228}Th of 0.01 nCi should be attainable by analyzing the samples after the ^{228}Th decay products have equilibrated, e.g., after 30 days in a sealed counting vial.

• FETAL AND JUVENILE RADIOTOXICITY

Person in Charge: M. R. Sikov

Many of the biological parameters used to calculate permissible levels of exposure to radioactive materials for adults are inappropriate for the rapidly growing infant or child, or for the pregnant female. These differences, when considered in conjunction with the greater intrinsic radiosensitivity of the immature organism, emphasize the need for more detailed information on the metabolism and toxicity of radionuclides in the prenatal and juvenile mammal. The aim of this project is to obtain such quantitative data.

Past efforts have included studies on the metabolism of ^{131}I, ^{137}Cs, ^{144}Ce, and ^{239}Pu relative to age and to a variety of nutritional and biochemical factors. Prenatal and neonatal rats were shown to be more sensitive than weanlings or adults to ^{131}I impairment of thyroid function and to carcinogenic effects. The metabolism and subacute toxicity of intravenously injected ^{239}Pu in newborn, weanling and adult rats showed patterns unique to each age. Studies of long-term effects at lower dose levels are nearing completion and a major effort is currently directed toward completing histopathologic evaluation and data analysis. Studies on postnatal physiology and long-term effects in rats exposed to ^{239}Pu at representative stages of gestation have recently been initiated.

The cross-placental transfer of ^{239}Pu, its distribution in the fetoplacental unit, and its effects on prenatal development have been studied in detail. To provide a basis for extrapolation to man, we are currently exploring the factors controlling transplacental passage and fetoplacental distribution in several species, including subhuman primates. Because prenatal exposure to plutonium results in a relatively high radiation dose to the yolk sac, where primitive cells of the gonads and the hematologic system originate, we are investigating the sequelae of prenatal exposure on developmental integrity. Organ culture techniques are being used to study embryotoxic effects, including the effects of single particles of plutonium oxide.

This year, studies were begun on the inhalation of $^{239}PuO_2$ particles by newborn rats. Differences in deposition, relative to age and particle size, were found and the results are being used to define experiments to increase the depth of the investigation and extend it to evaluations of effect relative to age.

Increased emphasis is being directed toward elucidating the biochemical and physiological processes in the immature mammal that may be responsible for the differences in metabolism and effects of radionuclides, as compared to their metabolism and effects in adults. A continuing effort will be made to interpret the findings of this project in terms of appropriate population exposure standards.

EFFECTS OF ^{239}Pu ADMINISTERED AT 9 DAYS OF GESTATION ON HEMATOLOGIC DEVELOPMENT OF THE RAT

Investigators:

H. Joshima, P. L. Hackett, M. J. Kujawa, P. G. Doctor, and M. R. Sikov

Technical Assistance:

J. O. Hess and L. D. Montgomery

Injection of pregnant rats with monomeric ^{239}Pu after 9 days of gestation decreased their leukocyte and reticulocyte counts at 5 and 10 days postexposure. Most of the fetal hematologic enumerative values were unaffected by injection of monomeric ^{239}Pu. There was, however, a major change in the maturation of the cells of the erythroid series, as indicated by a difference in the distribution between cell types. The weight of the yolk sac and fetal liver, and the cellularity of the fetal spleen were decreased.

Injection of ^{239}Pu at 9 days of gestation in the Charles-River CD rat produces dose-dependent embryolethality. Autoradiography has demonstrated most of the radioactivity in the fetoplacental unit (FPU) to be in the villus visceral splanchnopleure (yolk sac). Since the hematopoietic stem cells originate in the yolk sac at about this time of gestation, experiments were performed to determine whether plutonium injection would produce detectable alterations of the hematopoietic system.

After 9 days of gestation (dg) the experimental rats (Hilltop Wistar) received a single intravenous injection of 36 μCi/kg of a ^{239}Pu-citrate solution. Control rats received a citrate solution without plutonium. At 14 or 19 dg (5 or 10 days postinjection) maternal blood was obtained via cardiac puncture, the abdomen and thorax were opened, and the rat was killed by exsanguination. Individual FPUs were removed with the umbilical vessels attached to the placenta, placed in cold L-15 tissue culture medium, and divided into groups for assay. In some cases, the fetal jugular vein was cut and 5-20 μl blood was collected with disposable micropipettes for cell counts, hemoglobin determinations, and preparation of smears. The yolk sac, liver, spleen, or thymus was removed from other fetuses, the cells were dissociated, and total cells determined by counting an aliquot in a hemocytometer. Stained imprints of these tissues and the blood smears were examined by light microscopy to determine the relative distribution of cell types.

Tentative statistical analyses have been performed on the resulting data. The survival data were compared by a χ^2 test on an individual fetal basis and by a Wilcoxon Signed Rank Test (WSRT) on a litter basis. The data on body and organ weights were tested by either a 't' test or WSRT depending on the sample size ('t' for sample size >20, WSRT for samples size <20). The cell count data were compared exclusively by the WSRT. The significant level for all tests was 0.05.

There were slight but statistically significant increases in prenatal mortality in the exposed groups at both time periods

relative to the corresponding control groups, and to the combined control value. This was accompanied by a significant reduction in maternal weight gain in the plutonium-injected groups compared to the controls at both times of sacrifice. Embryonic weight, however, was unaffected by treatment (Table 12.1).

Plutonium exposure did not affect the maternal total erythrocyte count at 14 dg tion at 14 dg which was no longer demonstrable at 19 dg. Hematocrit and hemoglobin levels and reticulocyte counts, which were measured only at 19 dg, were unaffected by treatment.

The nucleated erythrocytes in the smears of fetal blood were categorized into three broad cell types: basophilic, polychromatic, and orthochromatophilic normoblasts, in order of increasing maturation. At both times of observation, ^{239}Pu exposure was

TABLE 12.1. Effect of ^{239}Pu Injection at 9 Days of Gestation on Weight, Prenatal Mortality, and Hematology

	DAY OF GESTATION			
	14		19	
	CONTROL	EXPERIMENTAL	CONTROL	EXPERIMENTAL
NUMBER OF LITTERS	7	13	4	8
MATERNAL Wt GAIN (% OF INJECTION Wt)	108 ± 5[a]	96 ± 3	124 ± 3	110 ± 7
FRACTION FETUSES DEAD	10/79	30/136	2/50	19/85
FETAL Wt (mg)	140 ± 23	140 ± 23	2112 ± 422	2070 ± 190
MATERNAL HEMATOLOGY				
ERYTHROCYTES (10^6/mm^3)	6.1 ± 0.5	5.8 ± 0.7	6.2 ± 0.5	5.4 ± 0.7
RETICULOCYTES (%)	1.4 ± 0.4	0.8 ± 0.4	1.2 ± 0.5	0.7 ± 0.2
LEUKOCYTES (10^3/mm^3)	10.1 ± 4.0	3.2 ± 1.9	8.0 ± 1.7	2.0 ± 0.8
FETAL HEMATOLOGY				
TOTAL BLOOD CELLS (10^4/mm^3)	21.8 ± 6.3	16.9 ± 5.5	216 ± 56	208 ± 49
NUCLEATED CELLS (10^4/mm^3)	5.1 ± 1.8	6.2 ± 1.8	7.6 ± 1.6	6.9 ± 1.3
NON-NUCLEATED ERYTHROCYTES (10^4/mm^3)	19.5 ± 4.5	9.2 ± 5.1	205 ± 56	201 ± 49
BASOPHILIC NORMOBLAST (%)	0.42 ± 0.42	0.14 ± 0.22	0.08 ± 0.1	0.02 ± 0.06
POLYCHROMATIC NORMOBLAST (%)	13.1 ± 5.8	17.2 ± 5.8	6.7 ± 2.7	13.1 ± 5.2
ORTHOCHROMATOPHILIC NORMOBLAST (%)	86.5 ± 5.9	81.5 ± 8.5	89.9 ± 3.6	83.7 ± 5.6

[a] STANDARD DEVIATION

although there was a significant depression by 19 days; the hematocrit and hemoglobin levels were not significantly affected. The percent reticulocytes and total leukocyte counts were significantly decreased in the treated adult animals at both times of sacrifice. The only effect on the differential counts was a slight decrease in the frequency of band forms of neutrophils in the treated animals.

The concentration of total blood cells in the fetus was slightly decreased in the exposed animals at 14 dg, although no difference was noted at 19 dg (Table 12.1). The slightly increased concentration of nucleated cells (leukocytes and nucleated [immature] erythrocytes) in the injected animals at 14 dg was not statistically significant; the decrease at 19 days was of equivocal significance. Calculation of non-nucleated (mature) erythrocyte concentrations as the difference between these two values yielded a significant reduc- associated with a decrease in the percentage of basophilic and orthochromatophilic normoblasts with a proportional increase in the percentage of cells classified as polychromatic normoblasts. These shifts in cell type distribution, together with the reduced concentration of non-nucleated erythrocytes at 14 dg, suggests a deficit in the maturation of the cells of the erythroid series.

Within the granulocytic series, there was a shift towards fewer band forms in the treated animals at 19 dg with a relative increase in metamyelocytes, although the frequency of segmented forms was largely unchanged. The percent of lymphoid cells, both lymphocytes and monocytes, was unaffected.

The weight of the yolk sac (Table 12.2) was significantly reduced by Pu exposure. The total cells in the suspensions prepared from the yolk sacs were also reduced, although the differences were not significant. No apparent differences were observed in the

TABLE 12.2. Effect of ^{239}Pu Injection at 9 Days of Gestation on the Weight and Cellularity of Selected Fetal Tissues

	DAY OF GESTATION			
	14		19	
ORGAN	CONTROL	EXPERIMENTAL	CONTROL	EXPERIMENTAL
YOLK SAC (mg)	21.4 ± 8.0[a]	13.7 ± 5.9	98.2 ± 26.3	60.3 ± 11.4
TOTAL CELLS (x 10^{-5})	17.3 ± 8.6	16.1 ± 10.4	197 ± 98	115 ± 83
LIVER (mg)	6.1 ± 3.7	5.2 ± 2.8	184 ± 28	186 ± 30
TOTAL CELLS (x 10^{-5})	17.1 ± 16.7	12.7 ± 6.7	874 ± 426	1103 ± 706
SPLEEN, TOTAL CELLS (x 10^{-5})	--	--	10.3 ± 4.5	3.5 ± 1.4
THYMUS, TOTAL CELLS (x 10^{-5})	--	--	33.5 ± 16.6	25.7 ± 19.8

[a] STANDARD DEVIATION

proportion of cell types (primarily nucleated erythrocytes and epithelial cells) in imprints of the yolk sac. The weight of the fetal liver was significantly decreased in the treated animals at 14 dg, although there was no difference at 19 days. Neither the total cells per liver nor the partition of these cells among the various morphologic categories was affected by treatment. The total cellularity of the spleen (determined only at 19 dg) was significantly decreased by plutonium exposure. No differences in the frequency of the various cell types in the imprint were noted. The total cells in the suspensions prepared from the thymus were slightly decreased by plutonium exposure, although this difference was not significant.

STRAIN DIFFERENCES IN THE EMBRYOTOXICITY OF ^{239}Pu

Investigators:

M. R. Sikov, D. D. Mahlum, and F. D. Andrew

Technical Assistance:

J. O. Hess, and M. J. Kujawa

Comparison of the embryolethality of monomeric ^{239}Pu injected at 9 days of gestation demonstrated that the sensitivity of Charles River CD strain was greater than that of Hilltop Wistar rats. Subsequent comparisons showed that rats derived from the Hilltop Fischer strain were more sensitive than the Wistar and, although not directly compared, more sensitive than the CD.

Previous studies in this laboratory demonstrated a dose-dependent embryolethality produced by injection of monomeric ^{239}Pu in Charles River CD rats. Subsequent studies using rats of Wistar derivation (Hilltop Farms) failed to provide quantitative replication of these results. A direct comparison of embryolethality was performed to establish whether rat strain, or some other unrecognized factor, was responsible for the differences.

Pregnant rats, from timed matings, were purchased from the two vendors. After 9 days of gestation (dg), the rats were injected intravenously with 10 or 40 μCi/kg of a monomeric ^{239}Pu or with an identical citrate solution not containing ^{239}Pu. Some rats from the 40 μCi/kg group were killed at 14 dg and the remaining rats from all groups were killed at 20 dg. Total fetuses and dead fetuses were counted for calculation of mortality (Table 12.3).

The lower dose, 10 μCi/kg, did not increase mortality above control levels in either strain, in keeping with past results. The higher dose, 40 μCi/kg, killed about 2/3 of the fetuses of the CD strain at both times of observation, also replicating earlier findings. There was a significant discrepancy between the mortalities seen at 14 and 20 dg with the rats of Wistar derivation. It should be noted that the 39% mortality at 20 dg following this dose is substantially higher than observed in earlier experiments or in subsequent experiments (see below). Nevertheless, the prenatal

TABLE 12.3. Prenatal Mortality (Dead/Total) at 14 and 20 Days of Gestation Following Injection of Monomeric ^{239}Pu at 9 Days of Gestation in Charles River CD and Hilltop Wistar Rats.

AMOUNT ^{239}Pu INJECTED (μCi/kg BODY WT.)	CHARLES RIVER CD		HILLTOP WISTAR	
	14 DG	20 DG	14 DG	20 DG
0	--	2/45	--	2/42
10	--	2/44	--	1/49
40	22/33	37/56	1/41	26/66

mortality values for the Wistar rats were both significantly less than for the CD, leading to the conclusion that there are marked differences in the embryolethality response of the two strains to ^{239}Pu at 9 dg.

These results led to inquiries into the responses of other strains. Rats of the Fischer strain (Hilltop Farms) were injected similarly with 0, 18, or 36 μCi/kg of a monomeric ^{239}Pu solution.

The 100% mortality observed in the Fischer fetuses at 20 dg, after 36 μCi/kg, was significantly greater than the mortality observed in the Wistar strain. Additional Fischer strain animals were injected with this and with lower doses to verify and extend this finding (Table 12.4). There was an increase in mortality with increased dose, the results demonstrating a much greater sensitivity to embryolethality in the Fischer relative to the Wistar rats, and suggesting a greater sensitivity than that observed in the earlier experiments with Charles River CD rats. These differences may provide the basis for a model system to evaluate the mechanisms involved in embryolethality following ^{239}Pu injection.

TABLE 12.4. Prenatal Mortality (Dead/Total) at 14 and 20 Days of Gestation Following Injection of Monomeric ^{239}Pu at 9 Days of Gestation in Hilltop Wistar and Hilltop Fischer Rats.

AMOUNT ^{239}Pu INJECTED (μCi/kg BODY WT.)	HILLTOP FISCHER		HILLTOP WISTAR	
	14 DG	20 DG	14 DG	20 DG
0	0/23	13/74	10/105	2/50
5	14/30	--	--	--
10	10/32	--	--	--
15-18	19/26	27/39	--	--
36	--	59/59	33/191	19/85

MOBILIZATION OF PLUTONIUM BURDENS DURING PREGNANCY

Investigators:

P. L. Hackett, D. D. Mahlum, and M. R. Sikov

Technical Assistance:

J. O. Hess, M. J. Kujawa, and M. J. Conger

The mobilization and distribution of previously deposited ^{239}Pu was compared in pregnant rats (15 and 20 days of gestation) and nonpregnant controls. Pregnancy had little effect on ^{239}Pu tissue burdens and only minimal activity appeared in the fetoplacental unit. Marked differences were observed in tracer ^{45}Ca deposition patterns between the experimental groups.

Pregnancy, and especially lactation, mobilizes maternal calcium stores. It seemed possible that plutonium might also be mobilized during gestation. Experiments were performed to determine the effects of pregnancy on predeposited tissue ^{239}Pu levels and its availability to the fetoplacental unit.

In a preliminary experiment, 15 female rats were injected with 5 μCi of monomeric ^{239}Pu and placed in metabolism cages for

excreta collection. Eight days later, they were placed with males in standard cages for 36 hr, during which time eight females became pregnant. All females were then returned to the metabolism cages. At 20 days of gestation (dg), the pregnant rats, together with the nonpregnant rats, which served as controls, were killed and tissues taken for radioanalysis.

There were no marked differences between the ^{239}Pu levels of the pregnant and nonpregnant animals (Table 12.5), although the results suggested that pregnancy may have caused some translocation from skeleton to liver. To examine this in more detail, 30 female rats were injected with 5 μCi of monomeric ^{239}Pu and held for 4 wk. At this time 20 animals were mated (vaginal smear positive for sperm = 0 dg) and 10 animals were designated as nonpregnant controls. At 14 and 19 dg, 10 pregnant and five nonpregnant rats were injected with 5 μCi of ^{45}Ca and sacrificed 24 hr later (15 or 20 dg). Excreta were collected during the last 20 experimental days. Maternal and fetal tissue radioactivity levels were determined by means of liquid scintillation counting.

TABLE 12.5. Effect of Pregnancy on the Metabolism of Previously Deposited Monomeric Plutonium

EXCRETA OR TISSUE	% OF INJECTED DOSE	
	CONTROL	PREGNANT
LIVER	2.46	3.52
KIDNEY	0.17	0.17
FEMUR	3.18	2.60
CARCASS	75.4	74.9
FECES	23.2	19.7
URINE	2.43	2.61

Pregnancy was associated with a significant decrease in plasma and skeletal ^{45}Ca values at 20, but not at 15 dg. The levels of ^{239}Pu in plasma and in the skeletal elements examined were not significantly affected by pregnancy at either time (Table 12.6). Neither the ^{45}Ca nor ^{239}Pu concentrations measured in soft tissues, such as the spleen, ovaries and mammary

TABLE 12.6. Percentage of Administered Dose per Gram Tissue ($\bar{x}$ ± SEM).

		15 DG		20 DG	
	TISSUE	CONTROL	PREGNANT	CONTROL	PREGNANT
^{45}Ca	PLASMA	0.057 ± 0.004[a]*	0.045 ± 0.002[a]	0.047 ± 0.006[a]	0.017 ± 0.002[b]
	LIVER	0.016 ± 0.001	0.019 ± 0.003	0.024 ± 0.003	0.022 ± 0.002
	UTERUS	0.044 ± 0.001[a]	0.047 ± 0.003[a]	0.043 ± 0.003[a]	0.022 ± 0.001[b]
	DECIDUA		0.045 ± 0.001[a]		0.018 ± 0.001[b]
	SKULL	1.61 ± 0.06[a]	1.68 ± 0.10[a]	1.74 ± 0.13[a]	1.02 ± 0.14[b]
	CALVARIUM	1.35 ± 0.11[a]	1.43 ± 0.08[a]	1.40 ± 0.09[a]	0.89 ± 0.10[b]
	VERTEBRAE	1.46 ± 0.06[a]	1.34 ± 0.12[a]	1.58 ± 0.20[a]	0.95 ± 0.11[b]
	RIBS	3.39 ± 0.26[a]	3.07 ± 0.23[a]	3.10 ± 0.33[a]	1.86 ± 0.20[b]
	UPPER INCISOR	3.21 ± 0.30[a]	2.83 ± 0.13[a]	2.38 ± 0.45[a]	1.09 ± 0.07[b]
	LOWER INCISOR	1.87 ± 0.20[a, b]	2.39 ± 0.21[a]	2.58 ± 0.20[a]	1.52 ± 0.18[b]
	MANDIBLE	2.47 ± 0.40[a]	2.36 ± 0.23[a]	2.30 ± 0.20[a]	1.22 ± 0.11[b]
	FEMUR	2.49 ± 0.21	2.18 ± 0.14	2.20 ± 0.31	2.09 ± 0.37
^{239}Pu	PLASMA	0.0044 ± 0.0015	0.0016 ± 0.0003	0.0040 ± 0.0008	0.0023 ± 0.0003
	LIVER	0.205 ± 0.015[a]	0.396 ± 0.006[b]	0.199 ± 0.015[a]	0.260 ± 0.059[a]
	UTERUS	0.080 ± 0.015[a]	0.033 ± 0.009[b]	0.085 ± 0.022[a]	0.009 ± 0.001[b]
	DECIDUA		0.054 ± 0.001[a]		0.009 ± 0.002[b]
	SKULL	1.41 ± 0.19	1.19 ± 0.12	1.59 ± 0.20	1.28 ± 0.12
	CALVARIUM	1.60 ± 0.21	1.31 ± 0.14	1.25 ± 0.08	1.46 ± 0.12
	VERTEBRAE	2.02 ± 0.12	1.51 ± 0.14	1.86 ± 0.16	2.04 ± 0.26
	RIBS	2.76 ± 0.26	2.05 ± 0.21	2.18 ± 0.20	2.72 ± 0.26
	UPPER INCISOR	1.19 ± 0.07	0.92 ± 0.10	1.17 ± 0.13	1.13 ± 0.16
	LOWER INCISOR	1.16 ± 0.14	0.75 ± 0.07	0.97 ± 0.11	0.87 ± 0.13
	MANDIBLE	1.08 ± 0.15	0.98 ± 0.09	0.98 ± 0.10	1.07 ± 0.05
	FEMUR	2.54 ± 0.23	2.06 ± 0.23	2.45 ± 0.16	2.38 ± 0.11

(a)*VALUES IN THE SAME ROW WITH DIFFERENT LETTERS ARE SIGNIFICANTLY DIFFERENT ($P > 0.05$)

glands, showed appreciable differences between control and pregnant animals. The hepatic values for ^{239}Pu were higher in pregnant than in nonpregnant animals, although the difference was significant only at 15 dg. The effects of pregnancy on ^{45}Ca and ^{239}Pu concentration in the uterus and decidua are probably due to marked growth and fluid accumulation.

The fetus showed a marked avidity for ^{45}Ca at 20 but not 15 dg, reflecting ossification, although neither the total activity nor concentration in the membranes or placenta differed by more than a factor of two between the two stages (Table 12.7). The total ^{239}Pu activity in the fetus increased somewhat between 15 and 20 dg although the concentration decreased. The total activity (and concentration) in the placenta also increased between 15 and 20 dg and were substantially greater than those in the fetus at both times. A similar relationship pertained in the fetal membranes, although the absolute values were much higher. These patterns were identical to those previously seen following injection of ^{239}Pu at these times of gestation, although the activities in the present study were markedly less, reflecting the low levels of ^{239}Pu mobilized. This would suggest that predeposited ^{239}Pu poses a minimal hazard to the conceptus.

TABLE 12.7. Partition of ^{45}Ca and ^{239}Pu Within the Fetoplacental Units (mean % of dose per strucutre [x10^3] ± SEM).

	^{45}Ca		^{239}Pu	
TISSUE	15 DG	20 DG	15 DG	20 DG
PLACENTA	11.8 ± 0.71	14.7 ± 0.59	0.75 ± 0.09	2.84 ± 0.19
MEMBRANES	3.41 ± 0.15	8.40 ± 0.40	1.59 ± 0.14	12.6 ± 0.81
FETUS	14.7 ± 0.59	3880 ± 211	0.14 ± 0.02	0.88 ± 0.16

We may calculate, assuming an average litter size of 10, that only 0.2% of the original ^{239}Pu dose is incorporated into the products of conception at 20 dg; this corresponds to only about 0.001% in each fetus. Although pregnancy may produce minimal mobilization and translocation of ^{239}Pu, the magnitude of any changes in maternal skeletal burden at these stages of gestation is too low to be detectable.

LATE EFFECTS OF ^{239}Pu ADMINISTERED AT REPRESENTATIVE STAGES OF GESTATION

Investigators:

F. D. Andrew and M. R. Sikov

Technical Assistance:

L. F. Haug and J. O. Hess

The protocol for a systematic comprehensive study of the influence of prenatal exposure on the tumorigenic and other adverse effects of ^{239}Pu is described. The study has been initiated, all animals have been weaned, and postnatal function is being evaluated, although results are not yet available.

Previous studies in this laboratory have provided extensive data indicating that there are age-related differences in the long-term responses to plutonium (^{239}Pu) injection. Since these earlier studies did not include life-span evaluations following exposure during early gestation, such studies have been initiated. These include estimates of radiation dosimetry obtained from concurrent distribution studies, and evaluation of effects on perinatal growth, functional capabilities, tumor incidence and survival times.

Pregnant Wistar rats were injected intravenously on days 9, 15, or 19 of gestation (dg) with ^{239}Pu citrate preparations to give dose levels of 0, 0.3, 3, or 30 μCi/kg, according to the matrix shown in Table 12.8. These dosages ranged from a threshold level for effect to approximately the maximum tolerated level for normal litter size. Based on statistical considerations, previous experience in this laboratory and practical husbandry constraints, a group size of 56 animals (approximately 1:1, male:female) was selected for each of the 12 offspring groups. Adult groups were derived empirically from the requirement of at least seven litters per group. Additional replicates received ^{239}Pu according to the matrix regimen and were sacrificed at intervals for radioanalysis and autoradiography to establish the dosimetry for target tissues of the adult, offspring and fetoplacental unit (FPU).

TABLE 12.8. Experimental Matrix and Group Size

		DOSE (μCi/kg)			
		0	0.3	3	30
AGE AT INJECTION		NUMBER RATS/GROUP			
DG 9	♂	28	27	29	27
	♀	28	29	27	28
DG 15	♂	28	27	29	27
	♀	28	29	27	29
DG 19	♂	30	28	27	30
	♀	25	27	29	26
ADULT					
PREGNANT		26	24	29	24
NONPREGNANT		7	6	2	6

Several parameters were measured for assessment of effects on reproduction and perinatal survival. Dams were weighed at intervals throughout gestation to test for maternal toxicity. At birth and on postnatal days 4 and 7, litter size was determined and reduced, if necessary, to 12, 10,

and 8, respectively. Rate of postnatal growth was followed to determine the degree of embryotoxicity. Surviving offspring were maintained with their mothers and were weighed periodically from day 4 until day 21, when they were weaned and marked to indicate dosage group, day of exposure and intrasibling identification.

Injected dams are housed 8-10/dosage group/cage, while their offspring are housed 3-5 littermates/sex/cage. All animals are weighed and examined at least once per month, and half of each group will receive a hematological evaluation every 6 months; other functional modalities will be evaluated periodically. The results of these examinations may suggest other functional alterations to be quantified at or prior to sacrifice, such as immunological competence or blood and tissue enzyme levels.

Tumor appearance and general growth and survival will be monitored throughout the natural life span without intervention, except for surgical removal of mammary tumors as soon as they are detected in any group. Moribund animals will be sacrificed prior to death. Organ weights will be obtained at necropsy whenever possible. Organs showing gross pathology will be studied microscopically. A representative sample of rats of each sex from each group will receive a more extensive postmortem analysis, including whole-body radiography and radioanalysis of index tissues.

POSTNATAL DEVELOPMENT OF THE RAT THYROID GLAND

Investigators:
J. L. Daniel, Jr., M. Goldman, D. D. Mahlum and M. R. Sikov

The postnatal development of the rat thyroid gland is being studied histologically and by autoradiography after tritiated thymidine injection. The second week of life appears to be the period of greatest cell proliferation and growth of follicles. It appears that new follicles are formed by subdivision of existing follicles, as well as by organization of interfollicular cells into new follicles.

Previous studies have demonstrated that there are qualitative and quantitative differences between the responses of juvenile thyroid glands and those of the adult to incorporated ^{131}I. Since it has been postulated that differences in growth and cell proliferation contribute to the observed elevated sensitivity in juveniles, the response of these factors to irradiation are being evaluated. Studies to define baseline development in unexposed rats have been completed.

Groups of rats, each comprising two litters, were injected intraperitoneally (i.p.) at < 1, 7, 14, and 21 days of age with 1 μCi/g body weight tritiated thymidine. Serial sacrifice of one rat from each litter occurred at 1/2, 1, 2, 3, 5, 7-1/4, 9-1/2, 12, 24, and 48 hr postinjection. Rats of another series (0, 6, 13, 21 days of age and adult) received five injections of 0.4 μCi/kg at 5-hr intervals. They were killed at 1 hr following the last injection. The thyroid glands attached to the trachea were removed, fixed, and autoradiographs prepared. They were evaluated histologically and enumeratively in two planes: one along the longest chord of the gland and the other along the longest chord at right angles to the first. Follicle size and cells per follicle were recorded, together with the number of labeled and unlabeled cells, and their locations.

Due to the infrequency of labeled mitoses, and to variations in grain counts with time postinjection, valid calculations of cell-cycle kinetics were not possible. Other measures, however, are providing some interesting insights into the postnatal development of the thyroid gland. The developing gland contains groups of cells between the follicles; these interfollicular cells (IFC) are distinct from the so-called interfollicular cells postulated to be associated with thyrocalcitonin secretion in adults. It is thought that these IFCs organize into follicles, which seems to be confirmed by their histologic appearance in this study. The percentage of the IFC and follicle cell (FC) populations labeled are the same, suggesting that they are of the same overall population. The total thymidine incorporated per IFC, as indicated by grains per cell, is greater than per FC, indicating nuclear differences. Also, there is histologic evidence that follicles invaginate, form connective tissue bridges, and bud into two or more follicles; this was most notable in the two youngest

groups. This observation indicates that the organization of IFCs into follicles is not the sole process for increase in follicle number.

There is a good correlation between the mean area and mean number of cells per follicle; both measures show a proportional increase with age, indicating that cell proliferation is the primary mechanism for size increase (Figure 12.1). Growth is not progressive, however, size remaining unchanged for the first few days of age and growth rate diminishing after about 2 wk of age. Proliferation, indicated by the percent of follicles or FC labeled, follows the same general pattern (Figure 12.2). Again, proliferation is low soon after birth, rises to a peak in the second week of life, and falls thereafter. Although surprising, it thus appears that cell proliferation and thyroid growth is relatively low in the neonatal period, reaches a peak about a week after birth, and decreases thereafter.

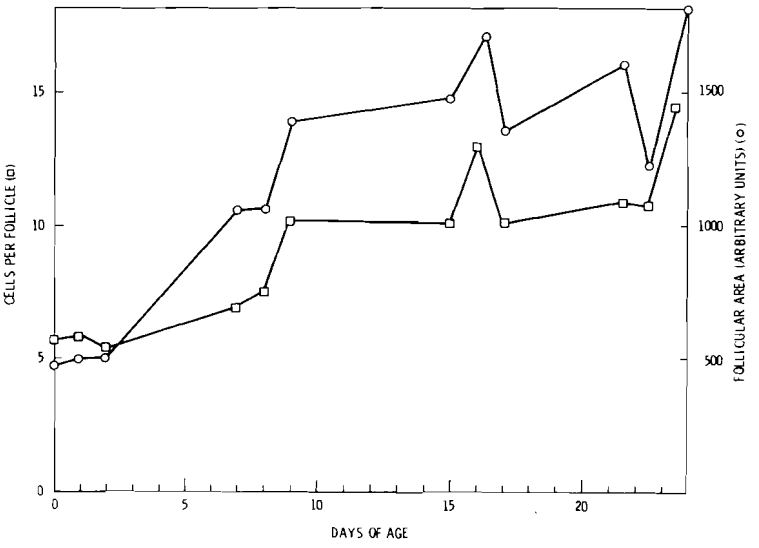

FIGURE 12.1. Growth of Thyroid Follicles in the Postpartum Rat, Expressed as Mean Areas and Cells per Follicle

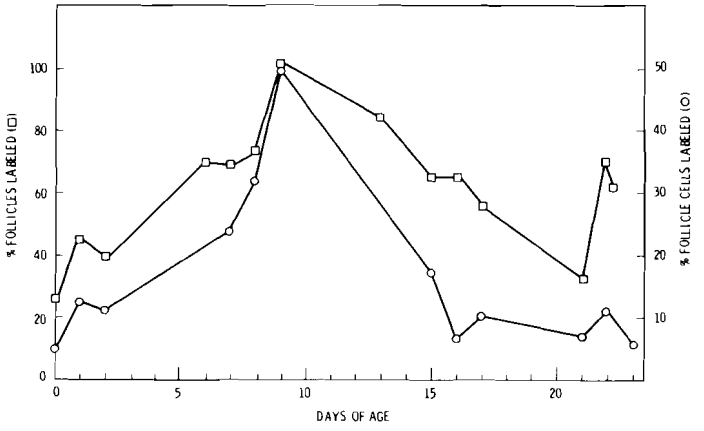

FIGURE 12.2. Percent of Thyroid Follicles and Follicle Cells Showing Autoradiographic Label After Injection of Tritiated Thymidine.

DEPOSITION AND RETENTION OF INHALED $^{239}PuO_2$ AEROSOLS IN NEWBORN AND ADULT RATS

Investigators:

M. R. Sikov, W. C. Cannon, R. L. Buschbom and D. D. Mahlum

Technical Assistance:

E. F. Blanton, M. J. Conger, J. O. Hess and M. J. Kujawa

Adult and newborn rats were exposed to $^{239}PuO_2$ aerosols of four different size distributions. Rats of both ages were killed at intervals between 1 hr and 60 days postexposure. There were marked age- and particle-related size differences in deposition, although retention was similar throughout. The differences in deposition are attributable to relatively greater deposition of larger particles in the upper respiratory tracts of newborns.

The biological disposition and effects of injected plutonium vary with age, and are related to the morphologic and biochemical development of the organism. Studies were performed to determine whether the deposition and translocation of inhaled plutonium also change with the age of the animals.

Air containing an aerosol of ^{239}Pu dioxide was drawn through an Andersen cascade impactor. The particles were collected and resuspended from four stages to give different size distributions characterized by their activity median aerodynamic diameter (AMAD). Aerosols were generated by nebulizing each suspension and were used to expose 35 adult and 35 1-day-old rats in our standard exposure facility with appropriate modifications for the newborns. Filter paper and cascade impactor samples were taken during exposure to determine concentrations and particle size distributions, respectively (Table 12.9). Five or six rats from each age and particle size group were killed at 1 hr and 1, 4, 12, 29, and 60 days after exposure and several tissues taken for radioanalysis. A tangential cross section of the left lung at the entrance of the bronchus was prepared for autoradiography. To compensate for concentration differences between exposures and at different levels within the chamber, all radioanalytic values were normalized to a unit exposure concentration of 20 nCi/ℓ.

TABLE 12.9. Effect of AMAD on Percentage Alveolar Deposition in Newborn and Adult Rats Exposed to $^{239}PuO_2$ Aerosol.

AMAD (μm)	% ALVEOLAR DEPOSITION	
	NEWBORN	ADULT
1.1	8.9	9.7
1.4	5.8	10.8
2.4	2.7	5.0
3.0	1.3	3.2

The retention curves for the adults were generally similar to those observed in other experiments (Figure 12.3) and conform to the model: $y = \alpha e^{\beta t}$, where y = nCi/lung, t = days postexposure, α is the 0 time intercept on the Y-axis and β is the slope.

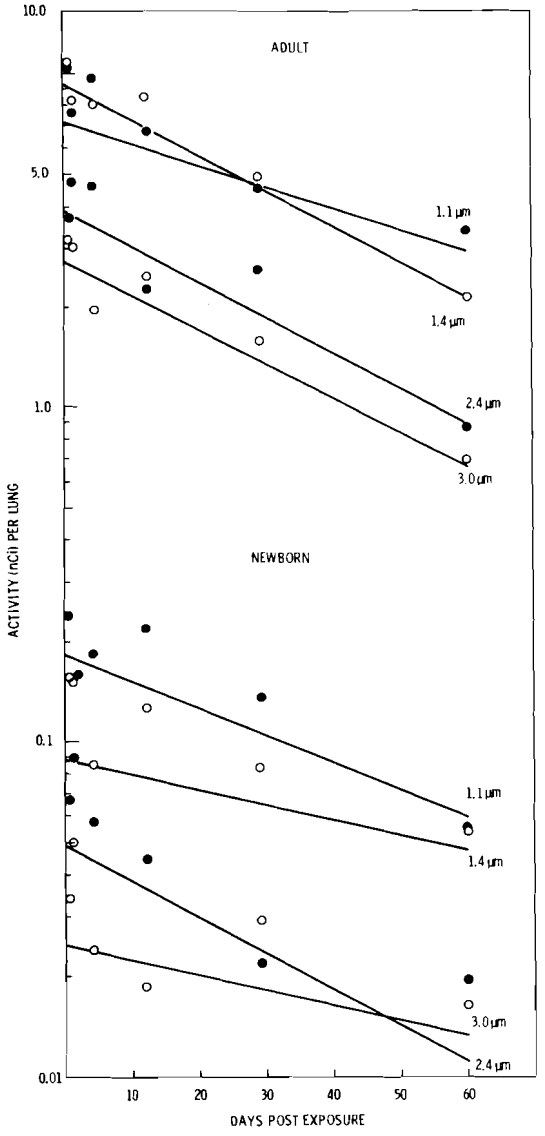

FIGURE 12.3. Deposition and Retention of $^{239}PuO_2$ After Exposure of Newborn and Adult Rats to Aerosols of Different AMADs. Mean values (normalized to aerosol concentration of 20 nCi/ℓ) and best fit lines to a $y = \alpha e^{\beta t}$ model are shown.

The newborns also follow this model, but with a marked displacement of the scale on the Y-axis. Estimates of β, the slope, among AMAD groups within adult and newborn categories are not significantly different at the 0.05 level, nor are the β estimates between adults and newborns. There were differences in initial deposition (α) which resulted in displacement of the regression lines on the Y-axis. The lines for the adult groups with AMADs of 1.1 and 1.4 µm are not significantly different, nor are those for the newborn groups with AMADs of 2.4 and 3.0 µm. All other lines are significantly different from each other at the 0.05 level of significance.

Most of this 100-fold difference in burden is attributable to difference in the size of the lung at the two ages. When the data at early postexposure times are calculated as concentration (pCi/g) to reflect the smaller size of the neonatal lung there still remains a 5- to 10-fold difference, which is greater at larger AMADs. These differences are partially explained by differential deposition in the upper portions of the respiratory tract. For example, the initial concentrations in the nasal bones (presumably mucosal deposition) were approximately 1 and 6% of the lung concentration with small and large particles, respectively, in the adults. In the newborns the corresponding concentrations were 40 and 1200%. Examination of lung autoradiographs demonstrates only smaller particles in the deep lung of newborns, even with the larger AMAD values, while the adult lungs contain a wider range of particle sizes.

The percentage alveolar deposition was calculated from the aerosol concentration by assuming a minute volume of 150 ml in the 300-g adults and a proportional 4 ml in the 8-g newborns. (Table 12.9). There was about 10% alveolar deposition in the adults for the distributions with an AMAD of 1.1 or 1.4 µm, which dropped to 5 at 2.4 µm and to 3.2 at 3 µm. The 9% value for the smallest particles in the newborns approximates that for the adults, suggesting that the assumed minute volumes are reasonable. Percentage deposition decreased somewhat at 1.4 µm and even more sharply at 2.4 µm and 3 µm, reflecting the differences in upper respiratory deposition.

• MODIFYING RADIONUCLIDE EFFECTS

Person in Charge: D. D. Mahlum

Studies of radionuclide metabolism and effects have usually employed a single radionuclide, administered under carefully controlled conditions. Animals are supplied adequate amounts of all essential nutrients and are maintained in an environment of controlled temperature and humidity; often a pathogen-free situation is created. These are common and reasonable experimental precautions taken to reduce effects from uncontrolled variables. People who may be exposed to radionuclides do not, however, live under such ideal conditions. They are subjected to many agents (ubiquitous, local, or self-imposed) and to a variety of environmental and health situations which may influence the biological disposition and effect of these radionuclides. Examples include suppressed or accentuated immunologic status, dietary deficiencies and excesses, use of drugs (those medically prescribed as well as those abused), normal variations in hormonal state, inadvertent exposure to harmful agents in the environment such as pesticides and known carcinogens, and various common physiopathologic disorders. The consequences of radionuclide exposure may either be exacerbated or ameliorated, depending on the conditions extant, and it is particularly important that we investigate those that may increase radiotoxicity.

This project was therefore designed to provide a quantitative assessment of the influence of various agents and health situations on the biological disposition and resulting effects of important radionuclides. The following factors are presently being investigated:

- The influence of iron reserves on plutonium metabolism. Iron deficiency is one of the most common nutritional diseases of young children and women and exposure of this population to plutonium or other radionuclides may result in effects not found in iron-replete individuals.
- The response of the mammary gland and uterus to plutonium. Data obtained thus far show that pregnancy and lactation increase the deposition and retention of plutonium in the mammary gland and uterus. The effect of pregnancy and lactation on the response of these tissues to plutonium will be evaluated, using tumorigenesis and reproductive capacity as indicators.
- The effects of alcohol on the metabolism of plutonium and other radionuclides. Alcohol ingestion results in a great number of physiologic perturbations, including morphologic and functional disturbances in the liver, as well as disturbances in iron metabolism. The use of alcohol by large numbers of people and the role of liver in the metabolism of Pu and other radionuclides suggest the possible importance of this factor in radionuclide toxicity.

ABSORPTION OF PLUTONIUM IN THE IRON-DEFICIENT RAT

Investigator:

H. A. Ragan

Technical Assistance:

M. J. Pipes, E. T. Edmerson, S. L. English,

M. C. Perkins, and K. H. Debban

Iron deficiency did not enhance absorption of plutonium following intragastric gavage of rats. Absorption of plutonium citrate in both control and iron-deficient rats was about 0.03% of the administered dose.

Previous Annual Reports (1973-1974) have described the enhanced absorption and retention of plutonium in iron-deficient mice, and the altered tissue distribution of plutonium in these animals following either intragastric gavage or intraperitoneal injection. In a subsequent study (Annual Report, 1975), iron-deficient rats given ^{239}Pu citrate by intraperitoneal injection were found to have plutonium body burdens and tissue distributions similar to litter-mate control rats. In a continuation of these studies, two groups of weanling rats were fed an iron-deficient diet until they were about 70 or 100 days of age. At that time rats were administered freshly prepared ^{239}Pu citrate (pH 3.5) by intragastric gavage. One group (70 days of age) was killed 48 hr later; the second group (100 days of age), 96 hr later. Littermates maintained on a control diet were gavaged with plutonium and killed at the same time as the corresponding iron-deficient group.

There were no significant differences in the plutonium body burdens of iron-deficient rats compared to the control groups (Tables 13.1 and 13.2). This was true regardless of whether the iron-deficient rats had been on the diet long enough to become anemic (100 days of age) or were nonanemic (70 days of age). Body-iron stores, as evaluated by histochemical staining for iron, were decreased in both groups compared to the controls.

TABLE 13.1. Body Burdens of Plutonium Following Gavage of Iron-Deficient and Control Rats

GROUP	n	BODY WEIGHT (g)	VOLUME OF PACKED RED CELLS (ml/100 ml)	PERCENT OF ADMINISTERED DOSE
IRON DEFICIENT	10	246 ± 13	43.7 ± 2.0	0.036 ± 0.011
CONTROL	10	289 ± 19	46.2 ± 0.6	0.046 ± 0.020

[a] RATS WERE 70 DAYS OF AGE AT GAVAGE, AND WERE KILLED 48 hr LATER
(MEAN ± STD. ERROR OF MEAN)

TABLE 13.2. Body Burdens of Plutonium Following Gavage of Iron-Deficient and Control Rats

GROUP	n	BODY WEIGHT (g)	VOLUME OF PACKED RED CELLS (ml/100 ml)	PERCENT OF ADMINISTERED DOSE
IRON DEFICIENT	10	291 ± 13	32.5 ± 1.9	0.030 ± 0.004
CONTROL	10	260 ± 11	44.1 ± 0.4	0.026 ± 0.004

[a] RATS WERE 100 DAYS OF AGE AT GAVAGE, AND WERE KILLED 96 hr LATER
(MEAN ± STD. ERROR OF MEAN)

From the results of these and the previous studies, it appears that rats and mice are distinctly different in regard to the effect of iron deficiency on their plutonium absorption and retention. These species differences are not easily explained, but aptly illustrate the need for data from several animal species in the estimation of human hazards.

EFFECT OF PREGNANCY AND LACTATION ON PLUTONIUM METABOLISM

Investigators:

D. D. Mahlum, J. O. Hess and M. R. Sikov

Technical Assistance:

M. J. Kujawa

Nulliparous, pregnant (19 days of gestation), and lactating (1 day postpartum) rats were intravenously injected with monomeric plutonium and the tissue distribution determined at 1 to 90 days after injection. The concentrations of ^{239}Pu in the mammary gland and uterus were increased by pregnancy and lactation while the skeletal values were decreased.

A preliminary study (Annual Report, 1974) suggested that the deposition of injected plutonium in the mammary gland and uterus was altered by pregnancy and lactation. In the present study, we determined both the deposition and retention of ^{239}Pu in pregnant and lactating rats. We also determined whether the retention and tissue distribution of ^{239}Pu were altered by subsequent pregnancy and lactation.

Nulliparous, pregnant (19 days of gestation), and lactating (1 day postpartum) rats (40/group) were intravenously injected with 5 μCi of ^{239}Pu citrate. Five rats of each group were killed at 1, 7, 21, and 45 days after injection. The remaining animals were caged with untreated males and bred until approximately half of each group showed sperm in the daily vaginal smears. Five of the pregnant rats from each group, along with nonpregnant group mates, were killed at 20 days of gestation or at 14 days postpartum. At sacrifice various tissues, including the mammary gland and uterus, were removed, weighed and analyzed for ^{239}Pu content.

Pregnancy and lactation resulted in an enhanced deposition of ^{239}Pu in the mammary gland (Figure 13.1), with concentrations highest in the lactating group. Subsequent pregnancy and lactation did not have a major effect on the clearance of Pu from the mammary gland.

Concentrations in the uterus at 1 day postinjection were similar for the three groups, but a marked effect of pregnancy and lactation was seen subsequently (Figure 13.2).

Although concentrations were similar at 1 day postinjection, the total ^{239}Pu content of the uterus was substantially higher in the pregnant and lactating animals because their organ weights were larger. Further examination revealed that the nidation sites (areas of placental attachment) in the pregnant and lactating groups had concentrations several times that of the remaining uterine tissue. Both the nidation sites and the uterine segments between them retained substantial ^{239}Pu over the course of the study.

Femoral concentrations of ^{239}Pu were also affected by pregnancy and lactation, with the concentration in the nulliparous rats being about 70% higher than in the other groups. Subsequent pregnancy had very little effect on the femoral concentrations.

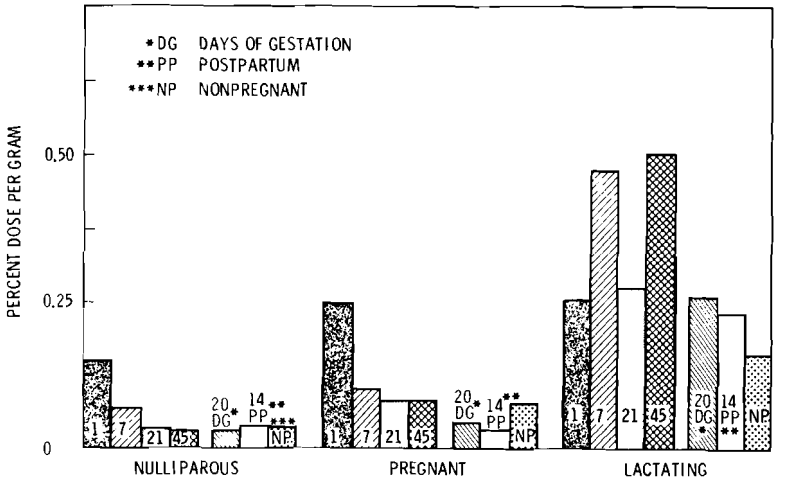

FIGURE 13.1. Concentration of ^{239}Pu in the Mammary Gland after Injection into Nulliparous, Pregnant or Lactating Rats. Numbers in bars indicate sacrifice times.

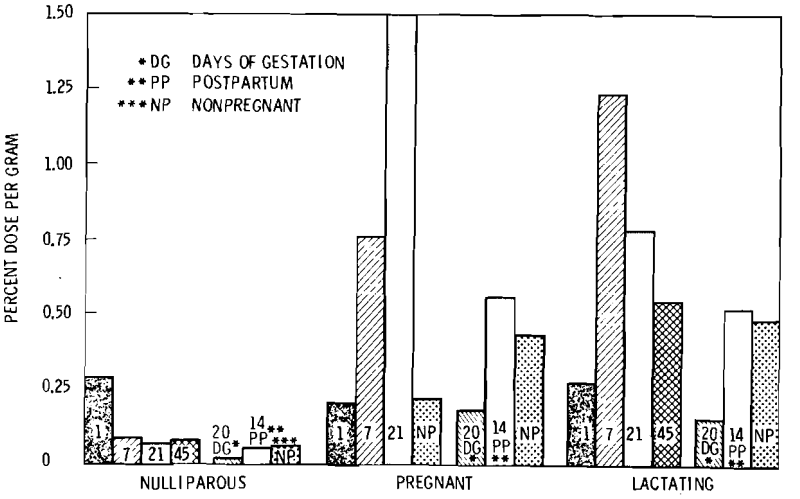

FIGURE 13.2. Concentration of ^{239}Pu in the Uterus after Injection into Nulliparous, Pregnant or Lactating Rats. Numbers in bars indicate sacrifice times.

• GUT-RELATED RADIONUCLIDE STUDIES

Person in Charge: M. F. Sullivan

This project is concerned with the fate of ingested radionuclides or of radionuclides translocated to the intestine after clearance from the lung. It is also concerned with the effects of radiation, either from an internally deposited radionuclide or from an external source, on the gastrointestinal tract and its functions.

Present emphasis in this project is placed on measurement of the gastrointestinal absorption of the actinide elements. It has long been known that absorption of plutonium is relatively higher in the very young rat. We are now studying this phenomenon in guinea pigs and swine neonates with ^{106}Ru-^{106}Rh, and find even more markedly increased retention in the intestinal mucosa of newborn swine. Guinea pigs show retention in the gastric and intestinal mucosa but the retention is of shorter duration than in rats and swine. Absorption studies involve both insoluble oxide forms and more soluble nitrate and organically complex forms. Of particular interest are current experiments involving metabolically incorporated actinides from plant and animal sources. Information from these studies will be of critical importance in evaluating the food-chain hazard from environmentally dispersed actinides over long periods of time.

Also included in this project are studies of the effects of neutrons from spontaneously fissioning californium-252 on normal tissues in both rats and miniature swine. The effects on the gastrointestinal and urinary tracts are of particular concern in radiation therapy, where clinical treatment for cancer of the cervix uteri may result in exposure of these normal tissues.

GASTROINTESTINAL ABSORPTION OF TRANSURANIC ELEMENTS BY RATS

Investigator:
M. F. Sullivan
Technical Assistance:
A. L. Crosby and T. M. Graham

Absorption of "organically bound" ^{233}U and ^{241}Am from gastrointestinal tracts of adult rats was twice that of the inorganic nitrate form. There was no difference between transport of ^{232}U and ^{233}U by adult rats, but ^{232}U absorption by newborn rats was four times that of ^{233}U. Absorption of ^{238}Pu nitrate through the gut of the newborn is relatively insensitive to dose but incorporation in the gut mucosa saturates at high dose levels. Absorption of ^{238}Pu is greater at 4 hr of age than at 24 hr.

Data on the absorption of ^{237}Np, ^{238}Pu, ^{239}Pu, and ^{241}Pu by adult rats were reported in the 1975 Annual Report, along with information about transport of metabolically incorporated ^{237}Np nitrate and ^{238}Pu nitrate or oxide. The binding of ^{237}Np in animal tissue appeared to decrease absorption, but ^{238}Pu transport was increased slightly in metabolically incorporated forms. Information was also presented on the effect of age on the capability of the intestine of the newborn rat to absorb either ^{237}Np or ^{238}Pu and also on the high quantities that are incorporated into the mucosa of the lower small intestine.

In this report we present additional data on the effect of metabolic binding on the absorption characteristics of ^{233}U, ^{241}Am, and ^{238}Pu. Data are also presented comparing absorption of ^{232}U and ^{233}U, and on the influence of plutonium dose on absorption through and incorporation in the intestine of newborn rats.

"Soluble" forms of the radionuclides were prepared by adjusting the pH of nitric acid solutions to a value between 1.5 and 2 with NaOH, and diluting the solution to a concentration of 20 μCi per ml. Further dilutions of the stock solutions were made where lower doses were desired for adult animals. Newborn animals received 0.1 ml of the stock solution through a polyethylene tube. Adult rats or guinea pigs received their dose in a 1.0 ml volume through a rubber stomach tube. The uranium isotopes were in the hexavalent state; ^{232}U was separated from daughter products not more than 2 wk prior to administration.

Newborn rats were gavaged or injected intraperitoneally with the radionuclide, killed 5 hr later, and fed in toto to adult rats as a source of biologically incorporated radionuclide. Uneaten fragments were collected, counted, and subtracted from the total dose fed, which was estimated by counting the radioactivity in several animals that were dosed but not fed to other animals.

Excreta were collected daily from each adult rat for 4 days; excreta for the following 3 days were pooled. At the completion of the collection periods the animals were killed. Only the femurs of most of the rats

were ashed and counted. The radioactivity of the total skeleton of 9-day-old rats was determined to be 0.165 times that in 1 g of femur.

Distribution and excretion data for adult rats gavaged or fed biologically incorporated radionuclides are shown in Table 14.1. The liver and skeleton contained the major fraction of absorbed radioactivity that was not excreted in the urine. Retention and urinary excretion of ^{232}U did not differ significantly from that of ^{233}U when administered as the hexavalent nitrate solution. Feeding of ^{233}U incorporated in newborn rats resulted in a 2- to 5-fold increase in the quantity retained in the liver ($P = 0.05$) and a 2-fold increase in the amount excreted in the urine ($P = 0.09$). There was little difference between absorption of ^{233}U by adult rats fed neonates injected intraperitoneally with the nuclide and those fed neonates gavaged with ^{233}U ($P = 0.13$ for the total amount absorbed).

The quantity of ^{241}Am nitrate absorbed after gavage (Annual Report, 1975) was similar to that of hexavalent uranium. The effect of biological incorporation on absorption was also similar for Am and U. Deposition of Am in both the skeleton and liver was increased by biological incorporation ($P = 0.01$) and so was urinary excretion ($P = 0.04$).

Our earlier studies (Annual Report, 1975) on absorption of transuranic elements by newborn rats showed that retention in the mucosa decreased rapidly between 2 and 8 days postgavage, and that about 2 to 3% of a 2-μCi dose of ^{238}Pu nitrate was transported across the mucosa. The results shown in Table 14.2 indicate that ^{233}U nitrate is absorbed to about the same extent as ^{238}Pu nitrate and very little is retained in the mucosa after gavage of 2-day-old rats. Although absorption by adult rats of ^{232}U and ^{233}U is similar, up to three times more ^{232}U is absorbed by the newborn, 2.0% vs 6.7% ($P = <0.01$). In addition, five times more ^{232}U is retained in the gut wall ($P = 0.01$).

TABLE 14.1. Distribution of Radionuclides in Adult Rats 7 Days After Gavage or Feeding Biologically Incorporated Nuclides

RADIONUCLIDE	NO. OF RATS	CONTENT AS PERCENT OF DOSE ADMINISTERED				
		SKELETON[a]	LIVER	SKELETON + LIVER	URINE	SKELETON, LIVER AND URINE
^{232}U - NITRATE	6	0.015 ± 0.005[b]	0.007	0.016	0.05	0.066
^{233}U - NITRATE	4	0.014 ± 0.006	0.0008 ± 0	0.015	0.07 ± 0.02	0.085
^{233}U - NITRATE (BIOLOGICALLY INCORPORATED IN GAVAGED NEONATES)	4	0.014 ± 0.009	0.002 ± 0.001	0.016	0.15 ± 0.02	0.116
^{232}U - NITRATE (BIOLOGICALLY INCORPORATED BY NEONATES INJECTED TP)	2[b]	0.021 ± 0.02	0.004	0.025	0.15 ± 0.02	0.175
^{241}Am - NITRATE[c]	11	0.012 ± 0.003	0.003	0.015	0.05 ± 0.006	0.065
^{241}Am - NITRATE (BIOLOGICALLY INCORPORATED IN GAVAGED NEONATES)	6	0.02 ± 0.005	0.01 ± 0.001	0.03	0.05 ± 0.08	0.08

[a] SKELETON ESTIMATED TO BE 23 TIMES FEMUR RADIOACTIVITY

[b] STATISTICAL VARIATION IS SEM EXCEPT RANGE IS SHOWN FOR GROUPS OF 2 ANIMALS

[c] DATA FROM 1975 ANNUAL REPORT

Measurements of absorption of a low dose (0.05 μCi) of ^{237}Pu showed that the percentage of administered dose transported across the gut and retained was similar to the amount of ^{238}Pu nitrate absorbed from a μCi dose 40 times higher (2 μCi, Annual Report, 1975) and a mass dose nearly 30,000 times higher. However, a much higher percentage of ^{237}Pu, than of ^{238}Pu, was retained in the gut wall. To further investigate the dose-dependency of these effects and to determine whether the mechanisms responsible for gut retention were saturated at higher doses, several different dose levels of ^{238}Pu nitrate were administered to groups in two separate litters of newborn rats. Groups of two or three rats from each litter were administered four different doses at two different ages. The results shown in Table 14.3 indicate little effect of dose on percentage absorption from the gut. The percentage absorption of ^{238}Pu was about the same as that for ^{237}Pu (Table 14.2) at an even lower mass level. Percentage retention in the intestine wall and contents was markedly decreased at the highest dose level ($P = <0.01$), indicating a saturation of the mechanisms responsible for this retention.

The 4-hr-old animals absorbed more ^{238}Pu from the gut than did the 24-hr-old rats ($P = 0.025$).

TABLE 14.2. Distribution of Radionuclides in Newborn Rats 7 Days After Gavage.

RADIONUCLIDE	DOSE (μCi)	NO. OF RATS	CONTENT AS PERCENT OF GAVAGED DOSE ± SEM				
			SKELETON[a]	LIVER	INTESTINE WALL	INTESTINE CONTENT	TOTAL ABSORBED
^{232}U - NITRATE	2	5	6.2 ± 0.6	0.054 ± 0	4.5 ± 0.7	2.5 ± 0.4	6.7 ± 0.4[d]
^{233}U - NITRATE	2	10	2.1 ± 0.2	0.02 ± 0	0.7 ± 0.1	0.5 ± 0.1	2.0 ± 0.2[d]
^{237}Pu - NITRATE	0.05	10	1.3 ± 0.7[b]	0.14 ± 0.01	40.6 ± 2.3	10.7 ± 1.4	2.9 ± 0.3[c]

[a] SKELETON ESTIMATED AS 0.165 x BODY wt(g) x CONCENTRATION IN FEMUR (%/g)

[b] ENTIRE SKELETON COUNTED ON 3 RATS

[c] DETERMINED BY WHOLE-BODY COUNTING AFTER REMOVAL OF THE INTESTINE

[d] DETERMINED BY COUNTING CARCASS AFTER REMOVAL OF THE INTESTINE

TABLE 14.3. Distribution of Plutonium-238 in Newborn Rats Killed 7 Days After Gavage

ADMINISTERED DOSE (μCi)	NO. OF RATS	AGE AT GAVAGE (h)	CONTENT AS PERCENT OF GAVAGED DOSE[a]				
			SKELETON[b]	LIVER	INTESTINE WALL	INTESTINE CONTENTS	TOTAL ABSORBED[c]
0.0036	2	24	6.2 ± 1.2	0.5 ± 0.1	90 ± 26	39 ± 14	10 ± 1.3
	2	4	7.7 ± 0.1	0.6 ± 0.1	83 ± 17	37 ± 6	29 ± 3.8
0.037	1	24	3.3	0.24	64.9	28	2.7
	2	4	3.4 ± 0.4	0.4 ± 0.01	51 ± 1	25 ± 6	4.8 ± 0.2
0.39	3	24	1.9 ± 0.2	0.2 ± 0.03	33 ± 7	26 ± 3	1.6 ± 0.2
	3	4	4.2 ± 1.0	0.7 ± 0.2	27 ± 6	24 ± 6	4.7 ± 1.4
4.14	3	24	2.1 ± 0.2	0.4 ± 0.03	1.3 ± 0.2	6.8 ± 1.4	2.4 ± 0.3
	3	4	4.7 ± 0.8	0.9 ± 0.2	1.7 ± 0.6	3.7 ± 3.1	5.9 ± 1.1

[a] STATISTICAL VARIATION IS SEM, EXCEPT RANGE IS SHOWN FOR GROUPS OF 2 ANIMALS

[b] SKELETON ESTIMATED AS 0.165 x BODY wt(g) x CONCENTRATION IN FEMUR (%/g)

[c] TOTAL ABSORBED IS SUM OF CARCASS, LIVER, LUNG, AND FEMUR ANALYSES, AND DOES NOT INCLUDE GUT OR GUT CONTENTS

GASTROINTESTINAL ABSORPTION OF RADIONUCLIDES BY THE NEONATAL RAT, GUINEA PIG AND SWINE

Investigator:

M. F. Sullivan

Technical Assistance:

A. L. Crosby, T. M. Graham, and P. S. Ruemmler

Ruthenium-106 administered to newborn rats and swine was incorporated into the epithelium of the lower small intestine and retained there for a few weeks after gavage; the stomach and small bowel of guinea pigs also incorporated ^{106}Ru but did not retain it.

Incorporation of high concentrations of ^{106}Ru-^{106}Rh, and of several transuranic elements, into the mucosa of the small bowel of the newborn rat was reported in the 1975 Annual Report. In this report we present additional results obtained with newborn guinea pigs and swine gavaged with ^{106}Ru-^{106}Rh for the purpose of comparing the functions and maturation rates of the GI tracts of these three different species.

Acid solutions of ^{106}Ru-^{106}Rh chloride were adjusted to pH 2 with NaOH and to a concentration of 15 μCi/ml for studies of whole body retention. Higher concentrations of 1.0 mCi/ml were prepared for treatment of animals to be killed and sectioned for preparation of autoradiographs. Rats 3 days old, guinea pigs 1 day old and swine 1 day old were gavaged with ^{106}Ru-^{106}Rh, 5 μCi each. Retention of radioactivity was measured by whole-body counting at intervals following administration. Some of the animals were killed to determine the radionuclide content of their intestines.

A comparison of the whole-body retention of gavaged ^{106}Ru-^{106}Rh is shown in Figure 14.1. Movement of the radionuclide from the intestines is much slower in newborn rats and swine than in guinea pigs. At 3 days 64% still remains in the rat and 77% in the swine, whereas only 6% remains in the guinea pig. Analysis of the gut showed that almost all of the radioactivity measured by the whole-body counter was due to gut retention. This difference in retention suggests differences in absorption by the mucosa. The quantity retained was not appreciably different in rats or guinea pigs if gavage occurred any time between a few hours and 3 days after birth. Later times were not studied in guinea pigs but rats retained a substantial amount of ^{106}Ru-^{106}Rh if injected any time during the first 2 wk after birth.

Autoradiograms made from sections taken from the lower ileum of rats and swine, where most of the radioactivity was concentrated, are shown in Figure 14.2; ^{106}Ru-^{106}Rh is concentrated in the mucosa. Figure 14.3 shows the very different pattern of ^{106}Ru-^{106}Rh localization in the guinea pig GI tract. Guinea pigs gavaged at 1 day and killed a day later showed much of the radioactivity concentrated in the glandular stomach; at 2 days incorporation in the ileum was more prominent, but at 3 days, most of the dose had left the mucosa of the intestine and some was visible in the central region of the villi.

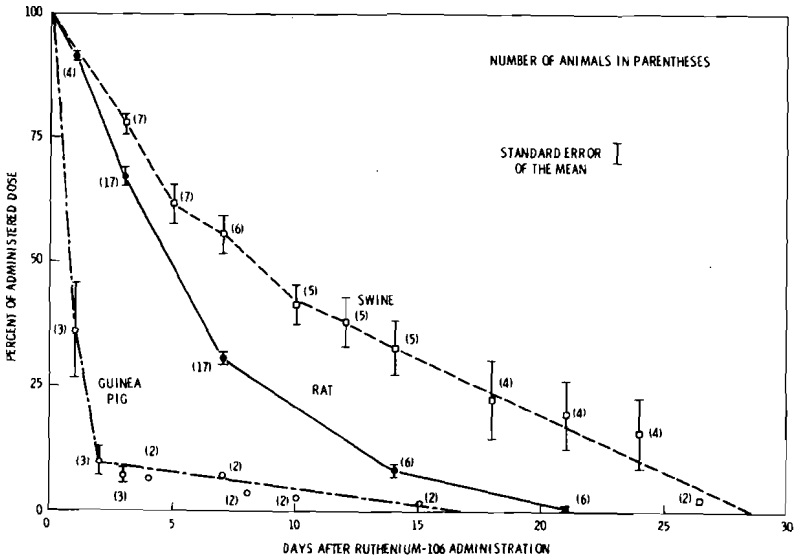

FIGURE 14.1. Measurements of Whole-Body Retention of Gavaged ^{106}Ru-^{106}Rh in Newborn Rats, Guinea Pigs or Swine at Various Intervals After Administration.

The intestine of the newborn rat is known to absorb large molecules such as immunoglobulins throughout the suckling period (3 wk) but the intestine of newborn swine, guinea pigs and humans absorbs such macromolecules for only about a day. The results of this study show that the internalization of ^{106}Ru-^{106}Rh in the mucosa of the swine intestine is similar to that observed in the rat and retention is also similar.

On the other hand, ^{106}Ru-^{106}Rh is handled much differently by the gut of the newborn guinea pig. The radionuclide is briefly incorporated by the gastric and small bowel mucosa, but is cleared into the feces within a few days. These results suggest that the process of incorporation within the mucosa is not directly related to the process responsible for the absorption across the gut wall of large molecules or radionuclides. Further studies are in progress to determine whether prolonged retention at the site where absorption probably occurs contributes to enhanced absorption of radionuclides by the newborn rat or swine.

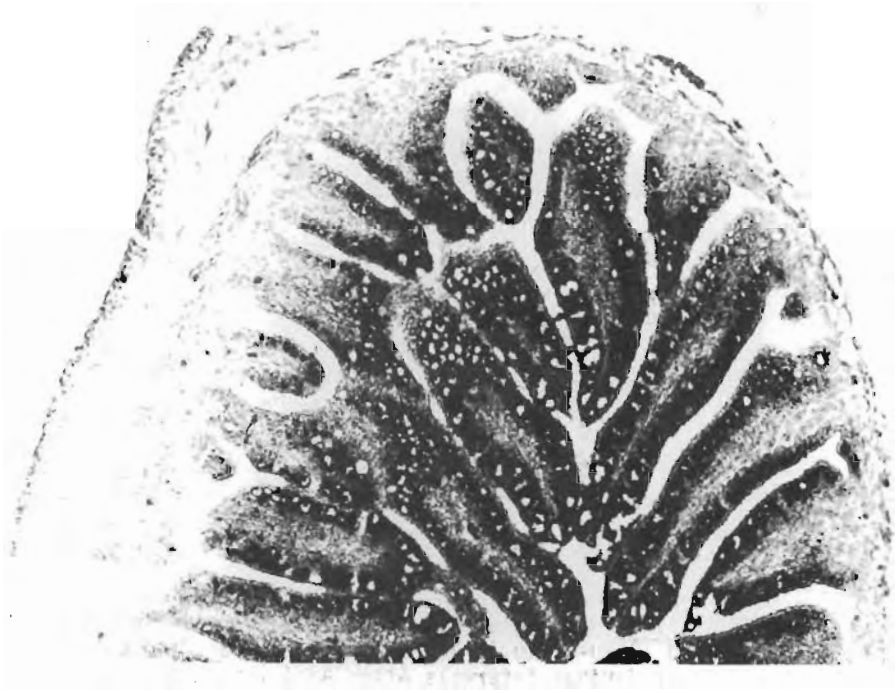

a

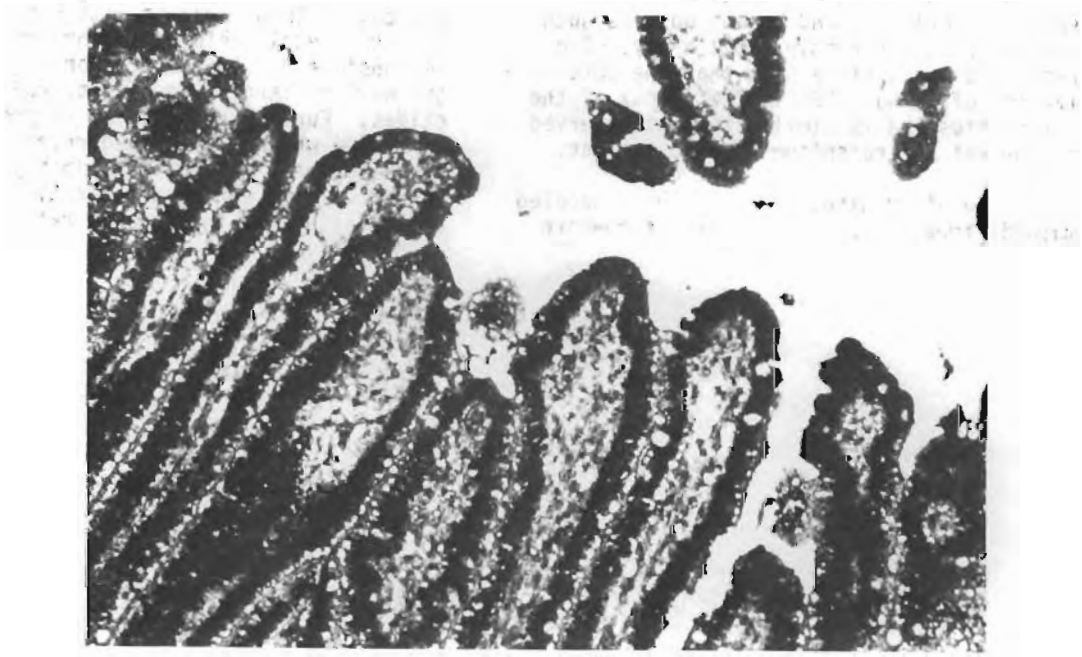

b

FIGURE 14.2. Autoradiograms of Sections of a) Rat Ileum and b) Swine Ileum Showing Incorporation of ^{106}Ru-^{106}Rh, Gavaged at 1 Day of Age and Killed a Day Later. (400X)

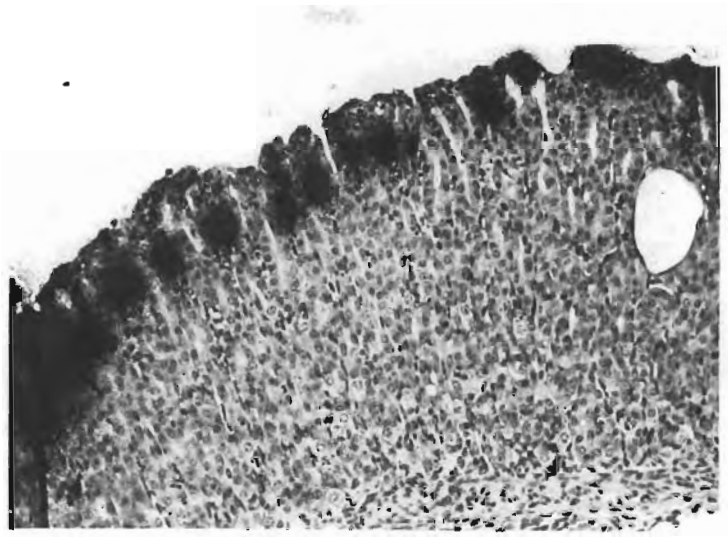

a

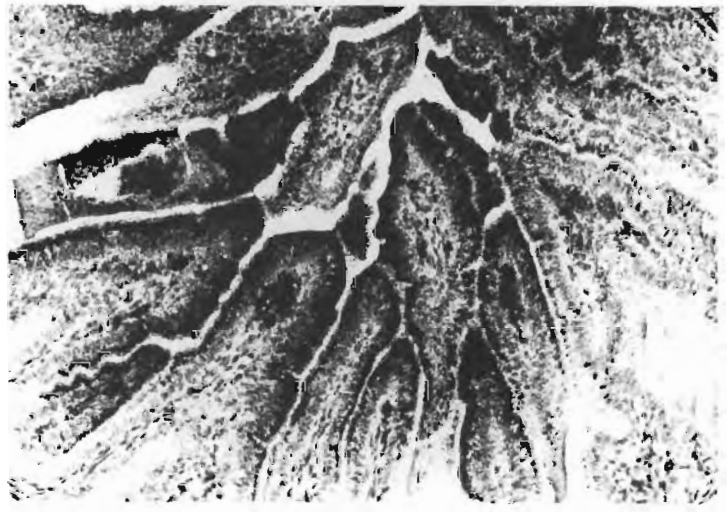

b

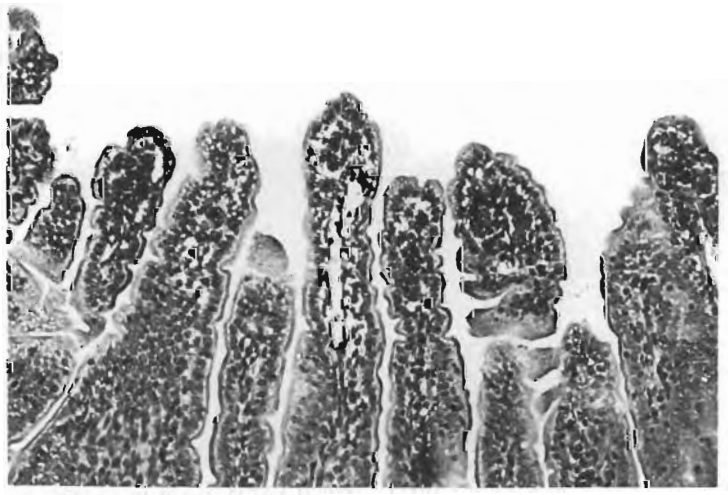

c

FIGURE 14.3. Autoradiograms of Guinea Pigs Gavaged with ^{106}Ru-^{106}Rh at 1 Day of Age and Killed at 1, 2, or 3 Days. (a) shows incorporation in the stomach at 1 day; (b) concentration in the ileal mucosa at 2 days; (c) concentration in the central area of the villus at 3 days after dosing.

• BIOHAZARDS OF REACTOR ACCIDENTS

Person in Charge: M. F. Sullivan

This project was initiated in FY 1974 to provide acute toxicity data on ingested, non-absorbed radionuclides such as might result from a reactor accident. The first phase, recently completed, furnished data used in revision of Appendix VI of the Rasmussen Report (WASH-1400). Acute toxicity information was derived for both a weak beta-emitter, ^{147}Pm, and a strong beta-emitter, ^{106}Ru-^{106}Rh, in rats. Data were also obtained with ^{106}Ru-^{106}Rh in the dog.

In FY 1976 a second phase of this program was begun, with cooperation from members of the Ecology Department, to determine the gastrointestinal absorption of an insoluble, slightly absorbed alpha-emitting nuclide that might be released to the environment in an accident, incorporated in the food chain, and subsequently ingested. Initial experiments employing ^{238}Pu incorporated in alfalfa are described in this report.

PREVENTION OF DEATH FROM INGESTED RUTHENIUM-106 BY COLECTOMY

Investigators:

M. F. Sullivan, J. L. Beamer and M. T. Karagianes

Technical Assistance:

T. Graham and A. J. Clary

Two dogs were given 3.0 mCi/kg body weight of ^{106}Ru-^{106}Rh and two were given 4.0 mCi/kg. At 5 days after treatment, one dog from each dose level was colectomized. The dog given the larger dose but not surgically treated was killed in extremis due to acute lower bowel injury at 18 days. The other dog, given 3.0 mCi/kg but not surgically treated, was killed in a moribund condition at 145 days after dosing. The rectum had perforated. The colectomized dogs recovered from intestinal injury and showed no radiation damage at the termination of the study.

Toxicity data reported in the 1975 Annual Report indicated that the LD_{50} of ^{106}Ru-^{106}Rh for dogs was approximately 3.5 mCi/kg, and that death from ingested ^{106}Ru-^{106}Rh was due primarily to lower bowel injury. Death from doses lower than 3.2 mCi/kg was usually delayed for several weeks and the principal cause of death was failure of the denuded lower bowel to recover from damage. In this report we will describe surgical treatment that prevented both the acute death and the delayed death, following ^{106}Ru-^{106}Rh ingestion.

The ^{106}Ru-^{106}Rh was fed as the chloride, mixed with 100 g ground meat. Two dogs, #1452 and #5374, were administered doses of 3.0 mCi/kg and two others, #1442 and #5375, given 4.0 mCi/kg. Passage time through the gut was measured.

Five days after ruthenium feeding, dogs #5374 and #5375 were anesthetized and the lower bowel, extending from the lower ileum to within 5 cm of the anus, was excised and fixed in 10% formalin. An end-to-end anastomosis of the ileum and rectum was performed. The colectomized dogs and the control dogs, not surgically treated, were given the same postsurgical drug treatment. Anorexia and diarrhea were common to all dogs both before and after the time of surgery. These symptoms ameliorated within about 10 days in the colectomized dogs but continued in the control animals. Histologic sections of the colon removed from the colectomized dogs are shown in Figures 15.1 and 15.2. The dog given 3 mCi/kg and colectomized, #5374, showed less severe damage to the colon than was seen in the dog given 4 mCi/kg, and the symptoms of injury to the gastrointestinal tract subsided more rapidly. The dog given 4 mCi/kg but not colectomized, #1442, was killed in extremis at 18 days; the colectomized dog given that dose recovered and was sacrificed at 81 days for pathologic evaluation.

The dog given 3.0 mCi/kg but not colectomized, #1452, regained its appetite but diarrhea continued for several months. The appearance of the feces suggested stenosis

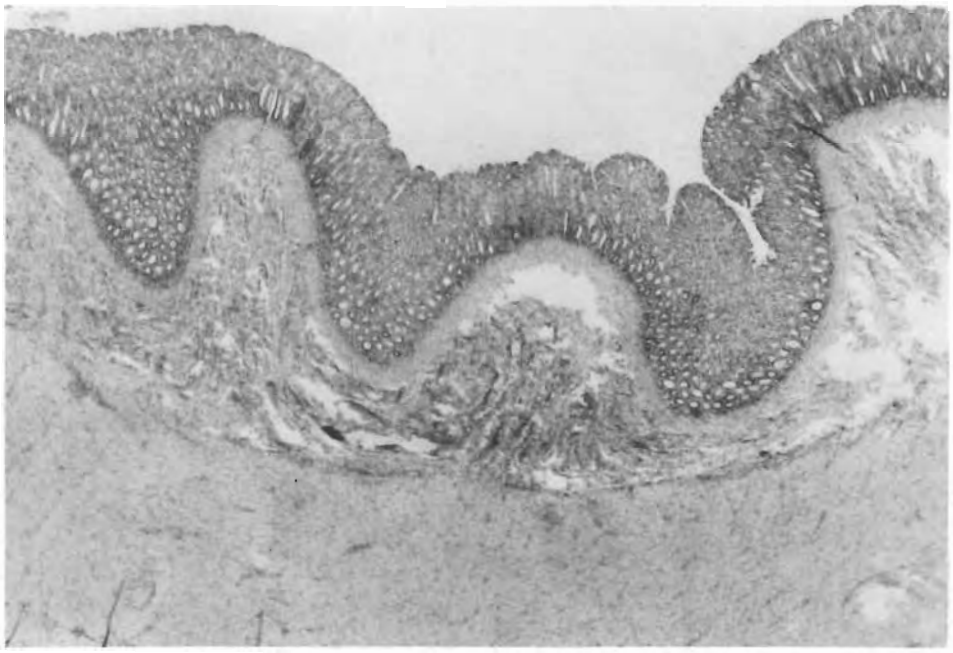

FIGURE 15.1. A Section of the Midcolon of Dog #5374 Removed During Colectomy at 5 Days After Ingestion of 3 mCi/kg of ^{106}Ru-^{106}Rh. There are numerous cystic crypts evident. (25X).

FIGURE 15.2. A Section of the Midcolon of Dog #5375 That was Removed During Colectomy at 5 Days After Ingestion of 4 mCi/kg of ^{106}Ru-^{106}Rh. Note the cystic crypts, some of which contain inflammatory cells. (25X).

of the large bowel. At 145 days both 3.0 mCi/kg dogs were sacrificed. The colectomized dog had fully recovered and there was no appreciable damage evident in the intestine at necropsy; the rectum of the control dog had perforated. Sections from the midcolon of both ruthenium-dosed but not surgically treated animals are shown in Figures 15.3 and 15.4.

This limited study would appear to demonstrate the effectiveness of colectomy in preventing both early and delayed death resulting from the ingestion of otherwise lethal doses of ^{106}Ru-^{106}Rh.

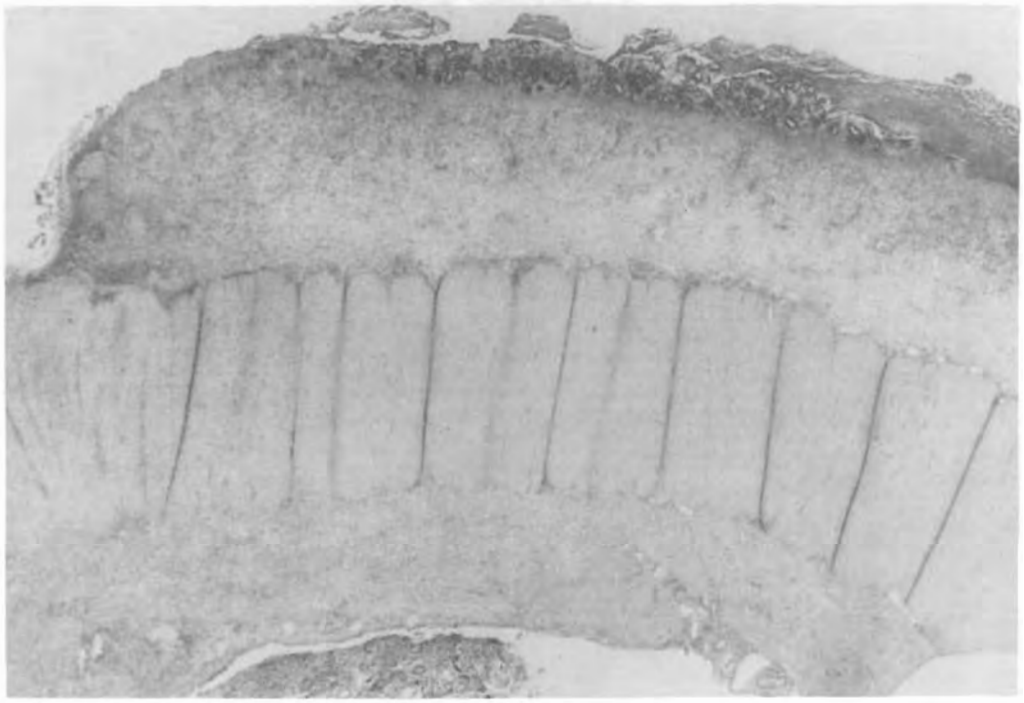

FIGURE 15.3. A Section of the Midcolon of Dog #1452, Fed 3 mCi/kg of ^{106}Ru-^{106}Rh 145 Days Before Necropsy. Note the ulcer at the left margin and the denuded surface on both ends of the section, some of which is covered by an inflammatory exudate. A few mucosal glands remain on the surface at the center. (16X).

FIGURE 15.4. A Section of the Midcolon of Dog #1442, Taken at Necropsy 18 Days After Ingestion of 4 mCi/kg of ^{106}Ru-^{106}Rh. The denuded surface is covered by a thin inflammatory exudate. (25X).

GASTROINTESTINAL ABSORPTION OF ALFALFA-BOUND PLUTONIUM-238 BY RATS AND GUINEA PIGS

Investigators:

M. F. Sullivan and T. R. Garland[a]

Technical Assistance:

T. M. Graham and A. L. Crosby

Rats and guinea pigs were fed ^{238}Pu either biologically incorporated into alfalfa (by growth of the plant on soil containing Pu) or added as a solution to alfalfa, or were gavaged with a Pu solution. Depending upon the plant material fed, there appeared to be a twofold increase in ^{238}Pu-gut absorption by the rat and a two- to fourfold increase in the guinea pig as compared with absorption from the Pu solution. The data, though limited and variable, suggest that Pu bound to plant tissue may have higher gut absorptivity than inorganic Pu in both herbivorous and nonherbivorous rodents.

Whether plutonium translocated from contaminated soil into plant tissue may be bound in a form that exhibits enhanced absorption from the gastrointestinal tract, was investigated in these preliminary studies employing rats and guinea pigs.

Alfalfa used in the first experiments was grown to maturity on ^{238}Pu-amended soils; leaves were dried, ground, and pelleted. Plutonium fed in this form will be referred to as "incorporated". Alfalfa grown on soil containing no Pu was mixed with a plutonium nitrate solution to produce ^{238}Pu levels equivalent to those found upon biologic incorporation (60,000 dpm/g plant tissue). Plutonium fed in this form will be referred to as "mixed". The plutonium nitrate solution (pH 2.0) was also given directly by gavage and is referred to as "solution". All animals were placed on an alfalfa ration one week prior to Pu administration.

Rats were killed 5 days after plutonium administration; pelt and viscera were carefully removed and discarded. Results of radiochemical analyses* on liver and carcass are shown in Table 15.1. Incorporated Pu was absorbed to a twofold greater extent than mixed Pu, the difference being statistically significant at P = 0.11. Incorporated Pu showed a 10-fold greater gut absorption than inorganic Pu (significant at the P = 0.08 level) administered by gavage at pH 2.0.

Guinea pigs were employed in a similar experiment, except that alfalfa leaves and stems were fed, as well as leaves alone. Skeletons were separately analyzed for some animals. Results are shown in Table 15.2. When leaves and stems were fed, incorporated Pu showed a fourfold higher gut absorption than mixed Pu (GP-1 vs GP-2), the difference being statistically significant at P = 0.13. However, when leaves-only were fed, mixed Pu showed a higher absorption than incorporated Pu (not statistically significant). Absorption of the Pu solution was not significantly different from that of either incorporated or mixed plutonium.

(a) Ecosystems Department

*Analyses by LFE Corp., Richmond, CA

TABLE 15.1. Absorption of Ingested ^{238}Pu by Rats

GROUP	ANIMAL	FORM ADMINISTERED	DOSE ADMINISTERED (dis/min)	ABSORBED LIVER (dis/min)	LIVER (%)	CARCASS (dis/min)	CARCASS (%)	TOTAL (dis/min)	TOTAL (%)
R-1	1	INCORPORATED	132,000	32 ± 6*	0.023	121 ± 3	0.091	153	0.115
	2	(LEAVES)	130,000	11 ± 6	0.008	43 ± 3	0.032	54	0.040
	3		136,000	24 ± 3	0.018	109 ± 2	0.080	133	0.098
	AVG			22	0.016	91	0.068	113	0.084
R-2	1	MIXED	154,000	8 ± 6	0.005	57 ± 3	0.037	65	0.042
	2	(LEAVES)	154,000	12 ± 6	0.007	50 ± 3	0.032	62	0.039
	3		154,000	10 ± 6	0.007	42 ± 3	0.027	52	0.034
	AVG			10	0.006	50	0.032	60	0.038
R-3	1	SOLUTION	161,000	5 ± 9	0.003	12 ± 5	0.008	17	0.010
	2		161,000	1 ± 23	0.001	6 ± 7	0.003	7	0.004
	AVG			2.8	0.002	9	0.006	12	0.007
R-4		NONE	0	0		0.1		0.1	

* PERCENT COUNTING ERROR

To obtain further data upon differences in gut absorption of Pu biologically incorporated into leaves or stems at higher tissue concentrations of Pu, a chronic feeding experiment was performed. Guinea pigs were fed, daily for ten days, either pellets made from leaves and stems, or leaves alone, containing incorporated or mixed Pu; other animals received inorganic Pu by gavage. Animals were killed 2 days after the last dosing. The results of tissue analyses are shown in Table 15.3. When leaves and stems were fed, there was, again, a fourfold increase in gut absorption of incorporated as compared to mixed plutonium (GP-6 vs GP-7), significant at $P = 0.12$. When leaves-only were fed, incorporated Pu was absorbed to about twice the extent of mixed Pu (GP-8 vs GP-9); significant at $P = 0.04$. Absorption of Pu from the gavaged solution was higher than that of any Pu fed with alfalfa except for that incorporated in leaves and stems, but the differences were not significant.

The high levels of Pu found in 2 of 5 gavaged animals could have been due to inspiration of solution during the 10 days of gavage. Radiochemical analyses of lung, however, showed excessive Pu in only one animal, which was omitted from the analyses. The variability in the data could not be explained by differences in skeleton versus total carcass levels of Pu; a 2:1 ratio of skeleton or carcass to liver Pu was determined for most of the animals.

The results of these preliminary experiments suggest that biological incorporation of Pu in plant tissue increases its gastrointestinal absorption. The variability of the data, especially for guinea pigs, precludes a quantitative evaluation of this increase and indicates a need for further study.

TABLE 15.2. Absorption of Ingested ^{238}Pu by Guinea Pigs

GROUP	ANIMAL	FORM ADMINISTERED	DOSE ADMINISTERED (dis/min)	ABSORBED							
				LIVER		SKELETON		CARCASS		TOTAL	
				(dis/min)	(%)	(dis/min)	(%)	(dis/min)	(%)	(dis/min)	(%)
GP-1	1	INCORPORATED	102,500	43 ± 3*	0.042	37 ± 3*	0.036			80	0.078
	2	(LEAVES AND STEMS)	100,500	30 ± 3	0.030	28 ± 3	0.027			58	0.057
	AVG			37	0.036	33	0.032			70	0.068
GP-2	1	MIXED	105,800	8 ± 5	0.008	11 ± 5	0.011			19	0.019
	2	(LEAVES AND STEMS)	105,600	8 ± 6	0.007	10 ± 5	0.010			18	0.017
	AVG			8	0.008	11	0.011			19	0.018
GP-3	1	INCORPORATED	135,500	34 ± 3	0.025			76 ± 3	0.056	110	0.081
	2	(LEAVES)	118,100	24 ± 3	0.020			15 ± 3	0.013	39	0.033
	3		123,000	7 ± 5	0.006			21 ± 3	0.017	28	0.023
	AVG			22	0.017			37	0.029	59	0.046
GP-4	1	MIXED	105,500	23 ± 2	0.021			44 ± 4	0.042	67	0.063
	2	(LEAVES)	106,100	16 ± 6	0.015			30 ± 4	0.028	46	0.043
	3		102,500	34 ± 3	0.033			162 ± 3	0.158	196	0.191
	AVG			24	0.023			79	0.076	103	0.099
GP-5	1	SOLUTION	110,300	10 ± 4	0.009			27 ± 3	0.024	37	0.033
	2		110,300	17 ± 4	0.016			21 ± 3	0.019	38	0.035
	3		110,300	19 ± 3	0.017			16 ± 4	0.015	35	0.032
	AVG			15	0.014			21	0.019	36	0.033
GP-C	1	NONE	0	1.0				0.3		1.3	
	2		0	0.1				0.1		0.2	
	3		0	0		2.0				2.0	
	AVG			0.4				0.8		1.2	

*PERCENT COUNTING ERROR

TABLE 15.3. Absorption of Chronically Ingested ^{238}Pu by Guinea Pigs

GROUP	ANIMAL	FORM ADMINISTERED	10-DAY DOSE ADMINISTERED (dis/min)	ABSORBED							
				LIVER		SKELETON		CARCASS		TOTAL	
				(dis/min)	(%)	(dis/min)	(%)	(dis/min)	(%)	(dis/min)	(%)
GP-6	1	INCORPORATED	587,000	80	0.014	76	0.013			156	0.027
	2	(LEAVES AND	499,000	282	0.057			402	0.081	684	0.138
	3	STEMS)	575,000	262	0.046	636	0.111			898	0.157
	AVG			208	0.039	356	0.062			579	0.107
GP-7	1	MIXED	666,000	84	0.013			155	0.023	239	0.036
	2	(LEAVES AND	663,000	52	0.008			111	0.017	163	0.025
	3	STEMS)	661,000	35	0.005	56	0.009			91	0.014
	AVG			57	0.009			133	0.020	164	0.025
GP-8	1	INCORPORATED	595,000	103	0.017			156	0.026	259	0.043
	2	(LEAVES)	597,000	52	0.009			162	0.027	214	0.036
	3		580,000	55	0.010	162	0.028			217	0.038
	AVG			70	0.012			159	0.027	230	0.039
GP-9	1	MIXED	558,000	35	0.006			143	0.026	178	0.032
	2	(LEAVES)	557,000	42	0.008	50	0.009			92	0.017
	3		505,000	26	0.005			60	0.012	86	0.017
	AVG			34	0.006			102	0.019	119	0.022
GP-10	1	SOLUTION	625,000	77	0.012	153	0.025			230	0.037
	2	(GAVAGED TO	625,000	91	0.015			448	0.072	539	0.087
	3	ANIMALS FED LEAVES)	625,000	34	0.005			85	0.014	119	0.019
	AVG			67	0.011			266	0.086	296	0.048
GP-11	1	SOLUTION	625,000	50	0.008			125	0.020	175	0.028
	2	(GAVAGED TO ANIMALS FED LEAVES AND STEMS)	625,000	302	0.048	216	0.035			518	0.083
	AVG			176	0.028					346	0.055
GP-C	1	NONE	0	0.7		0		0		0.7	

• TOXICOLOGY OF CHRONICALLY FED ^{90}Sr IN MINIATURE SWINE

Person in Charge: H. A. Ragan

This long-term project, first funded in 1958, was terminated in FY 76 and all remaining swine on the program have been killed. The project objective was to establish the dose-effect relationships following daily feeding of ^{90}Sr through the life spans of three generations of miniature swine. Present efforts are directed toward preparing for publication the data collected over the past 18 years.

COMMON TUMORS AND LESIONS IN CONTROL MINIATURE SWINE FED ^{90}Sr DAILY

Investigators:

H. A. Ragan and J. E. Lund

Technical Assistance:

S. Owzarski, D. Hunter and V. D. Tyler

Control miniature swine, averaging 9 yr of age had an approximately 45% incidence of benign tumors and 11% incidence of malignant tumors. Swine of comparable age, fed 1 or 5 μCi ^{90}Sr for their lifetime, had a similar incidence of benign tumors, but about a two-fold increase in malignant neoplasms. The occurrence of non-neoplastic lesions was similar in the three groups.

Annual Reports since 1958 have described the experimental design and effects of feeding ^{90}Sr daily to miniature swine for their lifetime. Histopathologic evaluations have been completed, computer-coded, and preliminary data accumulated for the control swine and the parent, F_1 and F_2 generations. The parent generation dams were started on daily feeding of ^{90}Sr at 9 mo of age; the F_1 generation was continued on the same feeding regimen and the females bred at 9 mo of age to produce the F_2 generation, which was fed ^{90}Sr on the same schedule as the F_1 generation. Periodic sacrifices were performed in both generations to determine ^{90}Sr body burdens, tissue distributions, and early biologic effects. This report is restricted to swine in the 1- and 5-μCi/day groups surviving at least 1 yr, most of which survived more than 5 yr.

Previous analyses of cumulative mortality data showed no differences in life spans of control swine and those from parent or offspring generations fed 1 or 5 μCi ^{90}Sr daily. The only biologic effect observed was a significant dose-related neutropenia in the F_1 and F_2 generations of both dose groups. Since radiation doses received in utero and after birth were the same for both groups, data from F_1 and F_2 generations were combined. Table 16.1 shows the percent of benign and malignant tumors in the various groups. The lowest incidence of both tumor types was seen in the parent generations of 1- and 5-μCi swine, but many of these swine were killed rather than left to complete their natural life span. There was no significant difference in benign tumor incidence in either the 1- or 5-μCi offspring generations when compared to the controls. There was, however, a significant increase ($P < 0.01$) in the incidence of malignant neoplasms in both the 1- and 5-μCi offspring, compared to controls.

Incidence figures for the most frequently observed tumors are shown in Table 16.2. The most common benign neoplasm was uterine leiomyoma; in some cases these became extremely large and necrotic, and were the immediate cause of death, usually because acute and chronic peritonitis developed. In other cases these tumors were small and their presence was unsuspected until necropsy. The other common benign tumor was hepatic

adenoma, in which a significant increase ($P < 0.05$) was observed in the 1- and 5-μCi offspring as compared to controls. The uterus was the tissue most frequently involved with malignant neoplasms in all groups. Lymphosarcoma, the other common malignant tumor, was increased in the 1-μCi offspring, but these were found at histologic examinations in isolated organs and were not the immediate cause of death.

Table 16.3 lists the most common non-neoplastic lesions observed. Only in rare instances were any of these lesions the immediate cause of death, but they contributed to the general age-related deterioration observed in all groups of elderly swine.

TABLE 16.1. Age at Death and Tumor Incidence in Control Miniature Swine and Those Fed 1.0 or 5.0 μCi ^{90}Sr Daily

GROUP	GENERATION	n	AGE (yr)[a]	BENIGN TUMORS (%)	MALIGNANT TUMORS (%)
CONTROL		94	8.8 ± 3.2	44.7	10.6
1 μCi/day	PARENT	24	7.0 ± 2.5	25.0	8.3
	F_1/F_2	62	9.8 ± 3.9	56.5	27.4
5 μCi/day	PARENT	10	6.2 ± 3.4	20.0	0
	F_1/F_2	33	8.8 ± 4.5	42.4	21.2

[a] MEAN ± 1 SD

TABLE 16.2. Percent Tumor Incidence in Control Miniature Swine and Those Fed 1.0 or 5.0 μCi ^{90}Sr Daily

	GROUP				
	CONTROL (94)[a]	1 μCi PARENT (24)[a]	1 μCi F_1/F_2 (62)[a]	5 μCi PARENT (10)[a]	5 μCi F_1/F_2 (33)[a]
ADENOMA					
LIVER	6.4	4.2	17.7	0	18.2
OTHER	3.2	0	4.8	0	0
LEIOMYOMA - UTERUS	38.3	20.8	25.8	20.0	30.3
CARCINOMA - UTERUS	4.3	4.2	8.1	0	6.1
CARCINOMA - OVARY	1.1	0	1.6	0	0
SARCOMA - UTERUS	1.1	0	0	0	6.1
MYELOPROLIFERATIVE DISORDER	4.3	0	0	0	3.0
LYMPHOSARCOMA	0	4.2	9.7	0	3.0

[a] NUMBER OF ANIMALS IN PARENTHESES

TABLE 16.3. Percent Incidence of the Most Common Lesions Observed in Control Miniature Swine and Those Fed 1.0 or 5.0 μCi ^{90}Sr Daily

LESION	CONTROL (94)[a]	1 μCi PARENT (24)[a]	1 μCi F_1/F_2 (62)[a]	5 μCi PARENT (10)	5 μCi F_1/F_2 (33)
ATHEROSCLEROSIS					
AORTA	23.4	4.2	40.3	0	18.2
CORONARY ARTERY	25.5	4.2	22.6	0	9.1
HEPATITIS	17.0	8.3	17.7	0	12.1
HYPERPLASIA - LIVER	16.0	0	25.8	0	15.2
NEPHRITIS	54.3	4.2	61.3	10.0	66.7
CYSTIC ENDOMETRIAL HYPERPLASIA	31.9	29.2	37.1	30.0	42.4

[a] NUMBER OF ANIMALS IN PARENTHESES.

• MALNUTRITION AND METAL TOXICITY

Person in Charge: H. A. Ragan

This is a new project, originally funded for FY 1976. Initial emphasis will be placed on evaluating the effects of iron deficiency on the absorption and tissue distribution of trace amounts of selected heavy metal pollutants given by intragastric gavage. Metals whose absorption is enhanced by iron deficiency will be further studied to determine their effects on hematopoiesis and immune competence when fed for prolonged periods to control and iron-deficient rats. Future studies will evaluate the toxicity of heavy metals in conjunction with other nutritional deficit states common in humans, e.g., protein, protein/calorie, and calcium deprivation.

Iron deficiency was selected for initial examination since it is probably the most common single nutritional disease in young children and women of child-bearing age. Despite the paucity of data on absorption of pollutant metals in iron-deficient subjects, it is known that some elements compete for iron-binding proteins in plasma and in cells, and some interfere with iron metabolism directly. Iron deficiency may enhance the absorption, translocation or transplacental passage of heavy metals, increasing the risk of toxic effects in the young, teratogenic effects in the fetus, or interference with iron metabolism in subjects already compromised in regard to their iron status. The effects of combined iron deficiency and exposure to heavy metal pollutants on immune competence are of particular concern with regard to carcinogenesis.

ABSORPTION OF POLLUTANT METALS IN IRON-DEFICIENT RATS

Investigator:

H. A. Ragan

Technical Assistance:

M. J. Pipes, E. T. Edmerson, S. L. English and M. C. Perkins

The gastrointestinal absorption of selected heavy metals was evaluated in rats with depleted tissue-iron stores and enhanced iron absorption, but prior to the development of severe anemia. The total body burden of lead, cadmium, mercury and zinc was significantly greater in iron-deficient rats than in litter-mate controls, whereas no difference in arsenic absorption was evident between the two groups. Control rats absorbed more vanadium than iron-deficient rats.

Previous annual reports have detailed the enhanced absorption and retention of plutonium, and alterations in its tissue distribution, in iron-deficient mice. These studies have been extended, in rats, to evaluate the influence of body-iron stores on the absorption of pertinent non-nuclear pollutant metals.

Female Wistar rats, weaned at 21 days of age, were fed either an iron-deficient or iron-replete diet until they were 70-90 days of age. Ten control and ten iron-deficient rats were then used to determine the absorption of each metal following intragastric gavage. Each gavage solution was prepared in citrate buffer with a final pH of approximately 3.5. After an 18-hr fast the appropriate solution was given by gavage and the rats killed 48 hr later to determine absorption and tissue distribution of the tracer dose of metal. In addition, just prior to necropsy a blood sample was obtained from each rat to evaluate the hematologic status; and sections of liver, spleen, and bone marrow were taken for histologic determination of tissue-iron stores. The GI tract was ligated and carefully excised from each carcass prior to obtaining other tissues.

Rats on the iron-deficient diet were only marginally anemic when compared with the control group, i.e., the mean combined values for volume of packed red cells (VPRC) of the iron-deficient groups were 39.9 ml/100 ml vs 46.6 ml/100 ml in an equal number of control rats. Although there was considerable variation in serum iron (SI) values, the mean for all iron-deficient rats was 197 $\pm$ 87 µg/dl vs 333 $\pm$ 35 µg/dl in the control groups. Histochemical staining of tissue revealed considerable particulate iron in the spleen, liver, and bone marrow of control rats and a paucity of nonheme iron in these tissues from iron-deficient rats. As an additional measure of iron status, nine iron-deficient and nine control rats were given ^{59}Fe by gavage. Control rats absorbed 11.1 $\pm$ 7.2% of the administered dose, whereas 35.1 $\pm$ 7.1% was absorbed by rats on the iron-deficient diet. This difference was highly significant ($P < 0.001$).

The total body burden of ^{210}Pb was approximately 28% of the administered dose in the iron-deficient rats, compared to approximately 5% in the control group (Table 17.1). There was considerable variation in body burden between rats, but excellent individual correlations, i.e., those with very high or low concentrations of lead in the carcass had corresponding levels in other tissues assayed. Bone, bone marrow, and muscle of iron-deficient rats accumulated greater relative concentrations of lead than did other tissues.

There was about an 8-fold increase in the absorption of ^{109}Cd in iron-deficient rats versus the control group, i.e., approximately 8% of the administered dose compared to 1% in the controls. Unlike lead, there was no tendency for one tissue to accumulate a greater concentration of cadmium than others (Table 17.2).

TABLE 17.1. Tissue Distribution of ^{210}Pb in Iron-Deficient and Control Rats 48 hr after Intragastric Gavage

			% DOSE/ORGAN					% DOSE/gram (x 10^3)			
VPRC (ml/100 ml)	SI (µg/100 ml)	CARCASS	LIVER	SPLEEN	KIDNEY	FEMUR	SERUM	BLOOD	MARROW	MUSCLE
IRON-DEFICIENT DIET (n = 10)										
45.2	188	26.5	0.63	0.031	--	0.54	0.30	58.4	5.83	0.90
4.7	119	21.3	0.54	0.046		0.43	0.70	48.3	5.00	1.00
CONTROL DIET (n = 10)										
49.9	282	4.4	0.13	0.003	--	0.03	0.04	10.5	0.25	0.04
3.3	53	4.2	0.12	0.003		0.03	0.09	7.6	0.24	0.09
P< 0.02	0.05	0.01	0.01	NS[a]		0.01	NS	0.01	0.01	0.02

[a]NS = NOT SIGNIFICANT

TABLE 17.2. Tissue Distribution of ^{109}Cd in Iron-Deficient and Control Rats 48 hr after Intragastric Gavage

		% DOSE/ORGAN					% DOSE/gram (x 10^3)			
VPRC (ml/100 ml)	SI (µg/100 ml)	CARCASS	LIVER	SPLEEN	KIDNEY	FEMUR	SERUM	BLOOD	MARROW	MUSCLE
IRON-DEFICIENT DIET (n = 10)										
45.6	251	5.9	1.86	0.011	--	0.0021	0.37	1.58	1.03	0.89
8.3	175	4.6	1.06	0.015		0.0016	0.64	2.07	0.89	0.51
CONTROL DIET (n = 10)										
52.8	333	0.8	0.28	0.001	--	0.0003	0.04	0.12	0.13	0.15
2.4	130	0.3	0.08	0.001		0.0001	0.03	0.07	0.06	0.07
P< 0.02	NS[a]	0.01	0.001	NS		0.01	NS	0.05	0.01	0.001

[a]NS = NOT SIGNIFICANT

The tissue distribution of vanadium is shown in Table 17.3. Interestingly, the control group had a mean body burden of vanadium 3.5 times greater than the iron-deficient group. The variation in absorption was considerable in the control group because of two animals; one absorbed greater than 6% and the other 4%. However, if these two are deleted, the absorption in the control rats is still 2-fold greater than in the iron-deficient group.

There were no significant differences in total body burdens of arsenic or in its tissue distribution in iron-deficient and control rats (Table 17.4).

The body burden of mercury was only slightly greater in the iron-deficient groups compared with the control groups (Table 17.5).

A highly significant difference in the whole-body burden of zinc was evident in the iron-deficient rats (Table 17.6).

TABLE 17.3. Tissue Distribution of ^{48}V in Iron-Deficient and Control Rats 48 hr after Intragastric Gavage

			% DOSE/ORGAN					% DOSE/gram (x 10^3)			
	VPRC (ml/100 ml)	SI (µg/100 ml)	CARCASS	LIVER	SPLEEN	KIDNEY	FEMUR	SERUM	BLOOD	MARROW	MUSCLE
					IRON-DEFICIENT DIET (n = 10)						
	37.0	96	0.52	0.076	0.0052	0.035	0.0092	5.1	--	0.36	1.12
	3.8	53	0.18	0.034	0.0020	0.013	0.0034	1.8		0.14	0.34
					CONTROL DIET (n = 10)						
	43.8	295	1.87	0.122	0.0082	0.117	0.0455	12.0	--	1.01	3.79
	3.3	50	1.88	0.120	0.0074	0.106	0.0485			1.09	5.44
P<	0.001	0.001	0.05	NS[a]	NS	0.05	0.05	NS		NS	NS

[a]NS = NOT SIGNIFICANT

TABLE 17.4. Tissue Distribution of ^{74}As in Iron-Deficient and Control Rats 48 hr after Intragastric Gavage

			% DOSE/ORGAN					% DOSE/gram (x 10^3)			
	VPRC (ml/100 ml)	SI (µg/100 ml)	CARCASS	LIVER	SPLEEN	KIDNEY	FEMUR	SERUM	BLOOD	MARROW	MUSCLE
					IRON DEFICIENT DIET (n = 10)						
	40.5	279	22.5	3.00	0.579	0.862	0.049	13.0	4771	40.3	58.3
	6.7	150	5.7	1.32	0.366	1.129	0.018	8.2	614	10.4	56.5
					CONTROL DIET (n = 10)						
	43.5	358	22.3	2.77	0.343	0.314	0.045	18.9	4427	44.1	41.7
	2.7	27	6.6	1.19	0.078	0.105	0.015	12.7	901	21.9	9.3
P<	NS[a]	NS	NS	NS	NS	NS	NS	NS	NS	NS	NS

[a]NS = NOT SIGNIFICANT

TABLE 17.5. Tissue Distribution of ^{203}Hg in Iron-Deficient and Control Rats 48 hr after Intragastric Gavage

	VPRC (ml/100 ml)	SI (µg/100 ml)	% DOSE/ORGAN					% DOSE/gram (x 10^3)			
			CARCASS	LIVER	SPLEEN	KIDNEY	FEMUR	SERUM	BLOOD	MARROW	MUSCLE
	IRON-DEFICIENT DIET (n = 10)										
	34.8	209	0.83	0.24	0.009	0.123	0.0018	5.7	8.7	0.67	1.11
	8.4	138	0.20	0.13	0.005	0.038	0.0005	2.5	3.7	0.17	0.41
	CONTROL DIET (n = 10)										
	40.9	365	0.66	0.15	0.005	0.091	0.0011	3.2	4.6	0.32	0.72
	1.3	59	0.16	0.07	0.002	0.037	0.0004	1.4	1.3	0.11	0.26
P<	0.05	0.01	0.05	NS[a]	0.05	NS	0.01	0.02	0.001	0.001	0.02

[a]NS = NOT SIGNIFICANT

TABLE 17.6. Tissue Distribution of ^{65}Zn in Iron-Deficient and Control Rats 48 hr after Intragastric Gavage

	VPRC (ml/100 ml)	SI (µg/100 ml)	% DOSE/ORGAN					% DOSE/gram (x 10^3)			
			CARCASS	LIVER	SPLEEN	KIDNEY	FEMUR	SERUM	BLOOD	MARROW	MUSCLE
	IRON-DEFICIENT DIET (n = 10)										
	37.8	287	19.9	4.29	0.25	0.44	0.22	38.0	84.9	26.2	101.1
	4.1	113	2.6	0.91	0.04	0.09	0.03	13.3	16.8	7.8	13.0
	CONTROL DIET (n = 10)										
	40.9	373	11.7	2.38	0.14	0.24	0.13	17.7	43.2	14.2	61.0
	1.5	30	3.3	0.84	0.05	0.08	0.04	7.8	16.6	6.1	19.5
P<	0.05	0.05	0.001	0.001	0.001	0.001	0.001	0.001	0.001	0.01	0.001

• LATE EFFECTS OF OIL SHALE POLLUTION

Person in Charge: J. E. Lund

This project, first funded in FY 1976 was designed to investigate the possible health hazard of dusts that may be produced in the processing of oil shale and the potential carcinogenicity of shale oil and shale oil fractions.

Dust generation from crushing and related operations and from the transportation of ore to crushing facilities is substantial. New equipment and methods can reduce this release of airborne particles to the atmosphere if a need for control measures is established. The extent to which such control measures are required may become a factor in the design of processes and facilities.

In view of the association of certain industrial dusts with pulmonary disease, it is important to investigate possible pulmonary effects from process or fugitive dusts early in the development of the technology.

Intratracheal instillation experiments were designed to define the toxic potential of oil shale materials. Two rodent species (rat and hamster) were given intratracheal doses of oil shale, spent shale, quartz (fibrosis control), methylcholanthrene and iron oxide (carcinogen positive control), and vehicle. The long-term study, consisting of repeated doses of the material, was begun in FY 1976.

Studies to be initiated in FY 1977 include a carcinogenesis assay of shale oil fractions determined to be mutagenic in the bacterial system (Ames assay) and aerosol exposure of rats and hamsters to oil shale particulates.

LATE EFFECTS OF OIL SHALE POLLUTION

Investigators:

J. E. Lund, K. E. McDonald, and L. G. Smith

Technical Assistance:

F. S. Gerber and L. S. Gorham

Studies on late effects of oil shale pollutants were initiated during FY 76. Tables 18.1 and 18.2 list the protocols for investigation of carcinogenic and fibrogenic potential of oil shale particulates. Animals in the long-term study (carcinogenesis) have one remaining intratracheal instillation of particulates to be given and will be observed for an additional 14 mo.

TABLE 18.1. Experimental Design for Study to Evaluate the Carcinogenic Potential of Oil Shale and Spent Shale Particulates.[a]

	NUMBER OF MALE AND FEMALE ANIMALS EXAMINED AT EACH SACRIFICE PERIOD						
	0 MO	12 MO		18 MO		24 MO	
TREATMENT GROUP		M	F	M	F	M	F
OIL SHALE (20 mg/DOSE)	10	5	5	5	5	20	20
OIL SHALE (5 mg/DOSE)	10	5	5	5	5	20	20
SPENT SHALE (20 mg/DOSE)	10	5	5	5	5	20	20
SPENT SHALE (5 mg/DOSE)	10	5	5	5	5	20	20
VEHICLE CONTROL (SALINE 0.4 ml)		5	5	5	5	20	20
SHELF CONTROL		5	5	5	5	20	20

[a] MATERIAL GIVEN INTRATRACHEALLY TO RATS AND HAMSTERS AT 5 BIMONTHLY INTERVALS.

TABLE 18.2. Experimental Design for Study to Evaluate the Fibrogenic Potential of Oil Shale and Spent Shale Particulates.[a]

TREATMENT GROUP	NUMBER OF MALE AND FEMALE ANIMALS EXAMINED AT EACH SACRIFICE PERIOD								
	0 MO	1 MO		2 MO		4 MO		6 MO	
		M	F	M	F	M	F	M	F
OIL SHALE (40 mg/DOSE)	5	8	8	8	8	8	8	8	8
SPENT SHALE (40 mg/DOSE)	5	8	8	8	8	8	8	8	8
POSITIVE CONTROL (QUARTZ, 40 mg/DOSE)	5	8	8	8	8	8	8	8	8
VEHICLE CONTROL (SALINE 0.4 ml)		8	8	8	8	8	8	8	8
SHELF CONTROL	5	8	8	8	8	8	8	8	8

[a] MATERIAL GIVEN INTRATRACHEALLY TO RATS AND HAMSTERS.

The animals held for 6 mo in the fibrosis study were recently killed, and lung tissues from all sacrifice periods are being analyzed for collagen content. Results are not available at this time; however it would appear, from examination of histologic sections, that oil shale and spent shale do not induce pulmonary fibrosis to the same degree as does quartz. Six months after intratracheal instillation, many of the shale particulates are present in macrophages in the alveolar spaces (Figure 18.1). Large granulomas and areas of fibrosis are not present in animals receiving these particulates but are common in those receiving quartz (Figure 18.2).

Preparations are under way to determine, by in vivo studies in rodents, whether the shale oil fractions which show mutagenic activity in bacterial assay (described elsewhere in this report) are carcinogenic in whole animals.

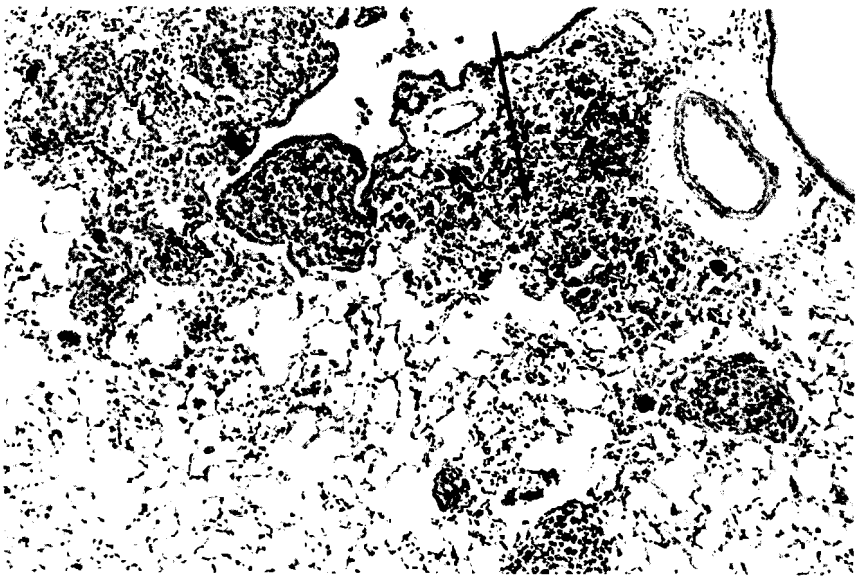

FIGURE 18.1. Accumulation of Spent Shale Particles in Peribronchiolar Alveolar Spaces 6 Mo Following Intratracheal Instillation

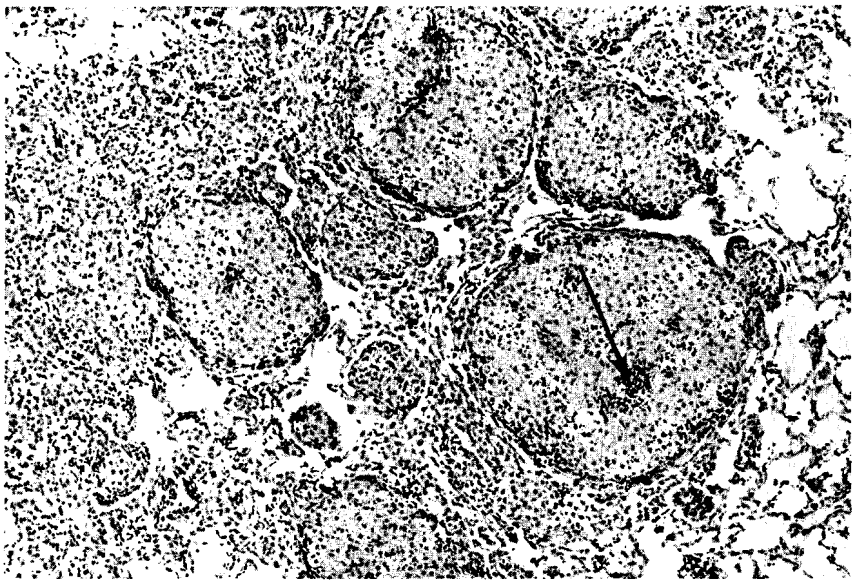

FIGURE 18.2. Multiple Granulomas in the Lung of a Hamster 6 mo Following Intratracheal Instillation of Quartz Particles

• MUTAGENICITY OF OIL SHALE

Person in Charge: R. A. Pelroy

Utilization of oil shale as a fuel source will release to the atmosphere many organic and inorganic materials. Many of these materials, especially the polyaromatic compounds and aromatic amines, are potentially carcinogenic. This project will test oil shale chemicals for potential carcinogenicity, using microbial and mammalian tissue-culture bioassays.

We have tested subfractions derived from crude shale oil for mutagenicity in the Salmonella typhimurium testor strains of Ames et al. Two fractions, one enriched in basic compound (e.g., aromatic amino acids), and one enriched in polynuclear aromatic compounds, were found to be highly mutagenic for S. typhimurium mutants, reverting both frame-shift and point mutations. These fractions are thus identified as potentially carcinogenic and will be tested to determine whether they cause tumor formation in mice employing techniques of tissue-culture cell transformation, followed by transplantation of transformed cells into recipient animals.

MICROBIAL TESTING OF SHALE OIL FOR POTENTIALLY CARCINOGENIC MATERIALS

Investigators:
R. A. Pelroy, V. G. Bushaw, and M. Petersen

Raw shale oil and the acidic, basic, polynuclear aromatic (PNA), and tar fractions from shale oil were tested for their mutagenicity against several of the Salmonella typhimurium testor strains of Ames et al., using a modification of their assay system. We identified two highly mutagenic fractions (the basic and PNA fractions) and one weakly mutagenic fraction, (the raw shale oil). Other fractions caused little or no increase in the frequency of mutation. We have been unable to demonstrate a requirement for metabolic activation of shale oil. On the other hand, addition of activating enzyme preparations from rat liver (S-9 enzymes) to the assay system consistently led to lower frequencies of mutation. Of all strains tested, S. typhimurium TA-100 is the most sensitive to mutation by the basic and PNA fractions.

The genetically marked S. typhimurium strains of Ames were used in three assay systems, each of which measured the frequency of mutation induced by a shale-oil fraction as compared to background mutation, i.e., in control or nonexposed cells. Increased mutational frequencies were considered as evidence that a given shale-oil fraction was potentially carcinogenic, requiring additional tests in animal or tissue-culture systems.

Initial experiments, employing the standard Ames assay system (Method 1), i.e., direct agar plating of shale-oil fraction plus testor strain onto selective medium, were unsatisfactory due to heavy killing of cells. Killing was not increased by activating (S-9) enzymes, suggesting that metabolic activation of chemical components present in the shale oil or its fractions was not responsible for loss of viability. At this time, we do not know the role that metabolic activation plays in shale-oil-induced mutagenesis of the Salmonella testor strains.

We attempted to overcome the killing problem by exposing the testor strains to shale-oil fractions in liquid media, with or without S-9 enzymes. At the end of the exposure time, cells were collected onto a 0.45-μ filter by filtration and washed. The cells were then resuspended in sterile nutrient broth and allowed to grow to stationary phase before plating an aliquot of the cells onto selective medium for visualizing mutated cells (Method 2). The results from these "timed" assays were an improvement over Method 1; however, mutational frequencies were still very low relative to control cultures.

As a final attempt to utilize the S. typhimurium testor strains, we modified Method 2 by omitting the filtration step and simply plating a small sample of exposed cells directly onto selective medium (Method 3). We also made viability counts of testor cells before and after exposure to shale-oil fractions. This method was employed in accumulating the data described in the balance of this report.

The mutation frequencies and viability data obtained after exposure of S. typhimurium TA-100 to shale oil are shown in Table 19.1. This strain responds to mutagens that cause both point and frame shift mutations, although it is generally more selective for the point mutagens. Included in the table are data from control experiments using the mutagen-carcinogens 2-aminoanthracine (2AA) and 2-nitrosofluorene (2NF). As can be seen, exposure of cells to raw shale oil or the tar fraction of shale oil resulted in, at most, a slight increase in mutation of TA-100. On the other hand, the basic and PNA fractions were highly mutagenic to the testor strain, increasing the frequency over unexposed controls 60- to 800-fold. The rat liver S-9 enzymes consistently lowered the mutation frequencies for the basic and PNA fractions, although enzymes present in the S-9 fraction were capable of converting inactive promutagens (carcinogens) to active mutagens, as shown by the data for 2-aminoanthracine. The latter compound requires metabolic activation.

TABLE 19.1. Mutational Frequencies of S. typhimurium TA-100 After Exposure to Shale-Oil Fractions

FRACTION TESTED	S-9[a]	REVERTANTS/10^8 VIABLE CELLS
BASIC[b]	+	600[c], 250[c]
BASIC	-	12000, 70000
PNA	+	1440, 800
PNA	-	16000, 25000
RAW	+	85, 160
RAW	-	120, 250
TAR	+	85, 120
TAR	-	125, 140
2AA[d]	+	800, 1550
2AA	-	18, 50
2NF[e]	-	375, 900
NO ADDITION	+	130, 125
NO ADDITION	-	67, 120

[a] S-9 = CRUDE MICROSOMAL ENZYME FRACTION FROM RAT LIVER; ANIMALS EXPOSED TO AROCLOR BY INTRA PERITONEAL INJECTION/ AMES et al. (1975)

[b] ALL SHALE-OIL FRACTIONS ADDED AS 25 µl FOR EACH (2 ml) SAMPLE. EXPOSURE OF CELLS BY METHOD 3.

[c] REPLICATE EXPERIMENTS

[d] 2AA = 2-AMINOANTHRACINE

[e] 2NF = 2-NITROSOFLUORENE

Comparable data on the mutational effects of exposing S. typhimurium TA-98 to these shale-oil fractions are shown in Table 19.2. This testor strain is highly specific for detecting frame-shift mutagens. As can be seen, the basic and PNA fractions caused significant increases in the mutational frequencies of TA-98. The crude S-9 microsomal enzymes lowered the mutational response, in this case nearly to background levels. In contrast to TA-100, strain TA-98 gave a weaker mutational response to all shale-oil fractions tested; on the other hand, this strain was almost as responsive to 2AA as strain TA-100. It should be noted that 2AA causes mutation only when "metabolically activated" by S-9 enzymes. Thus, the S-9 fraction used in this experiment was effective in such activation.

TABLE 19.2. Mutational Frequencies of S. typhimurium TA-98 After Exposure to Shale-Oil Fractions

FRACTION TESTED	S-9[a]	REVERTANTS/10^8 VIABLE CELLS
BASIC[b]	+	19
BASIC	-	100
PNA	+	27
PNA	-	267
RAW	+	18
RAW	-	30
TAR	+	4.0
TAR	-	4.0
2AA[c]	+	512
2AA	-	5
2NF[d]	-	5700
NO ADDITION	+	4
NO ADDITION	-	6

[a] S-9 = CRUDE MICROSOMAL ENZYME FRACTION FROM RAT LIVER; ANIMALS EXPOSED TO AROCLOR BY INTRAPERITONEAL INJECTION/ AMES et al. (1975)

[b] ALL SHALE-OIL FRACTIONS ADDED AS 25 µl FOR EACH (2 ml) SAMPLE. EXPOSURE OF CELLS BY METHOD 3.

[c] REPLICATE EXPERIMENTS

[d] 2AA = 2-AMINOANTHRACINE

Extensive testing of known carcinogens by the Ames assay has shown a correlation between carcinogenicity and bacterial mutation (mainly frame-shift) of greater than 90 percent. Thus, agents which induce frame-shift mutations especially warrant testing for carcinogenic activity. The observed increases in mutational frequencies in cells exposed to the PNA and basic fractions are not surprising. The PNA fraction is rich in polycylic aromatic compounds, which, as a class, contain many known carcinogens, and which are generally mutagenic for the special testor strains of S. typhimurium. The same can be said for the basic fraction, which contains aromatic amines. However, it is surprising that we have been unable to demonstrate metabolic activation for these fractions. Generally, polyaromatic hydrocarbons require metabolic activation for mutation of the testor strains. It may be

TABLE 18.2. Experimental Design for Study to Evaluate the Fibrogenic Potential of Oil Shale and Spent Shale Particulates.[a]

TREATMENT GROUP	NUMBER OF MALE AND FEMALE ANIMALS EXAMINED AT EACH SACRIFICE PERIOD								
	0 MO	1 MO		2 MO		4 MO		6 MO	
		M	F	M	F	M	F	M	F
OIL SHALE (40 mg/DOSE)	5	8	8	8	8	8	8	8	8
SPENT SHALE (40 mg/DOSE)	5	8	8	8	8	8	8	8	8
POSITIVE CONTROL (QUARTZ, 40 mg/DOSE)	5	8	8	8	8	8	8	8	8
VEHICLE CONTROL (SALINE 0.4 ml)		8	8	8	8	8	8	8	8
SHELF CONTROL	5	8	8	8	8	8	8	8	8

[a] MATERIAL GIVEN INTRATRACHEALLY TO RATS AND HAMSTERS.

The animals held for 6 mo in the fibrosis study were recently killed, and lung tissues from all sacrifice periods are being analyzed for collagen content. Results are not available at this time; however it would appear, from examination of histologic sections, that oil shale and spent shale do not induce pulmonary fibrosis to the same degree as does quartz. Six months after intratracheal instillation, many of the shale particulates are present in macrophages in the alveolar spaces (Figure 18.1). Large granulomas and areas of fibrosis are not present in animals receiving these particulates but are common in those receiving quartz (Figure 18.2).

Preparations are under way to determine, by in vivo studies in rodents, whether the shale oil fractions which show mutagenic activity in bacterial assay (described elsewhere in this report) are carcinogenic in whole animals.

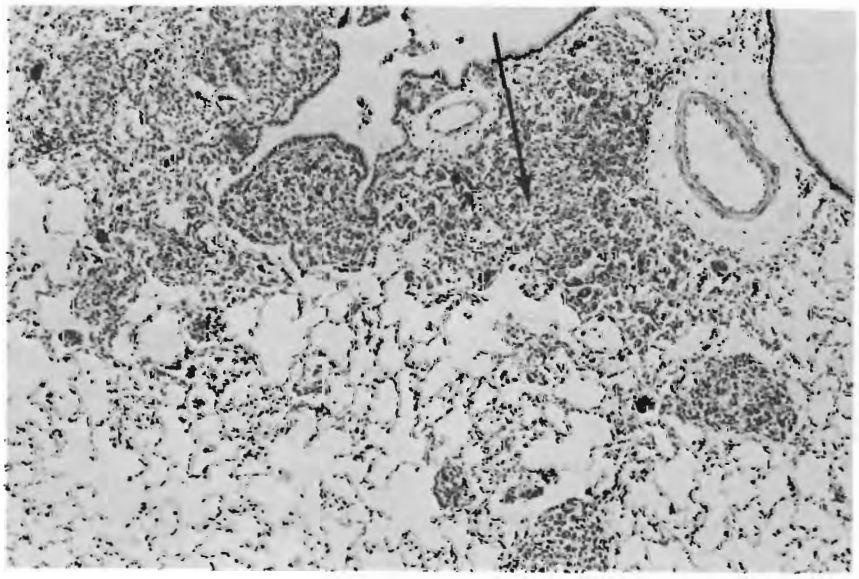

FIGURE 18.1. Accumulation of Spent Shale Particles in Peribronchiolar Alveolar Spaces 6 Mo Following Intratracheal Instillation

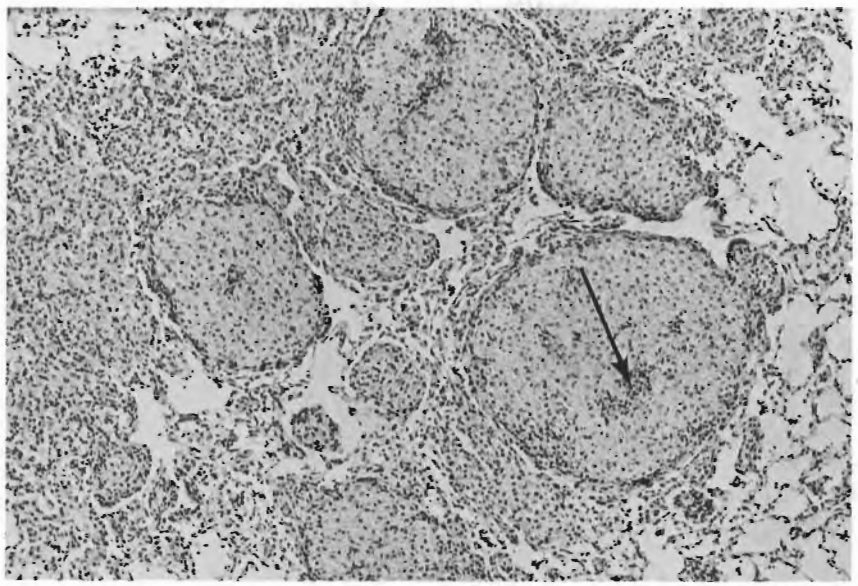

FIGURE 18.2. Multiple Granulomas in the Lung of a Hamster 6 mo Following Intratracheal Instillation of Quartz Particles

that the mutagenic components of the PNA and basic fractions do not require activation, and that we detect only these materials with our assay system. It is also possible that activating enzymes present in S-9 are inactivated by the shale-oil fractions, which seems likely, since mutational frequencies for 2AA are lowered in the presence of PNA.

On the basis of the work described here, both the basic and PNA fractions should be tested for their capacity to induce carcinogenesis in animal systems. We also feel that alternate microbial test systems should be developed. Specifically, we plan to develop microbial transformation systems that utilize DNA instead of living cells. Such systems should help to eliminate the severe killing problems which have been only partially solved by Method 3. Moreover, it will be desirable to have alternative microbial systems with the simplicity and flexibility of the Ames assay, but which can be used for testing toxic organic materials which may be produced from the refining and upgrading of raw shale oil.

H_2 PRODUCTION FROM GLUCOSE BY THE PHOTOSYNTHETIC BACTERIUM, *RHODOPSEUDOMONAS SPHEROIDES*

Investigator:
R. A. Pelroy

Hydrogen production from the photosynthetic decomposition (photodissimilation) of glucose by R. spheroides has been increased more than 4-fold by selection of a glucose-utilizing mutant; i.e., one capable of using the sugar as its sole source of carbon and energy. Physiological measurements of the effect of various gases and various soluble nitrogen sources implicate cellular nitrogenase as the enzyme which synthesizes hydrogen gas.

The nonsulfur photosynthetic bacterium, Rhodopseudomonas spheroides, is capable of catalyzing the synthesis of H_2 by coupling the photodissimilation of a carbon source to the anaerobic "photo-oxidation" of water. This process, unique to certain photosynthetic bacteria, is closely linked to cellular nitrogen metabolism, and is primarily dependent on two factors: First, it is absolutely necessary that cells are limited (starved) for reduced nitrogen. Second, it is necessary that molecular N_2 be either absent, or limited, in its exposure to a culture producing H_2. A third factor, which determines the yield of H_2, is the capacity of the cell to completely degrade or catabolize a given carbon source to CO_2. The more extensive this catabolism, the more electrons (meaning their biological equivalents, the reduced electron carriers) are potentially available for H_2 synthesis. Thus, H_2 biosynthesis by R. spheroides can be considered in terms of two separate physiologic functions: a) catabolism of a substrate to CO_2 plus a reduced electron carrier, and b) the enzymatic conversion of the electron carrier to H_2. It follows, therefore, that if the photodissimilation of carbon substrates by bacteria is to become a useful means of H_2 production, both of these functions must be controlled from the point of view of maximizing rates and total yields of H_2. Moreover, both functions can, to some extent, be changed by mutation to give strains particularly suited to H_2 biosynthesis. As one example of this approach we have selected glucose-utilizing mutants which are capable of a more efficient photodissimilation of glucose to H_2 plus CO_2, because glucose is a major

component of most of the materials which might ultimately serve as a source of substrates for H_2 biosynthesis (e.g., cellulosic wastes, sugar beets, etc.).

Tables 19.3 and 19.4 show the main features of H_2 synthesis from the photodissimilation of glucose by two strains of R. spheroides. A mutant strain, GLN, was selected for the capacity to use glucose as its sole source of carbon. Strain W, the parental type, is incapable of growth at the expense of glucose.

As can be seen in Table 19.3, column 4, the mutant GLN produced more H_2 than the wild type, W. This was true whether strains were grown under argon (Ar) or under molecular N_2, with a total H_2 yield 4-5 times greater for GLN than for W. The greatest amount of H_2 was produced by the culture incubated under Ar, where 36% of the maximum possible yield was obtained. On the other hand, growth of R. spheroides under a N_2 atmosphere substantially decreased the yields of H_2, with greater decreases occurring with increased surface area (from 2 cm^2 to 17 cm^2). Ammonium-ion also inhibited H_2 synthesis by GLN; however, as will be shown below, this inhibition was basically different from the inhibition caused by N_2.

The data presented in Table 19.4 show that both GLN and W formed about the same amount of H_2 during the photodissimilation of malate. The yields obtained from this dicarboxylic acid were much better than the corresponding values for glucose, with about a 71% conversion of malate by GLN, and approximately 78% conversion of malate by W. In all other respects, the behavior of GLN and W were qualitatively the same: H_2 synthesis was inhibited by N_2 and by ammonium ions, and the degree of H_2 inhibition was increased by increasing the surface-to-volume ratios of the cultures.

The distribution of carbon (from glucose) into cells, CO_2 and supernatant (CO_2-free, cell-free, spent medium) is shown by the data in Table 19.5. The samples are from the same experiment as the data in Table 19.3. The amount of glucose carbon taken up by cells (column 3) ranged from 16-32%, while

TABLE 19.3. H_2 Yields From Glucose: Strains GLN and W

SAMPLE	CO_2[a]	CELLS[a]	SUPERNATANT[a]	PERCENT	REMAINING SUBSTRATE[a]
GLN-Ar[a]	32.9	15.5	44.4	92.8	25.0
GLN-N_2	19.6	31.5	31.8	85	0
GLN-Ar PLUS NH_4Cl	5.7	20.8	54.0	80.5	6
W-N_2	5.4	18.5	69.9	93.8	0

[a] THE VALUES FOR CARBON ARE THE AVERAGE OF THREE REPLICATE SAMPLES, AND ARE EXPRESSED IN TERMS OF THE CONCENTRATION OF THE SUBSTRATE, ie IN μ MOLE EQUIVALENTS OF GLUCOSE

TABLE 19.4. H_2 Yields From Malate: Strains GLN and W

SAMPLE	SURFACE AREA, cm^2	NITROGEN SOURCE	H_2[a]	CO_2[a]	RATIO	% CONVERSION[e]
GLN-Ar[a]	17	0.05% YEAST EXTRACT	451.6	282.6	1.60	70.6
GLN-N_2[b]	2	0.05% YEAST EXTRACT	120.1	156.7	0.8	20
W-Ar[c]	17	0.05% YEAST EXTRACT	467	268	1.74	78
W-N_2[d]	2	0.05% YEAST EXTRACT	178.8	172	1.74	30
GLN-N_2	17	0.05% YEAST EXTRACT	10.4	197.8	0.08	1.76
GLN-Ar	17	5 mM NH_4Cl	55.2	122.3	0.45	9.0

[a] VALUES FOR CO_2 AND H_2 ARE THE AVERAGE OF THREE REPLICATE SAMPLES
[b] MUTANT GLN, Ar ATMOSPHERE
[c] MUTANT GLN, N_2 ATMOSPHERE
[d] WILD-TYPE W, Ar ATMOSPHERE
[e] WILD-TYPE W, N_2 ATMOSPHERE

TABLE 19.5. Carbon Recovery After Photodissimilation of Glucose[a]

SAMPLE	SURFACE AREA, cm^2	NITROGEN SOURCE	H_2[a]	CO_2[a]	RATIO	% CONVERSION[e]
GLN-Ar[a]	17	0.05% YEAST EXTRACT	435.6	197.3	2.21	36
GLN-N_2[b]	2	0.05% YEAST EXTRACT	167.1	128.5	1.30	14
W-Ar[c]	17	0.05% YEAST EXTRACT	98.7	48.2	1.02	9
W-N_2[d]	2	0.05% YEAST EXTRACT	32.9	32.4	1.02	3
GLN-N_2	17	0.05% YEAST EXTRACT	0	117.3	0	0
GLN-Ar	17	5 mM NH_4Cl	0	34.2	0	0

[a] VALUES FOR CO_2 AND H_2 ARE THE AVERAGE OF THREE REPLICATE SAMPLES
[b] MUTANT GLN, Ar ATMOSPHERE
[c] MUTANT GLN, N_2 ATMOSPHERE
[d] WILD-TYPE W, Ar ATMOSPHERE
[e] WILD-TYPE W, N_2 ATMOSPHERE

the amount present in the supernatant (column 4) ranged from 30 to 70% of the available carbon. Both N_2 and ammonium-ions increased the amount of nonglucose carbon in the supernates. Only the GLN samples incubated under Ar contained a significant amount of free glucose at the end of the experiment (column 6).

Figure 19.1 shows the probable identities of the small-molecular-weight carbon compounds remaining in the supernatant fractions shown in Table 19.4. Provisional identification of these compounds was made by gas liquid chromatography (GLC) of the corresponding silyated derivatives.

As can be seen (Figure 19.1A), α and β glucose were found in the supernates of GLN incubated under Ar constituting about 56% of the carbon in this fraction. No small-molecular-weight carbon compound was found in the CO_2-free supernatant fraction of the GLN samples incubated under N_2 (data not shown); whereas approximately 27% of the total glucose carbon (about half of the supernatant carbon) of W was present, mostly as gluconate, and a lesser amount as an unknown compound with a retention time suggesting a 5-carbon sugar or sugar-acid (Figure 19.1B).

The last observations are noteworthy since they pinpoint one of the slowest steps

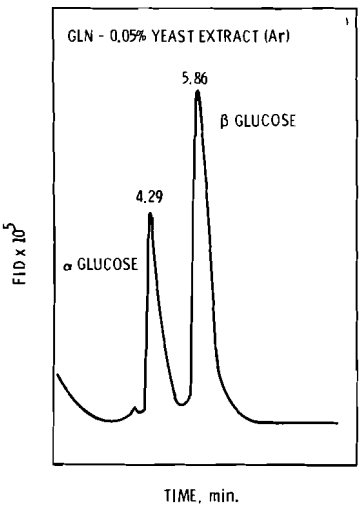

A

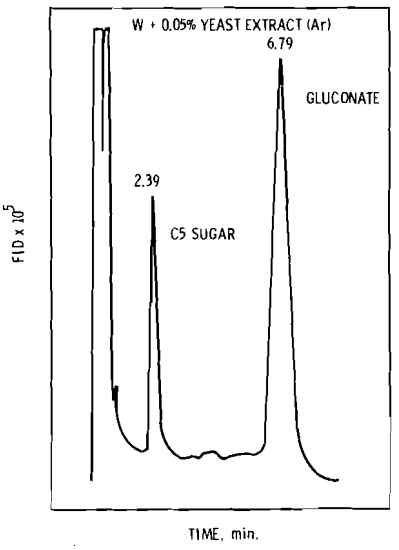

B

FIGURE 19.1. Metabolites in Supernates of Spent Media After Hydrogen Production by Strain GLN of R. spheroides. A. Samples from replicate cultures of W, incubated under an argon atmosphere. B. Samples from replicate cultures of W, incubated under argon. Provisional identification of the metabolites was made by gas liquid chromatography of the corresponding silyated derivatives using a flame ionization detector (FID).

in the metabolism of glucose by the wild-type strain W. The 6-carbon sugar-acid, gluconate, is the product of the first step in the sequence of reactions which constitute the pathway for glucose catabolism by R. spheroides. Since approximately 20% of the total glucose carbon was left as gluconate, the step responsible for converting gluconate to the next metabolite of the pathway was comparatively slow. Conversely, the mutant GLN did not accumulate gluconate to any appreciable extent. These two observations suggest that glucose metabolism in the wild type is blocked at the second step of the pathway, resulting in an inability to metabolize gluconate, thus leading to the accumulation of this metabolite in spent media. This interpretation is in agreement with the results of Doudoroff and Syzmona (J. Gen. Microbiol. 22:167, 1960). The origin of C5 is not known, but it may be formed through the action of one of the alternate pathways of glucose metabolism (e.g., hexose monophate shunt). Five-carbon sugars, it should be noted, are not formed via the main pathway of glucose catabolism used by R. spheroides.

There are several conclusions that can be drawn from these data. First and most important, genetic selection for glucose utilization yielded a strain of R. spheroides with increased capacity of H_2 production. Second, the final yield of H_2 was strongly influenced by two major factors: the concentration of ammonium ions, and the presence of molecular N_2. Third, a large amount of glucose carbon was incorporated in the cell material or excreted into the medium. This represents "wasted" energy from the point of view of H_2 synthesis and must be minimized. It is likely that much of this material is present in the form of polymeric carbohydrates (Ormerod et al.; Arch. Biochem. 94:449, 1961). The fact that we were unable to account for all of the carbon in terms of low-molecular-weight soluble compounds (i.e., in the supernatant fractions) also tends to support this idea.

Nitrogen inhibition of H_2 synthesis by R. spheroides suggests involvement of the enzyme nitrogenase (N_2ase) in the process. If this is so, then it is probable that N_2 inhibits by serving as an alternate acceptor for electrons generated during the catabolism of glucose to CO_2. The reduction in the ratios of H_2/CO_2 (Tables 19.3 and 19.5) observed for cultures incubated under N_2 is evidence for this interpretation. This conclusion can be supported by the following argument: For each mole of CO_2 produced from glucose, 4 molar equivalents of reduced electron carriers are available either for H_2 synthesis or for reduction of N_2 to ammonium ion. Thus, to the extent that N_2 (or any other acceptor) competes with hydrogen ions for these electrons, the ratio of H_2/CO_2 will be reduced. The fact that N_2 reduced the H_2/CO_2 ratio strongly suggests such a competition for electrons. It should be noted that N_2ase is one of the few enzymes capable of interacting specifically with molecular N_2, and the only enzyme that is known to reduce N_2 to ammonium ion.

A second line of experimental evidence also supports the idea that N_2ase is active in H_2 synthesis. The rationale for this set of experiments is based on the observation that acetylene can inhibit nitrogen fixation by serving as a substrate for N_2ase, thus effectively competing with N_2. Briefly, when acetylene and N_2 are both present, acetylene competes with the natural substrate in accepting electrons from the enzyme. This leads to the formation of ethylene, which can be accurately measured by gas chromatography. Thus acetylene reduction constitutes a sensitive in situ measurement of N_2ase activity. The data shown in Figure 19.2 are from an experiment designed to compare the effects of Ar, N_2 and acetylene on H_2 synthesis by the mutant GLN. The upper curve of Figure 19.2 shows H_2 production in a culture with an argon atmosphere. As can be seen, argon, which is an inert gas with respect to nitrogenase, allows the maximum evolution of H_2 gas under the experimental conditions of Figure 19.2. In separate experiments (data not shown), it was found that H_2 production in an argon atmosphere was not affected by changing the surface area of the culture. The middle curves were obtained using gas phases of argon + 5% (v/v) acetylene, or purified N_2. The surface areas for the

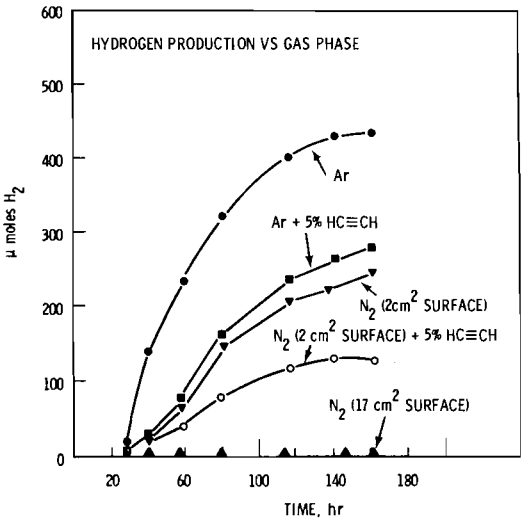

FIGURE 19.2. Hydrogen Synthesis by Mutant GLN as a Function of Gas Phase. Hydrogen was measured by gas chromatography using a thermal conductivity detector.

argon-acetylene and N_2 mixtures were 17 and 2 cm^2, respectively. As shown, both gas phases inhibited H_2 production to a level about 50% of that obtained for a pure argon atmosphere.

To some extent, the inhibitions caused by N_2 + acetylene appeared to be cumulative, as shown by the curve for N_2 gas plus 5% acetylene (surface area 2 cm^2, about 75% of that for the argon culture). However, as seen earlier in Tables 19.3 and 19.4, the strongest inhibition of H_2 synthesis occurred in the culture incubated under N_2, but with the surface area increased to 17 cm^2. Thus, H_2 production by R. spheroides was inhibited by both acetylene and N_2. These data, along with the data in Tables 19.3 and 19.4 on the effect of N_2 on H_2/CO_2 ratios, are strong evidence that the nitrogenase of R. spheroides is the terminal enzymatic step of H_2 production.

• OIL SHALE HYDROCARBON METABOLISM

Person in Charge: A. J. Gandolfi

The purpose of this project was to investigate the metabolism and disposition of possibly carcinogenic or mutagenic organic materials associated with the processing of shale oil. An example is the presence of polycyclic aromatic hydrocarbons in the crude oil and spent shale.

One task of this study was to investigate the effects of inhaled oil shale and spent shale dusts on the pulmonary enzyme systems responsible for the metabolism of polycyclic organic materials. A second task was to study the disposition of representative hydrocarbons from intratracheally administered spent shale. These initial studies were to give an overview of the possible fate and effects of particulate-bound polycylic organic material.

This project was first funded in FY 1976. Initial experiments were conducted but funding was subsequently terminated.

EFFECT OF INTRATRACHEALLY ADMINISTERED OIL SHALE AND SPENT SHALE ON PULMONARY BIOTRANSFORMATION ENZYME ACTIVITY

Investigators:

A. J. Gandolfi and C. A. Shields

Technical Assistance:

A. W. Endres

Rats were dosed intratracheally with suspensions of oil shale, spent shale, or methylcholanthrene/iron oxide. The activities of some important biotransformation enzymes in the lungs and liver were measured to determine any enzyme inductions. None were found.

The processes used to extract the shale oil produce polycyclic organic materials (POM), some of which are potentially carcinogenic or mutagenic (see Pelroy, et al. this Annual Report). Many POM are known to induce the enzymes that biotransform them to toxic intermediates, believed to be the ultimate carcinogens or mutagens. In this project, our primary objective is to evaluate oil shale and spent shale for their capacity to cause changes in the levels and activities of enzymes in the lung responsible for POM metabolism and, perhaps, formation of carcinogenic intermediates.

Many POM are biotransformed by the aryl hydrocarbon hydroxylase enzyme system to yield a phenol or an arene oxide intermediate. The arene oxide is a reactive intermediate which has been shown to covalently bind to nucleic acids and proteins, and it is this interaction which suggests arene oxide as the ultimate carcinogen derived from some POM. The arene oxide may be isomerized to a phenolic product, hydrolyzed by epoxide hydrase, or conjugated with glutathione by glutathione S-aryl epoxide transferase. Recent evidence has demonstrated that metabolites may be recycled to form additional toxic arene oxides. Thus, removal of the metabolites by immediate reaction with glucuronic acid via UDP-glucuronyl transferase also appears to be an important detoxification reaction (See Figure 20.1). Alterations in any of the above processes may alter the existing level of arene oxide and thus its efficacy as a carcinogen/mutagen.

Rats were anesthetized with ether and intratracheally injected, weekly, with 20 mg of one of the following: oil shale, spent shale, or standard POM (methylcholanthrene, 3 mg) attached to ferric oxide particles. Periodically, groups of rats were removed from the regimen and sacrificed 2 weeks following their last injection (to minimize the effects of the ether). The livers and lungs were removed and assayed for their content of the following biotransformation enzymes: aryl hydrocarbon hydroxylase, epoxide hydrase, UDP-glucuronyl transferase, and glutathione-S-aryl epoxide transferase. The enzyme levels were compared to a control group (ferric oxide alone) and to the animals dosed with the standard POM/ferric oxide mixture.

We expected the POM(s) to elute from the particulates over a period of time (see Gandolfi and Shields, this Annual Report) thus possibly resulting in inductions of biotransformation enzymes with the increased level persisting over several days. This was not observed. Figure 20.2

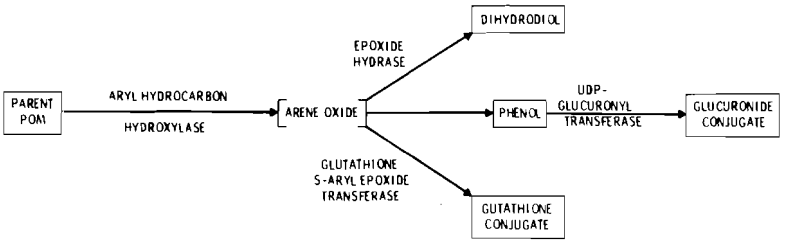

FIGURE 20.1. Biotransformation Pathways for Polycyclic Organic Material (POM).

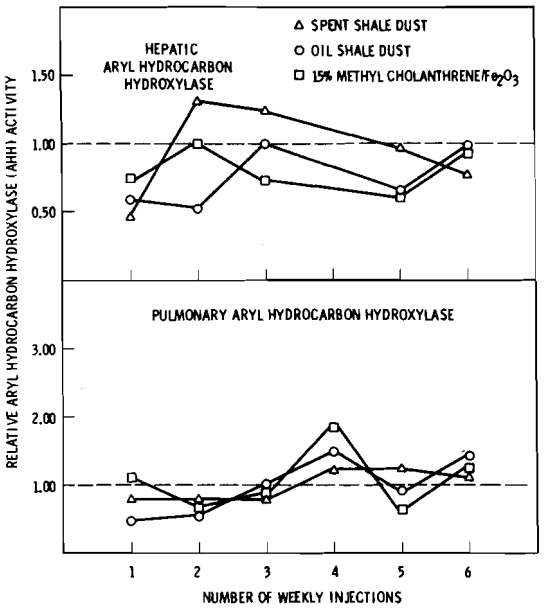

FIGURE 20.2. Effect of Intratracheally Administered Oil Shale and Spent Shale on Aryl Hydrocarbon Hydroxylase Activity

shows the relative aryl hydrocarbon hydroxylase level in the livers and lungs of animals exposed to POM-bearing particulates, compared to control animals. The enzyme levels were erratic, with no large or sustained inductions even with the methylcholanthrene/ferric oxide treatments. Very similar results were noted with the three other enzyme levels tested: epoxide hydrase, UDP-glucuronyl transferase, glutathione-S-aryl epoxide transferase.

To confirm that pulmonary biotransformation could be induced, rats received a single intratracheal injection of standard POM suspended in a gelatin solution. Two weeks later pulmonary aryl hydrocarbon hydroxylase activity in these animals was found to be induced at over twice the level observed in control animals.

These preliminary results suggest that POM bound to particulate, as administered by intratracheal injection in this experiment, may not be capable of inducing a general increase in the level of POM biotransformation enzymes in the lung.

ABSORPTION OF BENZO-α-PYRENE FROM INTRATRACHEALLY ADMINISTERED SPENT SHALE

Investigators:

A. J. Gandolfi and C. A. Shields

Tritiated benzo-α-pyrene was adsorbed onto spent shale particles at realistic processing levels. The rate of elution of this ^{3}H-benzo-α-pyrene from the spent shale was determined in vivo and in vitro.

During the processing of oil shale, aromatic hydrocarbons, such as benzo-α-pyrene, are produced and can adhere to the resulting spent shale dust.

We are investigating the elution of a polycyclic aromatic hydrocarbon (benzo-α-pyrene) from spent shale labeled with this hydrocarbon at a level normally produced during the processing of oil shale to spent shale. Spent shale was enriched with 6 ppm ^{3}H-benzo-α-pyrene by coating the spent shale with a benzene solution of the tritiated benzo-α-pyrene and then evaporating the residual benzene.

To test how well the benzo-α-pyrene was attached to the spent shale, the labeled spent shale particles were placed in saline or growth media and the rate of elution of the radioactivity from the particles determined. Figure 20.3 shows that even with changes in the media, a maximum of 7% of the attached radioactivity elutes in 12 days. Thus the benzo-α-pyrene is apparently tightly attached to the spent shale particles.

Male Wistar rats were injected intratracheally with 10 mg of the ^{3}H-benzo-α-pyrene-enriched spent shale (10^{7} dpm) and serially sacrificed. The lungs were removed in toto and the trachea, bronchi, and lung lobes individually isolated. The

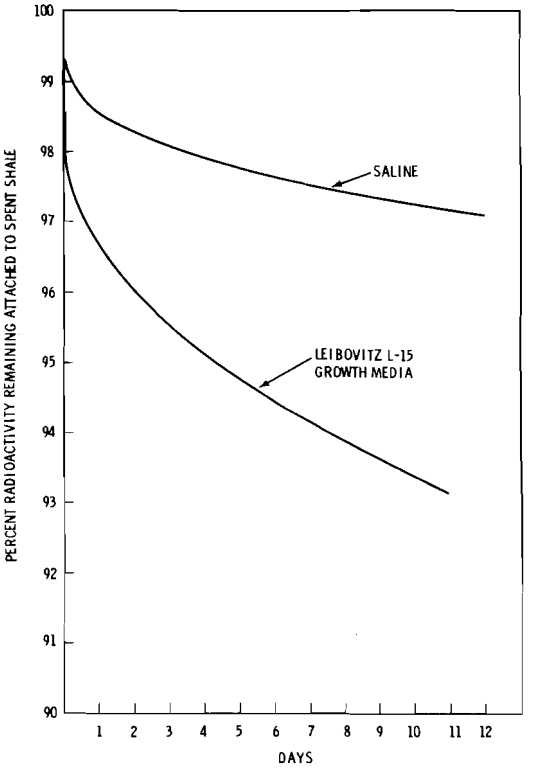

FIGURE 20.3. Elution of Radioactivity from ^{3}H-Benzo-α-Pyrene Enriched Spent Shale

radioactivity was determined in these tissues and is shown in Table 20.1. There was a rapid decrease in the radioactivity in the trachea and bronchi while that associated with the lungs decreased more slowly.

Investigations are in progress to determine if the ^{3}H-benzo-α-pyrene is still attached to the spent shale or is eluted and localized in the lung tissue.

TABLE 20.1. Distribution of ^{3}H Following ^{3}H-Benzo-α-Pyrene Spent Shale Injection

NO. DAYS AFTER DOSE	TOTAL DPM ± S.D.[b] TRACHEA x 10^{3}	BRONCHI x 10^{3}	LUNG HOMOGENATE x 10^{6}
0	77.8	252.6	11.7 ± 0.8
0.5	39.4	81.7	9.0 ± 0.8
1	27.1	33.6	10.4 ± 1.1
2	12.3	24.0	10.0 ± 1.3
3	13.9	23.8	8.0 ± 0.7
5	5.4	19.3	9.0 ± 1.0
6	(2.2)[c]	11.8	10.8 ± 1.7
8	2.2	14.8	7.0 ± 1.9
12	2.6	<17.3>	6.0 ± 0.9
15	4.1	17.9	6.3 ± 2.6
22	15.9	31.3	4.9 ± 1.5

[a] ANIMALS RECEIVED 10 mg SPENT SHALE / ^{3}H-BENZO-α-PYRENE (APPROXIMATELY 10^{7} dpm).

[b] FOUR ANIMALS WERE SACRIFICED FOR EACH TIME PERIOD

[c] <> WIDE VARIATION IN FOUR ANIMALS

• ALVEOLAR CLEARANCE OF METAL OXIDES

Person in Charge: C. L. Sanders

Metal oxides produced during the combustion of fossil fuels constitute a potential health hazard to human populations. The alveolar macrophage and the Type I alveolar epithelium are involved in the initial cellular response to metal oxides in the lung via the phagocytic process. Solubilization of the metal oxides in these cells leads to early cellular damage which, in the case of cadmium monoxide, leads to acute death at initial alveolar depositions of about 100 μg Cd. Investigations will continue into the early pathologic sequelae in the lung from Cd. Studies with radioactive Cd and Pb will be carried out to determine the sites of binding of these metals in the lung. Life-span investigations in rats will determine the pathologic (carcinogenic) properties of inhaled lead and cadmium monoxides.

EARLY FATE AND ACUTE MORTALITY FROM INHALED CADMIUM MONOXIDE

Investigators:

C. L. Sanders, R. R. Adee, and G. J. Powers

Severe pulmonary effects resulted from inhalation of cadmium monoxide by rats, possibly due to the rapid solubilization of cadmium monoxide and binding of cadmium to membrane sulfhydryl groups.

Female Wistar SPF rats approximately 70 days old were exposed to aerosols of cadmium monoxide (CdO). Exposure was for 30 to 60 min, nose-only, using the same technique as in lead monoxide exposures (see elsewhere in this Annual Report). The mass median aerodynamic diameter of the CdO aerosol was 3.72 ± 0.18 μm, with a geometric standard deviation of 1.98 ± 0.10; count median diameter was 0.35 ± 0.09 μm. The amount of Cd present in tissue samples was determined following wet ashing by atomic absorption.

Four groups of rats were exposed to CdO aerosols: (1) 101 rats were exposed to CdO in three separate subgroups, the lung burdens at 1 day after exposure being 38.1 ± 7.7 μg Cd; (2) 70 rats were exposed to CdO in one group with a lung burden at 1 day after exposure of 19.5 ± 9.3 μg Cd; (3) 16 rats were given an intraperitoneal injection of 0.5 mg $Zn(NO_3)_2$ just prior to CdO exposure; (4) 15 rats were given an intraperitoneal injection of 80 mg WR-2721 (S-2-[3-aminopropylamino]ethyl phosphorothioic acid hydrate) just prior to CdO exposure, and 18 rats were given an intraperitoneal injection of 80 mg WR-2721 just after CdO exposure. The amount of Cd found in the lungs at 1 day after exposure for rats in groups 3 and 4 was 35.0 ± 8.0 μg.

An additional group of 10 rats was given about 250 mg of CdO suspended in 1 ml of water by stomach tube and the rats were killed 7 days later. Tissue samples from these and all other animals were taken for Cd analysis and for histopathologic and electron microscopic examinations.

No particulate or other electron-dense material was seen in macrophages or epithelial cells of the alveoli following CdO exposure. The liver contained more Cd than the lung at 1 day after exposure (Table 21.1). Less than 10% of the initial alveolar deposition of Cd was found in the lung at 3 days after exposure (Table 21.1). Injection of either Zn or WR-2721 had no effect upon Cd clearance or translocation.

Only 0.017% of Cd given to rats by stomach tube was found in the liver at 7 days after gavage, indicating that less than 1% of the CdO was solubilized in the gut and transported into the body.

Rats with 20 μg or 38 μg Cd in their lungs at 1 day after exposure to CdO aerosols exhibited severe pulmonary reactions, which were fatal to most rats by 3 days postexposure (Figure 21.1). The pulmonary response to Cd consisted of acute pulmonary edema, resulting in swelling and lysis of

TABLE 21.1. Distribution of Cd in Lung and Liver at Various Time Intervals Following Inhalation of CdO.

TREATMENT	SURVIVAL TIME POST-EXPOSURE, DAYS	AMOUNT OF Cd, µg		NUMBER OF ANIMALS
		LUNG	LIVER	
CdO ONLY	1	38 ± 7.7	54 ± 19	73
	2	17 ± 3.4	15 ± 4.3	11
	3	11 ± 5.1	8.7 ± 6.4	4
	8	8.7 ± 3.1	--	6
	26	--	4.5 ± 0.4	2
CdO ONLY	1	20 ± 9.3	21 ± 7.8	18
	2	13 ± 3.2	--	25
	3	9.9 ± 1.5	--	13
	7	8.5 ± 2.0	--	4
	91	3.0 ± 0.8	5.6 ± 1.3	10
CdO + 0.5 mg $Zn(NO_3)_2$	1	37	26	1
	2	17 ± 9.6	18 ± 10	6
	3	13 ± 3.3	11 ± 1.8	4
CdO + 80 mg WR-2721 PRIOR TO CdO	4	13	11	1
	7	10	16	1
CdO + 80 mg WR-2721 AFTER CdO	1	34 ± 7.9	39 ± 9.0	7
	2	21 ± 8.3	9.5 ± 5.4	7
	3	20 ± 5.5	13 ± 4.9	3

alveolar cells and engorgement of capillaries with red blood cells. Pretreating rats with zinc caused only a slight decrease in mortality from inhaled CdO (Figure 21.2). Pretreating rats with WR-2721 had a marked effect on improving survival following CdO exposure; postexposure treatment with WR-2721 had no effect on survival of rats exposed to CdO (Figure 21.2).

Cadmium is known to have a strong affinity for sulfhydryl groups on the cell membrane. That the Cd may be influencing membrane function and integrity by binding to sulfhydryl groups is supported by the protection of WR-2721 against lethal pulmonary effects. Zinc is closely associated chemically with cadmium and biologically, both metal cations are bound to metallothionine; however, zinc did not protect against the lethal effects of Cd. The lethal acute action of CdO in lung may be due to the rapid solubilization of CdO and the binding of Cd to membrane sulfhydryl groups, resulting in profound changes in membrane function.

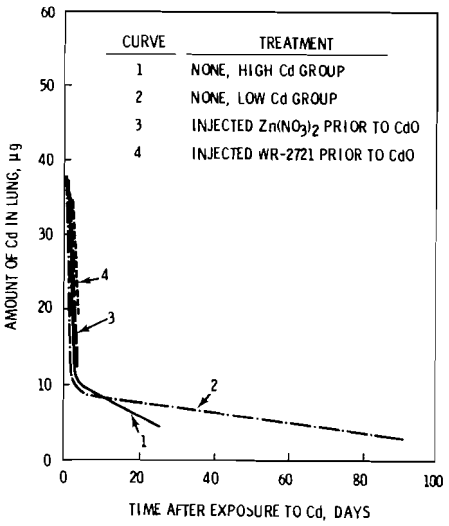

FIGURE 21.1. Amount of Cd Present in the Lung as a Function of Time After Inhalation and Treatment with $Zn(NO_3)_2$ and WR-2721.

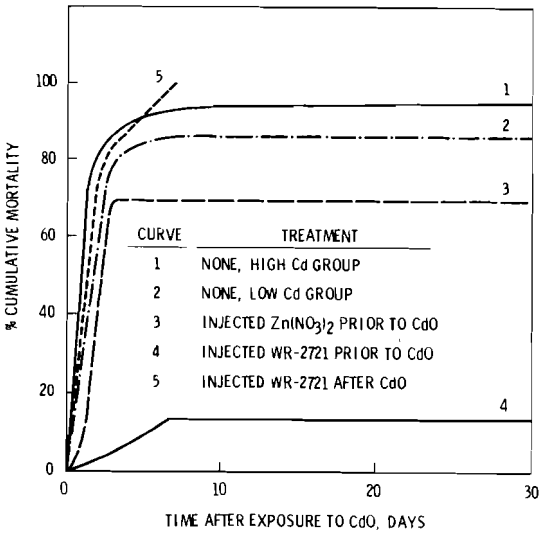

FIGURE 21.2. The Lethal Effect of Inhaled CdO on Rats as Influenced by Treatment With $Zn(NO_3)_2$ and WR-2721.

EFFECTS OF CADMIUM ON RED BLOOD CELL MEMBRANES

Investigators:

P. T. Johns, C. L. Sanders, and G. J. Powers

In vitro pretreating of rat red blood cells with WR-2721 protected them from the increased osmotic fragility and loss of potassium usually caused by incubation with cadmium.

A previous report described the acute pulmonary effects in rats resulting from the inhalation of CdO and the protection against these effects by pretreatment with the sulfhydryl compound WR-2721 prior to inhalation of CdO. The effect of Cd on red blood cell (RBC) membranes was also examined.

Red blood cells were obtained by heart puncture from female SPF, untreated Wistar rats. The RBCs were washed and diluted in 0.9% NaCl to a concentration of about 200 x 10^6 ml and incubated with various chemicals in a shaking water bath at 37°C. Osmotic fragility and loss of potassium into the medium were measured after incubation. The amount of Cd bound to RBC was also determined.

The Cd cation exhibited a damaging effect on RBC as demonstrated by an increased osmotic fragility (Figure 21.1) and by an increased loss of potassium (Figure 21.2). Cd was tightly bound to RBCs and was not removed by four washings. WR-2721 prevented the effects of Cd, the drug being more effective in preventing potassium leakage than in preventing osmotic lysis (Figures 21.3 and 21.4). Zinc totally prevented the effects of Cd on osmotic fragility at a level of 5 mM Zn (Figure 21.3). However, zinc did not prevent the Cd-induced potassium leakage nor did Zn by itself cause an increased potassium leakage from RBCs. Mercuric ions were at least an order of magnitude more effective than Cd in inducing a potassium leakage from RBCs (Figure 21.4).

In some ways the in vivo studies with inhaled CdO and injected WR-2721 paralleled in vitro observations with RBCs, in that WR-2721 protected against both the lethal effects of inhaled CdO in rats and against the effects of Cd on osmotic fragility and potassium leakage on RBCs. Both in vivo and in vitro studies indicate a toxic action of Cd upon membrane sulfhydryl groups.

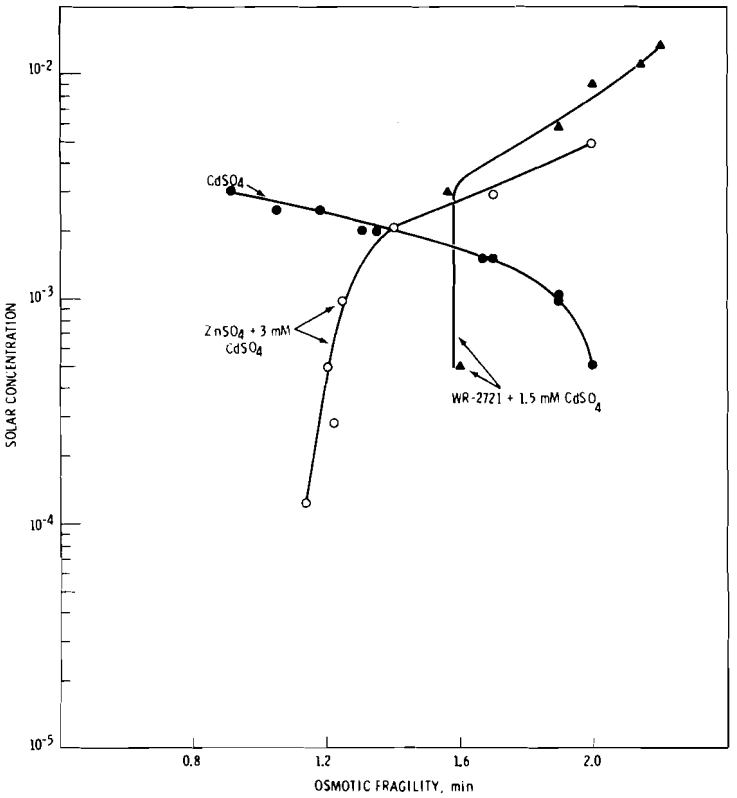

FIGURE 21.3. Influence of Increasing Concentrations of $CdSO_4$, Increasing Concentrations of $Zn(NO_3)_2$ in the Presence of 3 mM $CdSO_4$, and of Increasing Concentrations of WR-2721 in the Presence of 1.5 mM $CdSO_4$ Upon the Osmotic Fragility of Rat Red Blood Cells. Each sample was incubated for 100 min prior to measurement of fragility. Each point represents one sample.

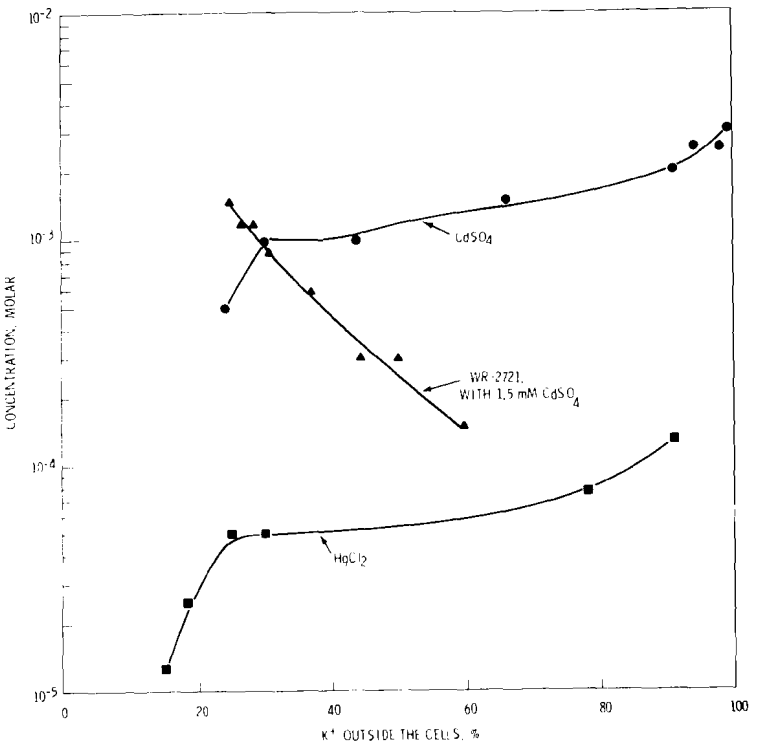

FIGURE 21.4. Influence of Increasing Concentrations of $CdSO_4$, Increasing Concentrations of WR-2721 in the Presence of 1.5 mM $CdSO_4$, and of Increasing Concentrations of $HgCl_2$ Upon the Leakage of Potassium into the Extracellular Medium. Samples containing Cd were incubated for 100 min. Samples containing Hg were incubated for 30 min. Each point represents one sample.

EARLY FATE OF INHALED LEAD MONOXIDE

Investigators:

C. L. Sanders and R. R. Adee

Inhaled lead monoxide is soluble in the lungs of rats, the particles being phagocytized by macrophages and Type I alveolar epithelium prior to their dissolution. It is also cytotoxic.

Lead exposure from combustion of fossil fuels and leaded gasoline continues to occur in the United States. Lead oxides and suboxides appear to be the primary chemical form produced by combustion of fuel, with lead monoxide being more toxic than metallic lead or other less soluble lead compounds. We are investigating the early fate and late pathologic effects of inhaled lead compounds in the lung.

Female Wistar SPF rats approximately 70 days old were exposed to an aerosol of lead monoxide (PbO) generated by a Wright Dust Feed Mechanism and an elutriator. The PbO dust was administered in an exposure chamber to rats placed in specially cut "Coke" bottles, resulting in a nose-only exposure of the animals. Rats were exposed for 1 hr. The mass median aerodynamic diameter of the PbO was 2.62 ± 0.20 μm, with a geometric standard deviation of 2.07 ± 0.14 and a count median diameter of 0.17 ± 0.04 μm.

Groups of five animals were killed by halothane overexposure at 1, 3, 7, 14, 21, 28, 35, 42, 49, 56, 63, 70, 77, and 91 days after exposure. The lungs were fixed at 20 cm H_2O with 2% glutaraldehyde following tracheal cannulation. Lead was determined in ashed and acid-dissolved samples by atomic absorption spectroscopy.

The initial alveolar deposition was 300 ± 118 μg Pb. Approximately 50% of the Pb deposited in the alveoli was cleared into the blood during the first day after exposure; about 90% of the initial alveolar deposition was cleared from the lung by 7 to 14 days after exposure. About 5% of the alveolar deposition was retained in the lung from 21 to 91 days after exposure with a comparatively long biological half-life (Table 21.2). While the skeleton is known to concentrate soluble lead, we are unable as yet to determine skeletal Pb content due to interference from the high salt content of the ashed and solubilized bone samples. Column chromatographic separation of the Pb is needed prior to measuring with atomic absorption spectroscopy.

TABLE 21.2. Fate of Inhaled Lead Monoxide in Rats

TIME AFTER EXPOSURE, days	% INITIAL ALVEOLAR DEPOSITION ($\bar{x}$ ± S.D.)			
	LUNG	PULMONARY LYMPH NODES	LIVER	KIDNEY
1	54 ± 21	5.0 ± 1.1	13 ± 8.3	8.0 ± 2.5
3	18 ± 4.3	4.7 ± 1.5	8.7 ± 3.1	5.0 ± 1.6
7	12 ± 3.0	4.0 ± 1.0	5.7 ± 1.6	3.2 ± 1.0
14	7.3 ± 2.5	6.0 ± 1.0	7.0 ± 1.6	3.3 ± 0.9
21	4.0 ± 1.6	4.3 ± 2.1	6.0 ± 1.9	4.7 ± 1.5
28	3.3 ± 1.1	2.1 ± 1.0	3.2 ± 0.5	2.1 ± 0.6
35	4.3 ± 2.9			
42	4.7 ± 1.0			
49	4.7 ± 0.6			
56	5.3 ± 1.1			
63	3.7 ± 0.7			
70	5.3 ± 0.7			
77	4.7 ± 2.3			
91	5.0 ± 2.1			

Uptake of inhaled Pb by the pulmonary lymph nodes, liver and kidney was rapid, occurring mostly during the first day after exposure, and accounting for 5% to 13% of deposited lead.

The intrapulmonary distribution of inhaled PbO was determined by examination of paraffin- and plastic-embedded samples of lung tissue. Sections were stained with Mallory's hematoxylin (saturated with calcium carbonate) for light microscopic examination or with uranyl acetate and lead citrate for electron microscopic examination. Lead oxide particles were seen in alveolar macrophages and alveolar epithelial cells with the light microscope (Figure 21.5). Lead particles were not seen later than 14 days after exposure.

Five lung samples were examined with the electron microscope at 1, 3, 7, 14, 21, and 28 days after exposure. Lead monoxide particles were found almost exclusively either in alveolar macrophages or within Type I alveolar epithelial cells (Figures 21.6-21.9). No lead particles were seen in lung samples taken later than 21 days after exposure.

Based on both light and electron microscopic observations, it was estimated that at 1-14 days after exposure, about 80-90% of the inhaled PbO was phagocytized and retained within macrophages, and 10-20% was retained by Type I alveolar epithelium.

Uptake of PbO by alveolar epithelium usually occurred in perinuclear regions of the Type I cell rather than in the more attenuated cytoplasmic regions of the cell. Individual epithelial cells contained only one aggregate of PbO in their cytoplasm (Figures 21.6 and 21.7). Macrophages, on the other hand, contained numerous phagolysosomes loaded with PbO (Figures 21.8 and 21.9). Evidence of solubilization of phagocytized PbO and recrystallization of ions was seen in some macrophages (Figure 21.8). Lead was markedly toxic to macrophages, as shown by the numerous cells with cytotoxic alterations, and the macrophage-related cell debris associated with lead particles in alveolar air spaces (Figures 21.8 and 21.9).

An inflammatory reaction was seen soon after lead inhalation as evidenced by an intravascular accumulation of neutrophils in the alveolar capillaries, proliferation of macrophages and a hypertrophy of Type I alveolar epithelial cells (Figure 21.7). The inflammatory response appeared to have subsided by 91 days after exposure.

These studies indicate that (1) inhaled lead monoxide is highly soluble in the lung, being rapidly cleared from the lung into the blood stream, where it is carried to extrapulmonary tissues; (2) both alveolar macrophages and Type I alveolar epithelium participate in the phagocytosis of PbO, with solubilization of PbO probably occurring mostly within these cell types; and (3) PbO is cytotoxic to macrophages and alveolar epithelium.

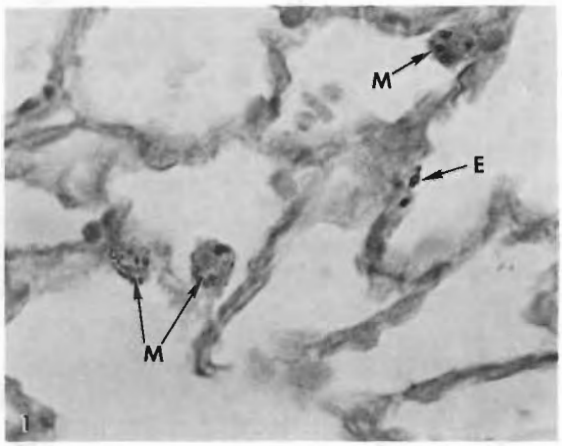

FIGURE 21.5. Localization of Lead Monoxide with Alveolar Macrophages (M) and Epithelial Cells (E). Stained with Mallory's hematoxylin saturated with calcium carbonate 3 days after inhalation. (800X).

FIGURE 21.6. Epithelial Localization of Inhaled Lead Monoxide in Type I Cells 3 Days After Exposure. The lead must pass through epithelium (E), interstitium(I), and endothelium (En) to reach the blood stream. (7500X)

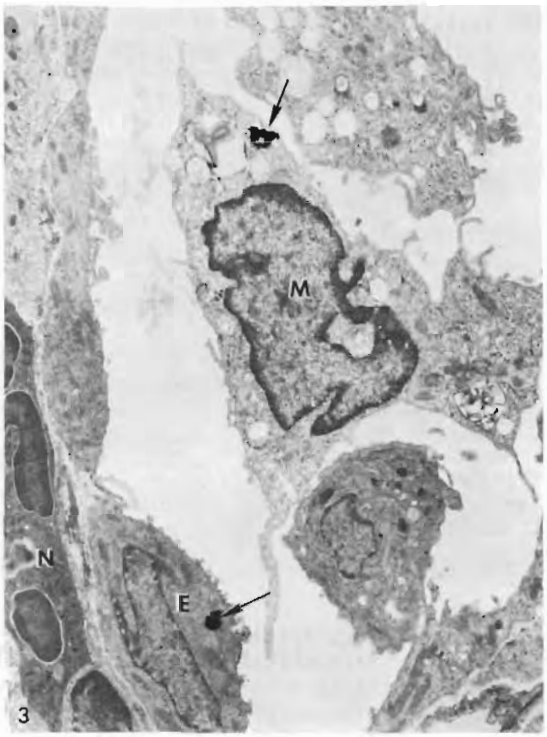

FIGURE 21.7. Localization of Lead Monoxide (3 Days After Exposure) in Alveolar Macrophage (M) and Alveolar Epithelium (E). Note the presence of a neutrophil (N) in the capillary and the hypertrophy of the Type I alveolar epithelium. (3000X).

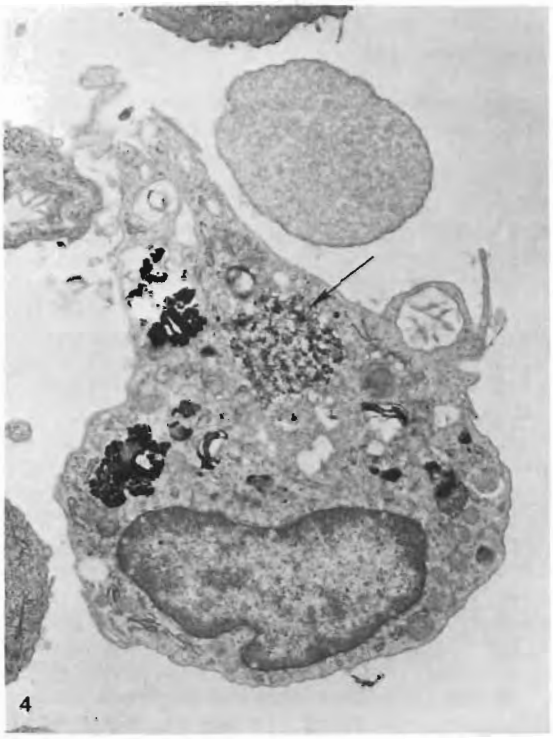

FIGURE 21.8. Localization of Lead Monoxide (3 Days After Exposure) in Phagosomes of an Alveolar Macrophage. Note the apparent recrystallization of lead ions (arrow) following solubilization of PbO in the cell. (4000X).

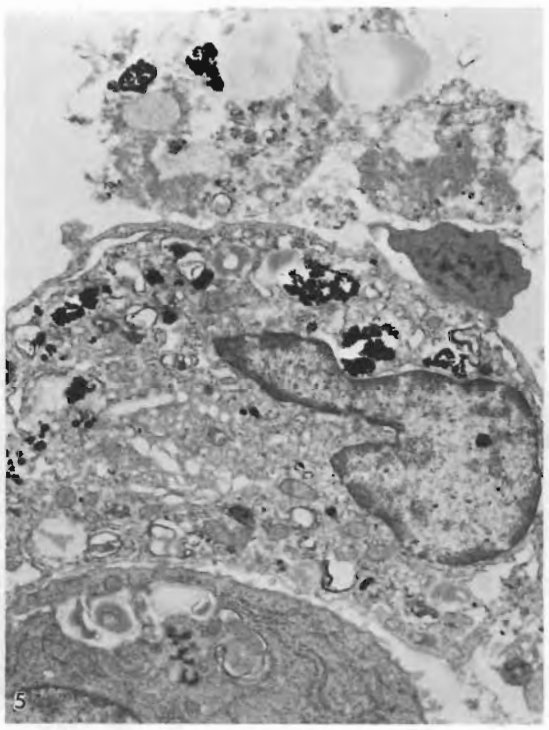

FIGURE 21.9. Damage of Alveolar Macrophages (3 Days After Exposure) Which had Phagocytized Lead Monoxide. Note the vacuolization in the cytoplasm of the intact macrophage and the cell debris associated with lead particles from a macrophage that has died and lysed. (4000X).

ULTRASTRUCTURAL STUDIES OF ALVEOLAR EPITHELIUM FOLLOWING TANNIC ACID FIXATION

Investigator:
R. R. Adee

Additional treatment with tannic acid provides better preservation of biological specimens prepared for transmission electron microscopy. The tannic acid also acts as a mordant for binding heavy metals for obtaining greater contrast. This was demonstrated in the preservation of lamellar bodies of Type II alveolar epithelial cells.

Recently the value of tannic acid, which contains low molecular weight galloylglucoses, has been recognized for its ability to better preserve biological specimens prepared for transmission electron microscopy. The tannic acid penetrates the tissues rapidly, stabilizing membranes and fibrillar components, with better retention of soluble protein in the cytoplasmic matrix. Tannic acid apparently also acts as a mordant between osmium-treated structures and heavy metals, enabling much greater contrast in thin sections viewed with the electron microscope.

Adequate fixation of lung tissue is of particular concern in our laboratory. Previously, the lung was instilled with an aldehyde, cut into small tissue blocks, post-fixed in osmium tetroxide, dehydrated and embedded in epoxy resin. Thin sections obtained from these blocks were doubly grid-stained with uranyl acetate and lead citrate. When we treated the tissues after osmium fixation with 2% tannic acid (Eastman P422) in cacodylate buffer (0.2 M pH 7.2) for 1/2 hr, it was apparent that the extra- and intracellular structures, especially membranes, were better preserved and showed higher contrast.

Of special interest to us were Type II epithelial cells (Figure 21.10). The cytoplasm is differentially and heavily stained compared to the surrounding lung parenchyma. Without tannic acid treatment,

FIGURE 21.10. Type II Epithelial Cell of Rat Lung. M = mitochondria, LB = lamellar bodies, arrow indicates site of lamellar body formation within mitochondria. (12,500X).

the lamellar (LB) bodies would be extracted during the dehydration process. In this photomicrograph, the mitochondria (M) and lamellar bodies are well preserved. Note the formation of lamellar bodies within some of the mitochondria (arrow).

Figure 21.11 shows excellent preservation of the fine structure of the membranous whorls of the lamellar bodies. At higher magnification (Figure 21.12) the periodicity of these membranes can easily be measured (in this case, about 40Å - 45Å). This measurement is of special importance in determining the origin of lung tumor cells. For example, if there were some doubt whether a tumor cell had evolved from a Type II cell or a macrophage, this could be resolved by comparing the lamellar body of the Type II cell with lamellar structures in other cells such as macrophages (Figure 21.13).

Tannic acid treatment appears very promising in studies of membranes in the lung and other tissues.

FIGURE 21.11. Lamellar Body of a Type II Epithelial Cell Showing Good Membrane Preservation with Tannic Acid Treatment. (50,000X).

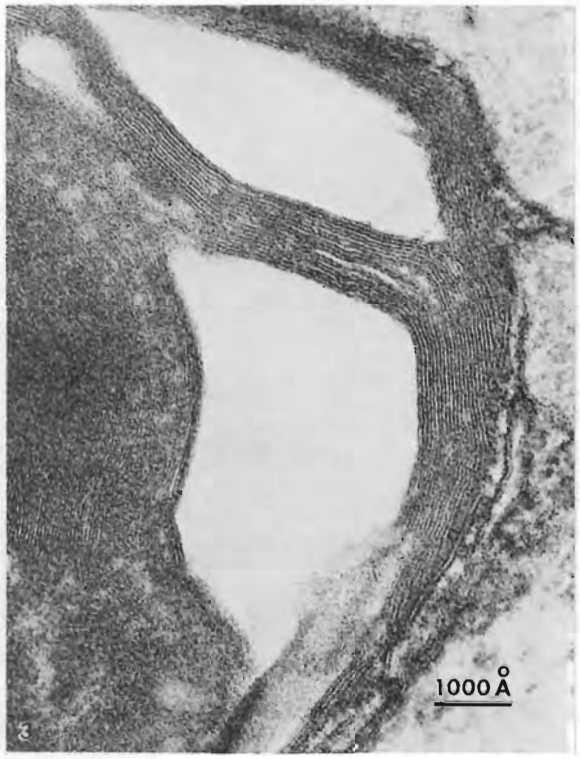

FIGURE 21.12. With Higher Magnification of a Lamellar Body, the Periodicity of the Membrane Structure (40Å - 45 Å) Can Easily be Measured. (125,000X).

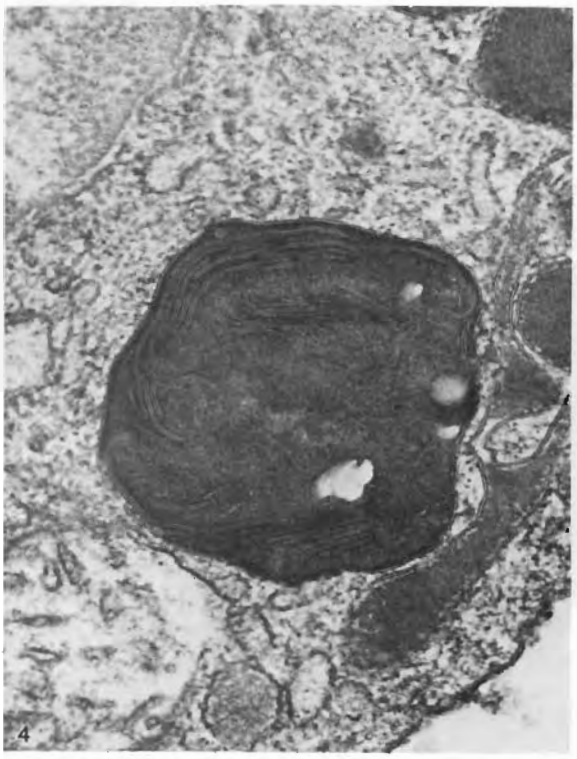

FIGURE 21.13. Lamellar Structure Within a Pulmonary Macrophage is Clearly Defined for Comparison with the Structure Shown in Figure 21.12. (62,000X).

• TOXICITY OF CO, NO_x, SO_x, AND FLY ASH

Person in Charge: A. J. Gandolfi

This project sought to define, in an animal model, the biological effects of exposure to pollutant atmospheres which might develop around large-scale fossil-fuel-burning power plants. Most previous studies related to the health effects of air pollutants have focused on one pollutant material administered at levels higher than actual environmental concentrations; this study was to have been concerned with health effects of combinations of pollutants administered at realistic concentrations.

This project received EPA "Pass Through" funding in FY 1976, but was terminated by ERDA as of September 30, 1976.

DESIGN AND PERFORMANCE OF AEROSOL EXPOSURE SYSTEM

Investigators:

A. J. Gandolfi, W. H. Hodgson, and J. H. Chandon

Technical Assistance:

R. Roadifer

An exposure system designed to deliver precise levels of NO_x, SO_x, and CO in combination with a fly ash aerosol is described.

Most of the effort in this project was directed towards the design, construction, and testing of an atmospheric pollutant animal exposure system. Due to the importance of humidity and temperature in determining the toxicity of atmospheric pollutants, a system was installed that could supply temperature- and humidity-regulated air to the exposure chambers. The exposure system (Figure 22.1) consisted of four hexagonal chambers, each capable of housing 48 rats on a single level, connected to a filtered controlled source of humid, temperature-regulated air. Gas lines delivered precise amounts of SO_2, NO_2, and CO via a series of metering valves to the individual chambers. Fly ash aerosols were generated with a Wright Dust Feed Mechanism and mixed with the incoming humid air just prior to entering the chamber. The chamber gas concentrations were monitored with a battery of calibrated gas analyzers (NO_x, SO_x, CO, and ozone). The aerosols were characterized from filter paper and cascade impactor samples.

At a chamber air flow rate of 10 cfm, consistent and reproducible concentrations of CO, SO_2 and NO_2 could be produced daily. The relative humidity could be easily adjusted from 50-90% with the aid of a Bemco Temperature-Humidity Controller. The fly ash samples used for these tests were from the Colstrip, Montana and Centralia, Washington coal-fired power plants. In order to generate an aerosol of suitable particle-size distribution, the fly ash was extensively ball milled and sieved to less than 38 microns dia (-325-mesh sieve) before packing in the Wright Dust Mill cylinder. An aerosol concentration of over 50 mg/m^3 could be generated from this material with equal and consistent distribution throughout the exposure chambers.

Future plans for the exposure system include total automation and control of the gas concentrations and aerosol levels by a micro-processor and a system of solenoids and motorized valves.

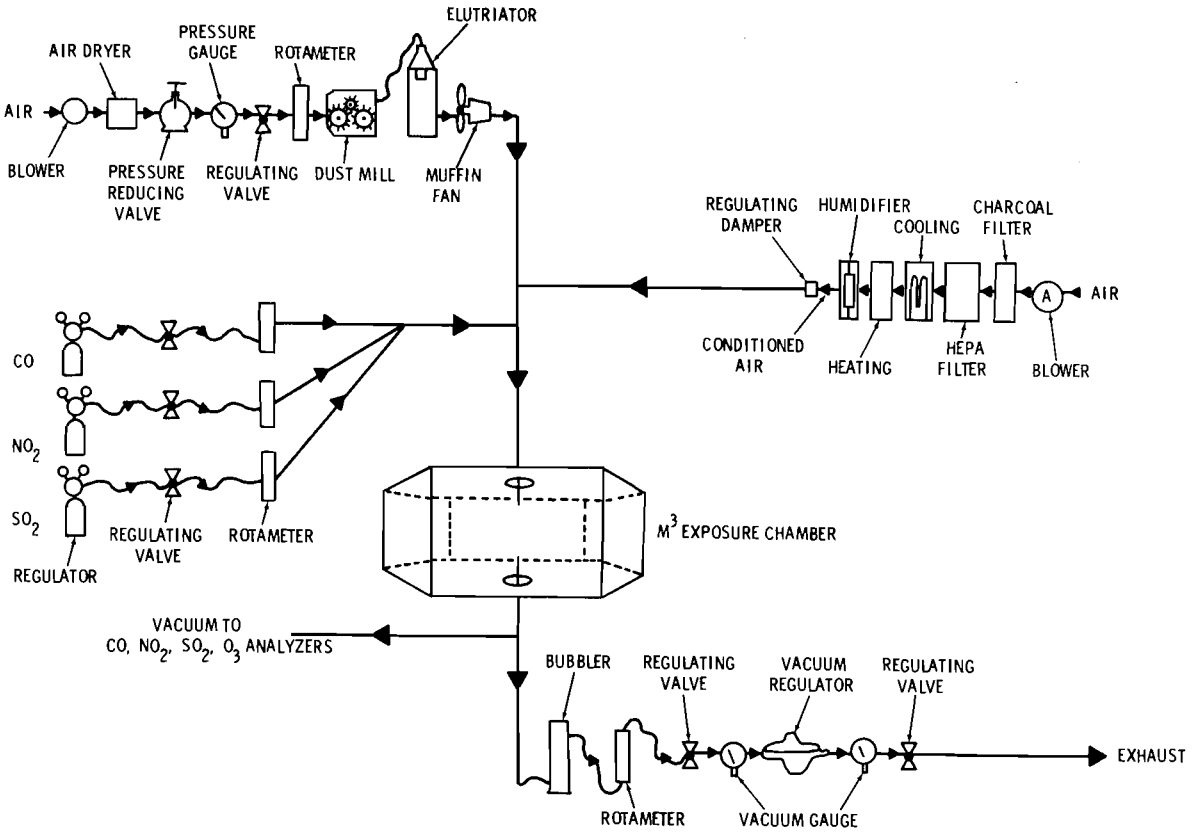

FIGURE 22.1. Atmospheric Pollutant Animal Exposure System

• LUNG TOXICITY OF SULFUR POLLUTANTS

Person in Charge: S. M. Loscutoff

Sulfur oxides released during the combustion of fossil fuels for energy production constitute a health hazard to exposed individuals. Certain individuals are particularly sensitive to harmful effects of sulfur oxides, including individuals with pre-existing pulmonary and cardiovascular diseases. This sensitive population shows an increased morbidity and mortality during episodes of high ambient sulfur oxide pollution. Since sources of sulfur pollution appear to be increasing with the use of catalytic converters in automobiles and the growing reliance on coal burning for energy, sulfur pollutants will continue to pose a health hazard.

The goal of this project is to evaluate possible means of protecting sensitive humans during episodes of high sulfur pollution, by using animal models which simulate human disease states. Using specific pharmacologic blockade, we are investigating the possibility of inhibiting the increased pulmonary resistance and decreased pulmonary compliance which occur during inhalation of sulfuric acid aerosols. Sulfuric acid inhalation effects are compared in animals with pulmonary changes blocked and in unblocked animals to determine if pharmacologic blockade protects animals from damaging effects of sulfuric acid exposure. Protection will be evaluated from morbidity and mortality data and pathologic and physiologic characterizations of pulmonary lesions. If pharmacologic blockade protects experimental animals from sulfuric acid exposure, a means of protecting sensitive humans during high sulfur pollution episodes may be suggested.

EFFECT OF PHARMACOLOGIC BLOCKADE ON PULMONARY FUNCTION IN AWAKE GUINEA PIGS

Investigator:

S. M. Loscutoff

Technical Assistance:

B. W. Killand and P. L. Savignac

In preliminary experiments, pulmonary function and cardiac functions were monitored in control guinea pigs and in animals injected with specific inhibitors of histamine, prostaglandins, acetyl choline and catecholamines (β-receptors). Tidal volume, minute volume and respiration rate were not significantly different between control and blocked animals. Pulmonary resistance was significantly higher in animals treated with antihistamines and antiprostaglandins. Pulmonary compliance was significantly lower in animals treated with antihistamines and heart rate was significantly lower in animals treated with β-blockers. Results of these studies will be used in establishing conditions for sulfuric acid aerosol exposures. To avoid confusion between sulfuric acid and drug-related effects, concentrations of sulfuric acid will be used which produce changes in pulmonary resistance and compliance significantly greater than changes caused by administration of drugs.

Before evaluating the effects of pharmacologic blockade on pulmonary responses to sulfuric acid exposure, control experiments evaluating the effects of pharmacologic blockade alone were performed. Results of these preliminary studies will be used in establishing conditions for sulfuric acid aerosol exposures.

Male, Hartley-strain guinea pigs were tested for 90 min in the apparatus shown schematically in Figure 23.1. Before insertion in the plethysmograph, animals were anesthetized with ether for placement of the pleural catheter and electrocardiograph (ECG) leads. The plethysmograph is designed so that the neck opening can be sealed, allowing respiratory flow and volume to be recorded from a pneumotachometer (resistance flow meter) affixed to the back of the plethysmograph. Pulmonary resistance and compliance were calculated from simultaneous recordings of pleural pressure, flow and volume.

Drugs used for pharmacologic blockade, their dosage, time preadministration, and affected endogenous vasoactive compounds are listed in Table 23.1. All drugs were given by intraperitoneal injection, except indomethacin, which was given orally. Ten animals were tested with each drug and there were ten untreated controls.

Measurements were made, periodically throughout the 90-min test period, of respiratory pattern, pulmonary mechanics,

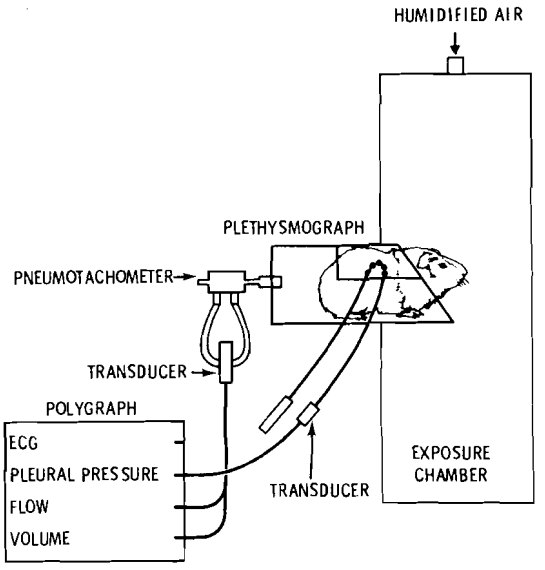

FIGURE 23.1. Apparatus for Testing Awake Guinea Pigs

and heart rate. Results of respiratory pattern measurements (respiration rate, tidal volume and minute volume) at 50 min are summarized in Table 23.2. Tidal volume in β-blocked animals was the only parameter affected by pharmacologic blockade. Pulmonary mechanics (resistance and compliance) and heart rate data are shown in Figures 23.2-23.4. Mean control values, ± 95% confidence intervals for controls, and mean values for drug-treated animals are presented for the 90-min test period. Responses of the animals were relatively constant throughout the 90-min test period. Resistance in histamine-blocked and prostaglandin-blocked groups was significantly higher than in controls, while compliance in the histamine-blocked group was significantly lower than in controls. Heart rate was significantly reduced in the β-blocked group.

These data, particularly the results of resistance and compliance measurements, will be important in establishing conditions for sulfuric acid aerosol exposures. Exposures will be carried out at a concentration of sulfuric acid which changes resistance and compliance more than any of the drugs. The influence of pharmacologic blockade on the pulmonary response to sulfuric acid aerosol exposure can then be evaluated.

TABLE 23.1. Drug Protocol for Pharmacologic Blockade

DRUG	DOSE	TIME PRE-INJECTION (min)	AFFECTED ENDOGENOUS COMPOUND
ATROPINE	5 mg/kg	45	ACETYLCHOLINE
PROPRANOLOL	10 mg/kg	60	CATECHOLAMINES (β-RECEPTORS)
CHLORPHENIRAMINE	10 mg/kg	15	HISTAMINE
INDOMETHACIN	50 mg	120	PROSTAGLANDINS

TABLE 23.2. Respiration Rate, Tidal Volume and Minute Volume in Control and Drug-Treated Guinea Pigs at 50 Min of the 90-Min Test Period

TREATMENT GROUP	RESPIRATION RATE (BPM)	TIDAL VOLUME (ml)	MINUTE VOLUME (ml/min)
CONTROL	86.5 ± 23.5	2.73 ± 1.02	233 ± 88
ACETYLCHOLINE-BLOCK	77.0 ± 16.5	2.90 ± 0.56	225 ± 63
β-BLOCK	74.5 ± 12.6	3.91 ± 0.49*	294 ± 49
HISTAMINE-BLOCK	88.5 ± 23.5	2.01 ± 0.29	176 ± 31
PROSTAGLANDIN-BLOCK	68.3 ± 16.5	3.20 ± 0.89	210 ± 30

*SIGNIFICANT DIFFERENCE FROM CONTROL $P < 0.05$, BASED ON UNPAIRED 'T' TEST

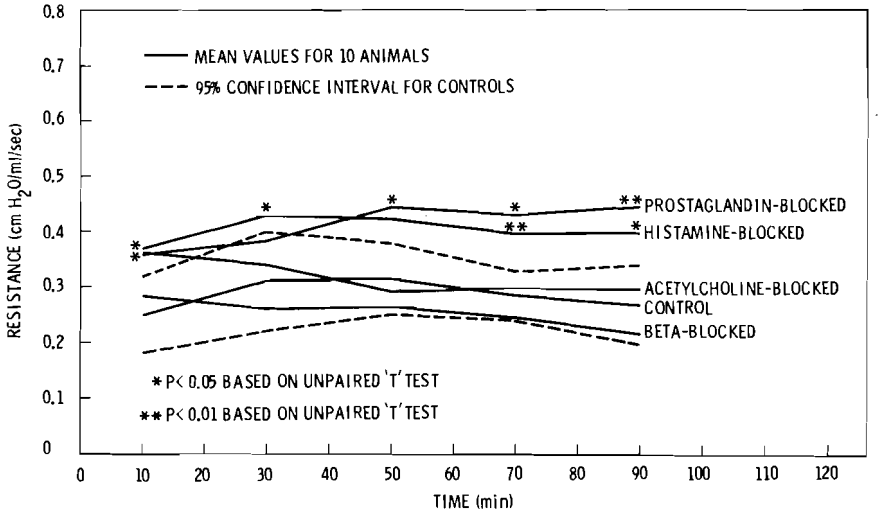

FIGURE 23.2. Pulmonary Resistance During a 90-Minute Test Period for Guinea Pigs Treated with Pharmacologic Blocking Agents

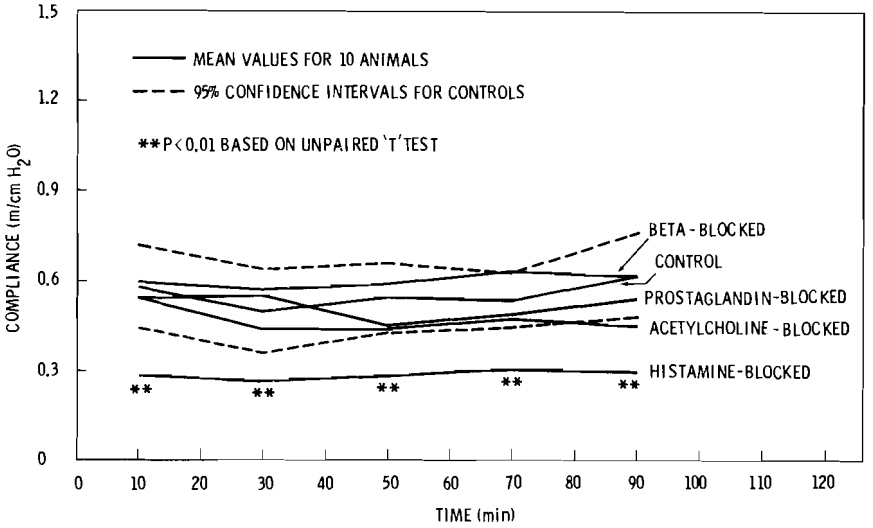

FIGURE 23.3. Pulmonary Compliance During a 90-Minute Test Period for Guinea Pigs Treated with Pharmacologic Blocking Agents

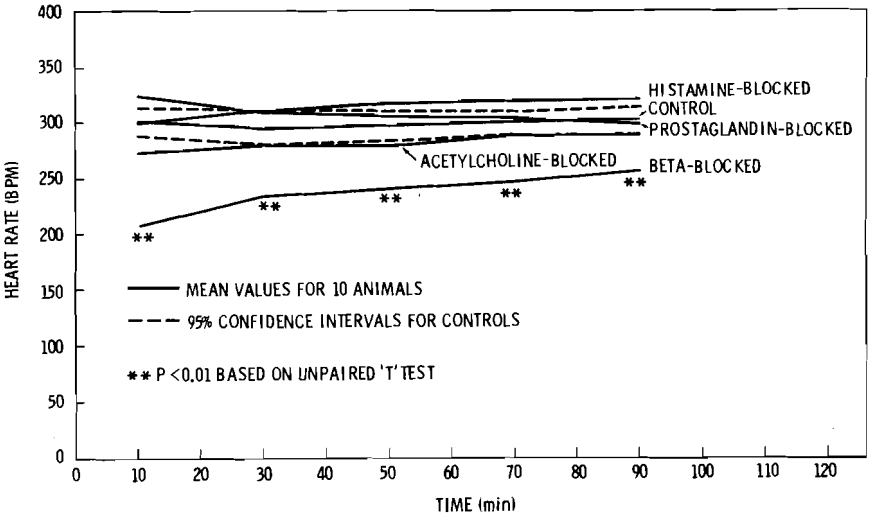

FIGURE 23.4. Heart Rate During a 90-Minute Test Period for Guinea Pigs Treated with Pharmacologic Blocking Agents

• CHEMICAL RADIATION PROTECTION

Person in Charge: J. C. Hampton

This project was terminated in FY 1976. It was aimed at developing ways of protecting individuals from the damaging effects of radiation and was based upon the use of compound ^{35}S-WR-2721 [S-2 (3-aminopropylamino) ethyl phosphorothioic acid hydrate] injected prior to exposure. During the course of the work, it was determined that a dose of 400 mg/kg body weight afforded protection to mice exposed to 1500 R X-rays such that they showed no evidence of gastrointestinal syndrome nor of marrow failure, and survived until they were killed 9 months postexposure. Studies on proliferative cells in the gut suggested that the protective effect was more likely on postmitotic cells rather than on the dividing population, based upon the appearance of mature cells at the time when unprotected animals usually died of the gut syndrome. The uptake of ^{35}S-WR-2721 in liver, gut and kidney showed that nearly all of the label was bound to the ribosome-rich microsome fraction, suggesting that, somehow, the pathways for protein synthesis were protected.

• REMOVAL OF DEPOSITED RADIONUCLIDES

Person in Charge: V. H. Smith

The objective of this project is to decrease the potential damage from inhaled, skin- or wound-absorbed, or ingested radionuclides. While primarily addressed to the needs for worker protection in the nuclear industries and laboratories, it also looks to the possible treatment needs arising from exposure of larger segments of the population. The approach is to develop methods that will prevent absorption, hasten excretion, improve decontamination, or alter translocation of the radionuclides--all for the purpose of minimizing radiation dose to sensitive tissues. Associated studies include mechanisms of radionuclide absorption, transport, mobilization and tissue distribution, preparation of new treatment agents and methodology, and the toxicology, pharmacology, pharmaceutics, and pharmacodynamics of treatment agents.

Research continues in the effort to obtain information for the IND on Zn-DTPA and inhaled Ca-DTPA. An inhalation study is underway in rats to check earlier indications of emphysema due to inhalation of Ca-DTPA. For patient and physician convenience, an oral treatment for Pu poisoning would be highly desirable. A compound related to bacterial siderochromes was found to be moderately effective in decreasing Pu retention when given orally 1 hr after administration of Pu to rats. As part of the pharmaceutical effort to direct Pu removal agents into cells to attack Pu pools not available to the standard Ca-DTPA treatment, DTPA has been incorporated into polylactide particles of respirable size. Before testing in animals, the behavior of new pharmaceutics will be tested in vitro, employing Pu-containing lung macrophages. Macrophages in the in vitro test system engulf plutonium into phagolysosomes just as the in vivo cells. The behavior of Pu in these cells thus provides an opportunity to study Pu uptake and release mechanisms and the effects of treatments and their vectors.

AN IN VITRO STUDY OF PLUTONIUM IN MACROPHAGES

Principal Investigators:
R. P. Schneider and A. V. Robinson
Technical Assistance:
L. M. Butcher

An in vitro system for studying Pu uptake by, and removal from, macrophages was developed to provide data for the actinide therapy program. We have shown that $^{239}PuO_2$ particle uptake in vitro resembles the process in vivo with respect to the intracellular localization of phagocytized particles. At the end of 7 days of culture of Pu-loaded cells, 54% of the cells were viable even though 71% of the cells in the culture initially contained enough $^{239}PuO_2$ to deliver more than 53 intracellular α-disintegrations.

Particulate Pu in the body is sequestered primarily in the macrophages of lungs, liver, lymph nodes, and bone marrow. Monomeric Pu in the extracellular space can be chelated by diethylenetriamine penta-acetic acid (DTPA) and excreted in the urine. Intracellular Pu, however, is resistant to such therapy since DTPA cannot penetrate cells. We are developing an in vitro test system using pulmonary macrophages in order to study actinide incorporation into these cells as well as means for removing the radionuclides from cells. Since most accidental exposures involve inhalation, the use of pulmonary macrophages is appropriate. Plutonium will be used initially in this system, due to its importance in the nuclear industry and the wealth of available data describing its in vivo behavior, for comparison to in vitro work. This report discusses some of the data necessary to define the test system.

The basic plan is to allow macrophages to ingest Pu (oxide, hydroxide and polymer) and then to culture the cells for several days. We will measure appearance of soluble Pu during various treatments, including macrophage-activating agents and chelators packaged in particles which will be phagocytized. Rabbit pulmonary macrophages are used because they can be easily harvested by lung lavage in sufficient quantity, and because they are the most extensively characterized pulmonary macrophages with respect to physiology and methodology. In culture, the cells must remain attached to the flask surface in order to maintain normal viability and function. We have found that attachment of the cells to the culture flask surface is promoted by increasing the charges on the flask surface by sulfonation of the polystyrene. The macrophages are the only cells in fluid from lung lavages which attach to the flasks, hence the cultures are pure (after washing away unattached cells). The cells survive for more than 8 days in culture with loss of 5% or less of the cells per day. During this period there is no change in morphology, except for increased flattening. The cells maintain the ability to phagocytize polystyrene spheres.

We have studied phagocytosis of $^{239}PuO_2$ by freshly harvested cells in order to

characterize a standard method for loading the cells prior to culture. The particles in the PuO_2 suspension used have a count median diameter of 0.14 μm and a mass median diameter of 0.529 μm. The cells (2.5×10^6/ml) were agitated while incubated with the PuO_2 suspension (0.15 μCi/ml) at 37° in Hank's balanced salt solution. At the sampling interval, a 2-ml aliquot was removed, the cells were concentrated by centrifugation and smeared on microscope slides. The smears were coated with photographic emulsion, autoradiographed for 5 or 12 days, and then stained.

Electron micrographs of the Pu-loaded cells revealed that they contained intracellular $^{239}PuO_2$. As shown in Figure 25.1, the particles were enclosed in membrane-limited structures within the cells, presumably phagosomes and phagolysosomes. Pu in pulmonary macrophages lavaged from aerosol exposed animals is enclosed in similar structures, showing that the actinide is handled by the cells in vitro in a manner similar to its handling in vivo

The appearance of the autoradiographed and stained cells and the α tracks which result from Pu disintegrations are shown in Figure 25.2. This photomicrograph also illustrates the nonhomogeneous nature of the particle uptake within the population. To obtain a rough estimate of the dose per cell in these preliminary studies, cells were classified into three categories, i.e., cells with no visible tracks, cells with one to five tracks, and cells with more than five tracks per cell.

The data in Table 25.1 show that while uptake of $^{239}PuO_2$ particles occurred in the absence of protein, the number of cells with more than five tracks increased three-fold in the presence of 4% bovine serum albumin (BSA). Pretreatment of the particles by incubating them with 4% BSA for 1.5 hr did not increase uptake relative to Hank's salt solution alone. This indicates that the effect of BSA is on the cells and that it does not exert its effect by coating the PuO_2 (opsonization). The behavior of these cells in the presence of

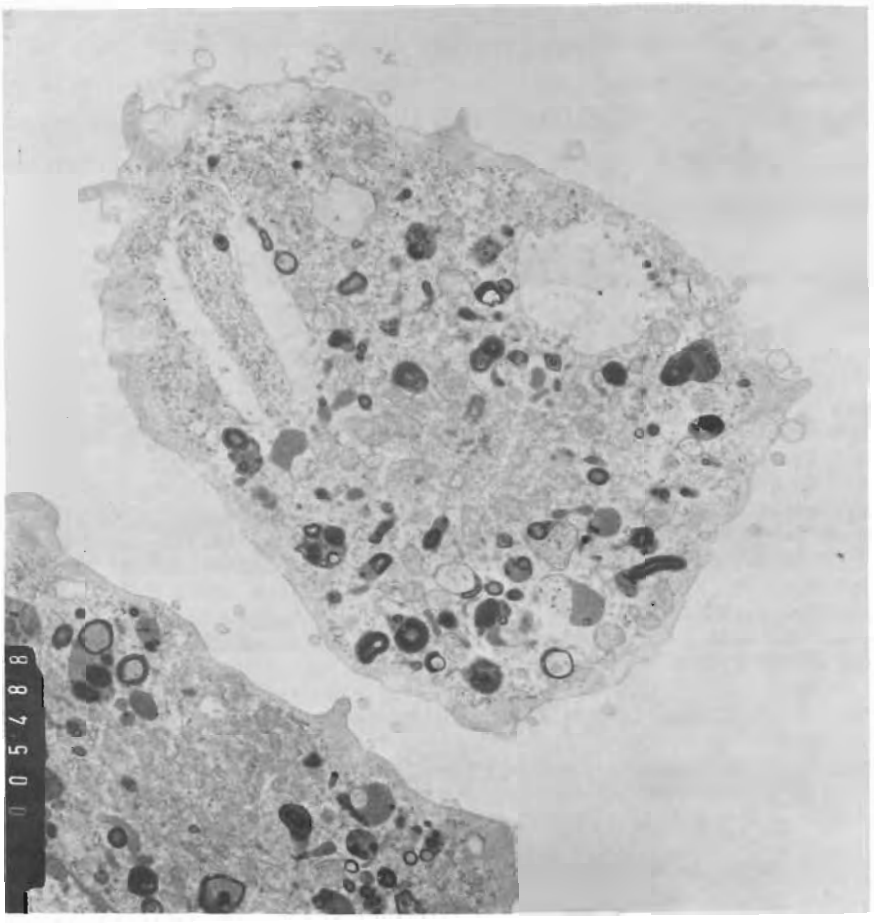

FIGURE 25.1. Autoradiograph of a Smear of Rabbit Pulmonary Macrophages Exposed to $^{239}PuO_2$ Particles in vitro. The emulsion was exposed to the cells for 5 days prior to development and staining.

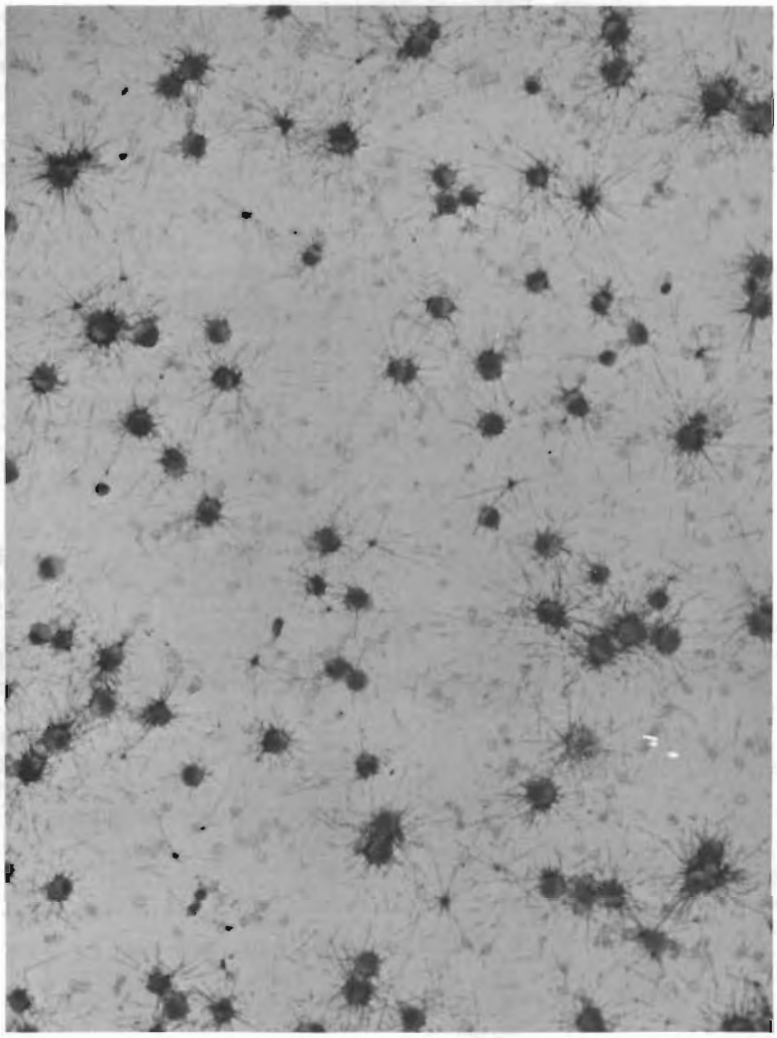

FIGURE 25.2. Electron Micrograph (14000 X) of $^{239}PuO_2$ Particles in Rabbit Pulmonary Macrophages. The cells were exposed to PuO_2 particles in vitro in Hank's balanced salt solution containing 4% bovine serum albumin. The arrows point to the electron-dense PuO_2.

BSA is consistent with the demonstrated ability of BSA to increase endocytosis or uptake of small particles in rabbit pulmonary macrophages. In the presence of BSA, virtually all of the cells contained Pu and about three-fourths of these contained more than five tracks after 5 days of autoradiography. The presence of rabbit serum was mildly inhibitory to uptake when compared to Hank's solution alone. We intend to use Hank's solution containing 4% BSA for a 0.5-hour incubation for the routine loading of the cells.

The effect of $^{239}PuO_2$ on the survival of macrophage cultures is shown in Figure 25.3. The cells were loaded with $^{239}PuO_2$ for 1 hr in Hank's solution containing 4% BSA, as described above. The cells were then pelleted, resuspended in medium M-199 with 20% rabbit serum, and added to the treated culture flasks to a density of $0.2 \times 10^6/cm^2$, or 1×10^6/ml of medium. After 1 hr the unattached cells and PuO_2 were removed by pouring the medium from the flask and washing the cells. Ninety percent of the cells applied to the flasks attached and there was no discernible difference in the number of control and Pu-containing cells which attached. The cells were then incubated at 37° after adding fresh medium to the flasks. The number of cells remaining attached was estimated by counting the cells (with an ocular grid) in three randomly selected sites of fixed area on each flask. The cells were counted at 1, 3, and 7 days of culture. The total number of cells (251-510) counted in each

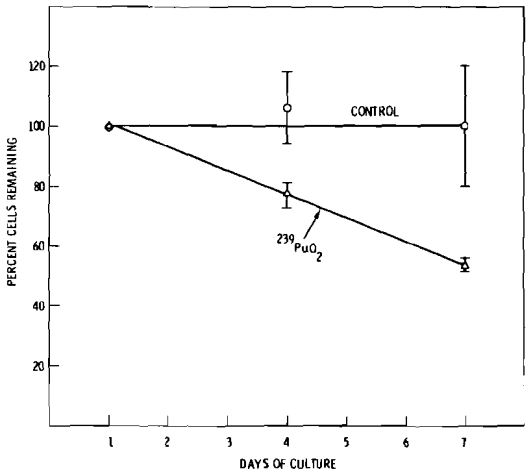

FIGURE 25.3. The Effect of Phagocytized $^{239}PuO_2$ on Survival of Rabbit Pulmonary Macrophages. The cell numbers were estimated by counting at three sites on four control and four Pu-containing flasks. The standard deviations of the percent counted in each flask relative to those counted on the first day are shown as bars.

of the four control and four Pu-containing flasks at 4 and 7 days was used to calculate the percent of cells present relative to the first day. The cells in the control flasks remained attached throughout the 8-day culture period, while the cultures containing $^{239}PuO_2$ lost about 46% of the cells in 7 days.

The efficiency of counting α tracks in emulsion-exposed cells is about 13% [Sanders, C. L., Health Phys. 22:607 (1972)]. It follows that the 71% of cells with more than five tracks (Table 25.1) were exposed to at least 53 intracellular disintegrations in 7 days. Since 54% of the cells were viable at the end of this period, the accumulation of 53 disintegrations alone must be insufficient to kill them outright.

The basic purpose of the experiments described above was to establish dose levels of ^{239}Pu which can be used for experiments which aid the therapy program. We now have procedures developed for loading the macrophages with desired levels of $^{239}PuO_2$. This knowledge will be used for the second stage of the study, i.e., culturing the cells and measuring the appearance of intra- and extracellular monomeric Pu when treated with various chelators and immunologically reactive agents.

TABLE 25.1. In Vitro Uptake of $^{239}PuO_2$ by Pulmonary Macrophages

INCUBATION MEDIA	DURATION OF INCUBATION (hr)	PERCENT OF CELL CONTAINING[a]		
		0 α TRACKS	<5 α TRACKS	>5 α TRACKS
HANK's BALANCED SALTS	0.5	31	46	23
	1	28	42	30
	2	1	22	77
HANK's BALANCED SALTS + 4% BSA	0.5	2	25	73
	1	3	26	71
	2	2	7	91
HANK's BALANCED SALTS (PuO_2 PREINCUBATED IN 4% BSA FOR 1.5 hr)	0.5	21	60	19
	1	22	57	21
	2	8	37	55
HANK's BALANCED SALTS + 20% RABBIT SERUM[b]	1	27	60	13

[a] DETERMINED BY AUTORADIOGRAPHY. CELL SMEARS WERE EXPOSED FOR 5 DAYS AND MORE THAN 100 CELLS ON EACH SLIDE WERE CLASSIFIED ACCORDING TO THE NUMBER OF α TRACKS ORIGINATING IN THEM.

[b] AUTORADIOGRAPHED FOR 12 DAYS

MASS EFFECT AND Pu REMOVAL FROM RATS WITH Ca- OR Zn-DTPA

Investigator:
V. H. Smith
Technical Assistance:
K. A. Poston

Eight percent of an intramuscular injection of 27.6 nCi of $^{237}Pu(NO_3)_4$ was retained by rats at the injection site, after 22 days. More than 30% is usually retained following injection of more massive quantities of ^{239}Pu. Treatment with Ca- or Zn-DTPA showed the former to be more effective when treatments were initiated 1 hr after Pu administration. When treatments were begun 7 days after the Pu injection, 416 nmol Ca-DTPA/kg was more effective in removing Pu than 28.7 nmol/kg (human dose level) of Zn- or Ca-DTPA. Due to its high specific activity and ease of detection, ^{237}Pu permits facile experimentation in small animals at Pu mass levels comparable to those encountered in most human exposures.

To achieve concentrations of Pu in rats similar to those usually treated in man, and still retain ease of radioassay, one can use the short half-life (45.6 days) ^{237}Pu. The present study was performed to gain experience with ^{237}Pu and to lay a background for more extensive experiments on mass effects and their relation to effectiveness of removal agents.

Groups of 6 adult female Wistar rats, weighing 330-385 g, were administered 27.6 nCi of ^{237}Pu in 10 µl pH 4 HNO_3 in the left gluteus maximus. One hour after injection (prompt treatment), 1 HDL (human dose level, 28.7 nmoles DTPA/kg) of Ca- or Zn-DTPA was given intraperitoneally, with the treatment repeated on days 2, 4, and 7 postinjection. Starting on day 7 after the radionuclide injection (delayed treatment), when the ^{237}Pu should be well-fixed in tissues, groups of rats were treated with 1 HDL Ca- or Zn-DTPA and with 18 HDL of Ca-DTPA. Treatments were repeated on days 9, 11, and 14. All rats were sacrificed on the 22nd day. Control rats received no treatment. All data were corrected for physical decay.

Results of whole-body counting are shown in Figure 25.4. After day 2 the biological half-life of ^{237}Pu for the control animals is about 68 days as estimated from these 21 days of data. The hump in the curve about day 1 may be due to early changes in plutonium distribution and counting geometry differences from the "standard" rat frozen 1 hr after Pu administration. In control rats sacrificed after 24 hr, the injection site retained about 25% of the initial ^{237}Pu dose, the liver retained 6%, the skeleton about 40% and the pelt, 12%. Control rats killed at 7 days showed only 7.6% of the Pu dose still at the injection site, 3.2% in the liver, 48% in the skeleton, and 2.7% in the pelt; this distribution was statistically indistinguishable from that seen at 22 days postinjection.

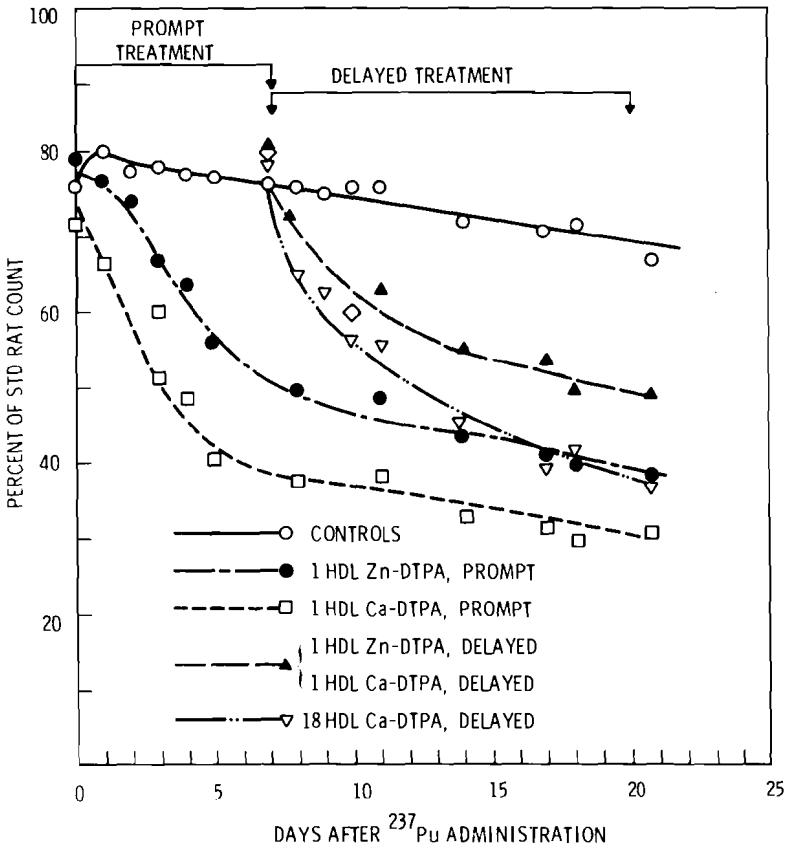

FIGURE 25.4. Total-Body Retention of Intramuscularly Injected ^{237}Pu in the Rat.

Under prompt treatment conditions Ca-DTPA is more effective in removing Pu than the Zn salt. This difference is not apparent in the delayed treatment situation, but an 18-HDL dose of the Ca salt is more effective than the 1-HDL dose of either Zn- or Ca-DTPA. At the time the delayed treatment regime was instituted, the concentration of Pu was about 25 fmol/kg of rat and treatment with 1 HDL Ca-DTPA provided a mole ratio of at least 1.3×10^9 DTPA:^{237}Pu. At the higher dose, this ratio increased to 2×10^{10}, a trivial change, one would have thought, in light of the already huge excess of DTPA available from the lower dose. These results may indicate that some of the DTPA dose is tied up on biological substrates and is unavailable, at least in sufficient concentration, to participate in removing Pu from body ligands. Or it may be that the larger dose maintains an effective chelon concentration over a longer period, allowing greater probability for ligand-metal interaction.

Tissue retention of Pu (Tables 25.2-25.4) reflects the same general order of treatment effectiveness shown in Figure 25.4. At 22 days the kidneys and spleens of the untreated rats have greater concentrations of Pu than the liver, which is not usually the case for monomeric ^{239}Pu in rats, and may be a mass effect. The inguinal lymph nodes in the region close to the injection site have almost twice the Pu concentration of the contralateral inguinal nodes. Prompt treatment had no effect on the Pu in the lymph nodes, while there was statistically significant removal when treatment was delayed. DTPA treatments enhanced Pu concentration in the ovaries. Despite their statistical validity in this experiment, these findings in lymph nodes and ovaries have not been previously observed in experiments with other Pu isotopes, and are contrary to expected results. The heart retains about a 5 times higher concentration of Pu than the other muscle tissues sampled, probably reflecting the great blood flow through that organ and the greater opportunity for Pu to contact the muscles of the heart. Removal from the heart is comparable to that from other muscle tissues.

TABLE 25.2. Percent of Intramuscularly Injected ^{237}Pu in Rat Tissues 22 Days Postinjection and After Treatments With Ca- or Zn-DTPA

	% ^{237}Pu DOSE / TISSUE[1]					
		PROMPT TREATMENT[2]		DELAYED TREATMENT[2]		
TISSUE	CONTROLS	1 HDL[3] Ca-DTPA	1 HDL Zn-DTPA	18 HDL Ca-DTPA	1 HDL Ca-DTPA	1 HDL Zn-DTPA
CARCASS[4]	56	20	33a, b	28a	34a, b	38b
PELT	2.3a	1.2b	3.3	1.5b, c	1.8a, c	1.8a, c
INJECTION SITE[5]	8.4a	5.6b	7.0a	4.7b	13c	18c

[1] MEANS IN THE SAME ROW WITH THE SAME LETTER SUFFIX ARE NOT SIGNIFICANTLY DIFFERENT AT THE 0.05 SIGNIFICANCE LEVEL ACCORDING TO DUNCAN's NEW MULTIPLE RANGE TEST.

[2] PROMPT TREATMENTS STARTED 1 hr AFTER ^{237}Pu ADMINISTRATION; DELAYED TREATMENTS STARTED 7 DAYS LATER.

[3] 1 HDL = 1 x 28 μmol DTPA / kg (HUMAN DOSE LEVEL); 18 HDL = 18 x 28 μmol DTPA / kg

[4] SKINNED, DEVOID OF MAJOR ORGANS AND THE INJECTION SITE MUSCLE. IT THUS REPRESENTS MAINLY SKELETAL ^{237}Pu.

[5] ABOUT 3 GRAMS OF MUSCLE, FASCIA, etc. SURROUNDING THE INJECTION SITE CONSTITUTE THIS SAMPLE

TABLE 25.3. Concentration of Intramuscularly Injected ^{237}Pu in Rat Tissues 22 Days Post-injection and After Treatments with Ca- and Zn-DTPA

	PERCENT OF ^{237}Pu DOSE x 10^{-2} / GRAM OF TISSUE[1]					
		PROMPT TREATMENT[2]		DELAYED TREATMENT[2]		
TISSUE	CONTROLS	1 HDL[3] Ca-DTPA	1 HDL Zn-DTPA	18 HDL Ca-DTPA	1 HDL Ca-DTPA	1 HDL Zn-DTPA
LIVER	46	18a	28b	7.3	24a, b	27b
KIDNEYS	91	26a	30a, b	38b	45b	47b
SPLEEN	51	13	18	25a	27a	27a
LUNGS	7.9	4.1a, b	3.4a	4.3a, b	5.0b	4.6b
HEART	6.3	2.3a	2.2a	4.2b	3.7b	3.5b
MUSCLE	1.3	0.55a	0.48a	0.74b	0.77b	0.81b
BRAIN	1.6	1.0a	0.99a	1.2a	0.90a	0.86a
OVARIES	6.9a	7.7a	9.0b	6.1a	9.4b	12
ADRENALS	24	7.1a	14b	6.5a	10b, c	9.2c
INGUINAL LYMPH NODES	44a	49a	40a	16b	11b	35a
INGUINAL LYMPH NODES NEAR INJECTION SITE	73a	67a	82a	29b	43b	36b

[1] MEANS IN THE SAME ROW WITH THE SAME LETTER SUFFIX ARE NOT SIGNIFICANTLY DIFFERENT AT THE 0.05 SIGNIFICANCE LEVEL ACCORDING TO DUNCAN's NEW MULTIPLE RANGE TEST

[2] PROMPT TREATMENTS STARTED 1 hr AFTER ^{237}Pu ADMINISTRATION; DELAYED TREATMENTS STARTED 7 DAYS LATER

[3] 1 HDL = 1 x 28 μmol DTPA / kg (HUMAN DOSE LEVEL); 18 HDL = 18 x 28 μmol DTPA / kg

TABLE 25.4. Comparison of the Concentration of Intramuscularly Injected ^{237}Pu in Selected Bones of the Rat 22 Days After Intramuscular Injection and After Treatments with Ca- or Zn-DTPA

		% OF ^{237}Pu CONCENTRATION IN CONTROL RAT TISSUES[1]				
	CONTROLS (% OF ^{237}Pu PER GRAM OF TISSUE)	PROMPT TREATMENT[2]		DELAYED TREATMENT[2]		
BONE		1 HDL[3] Ca-DTPA	1 HDL Zn-DTPA	18 HDL Ca-DTPA	1 HDL Ca-DTPA	1 HDL Zn-DTPA
VERTEBRAE	(0.2)	42a	65b	44a	56b	70b
OSSA COXARUM	(4.8)	35a	54b	38a	53b	62b
FEMORA	(4.4)	37	57a, b	49a	54a, b	64b
RIBS	(2.7)	12a	61b	44a	61b	72b
CALVARIA	(1.6)	9a	69b	54a	63b	82

[1] MEANS IN THE SAME ROW WITH THE SAME LETTER SUFFIX ARE NOT SIGNIFICANTLY DIFFERENT AT THE 0.05 SIGNIFICANCE LEVEL ACCORDING TO DUNCAN'S NEW MULTIPLE RANGE TEST

[2] PROMPT TREATMENTS STARTED 1 hr AFTER ^{237}Pu ADMINISTRATION; DELAYED TREATMENTS STARTED 7 DAYS LATER

[3] 1 HDL = 1 x 28 µmol DTPA/kg (HUMAN DOSE LEVEL); 18 HDL = 18 x 28 µmol DTPA/Kg

The delayed 18-HDL Ca-DTPA treatment was almost as effective in removing Pu from bone (Table 25.4) as the 1-HDL prompt treatment, suggesting that at the low Pu mass level employed, a considerable portion of the Pu had not become tightly bound to bone and was still available to the DTPA after 7 days. Plutonium-239, at the mass levels required for study, is more difficult to remove from bone if treatment is delayed for a similar period. Using a simple ranking procedure, the ossa coxarum appeared to be consistently most susceptible to Pu removal by DTPA and the calvaria least susceptible, with the other three bones about equally susceptible. These differences may be due to the amounts of trabecular bone, cellular activity and blood supply in the individual bones.

In previous experiments, intramuscularly injected $^{238}Pu(NO_3)_4$, at about 7000 times the mass used in this experiment, was retained to about 22-35% of the quantity injected; $^{239}Pu(NO_3)_4$, at a mass 10^6 that used in this experiment, was retained to about 50%. The retention of more Pu at the site is, of course, reflected in the amounts translocating to other tissues. This is one aspect of the mass effect, i.e., the propensity for larger amounts of Pu to hydrolyze and polymerize before being bound and transported by tissue ligands to other parts of the body. Although expensive, ^{237}Pu is an excellent tool for estimating behavior and treatment effects in small animals at Pu concentrations similar to those associated with exposure incidents in man.

EXPERIMENTS TOWARD MEDICAL MANAGEMENT OF RADIONUCLIDES IN THE GUT: EFFECT OF DEFEROXAMINE ON $^{238}Pu(NO_3)_4$ ABSORPTION FROM RAT GUT

Investigator:
V. H. Smith

Deferoxamine (DFA) (250 mg/kg), orally administered to rats, decreased Pu absorption from orally administered $^{238}Pu(NO_3)_4$ by about 1/3. The calcium salt of diethylenetriaminepentaacetic acid (Ca-DTPA), given orally 5-10 min after the Pu, increased absorption about four times. DFA given 10 min before the DTPA decreased the effect of the latter by a factor of two. Deferoxamine administration prior to inhalation treatment of man with DTPA may be one way to decrease possible DTPA-enhanced gut absorption of Pu.

Gut absorption of Pu may be increased severalfold by the presence of a strong chelator, e.g., DTPA. This is of special concern when DTPA is administered by aerosol for treatment of the inhalation of a radionuclide. In typical inhalation exposure, greater than 50% of the inhaled material is swallowed and the chelation of the radionuclide provides the possibility for increased absorption from the gut. Among the possible remedies is the administration of a compound that forms stronger complexes with the radionuclide than DTPA and is less well absorbed. A compound used to decrease iron absorption in the case of iron overdose in humans, deferoxamine (DFA), forms stronger chelates with Pu and Fe than does DTPA. The purpose of this experiment was to see if DFA given before DTPA treatment would decrease gut Pu absorption.

Female Wistar rats, weighing between 300 and 400 g, were administered 103 μCi $^{238}Pu(NO_3)_4$ in 0.40 ml 0.2 M HNO_3 by gavage. Five to 10 min later the first treatment was given by gavage, followed by a second treatment 10 min later. Eight rats constituted a treatment group, with treatments given as shown in Table 25.5.

TABLE 25.5. Treatments Administered by Gavage

GROUP	FIRST TREATMENT	SECOND TREATMENT
CONTROLS	SALINE[a]	SALINE
DFA	DFA[b]	SALINE
DTPA	DTPA[c]	SALINE
DFA, THEN DTPA	DFA	DTPA
DTPA, THEN DFA	DTPA	DFA

[a] 0.5 ml 0.9% NaCl
[b] 0.1 g DEFEROXAMINE AS DESFERAL® (CIBA-PHARMACEUTICAL CO.)/RAT IN 0.5 ml SOLUTION
[c] 0.01 g Ca-DTPA IN 0.5 ml SOLUTION/RAT

Rats were housed four/cage, and urine from each cage was collected on filter paper for 2 days following Pu administration. Feces were removed from the paper, the paper muffled, the ash dissolved in nitric acid, and analyzed by standard scintillation

techniques. Rats were killed 2 days after treatment. The liver and both femurs were analyzed for Pu in the same manner as the urine. Results are shown in Table 25.6.

Absorption of Pu was decreased by DFA, as evidenced by lower concentrations in tissues and urine; DTPA caused a marked increase in absorption and in retention. DFA administered before the DTPA decreased the enhanced absorption due to DTPA, as shown by the approximately 2.5-fold higher levels of Pu in urine and tissues when DTPA is given alone.

While it is difficult to predict the effect in man because of physiological/anatomical differences from the rat, and the usually much higher chelon to Pu ratios used in man, large doses of deferoxamine orally before the inhalation administration of Ca-DTPA would likely prevent some Pu absorption from the gut. There may well be better ways of accomplishing this, such as alkalinization of stomach contents or administration of a cathartic. Such procedures are under study.

TABLE 25.6. Percent of Administered $^{238}Pu(NO_3)_4$ Absorbed from the Rat Gastrointestinal Tract Within 2 Days Following Administration and Various Treatments

	% OF DOSE x 10^{-3}[b] AND (FRACTION OF CONTROL VALUES)		
TREATMENT BY GAVAGE[a]	LIVER	SKELETON[c]	URINE
NONE	0.39a (1.0)	3.1a (1.0)	17 ± 13 (1.0)
DFA	0.26[b] (0.67)	0.91 (0.29)	4.9 ± 1.9 (0.29)
DTPA	1.2 (3.2)	4.8 (1.5)	68 ± 17 (4.0)
DFA, THEN DTPA	0.31a,b (0.80)	2.0 (0.64)	27 ± 1.0 (1.6)
DTPA, THEN DFA	0.78 (2.0)	3.6a (1.2)	48 ± 8.2 (2.8)

[a] DEFINED IN TABLE 1

[b] THE PERCENT OF DOSE RESULTS WERE CALCULATED USING DUNCAN'S NEW MULTIPLE RANGE TEST. MEANS IN THE SAME COLUMN WITH DIFFERENT LETTER SUFFIXES ARE SIGNIFICANTLY DIFFERENT AT THE 5% LEVEL. URINE VALUES ARE THE MEAN ± RANGE FOR 2 CAGES OF 4 RATS/GROUP COLLECTED FOR 2 DAYS.

[c] PERCENT DOSE IN 2 FEMURS x 12 = SKELETON % DOSE

REMOVAL OF ^{239}Pu FROM THE RAT WITH AN ORALLY ADMINISTERED CHELON

Investigator:
V. H. Smith

The oral administration of 2,3-dihydroxybenzoic acid (DHB) to rats injected intravenously 1 hr previously with ^{239}Pu citrate caused an increase in urinary excretion of Pu about 8 times that of animals treated with 0.9% NaCl (controls). Liver retention of Pu was decreased from 18% at 2 days in the control animals to 11% in DHB-treated rats. The skeletal retention was similarly reduced from 56% in the control group to 40% in the DHB-treated animals.

Iron-removing agents appear useful in effecting Pu removal. Both diethylene-triaminepenta-acetic acid (DTPA) and deferoxamine (DFA) have been used to treat excess iron storage diseases and are also among the most effective agents for removing Pu. DFA is a hydroxamic acid-based siderochrome of bacterial origin. The other commonly occurring structural base for siderochromes of microbiological origin is 2,3-dihydroxybenzoic acid (DHB), which is capable of increasing Fe excretion from Fe-overloaded animals and man [R. W. Grady, et al., J. Pharm. Exp. Therap. 196:478-85 (1976)]. This compound is orally effective, of low toxicity, and would be very convenient for therapy, in contrast to DTPA and FDA, which are effective only if given parenterally. The possible oral effectiveness of DHB in removing Pu was tested in the rat.

To evaluate the effectiveness of the drug, experiments were initiated in which female Wistar-strain, Sprague-Dawley rats, weighing 300-340 g, were held off food for 24 hr, then anesthetized lightly with diethyl ether and injected via the tail vein with 1.02 μCi ^{239}Pu in 200 μl of 0.5% citrate buffer (pH 5). The rats were caged in groups of five, and 1 hr after Pu administration, groups were treated by intraperitoneal injection with 1 ml of 0.9% NaCl (controls), or 162 μmol DHB or Ca-DTPA/kg, equivalent to 25 or 80.6 mg/kg, respectively. The DHB and Ca-DTPA solutions used for the treatments were both 40.5 μmol/ml, adjusted to pH 7.2 with NaOH. Another group of rats was treated by gavage with 650 μmol (100 mg) DHB/kg in 1 ml of 1% $NaHCO_3$. Urine and feces were collected from each group of rats for 2 days, ashed, and the Pu content assayed in a liquid scintillator system. One femur and the liver from each rat were similarly analyzed for Pu.

From results shown in Table 25.7, all treatment groups had less Pu retention than controls, with the DTPA group having the least. The orally administered DHB, at 4X the intraperitoneal dose, gave essentially the same degree of removal. While less effective than DTPA, the effectiveness of oral DHB may be sufficient to qualify it as a convenient treatment for protracted use. Still to be ascertained are its effectiveness compared to DTPA under delayed treatment conditions and whether it is tapping the same Pu pools. Both DFA and DHB are iron-binding chelons of natural origin. The behavior of these two agents in effecting Pu removal suggests that the study of compounds of similar origin may turn up more effective Pu-excorporating agents.

TABLE 25.7. Influence of Ca-DTPA[c] or DHB[d] Treatment on the Amount of Intravenously Injected ^{239}Pu-Citrate in Excreta or Retained in Rat Skeleton and Liver.

	PERCENT OF ^{239}Pu DOSE PRESENT 48 hr AFTER INJECTION			
	MEAN ± STANDARD DEVIATION[e]			
TREATMENT AND ROUTE	LIVER	SKELETON[a]	URINE[b]	FECES[b]
0.9% NaCl, 1 ml INTRAPERITONEAL	18 ± 2.6	56 ± 4.8	2.9	1.4
0.162 mmol DHB / kg INTRAPERITONEAL	8.3 ± 0.97	36 ± 3.8	34	1.8
0.162 mmol Ca-DTPA kg INTRAPERITONEAL	3.6 ± 0.63	8.9 ± 1.4	52	6
0.65 mmol DHB / kg GAVAGE	11 ± 2.1	40 ± 4.3	24	2

[a] 24 X % Pu DOSE IN THE FEMUR.

[b] COLLECTED FROM THE GROUP OF 5 RATS AND DIVIDED BY 5. THESE ARE SINGLE VALUES, SO NO STATISTICAL LIMITS CAN BE CALCULATED.

[c] CALCIUM TRISODIUM SALT OF DTPA

[d] 2,3-DIHYDROXYBENZOIC ACID, Na SALT.

[e] DHB TREATMENT RESULTS ARE DIFFERENT FROM CONTROLS AND DTPA TREATMENT RESULTS AT $p > 0.95$ BUT DO NOT DIFFER FROM EACH OTHER.

TOXICITY OF HEAVY METALS AND CHELATING AGENTS IN VITRO

Investigators:

M. E. Frazier, T. K. Andrews, and V. H. Smith

The clonal growth assay using VERO (monkey kidney) cells has been investigated as a method of screening chemical and biological chelating agents for cytotoxicity. The technical aspects of the procedure were established and a scale of toxicity for several elements and for chelons was determined.

A stable cell line, VERO (monkey kidney), is being evaluated as a screening device for determination of metal and chelon toxicity and potential chelon effectiveness. We will report here a series of exploratory tests to determine toxicity of metals and chelons. The compounds under test at varying concentration are added to a known number of cells and the degree of clone (colony) formation relative to control cultures is observed. Any cluster of eight cells present at the end of the experiment is scored as a clone. The test material is diluted in culture medium (RPMI 1640 supplemented with 10% fetal bovine serum) and thus the cells were exposed to the test material throughout the 5-day experiment. Due to the high dilution

factors inherent in the test system there is minimal cellular interaction before clone formation and, as a result, the cloned cells are more sensitive to toxic agents and more stringent in their nutritional requirements than high-density cultures of the same cells.

The clonal growth assay provides several kinds of data. Measuring the plating efficiency (the number of colony-producing cells/total number of cells plated) allows objective numerical comparisons of cell survival following exposure to various chelons and/or chelated metal complexes. Studying growth rate, and variations in this rate, among individual colonies allows a more complete analysis of cell population than can be obtained in mass culture. Observed variations in the growth rate may reflect subtle toxic mechanisms not immediately apparent in the plating efficiency tests. Finally, if a metal, chelator, or metal complex causes cellular transformation, quantitative measurements can be made to provide us with a measure of the carcinogenic potential of the compound being tested.

The results (Table 25.8) indicate a scale of metal toxicity (Cd > Hg > Cu > Fe >> Ca) which mimics mammalian in vivo toxicity. The values obtained with several potential chelators indicate that an ordering of these compounds is also possible. Our preliminary findings indicate that three siderochromes are somewhat intermediate in toxicity between EDTA and PCDT (1-pyrolidine carbodithioic acid). The siderochromes tested do not appear to be more toxic to cell cultures than some antibiotics (e.g., amphoterin B) currently in use.

While initial studies with the clonal growth assay indicate it can serve as a rapid screening method for toxic agents, additional studies are necessary before the limitations of the method can be more clearly defined. The technique appears to be useful where only small amounts of the agent are available (i.e., siderochromes) for test as removal agents. Furthermore, a toxicity estimate of the chelon, compared to its metal complexes, is readily obtained.

TABLE 25.8. Relative Plating Efficiency of VERO Cells in the Presence of Metals and Chelons

	CONCENTRATION OF TEST AGENT (µg/ml)									
TEST AGENT	0.01	0.1	0.2	1.0	2.0	10	50	100	500	1000
Na_2 EDTA	NT[a]	NT	NT	NT	NT	NT	100	100	85	0
PCDT	95	61	0	0	0	0	0	0	0	0
SIDEROCHROME I *E. COLI*	NT	NT	NT	100	100	82	47	0	0	NT
SIDEROCHROME II *P. NITRIFICANS*	NT	NT	NT	100	100	100	64[b]	0	0	NT
SIDEROCHROME III *P. NITRIFICANS*	NT	NT	NT	100	100	100	89	0	0	NT
Cd	NT	NT	52	0	0	0	NT	NT	NT	NT
Hg	NT	NT	100	NT	47	4	NT	NT	NT	NT
Cu	NT	NT	100	100	100	60	0	0	NT	NT
Fe	NT	NT	100	100	100	100	82	70	0	0
Ca	NT	NT	NT	NT	NT	100	100	100	100	100
Zn	NT	100	NT	100	95	89	0	0	NT	NT

[a] NT = NOT TESTED

[b] VALUE FOR 35 µg/ml

• MOBILIZATION OF DEPOSITED METALS

Person in Charge: V. H. Smith

This project has the broad objective of developing treatments for overexposure to toxicants encountered in some of the new non-nuclear energy technologies. Necessarily associated with this effort is the identification of toxic agents, their effects and the mechanisms of their toxicity, the development of suitable test models and exposure procedures, and the formulation of this information into effective treatment procedures.

Initial efforts are being directed toward the toxic metals cadmium, lead, ruthenium, vanadium, nickel, cobalt, chromium, and arsenic, which are associated with catalytic processes used in shale oil production and synthetic fuel preparation, and are products of fossil fuel combustion. In the hope of finding complexing agents combining high selectivity for metals with low toxicity in mammals, biologically derived chelons are being tested. The siderochromes produced by some bacteria chelate several metals with a high degree of specificity, transport them across biological membranes, and may be capable of removing toxic metals from within cells and from the circulatory system. They have the advantage of small molecular size, which should make them poor antigens. A technique for inducing organisms to produce siderochromes against specific metals is also being investigated.

SIDEROCHROME PRODUCTION, PURIFICATION AND METAL BINDING

Investigators:

A. V. Robinson and R. A. Pelroy

A new method, involving polyamide chromatography, for quick purification of bacterial siderochromes has been developed and is compared to a previous method using silica gel chromatography and solvent extractions.

Siderochromes (SCs) are natural chelating agents, secreted by many microorganisms in response to iron deficiency conditions. These agents scavenge the medium for iron. Two main classes of SC compounds are known: catechol derivatives, which we are currently investigating, generally consist of a 2,3-dihydroxybenzoic acid moiety bound to an amino acid. The second class, which we will study in the future, are the hydroxamic acid derivatives.

Siderochromes are reported to form stable complexes with binding constants for Fe^{+3} in excess of 10^{30}, which is greater by two to four orders of magnitude than the corresponding values for EDTA or DTPA. The binding of other metals (such as Al^{+3}, Cr^{+3}, La^{+3}, Cd^{+2}, Tl^{+3}) to siderochromes has been shown, and as a result of this known chelation ability and the lipophilic nature of these compounds, they present a type of agent with potential for excorporation of toxic metals. Toxicity of SCs tested has been low, for example, when desferrioxamine B (isolated from actinomycetes) was used to treat excess iron storage disease in humans.

To date, our major effort has been directed toward the purification and preparation of a catechol-type SC produced by Paracoccus denitrificans. Using a standard iron-deficient medium we have produced crude siderochrome preparations from the following bacteria: Paracoccus denitrificans, Bacillus megatherium, Bacillus subtilis, Klebsiella pneumococcus and Escherichia coli. Siderochrome production began in the stationary phase and the SCs produced (usually yellow to yellow-orange) were excreted into the culture media. P. denitrificans was grown using succinate as the carbon source, while the other bacteria were grown on glucose. In all cases, the total catechol content of the media ranged from 10-30 mg per liter of cell-free culture supernatant.

Medium containing siderochrome from P. denitrificans was acidified to pH 2 with HCl, freeze-dried, and extracted with ethanol. The pooled ethanol fractions were dried under reduced pressure at 30-40°C, the residue dissolved in water, and the solution extracted with ethyl acetate. The aqueous phase was kept for further purification of SC II (N^1N^8-bis-(2, 3-dihydroxybenzoyl) spermidine). The ethyl acetate fraction was extracted with 10% (w/v) $NaHCO_3$. The $NaHCO_3$ extracts were set aside for purification of SC I (2,3-dihydroxybenzoic acid), and the ethyl acetate fraction was kept for purification of SC III (2-hydroxybenzoyl-N-1-threonyl-N^4 [N^1N^8-bis-(2,3-dihydroxybenzoyl) spermidine.)

Further purification of SC I and SC III was accomplished using a silica gel column (approximately 0.5 X 15 cm) equilibrated

with benzene-ethyl acetate (3:1, v/v). The $NaHCO_3$ fraction (containing SC I) was reacidified to pH 2 with HCl and extracted with ethyl acetate. The pooled fractions were dried under reduced pressure over Na_2SO_4. The residue was then dissolved in benzene-ethyl acetate (3:1 v/v) and an aliquot applied to the silica gel column with an eluotrophic series of solvents consisting of benzene-ethyl acetate (1:1, v/v), ethyl acetate, methanol, and H_2O. Fractions from each series were collected and assayed for catechol activity by the method of Arnow (Biochem. 8: 757-762, 1969). The ethyl acetate fraction (containing SC III) was dried under reduced pressure and the residue redissolved in benzene-ethyl acetate (3:1 v/v). SC III was then placed on a column and eluted exactly as detailed above for SC I.

Table 26.1 illustrates the results of this final step in terms of the percent of catechol recovered from the original medium in each fraction. The identity of each compound was established by thin-layer chromatography (TLC) on cellulose support in an aqueous solution of 5% ammonium formate (w/v) 0.5% formic acid (v,v). In this system SC I moves with Rf of approximately 0.6, SC II moves with Rf 0.4 and SC III has Rf of 0.0.

TABLE 26.1. Recovery for Siderochrome Purification by Method I.[a]

	SIDEROCHROME RECOVERY (% OF INITIAL AMOUNT)			
PURIFICATION STEP	SC I	SC II	SC III	TOTAL CATECHOL
1. FREEZE-DRYING	-	-	-	-
2. SOLVENT EXTRACTION	-	53	16(I + III)	69
3. SILICA GEL COLUMN CHROMATOGRAPHY	9	47[b]	14	70

[a] SILICA GEL CHROMATOGRAPHY OF SOLVENT-EXTRACT FRACTIONS (SEE TEXT)
[b] SC II WAS NOT CHROMATOGRAPHED ON SILICA GEL

The above procedure was time consuming and led to loss of product during the lyophilization and evaporation steps. An alternative method of concentrating and purifying siderochromes using a polyamide support was therefore investigated. Conditions necessary for adsorption and elution of catechols were established using TLC plates coated with polyamide. In preliminary work it was found that catechols in aqueous solutions were strongly adsorbed to polyamide support. Development of plates in a solvent system of methanol:acetone:10% (w/v) ammonium formate:N,N dimethyl formamide (1:1:1:1, v/v/v/v) resulted in migration of catechols. Using the results of the TLC data, the method was scaled up to a preparative 2.5 X 50-cm column. The column was equilibrated with distilled H_2O and 800 ml of siderochrome-containing media from P. denitrificans was passed through the column. The eluate from the column contained no catechol. The siderochrome compounds were adsorbed as a yellow band in the top 10-15 cm of the column and were washed free of nonadsorbing material by passing 200-300 ml of distilled H_2O through the column. Adsorbed compounds were then eluted with the previously mentioned solvent system. Four fractions of 30-50 ml each were collected as the yellow compounds were eluted. The recovery of catechol in eluted fractions 1 through 4 was 61%, relative to the total catechol applied.

Moreover, TLC analysis of eluted fractions for siderochrome (i.e., 30- to 50-ml fractions 1, 2, 3 and 4, Table 26.2) showed that fraction 1 contained only SC II and SC III, with SC III as the major component; fractions 2 and 3 contained only SC III; and fraction 4 contained no iron-binding component. It would appear that this method results in a substantial enrichment of SC III relative to SC I and SC II. This enrichment is desirable for several reasons: from the point of view of function it is likely that SC III is the significant species in Fe^{+3} transport in bacteria, and it is noteworthy that Fe^{+3} binds less strongly to SC II than to SC III, (Tait, Biochem. 146: 191-204, 1975). The ability of a catechol trimer (such as SC III) to bind Fe^{+3} more strongly than the dimer (such as SC II) or monomer (SC I) was also noted with enterochelin (a catechol trimer) and its dimeric and monomeric hydrolysis

TABLE 26.2. Distribution and Recovery of Catechols from Polyamide Column Chromatography.

POLYAMIDE COLUMN FRACTION	APPLIED CATECHOL RECOVERED, %	SIDEROCHROMES PRESENT[a]
1	21	SC III, SC II
2	36	SC III
3	9	SC III
4	1	UNDETECTABLE
TOTAL	67	

[a] AS DETECTABLE BY $Fe(NO_3)_3$ SPRAY, FOLLOWING TLC DEVELOPMENT ON POLYAMIDE PLATES IN ACETONE: METHANOL: 10% (w/v) AQUEOUS AMMONIUM FORMATE (1:1:1, v/v/v)

products (O'Brien, Biochim. Biophys. Acta 237: 537-549, 1971). These results suggest that SC III may bind other metals more strongly than SC II or SC I. We have also noted that brief treatment of SC III with 0.025 N HCl prior to analysis by TLC results in the appearance of a new iron-binding component. The extraction procedure exposes the SCs to 0.1 N HCl for 12-24 hr; thus, where high yields of unaltered SC III are desired, acid should be avoided.

Using the polyamide method, we hope to obtain significant quantities of purified representative siderochromes for future chemical and biological evaluation.

Such work will be directed toward preparation of milligram to gram quantities of microbially produced siderochromes, which will then be tested as possible excorporation agents in mammalian tissue culture and, ultimately, in animals. Preliminary experiments have been carried out which suggest that thin-layer chromatography and absorption spectrophotometry of siderochrome-metal chelates will be useful assay methods to detect metal binding by these agents. Only those siderochromes which demonstrate extensive chelation of heavy metals (other than Fe^{+3}) will be tested.

• DEVELOPMENT OF BLOOD IRRADIATORS

Person in charge: F. P. Hungate

Extracorporeal irradiation of blood, using repeated brief exposures, has been shown to suppress rejection of tissue transplants and to inhibit progression of chronic lymphocytic leukemia. There remains a need to establish the conditions of dose administration which optimize therapeutic effect, to study the basic processes by which blood irradiation produces such effects, and to improve the technique of blood irradiation through the development of improved and portable blood irradiators. Irradiators now in use are large, expensive and consequently available to relatively few patients. It also appears probable that continuous irradiation of blood during critical periods, with lower dose rates, may constitute a more effective treatment.

Tests since FY 1969 on a number of photon-, alpha-, and beta-emitting isotopes, for their ability to deliver effective doses to blood, have resulted in the choice of ^{170}Tm, encapsulated in vitreous carbon, as the source material. The ^{170}Tm beta radiation passes through the carbon layer and effectively irradiates blood; the direct and indirect (bremsstrahlung) radiation is readily shielded; the containment and blood interface material is unaffected by radiation doses in excess of 10^{10} rads and is relatively nonthrombogenic. An additional advantage is the fact that irradiation units can be totally fabricated with stable ^{169}Tm, which is converted to radioactive ^{170}Tm by a final neutron activation. Total weight of shielded prototype units is about 500 g. Goats wearing these units show rapid loss of circulating lymphocytes with daily doses to blood of <1,000 rads.

Current and projected future efforts include: (1) continued materials and design research leading to improved portable irradiators, and their preclinical evaluation in animals; (2) basic hematologic and immunologic studies relating to blood irradiation and its effects on cellular and humoral immune response; (3) liaison with regulatory bodies to provide them with information pertinent to ultimate licensing; and (4) continued and expanded support of, and collaborative research with, clinical groups interested in using blood irradiation as an adjuvant in the suppression of transplant rejection and the treatment of certain lymphocytic neoplasms.

PROGRESS IN DEVELOPING A PORTABLE BLOOD IRRADIATOR FOR MEDICAL APPLICATIONS

Investigators:

F. P. Hungate, L. R. Bunnell, and W. F. Riemath

Technical Assistance:

A. J. Clary

This year was spent in perfecting details of the new design blood irradiator, i.e., having male fittings made for shunt insertion and in acquiring preliminary biological data on its effectivness. Fabrication of units was slowed by an unanticipated reaction of the resin with the steel injection mold, by occasional thrombogenic flaws in the blood interface layer, by thrombus formation at the points of connection to the shunt and by nonavailability of a reactor for activating the ^{169}Tm to ^{170}Tm. The remaining unsolved problem is that of thrombus formation at the connectors.

Ionizing radiation can be effective in reducing the number of circulating lymphocytes and suppressing cellular immune responses. We are developing a fully portable blood irradiator capable of being attached in an arteriovenous (AV) shunt and irradiating circulating blood continuously for extended periods. A patent for the device has been granted and we are now perfecting fabrication techniques and acquiring animal data relevant to the development and use of the irradiators.

The irradiators are one-piece units of vitreous carbon (VC) with thulium oxide placed within the carbon matrix to optimize dose to blood, yet assure full containment. The present design was described and illustrated in the 1975 Annual Report. The tubular units used in animal studies are 48 mm long, 7 mm in dia and have an internal 3.1-mm diameter hole through which the blood flows. Extensions on the ends of the irradiators permit easy connection to silastic shunt tubing using standard shunt connectors typical of those used in blood dialysis of human patients.

To construct units with shunt connector ends, a steel mold was fabricated and initial units were produced by sequentially: 1) applying a Tm_2O_3 polyfurfuryl resin slurry on a wax rod; 2) casting the resin body around the wax rod and polymerized slurry; 3) following polymerization of the body and removal of the wax, flowing a thin inner containment and blood interface layer onto the inner surface. These steps were completed by trimming the ends to length, vitrifying the unit in a controlled atmosphere at 1000°C and neutron-activating the ^{169}Tm to ^{170}Tm. Several problems developed with this procedure: chiefly reaction of the resin with the steel mold, imperfections in the inner containment layer, and thrombogenesis at the end connectors. Reaction with the steel mold was not anticipated, since earlier castings made on a steel plate had released easily with a good surface. However, in the enclosed mold severe bubbling occurred with resulting defective units. Following prolonged evaluation of methods to coat the mold, this problem was recently overcome by forming a massive silastic

rubber mold. This silastic mold is easier to use and produces easily cleaned flaw-free surfaces.

The problem of imperfections in the inner containment layer appeared when some VCTm units were observed to release small amounts of ^{170}Tm after activation. Also, some units with fully contained ^{170}Tm caused localized thrombus formation when used in an AV shunt. This problem was overcome by centrifugally casting the inner layer (0.1-0.2 mm thick) in a mold at 10,000 rpm. Following polymerization and removal from the mold, the Tm_2O_3-resin slurry is then applied to the outer surface of this tube, using vacuum to remove any trapped bubbles. This spin casting produces a superior inner surface with assured containment of the thulium.

In early tests of the irradiator units in AV shunts on goats, ring thrombi formed at the ends. Early testing had indicated that VC subjected to machining is thrombogenic, while pristine surfaces are non-thrombogenic. Thus, following trimming the ends to precisely fit the connector hardware, a thin film of resin is now applied to the cut surface. Thrombus induction is now no greater than where the connectors are used without inclusion of an irradiator.

VCTm units showing full containment of the ^{170}Tm are being tested in carotid-jugular AV shunts on goats. When the shunt surgery is well-healed, and prior to insertion of the irradiator into the shunt, the goats are given 10-15 grains of aspirin per day and sufficient dicoumarol to maintain a prothrombin time of 2-3 times normal. There is essentially no problem with shunt occlusion by thrombi so long as this anticoagulation therapy is maintained. The typical response of lymphocytes to daily blood doses from 485 to 1090 rads per day is shown in Figure 27.1. An

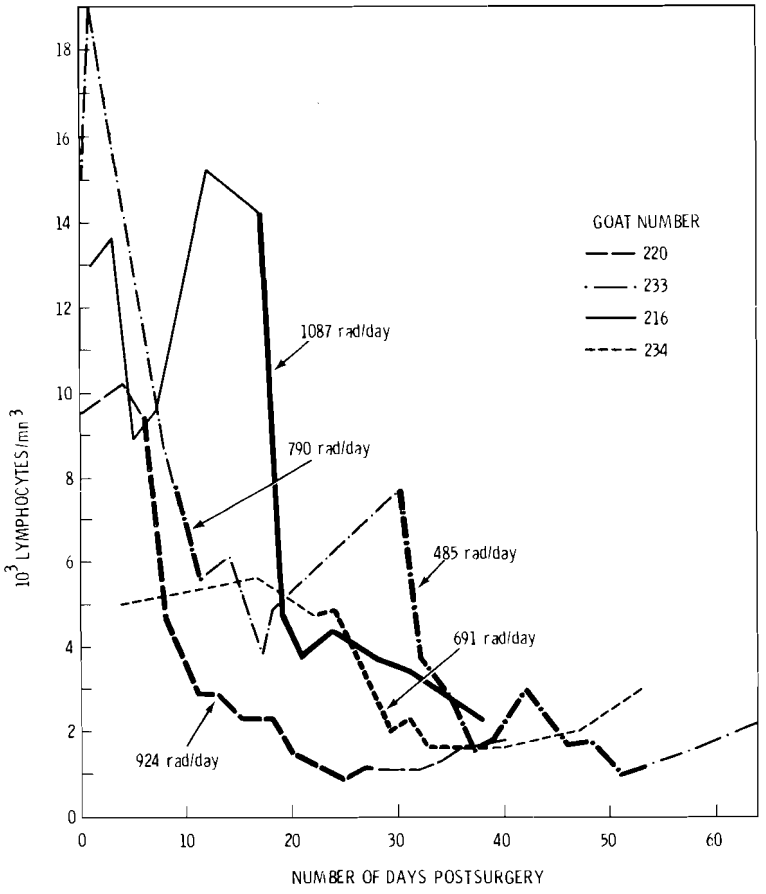

FIGURE 27.1. Typical Goat Lymphocyte Response to VCTm Blood Irradiator Units. Animal number and daily dose to the blood are indicated on each curve. Heavy portion of curve indicates time during which irradiator was in place.

approximately 5-fold reduction in circulating lymphocytes is achieved within 10 days at the dose rates tested; this is followed by a slow subsequent decline while the VCTm unit remains functional. With the doses used, no effects on red cell numbers or on blood cell components other than lymphocytes were noted.

The profile of the radiation dose to blood was calculated using a modified Betblud code and is shown in Figure 27.2. While there is an order of magnitude difference between central and peripheral dose rates, it is doubtful that this materially affects the results. Marsaglia and Thomas (Rad. Res. 25:269-76 [1965]) have discussed the statistical nature of dose accumulation under similar conditions.

Reciprocal skin allo- and autografts were performed on these animals approximately 10 days after radiation treatment commenced. Two animals maintained on anticoagulant therapy developed subgraft hemorrhage 3-5 days following placement of the grafts. A regraft on one of these (233) gave a full "take" with vascularization, and hair growth at 2-1/2 months. Two other pairs of animals failed to show typical rejections in either the control or treated animals, although the allografts slowly dried and were dropped 5-8 weeks following placement. Due to the absence of the typical rejection syndrome in these animals, all of which were unrelated, the presence of an allograft "take" in a treated animal is not readily interpreted. We are now testing African pygmy goat skin for rejection and will use these animals in subsequent tests if a typical rejection syndrome is obtained.

The problem of maintaining functional shunts during the period immediately following skin transplant is not yet resolved. Thrombus formation begins at the connectors between shunt tubing and the VCTm units. We have examined the surface by injecting nonadhering silicone rubber into these joints and forming a replica of the surface seen by the blood. These replicas indicate the existence of a nonconformity caused by nonconcentricity of the tubing extensions which butt together within a connector to close the shunt. When the extensions are used without VCTm intervention, the nonconformity can be minimized by appropriately matching the two extensions, and thrombus formation is not a problem. When the extensions are rotated to maximize the nonconformity a thrombus forms and stoppage of flow occurs within a few hours. We now minimize the effect of the nonconformity by frequently opening the connectors and removing the small thrombi. The vendor who supplies the shunt hardware is also working with us to develop more concentric hardware for these animal shunts, which are slightly larger than those typically used on humans.

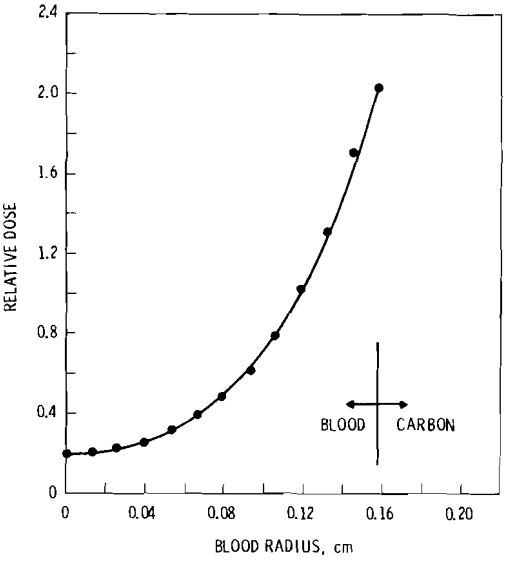

FIGURE 27.2. Relative Blood Dose Profile With 1/8 in. (0.32 cm) Dia Tube

• MECHANISMS OF RADIATION EFFECTS

Person in Charge: M. E. Frazier

This project is composed of two related but separate studies. Our primary objective is to determine the role of virus in "radiation-induced" malignancies and, in the process, to identify those parameters (biochemical, virological, immunologic, etc.) which might serve to monitor the oncogenic process.

Previous work under this project has demonstrated a virus associated with leukemia which developed in miniature swine following exposure to internally deposited ^{90}Sr. The immediate goal of the leukemogenesis study is to determine the nature of the porcine virus and its role in the oncogenic process. In other words, does radiation convert a normal cell to a malignant cell by the expression of pre-existing genetic information (viral or nonviral) through the action of gene repressors or modulators of metabolic function in the cytoplasm or at the cell membrane; or, is the malignant transformation preceded by the entry and insertion of new viral information?

Studies at this laboratory have also shown that plutonium in the form of inhaled particles produces a dose-related lymphopenia in the beagle dog, with pulmonary neoplasia or osteosarcoma as the principal causes of death. Plutonium-exposed beagles are currently being examined for evidence of impaired immune function resulting from the plutonium-induced lymphopenia. If such an impairment is present we will examine any relationship to the induction of bone and lung tumors. Similar studies are investigating the role of virus (initially, oncornavirus) in the genesis of these tumors. To facilitate these studies, tumor cells are being grown and investigated in cell culture.

CULTURE OF CELLS FROM BEAGLES WITH BRONCHIOLO-ALVEOLAR CARCINOMA

Investigators:
M. E. Frazier and T. K. Andrews

Cell cultures were prepared from lung tumors occurring in beagles following exposure to inhaled plutonium. Morphologic and growth characteristics of two of these cell lines are described.

The purpose of this in vitro study of Pu-induced bronchioloalveolar carcinomas in beagles was to attempt to determine the mechanism by which Pu causes lung tumors and, in the process, to identify any unusual parameters (whether biochemical, immunological, virological, etc.) which might serve to monitor the oncogenic process. Within this admittedly broad objective we have concentrated on the more immediate objective of growing lung tumor cells in culture, in order to provide a readily available source of material for the broader study. For example, an immunological study of these radiation-induced tumors requires the availability of a large number of cells from an individual animal, as well as a battery of cells cultured from many other tumor-bearing animals.

During the past year we have attempted to culture tumor cells from 12 dogs. We have established cell lines from 10 of these animals (Table 28.1); these were cloned and aliquots frozen for future use. Two cell lines (AF 759 and FA 772) were chosen for further study.

After 30+ passages in culture, certain stable growth characteristics were measured. The plating efficiency of these cells in NCTC 109, supplemented with 10% fetal bovine serum (FBS), was 19% for AF 759 and 34% for FA 772. The doubling time of these cell lines, determined using both the Elkinds procedure and total protein, was found to be about 20-22 hr in 10% FBS and about 54 hr in 1% FBS. Morphologically these cultures consist of oval to polygonal cells, 14-18 μm in diameter. The nuclei are usually oval, with distinct but delicate nuclear membranes. Mitotic figures are apparent, including some of abnormal appearance. Actively growing cultures display some intracytoplasmic vacuoles which contain PAS-positive material. Scanning electron micrographs reveal microvilli on the surface of the cells, a finding consistent with the probable origin of these tumors from secretory type II alveolar cells. These microvilli are fairly uniform in

TABLE 28.1. Tumor Cell Lines Established During FY 1976

DOG NUMBER	TYPE OF TUMOR (TENTATIVE DIAGNOSIS)	ESTABLISHMENT OF CELL LINE
759	LUNG	+
796	LUNG	+
480	LUNG, (POSSIBLE OSTEOSARCOMA METASTASIS)	-
271	LYMPHOMA	+
772	LUNG	+
792	MELANOMA	+
873	LUNG	+
783	LUNG	-
761	LUNG	+
753	LUNG	+
727	LUNG	+
LIL*	LUNG	+

*SPONTANEOUS LUNG TUMOR

diameter but vary in length. Transmission electron micrographs also show the presence of these microvilli. In addition, intracellular organelles, similar to the osmophilic lamellar bodies of type II alveolar cells, can also be seen in some of these cells.

Both cell lines were negative for spontaneous expression of C-type RNA virus and for mycoplasma contamination. Results of karyotyping indicate a definite hypodiploidy, which may be partially the result of translocation. Chromosome-banding studies are currently underway to test this hypothesis.

Additional studies are contemplated for obtaining information about the biochemical parameters and growth characteristics of these cultured cells, including a search for remnants of lung cell function.

PURIFICATION OF DNA POLYMERASE ACTIVITY IN TISSUES FROM LEUKEMIC MINIATURE SWINE

Investigators:
M. E. Frazier and L. Mallavia[a]

An RNA-instructed DNA polymerase (RIDP), also called reverse transcriptase, has been purified from the lymph node of a leukemic miniature swine. The procedure resulted in a 36-fold purification of the enzyme. The isolated enzyme has a sedimentation coefficient of ∿ 4.5, a value consistent with the 70,000-80,000 MW of mammalian viral reverse transcriptases.

An RIDP-like activity has been found associated with a virus from swine with radiation-induced leukemia. In order to demonstrate that this was a true viral RIDP it was necessary to purify and characterize the enzyme.

Purified porcine virus from a leukemic pig was pelleted, solubilized and added to diethylaminoethyl (DEAE) cellulose as a first step in the purification of RIDP (Figure 28.1). The column was initially washed in an effort to elute undesired enzymes. The DEAE was then washed with 0.4 M potassium phosphate buffer (KPB) to obtain the desired polymerase. This material was dialyzed to remove the KPB and then added to a phosphocellulose (PC) column. The enzyme activities were then eluted with a linear KPB gradient in an attempt to separate α polymerase from the viral RIDP. Fractions were assayed for reverse transcriptase (RIDP) activity using either polydeoxyguanylate, polyribocytidylate (dGrC) or polyriboadenylate polydeoxythymidylate (rAdT) as template. Activated (nuclease nicked) calf thymus DNA was used as a template to detect DNA-dependent DNA polymerase activity. A peak of dGrC and rAdT activity was eluted from the PC column between 0.1 and 0.25 M KPB. This partially purified enzyme preparation preferred the rAdT template, giving approximately three times more incorporation of label than was obtained using dGrC as a template. While these two templates are considered the most discriminating in assaying for RIDP, other polymerases can utilize these templates. However, the lack of activity with activated DNA in this region indicated this was a remote possibility.

In addition to this possible source of error in the assay, mitochondria-associated DNA polymerase and heavy-molecular-weight DNA-dependent DNA polymerase have been

[a]Washington State University

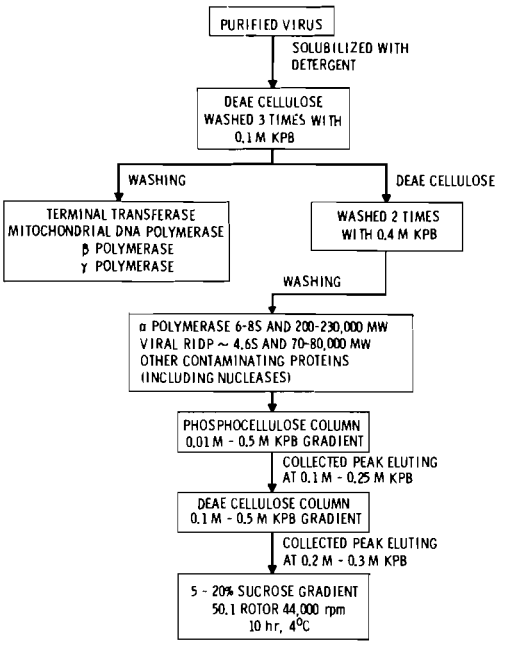

FIGURE 28.1. Purification Scheme for Isolation of Viral RIDP from Porcine Cells

reported to elute at the same KPB concentration on PC columns as viral reverse transcriptase (RIDP). Therefore, in order to assure separation from contaminating enzyme, fractions of the active peak were pooled and concentrated by filtration to exclude proteins with molecular weights less than 50,000 daltons. This material was then applied to a second DEAE cellulose column. The protein was eluted with a linear KPB gradient and the fractions assayed. A peak of dGrC- and rAdT-templated polymerase activity was eluted (between 0.2 and 0.3 M KPB) which was distinct from a peak of DNA-templated activity eluting at a higher KPB concentration. The first peak was collected and concentrated. This material was further purified and sized in a sucrose velocity gradient, along with various marker proteins (bovine serum albumin, 4.4S, and aldolase, 7.4S). As can be seen in Figure 28.2 the enzyme activity was found in the same region of the gradient as the albumin (4.4S). This value is consistent with the 70,000-80,000 MW of known mammalian viral reverse transcriptases. Table 28.2 shows the results of purification procedure. The final protein concentration was approximately 1% of the solubilized virus preparation and the procedure resulted in an approximately 36-fold purification of the enzyme.

The pH optimum for this enzyme activity (with an rAdT template) is 7.8-9, with maximum synthesis at 8.1-8.3. Divalent cations (Mg^{++}, 5 mM or Mn^{++}, 1mM), sulfhydryl reducing agents dithiothreitol (DTT) and all four deoxynucleotide triphosphates are necessary for maximum synthesis.

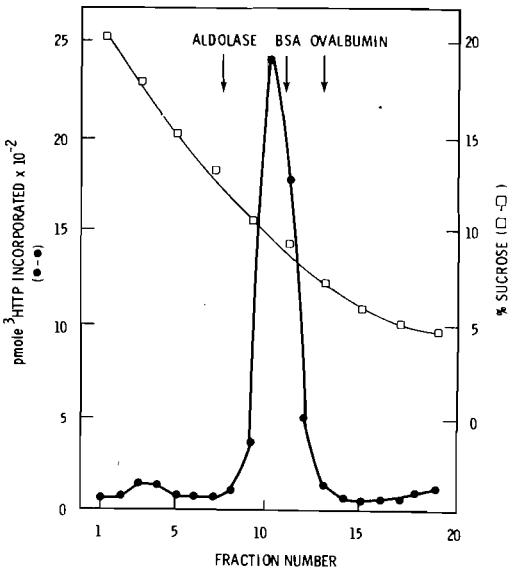

FIGURE 28.2. Sedimentation Pattern of Purified Porcine RIDP in Sucrose Gradient. The fractions obtained were ∿ 250 µl, of which 50 µl were used to determine activity. The remainder of the enzyme preparation was used to determine total protein and the catalytic properties of the purified enzyme.

TABLE 28.2. Purification of RIDP from Virus Extracted from the Lymph Node of a Leukemic Miniature Pig

FRACTION	TOTAL PROTEIN (mg)	SPECIFIC ACTIVITY (units/µg)	TOTAL ACTIVITY[a] (units)	% YIELD
SUCROSE GRADIENT (SOLUBILIZED VIRUS)	181	0.344	621	100
DEAE CELLULOSE	14	4.1	585	93
PHOSPHOCELLULOSE-II	3.1	9.0	281	46
DEAE CELLULOSE	2.4	11.2	266	43
SUCROSE GRADIENT	2.0	12.4	252	40

[a] ASSAYED USING rAdT AS A TEMPLATE; dGrC - TEMPLATED REACTIONS WERE APPROXIMATELY 1/3 OF THE rAdT VALUES. A UNIT IS THE AMOUNT OF ENZYME ACTIVITY WHICH INCORPORATES ONE pmole OF dTTP/min INTO AN ACID-INSOLUBLE PRECIPITATE

The properties of the enzyme (template specificity, molecular size and optimum reaction conditions) isolated in these initial studies are consistent with viral reverse transcriptase activity. The capacity of reverse transcriptase to copy a natural RNA template with fidelity is its single most important functional characteristic. Further, the DNA produced must be complementary to heteropolymeric regions of the natural RNA template, as determined by back hybridization of product to natural RNA template. To perform this important element of characterization, additional enzyme must be purified. In future efforts, we intend to study the catalytic and physical properties of this porcine viral enzyme, in addition to determining, immunochemically, its relationship to similar enzymes from various mammalian oncornaviruses and retraviruses. An assay system (preferably a radioimmune assay) for the porcine viral RIDP will also be attempted. Such a system could provide important qualitative and quantitative measurements of RIDP activity in a variety of materials (e.g., cell cultures, "normal" tissues, myeloblastic leukemias, lymphocytic leukemias, myeloid metaplasia, etc.).

USE OF MOLECULAR HYBRIDIZATION TECHNIQUES TO INVESTIGATE RADIATION-INDUCED MALIGNANCIES

Investigators:

M. E. Frazier and F. Akiya[(a)]

Technical Assistance:

J. Engstrom

A virus has been isolated from miniature swine with "radiation-induced" leukemia. In order to determine the role of this agent in the oncogenic process hybridization studies must be carried out to determine the nature of this virus. To facilitate these studies DNA from a variety of sources has been purified and tested. A number of available RNA tumor viruses have been produced or procured in amounts sufficient to allow preparation of DNA probes and purification of RNA.

RNA tumor viruses can be classified on the basis of hybridization patterns. Class I viruses have nucleotide sequences identical or nearly identical to those found in DNA of the species of origin. These viruses exhibit more than 50% homology with progenitor cells and will hybridize to both repetitive and infrequent sequences present in the DNA of these cells. Class II viruses, on the other hand, are transmitted horizontally, and have RNA sequences not highly related (less than 30%) to the DNA from the species of apparent origin. Those viruses hybridize only to the nonrepetitive (or infrequent) sequences of the host-cell DNA. To understand the role of viruses isolated from animals with radiation-induced malignancies it is necessary to understand the nature and origin of the viral agent. To do this, the following types of hybridization studies must be carried out:

1) viral DNA probe (^{3}H-DNA) to cell DNA
2) viral DNA probe (^{3}H-DNA) to viral RNA
3) viral RNA (^{125}I RNA) to cell DNA

The information provided by these studies will allow us to classify the porcine

(a) NORCUS Fellow

isolate, to determine the complexity of the viral genome, to analyze the degree of complementarity (relatedness) to other RNA tumor viruses (and retraviruses), and allow a quantitative assay of the viral genome in DNA from infected and "normal" cells.

Reagents are being prepared for such a study, and DNA has been isolated from a variety of sources in a large number of animals (Table 28.3). The DNA extraction procedure is shown in Table 28.4. Following purification the DNA is tested prior to use in hybridization experiments. We use only DNA with an O.D. 260/280 of greater than 1.8. The DNA to be used is sized in a velocity gradient and shown to be between 400-650 nucleotides in length. Finally, the DNA is melted and the reannealing properties tested.

Purified RNA tumor viruses from a number of species (Table 28.5) have been obtained for these studies. The production of ^{3}H-DNA probes (Frazier, Annual Report 1974) from a number of these viruses has been completed. Similarly, the purification of viral RNA (both unlabeled and ^{125}I-labeled) for hybridization experiments is currently in process.

TABLE 28.3. Source of DNA Preparations

PORCINE:	LEUKEMIA, NORMAL, METAPLASTIC
CANINE:	NORMAL, OSTEOSARCOMA, LYMPHOMA, LUNG TUMOR
FELINE:	NORMAL, LEUKEMIA
MOUSE (SEVERAL SPECIES):	NORMAL, LEUKEMIA, BONE TUMOR, MAMMARY TUMOR
RABBIT:	NORMAL
SHEEP:	NORMAL, LUNG TUMOR, MAEDI LUNG
BOVINE:	NORMAL, LYMPHOMA
HORSE:	NORMAL, EQUINE INFECTIOUS ANEMIA
HUMAN:	NORMAL, LEUKEMIA, LUNG TUMOR
CHICKEN:	NORMAL, LEUKEMIA
GOAT:	NORMAL
PRIMATE:	NORMAL

TABLE 28.4. DNA Extraction Procedure

LYSIS:	NUCLEI PREPARED BY DIFFERENTIAL CENTRIFUGATION; NUCLEI LYSED IN 8M UREA, DETERGENT, SODIUM PERCHLORATE, AND PHOSPHATE BUFFER
EXTRACTION:	CHLOROFORM ISOAMYL ALCOHOL
ABSORPTION:	DNA IS ABSORBED TO HYDROXYAPATITE
WASHING:	1) WASHED WITH 8M UREA IN PHOSPHATE BUFFER (TO REMOVE RNA AND PROTEIN) 2) WASHED WITH PHOSPHATE BUFFER TO REMOVE UREA
ELUTION:	DNA IS ELUTED FROM HYDROXYAPATITE WITH 0.4M PHOSPHATE BUFFER
SHEARING:	DNA IS PELLETED, RESUSPENDED, THEN SHEARED IN RIBI CELL FRACTIONATOR: A 50,000 psi YIELD -- 500 NUCLEOTIDE PIECES
FILTER:	FILTERED THRU MILLIPORE FILTER

TABLE 28.5. Virus Preparations

	^{3}H-DNA PROBE	PURIFIED RNA	SOURCE OF VIRUS
BABOON PLACENTA VIRUS (ENDOGENOUS VIRUS)			NCI[a]
GIBBON APE LYMPHOSARCOMA VIRUS			NCI
SIMIAN SARCOMA VIRUS			NCI
RD114 (FELINE ENDOGENOUS) VIRUS			NCI
FELINE LEUKEMIA VIRUS			BNW[b] NCI
RAUSCHER LEUKEMIA VIRUS	X	X	BNW NCI
MOLONEY LEUKEMIA VIRUS	X	X	BNW NCI
AVIAN MYELOBLASTOSIS VIRUS	X	X	BNW
MASON-PHIZER MONKEY VIRUS	X	X	BNW
MOUSE MAMMARY TUMOR VIRUS	X	X	BNW
EQUINE INFECTIOUS ANEMIA VIRUS			BNW
KIRSTEN SARCOMA VIRUS	X		BNW
PORCINE LEUKEMIA VIRUS	X		BNW
ROUS SARCOMA VIRUS		X	BNW

[a] NCI - OBTAINED FROM DR. JACK GRUEBER, NATIONAL CANCER INSTITUTE

[b] BNW - PREPARED AT PACIFIC NORTHWEST LABORATORY

TESTS FOR MUTAGENCITY OF FREE RADICALS FORMED IN IRRADIATED SUGARS AND AMINO ACIDS

Investigators:

D. R. Kalkwarf and R. A. Pelroy

Radicals formed in gamma-irradiated crystals of galactose and glycine were found, upon dissolution, to cause mutagenesis of Salmonella typhimurium strains TA-98 and TA-100. Although the reproducibility of the results has not been adequately determined, they suggest the possibility of developing a test to measure the mutagenic-carcinogenic potential of radiation-induced free radicals with a microbial system.

Several of the chemical effects of organic free radicals released from irradiated crystals during dissolution have been described in previous Annual Reports. If the radicals escape recombination, they can initiate oxidation, reduction, and polymerization reactions with suitable substrates in the media. Their demonstrated abilities to lyse both red blood cells and vesicular phospholipid bilayers prepared from common membrane constituents suggested that they might also be able to enter or disrupt living cells so as to cause mutagenesis. In addition, organic free radicals may represent a threat to living cells in terms of their capacity to induce mutation and/or carcinogenesis as a result of damage to cellular deoxyribonucleic acid (DNA). Such attack might be direct, i.e., DNA + radical, or indirect, e.g., mediated by a transmitter molecule which is first modified by radical attack.

To assess the potential for radical-induced mutagenesis, we have begun a series of experiments using bacteria as indicator, or target, cells. The assay system is highly specific for both point and frame-shift mutations, and depends on back-mutation of histidine-requiring S. typhimurium (the testor strains of Ames, et al.) to nonhistidine-requiring or wild-type strains. This is the most common and reliable system now in use for detecting chemical carcinogens. In particular, agents which cause a significant increase in frame-shift mutations are highly suspect as carcinogens.

The free radicals tested were those formed by exposing crystals of glycine, DL-α-alanine, D-galactose and D-lactose to ^{60}Co-gamma radiation at room temperature. Electron spin resonance (ESR) studies on single crystals have shown that the $\dot{C}H_2COO^-$ and $H_3\overset{+}{N}-\dot{C}H-COO^-$ radicals are formed in irradiated glycine and $H_3\overset{+}{N}-\dot{C}(CH_3)COO^-$ is formed in irradiated alanine, but the structures of the radicals in the irradiated sugars have not yet been clearly identified. Prior to irradiation, the crystals were dried, ground into particles <125 μ in size, and weighed into polypropylene containers that were then sealed. Half of the specimens received 5.0 megarads, which served both to form the radicals in the crystalline matrices and to sterilize the contents. The other half were not irradiated but were sterilized by heating to 110°C for 2 hr to serve as control specimens. In order to minimize radical decay, all samples were stored at -10°C. Shortly before use, one sample of each irradiated type was opened and the crystals were assayed for free-radical

content by ESR spectrometry. The radical concentrations were found to be in the range of 1 to 5 x 10^{19} radicals/g.

Both the TA-98 and TA-100 strains of S. typhimurium were used as test organisms. Reversions of the former indicate frame-shift mutations, whereas reversions of the latter indicate point mutations. In each test, approximately 10^7 cells were first separated from a log-phase culture of nutrient broth by filtering a 2-ml aliquot through a sterile Millipore HA, 0.45-μ pore filter. The cells were then washed with sterile phosphate buffer at pH 7.8 (ionic strength 0.1), and then resuspended in 2 ml of this buffer.

The samples of irradiated crystals, weighing either 40 or 200 mg, were warmed to room temperature and then dissolved rapidly in the bacterial suspensions, using sterile technique. Preliminary tests had shown that dissolution of these crystals decreased the pH of the suspension by only 0.1 to 0.4 units. After 1 min of exposure, a 1-ml aliquot of the suspension was removed and filtered through another Millipore filter. The collected cells were then washed with sterile buffer and resuspended in 10 ml of histidine-free nutrient broth. Control tests were made by exposing both strains of S. typhimurium to the nonirradiated crystals under the same conditions.

Results from two of these experiments are shown in Table 28.6. Exposure of cells in one set of experiments to the radicals in irradiated glycine and galactose produced significant increases in the frequency of both frame shift (TA-98) and point mutations (TA-100). In a second set, the response was considerably lower for radicals from the related compounds, alanine and lactose. These results, however, are evidence that organic radicals are capable of causing mutation in S. typhimurium.

TABLE 28.6. Response of Salmonella Typhimurium Strains to Free Radicals from Irradiated Compounds

STRAIN	COMPOUND	RADICALS ADDED TO SAMPLE (x 10^{18}/ml)	REVERSIONS[a] SAMPLE	REVERSIONS[a] CONTROL
TA-98	D-GALACTOSE	1.6	606[b]	23[c]
TA-98	GLYCINE	2.0	2600	15
TA-98	DL-α-ALANINE	1.0	23	11
TA-98	D-LACTOSE	0.4	23	11
TA-100	D-GALACTOSE	1.6	1680	33
TA-100	GLYCINE	2.0	1232	211
TA-100	DL-α-ALANINE	1.0	57	85
TA-100	D-LACTOSE	0.4	95	54

[a] REVERSION OF MUTANT HISTIDINE-REQUIRING STRAINS TO NONHISTIDINE REQUIRING PHENOTYPE

[b] NUMBER OF REVERTANTS PER 10^7 MUTANTS EXPOSED TO RADICAL-CONTAINING IRRADIATED COMPOUND

[c] NUMBER OF REVERTANTS PER 10^7 MUTANTS EXPOSED TO RADICAL-FREE NONIRRADIATED COMPOUND

Our plans are to continue such tests with other organic-free radicals, and to initiate experiments for testing the capacity of these radicals to activate nonmutagenic carcinogens (e.g., polynuclear aromatic hydrocarbons) to biologically active carcinogen-mutagens. The latter experiments will be designed to test the extent to which organic free radicals are capable of duplicating the action of microsomal enzymes in activating procarcinogens to carcinogens.

LYSIS OF PHOSPHOLIPID MEMBRANES WITH RADIATION-INDUCED FREE RADICALS

Investigators:
D. R. Kalkwarf[1] and D. L. Frasco[2]

Phospholipid vesicles were found to be lysed by exposure to free radicals derived from irradiated glycine and galactose. The decomposition yield increased with vesicle concentration, and attained values of 0.0006 vesicles destroyed per radical added. Ionic charge at the phospholipid end groups was found to be more important than degree of unsaturation in determining this yield. Radicals derived from irradiated serine and alanine had no detectable lytic action at the vesicle concentrations tested.

Vesicular phospholipid membranes were used as model structures to determine which components in cell membranes are most susceptible to attack by radiation-induced free radicals. These membranes possess a bilayer structure similar to those of cell membranes, but were of simple composition so that the sites of radical attack would be more clearly defined.

Phospholipids with different polar end groups and different degrees of unsaturation were made into vesicles in order to examine the effect of these factors on radical-induced lysis. These compounds and their analyses are shown in Table 28.7. Each of these compounds was used to prepare vesicular membranes by the method of Huang. Aqueous emulsions of the phospholipids were prepared in 0.10 M tris, and these were then sonicated to form vesicles enclosing a buffered solution of fluoride ion and bounded by a single phospholipid bilayer. When unsaturated fatty-acid residues were present, the preparations were conducted in a nitrogen atmosphere to prevent oxidation. Figure 28.3 illustrates the structure of these vesicles using dimensions determined by Huang.

The free radicals tested were those formed in crystals of glycine, DL-α-alanine, L-serine and D-galactose during ^{60}Co gamma irradiation at room temperature. Electron spin resonance (ESR) studies on single crystals have shown that the $\dot{C}H_2COO^-$ and $H_3\overset{+}{N}\text{-}\dot{C}H\text{-}COO^-$ radicals are formed in irradiated glycine, $H_3\overset{+}{N}\text{-}C(CH_3)COO^-$ is formed in irradiated alanine and $HO\text{-}CH_2\text{-}\dot{C}H\text{-}COO^-$ is formed in irradiated serine. The structure of the radicals in irradiated galactose has not yet been clearly identified. After irradiation, the crystals were assayed by ESR spectrometry and found to contain radical concentrations in the range of 1 to 5×10^{17} radicals per gram.

Vesicles were exposed to the radicals by rapidly dissolving weighed amounts of the irradiated crystals into vesicle suspensions that had just been passed through a Sephadex G-75 gel-filtration column to remove sodium fluoride from the external solution. The fluoride-ion concentrations in these solutions were then monitored continuously with a selective fluoride-ion electrode and any increase was taken as a measure of vesicle lysis. In control experiments, the vesicles were exposed to solutions of the same amount of irradiated crystals predissolved in buffer to dissipate the radicals. The lytic

[1] Radiological Sciences Department.
[2] NORCUS Fellow

TABLE 28.7. Analysis of Phospholipids Used in Vesicle Preparations

PHOSPHOLIPID	POLAR END GROUPS	FATTY ACID RESIDUES
SPHINGOMYELIN (FROM BOVINE BRAIN)	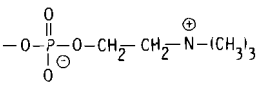	9 mol% PALMITOYL 91 mol% STEAROYL
LECITHIN (FROM EGG YOLK)	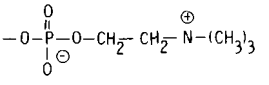	27 mol% PALMITOYL 10 mol% STEAROYL 23 mol% OLEOYL 40 mol% LINOLEOYL
DIPALMITOYLPHOSPHATIDYLCHOLINE	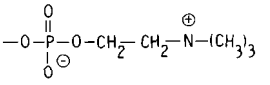	100 mol% PALMITOYL
PHOSPHATIDYLETHANOLAMINE (SOURCE UNSPECIFIED)	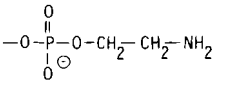	11 mol% PALMITOYL 34 mol% STEAROYL 55 mol% OLEOYL
PHOSPHATIDYLINOSITOL (FROM BEEF BRAIN)	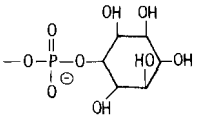	4 mol% PALMITOYL 50 mol% STEAROYL 46 mol% OLEOYL
PHOSPHATIDYLSERINE (FROM BEEF BRAIN)	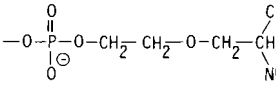	2 mol% PALMITOYL 44 mol% STEAROYL 54 mol% OLEOYL

effect of these solutions was slight and probably caused by nonradical radiolysis products. Finally, samples of the vesicle suspensions were completely lysed by addition of acetone, and the measured concentrations of fluoride ion were used together with Huang's value of 60 Å for the internal radius of the vesicle to calculate the original numbers of vesicles in the suspensions. The numbers of vesicles lysed by the radicals were calculated in the same way after correction of the fluoride concentrations by the control values.

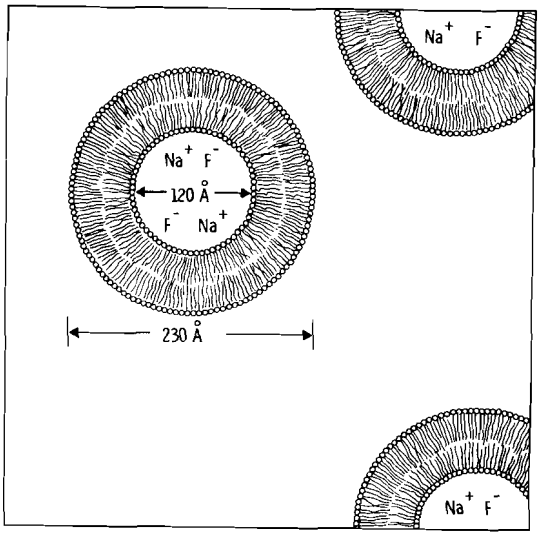

FIGURE 28.3. Cross-Sectional View of Spherical, Fluoride-Loaded Vesicles Bounded by a Phospholipid Bilayer with the Polar Head Groups (O) Directed Toward the External and Internal Aqueous Phases. The dimensions are those for vesicles bounded by egg-yolk lecithin reported by Huang in Biochemistry 8:344-352 (1969).

Vesicle lysis was readily measured after addition of irradiated glycine or D-galactose, and the decomposition yield was evaluated in terms of vesicles lysed per radical added. The results are shown in Table 28.8. In the case of sphingomyelin vesicles exposed to glycine radicals, the decomposition yield steadily increased as the vesicle concentration increased, supporting the view that radical-vesicle and radical-radical reactions competed with each other. Table 28.8 also indicates that vesicles prepared from phospholipids with net-neutral polar groups, e.g., sphingomyelin, egg-yolk lecithin, dipalmitoylphosphatidylcholine, were more readily lysed than those with negatively charged polar groups, e.g., phosphatidylserine, phosphatidylinositol and phosphatidylethanolamine. In the case of glycine radicals, this lesser effect may be due to electrostatic repulsion between the glycine radical-anions and the negatively charged vesicle surface. In any case, the effect of vesicle surface charge appears to outweigh any differences in unsaturation of the fatty acid chains. This suggests that lysis was triggered by radical attack at the vesicle surface and proceeded irrespective of the

TABLE 28.8. Decomposition Yields of Vesicles Due to Radical Attack

VESICLE CONCENTRATION	MEMBRANE PHOSPHOLIPID	RADICAL	YIELD[a]
1 μM	SPHINGOMYELIN	GLYCINE	1×10^{-4}
2 μM	SPHINGOMYELIN	GLYCINE	2×10^{-4}
3 μM	SPHINGOMYELIN	GLYCINE	3×10^{-4}
5 μM	SPHINGOMYELIN	GLYCINE	5×10^{-4}
1 μM	SPHINGOMYELIN	GALACTOSE	1×10^{-4}
2 μM	SPHINGOMYELIN	GALACTOSE	2×10^{-4}
2 μM	DIPALMITOYLPHOSPHATIDYLCHOLINE	GLYCINE	2×10^{-4}
2 μM	DIPALMITOYLPHOSPHATIDYLCHOLINE	GALACTOSE	2×10^{-4}
8 μM	EGG-YOLK LECITHIN	GLYCINE	6×10^{-4}
4 μM	EGG-YOLK LECITHIN	GALACTOSE	6×10^{-4}
3 μM	PHOSPHATIDYLSERINE	GLYCINE	1×10^{-4}
2 μM	PHOSPHATIDYLSERINE	GALACTOSE	0×10^{-4}
7 μM	PHOSPHATIDYLINOSITOL	GLYCINE	2×10^{-4}
8 μM	PHOSPHATIDYLINOSITOL	GALACTOSE	2×10^{-4}
1 μM	PHOSPHATIDYLETHANOLAMINE	GLYCINE	0×10^{-4}
1 μM	PHOSPHATIDYLETHANOLAMINE	GALACTOSE	0×10^{-4}

[a]NUMBER OF VESICLES LYSED PER RADICAL ADDED

number of double bonds buried in the hydrocarbon center of the bilayer.

No lysis was observed after addition of irradiated L-serine or DL-α-alanine. Since the radicals were added in numbers comparable to those used in the glycine and galactose experiments, it was concluded that either radical-radical reactions outcompeted radical-vesicle reactions completely at the vesicle concentrations tested or no reaction leading to vesicle lysis was mediated by the radicals.

Future experiments will be directed toward measuring radical-induced lysis of phospholipid vesicles containing membrane proteins and cholesterol in their bounding surface. Preparation of more concentrated vesicle suspensions will also be attempted for use in testing the effects of radicals which react rapidly with themselves.

DIFFERENTIATION OF PERIPHERAL LYMPHOCYTE POPULATIONS IN Pu-EXPOSED BEAGLE DOGS

Investigators:
J. E. Morris
Technical Assistance:
R. S. Moore

The percentage of peripheral lymphocytes binding fluorescent-labeled anticanine antibodies was measured in plutonium-oxide-exposed and unexposed beagle dogs. With this assay system, there was a significant decrease in the percentage of lymphocytes binding the labeled antibody in exposed animals compared to control animals.

Studies at this laboratory with inhaled plutonium oxide ($^{239}PuO_2$ or $^{238}PuO_2$) in beagle dogs have demonstrated a pronounced lymphocytopenia preceding tumor appearance. The development of this lymphocytopenia was both dose- and time-dependent. Data reported in last year's Annual Report on normal humoral immunity as mirrored in levels of circulating immunoglobulins suggested that the levels were not altered by exposure to plutonium, even in animals suffering pronounced lymphocytopenia as a result of such exposures.

To further define the immunological implications of the observed lymphocytopenia, fluorescent-labeling studies were initiated to differentiate peripheral lymphocyte populations of exposed and control animals into T cells (thymus-dependent) and B cells (thymus-independent), and to determine if differences in percent population of these cell types occurred as a function of exposure to Pu.

In the fluorescent-labeling studies, the binding of goat anticanine immunoglobulin antibodies was used as a measure of B-cell populations. Peripheral lymphocyte preparations were derived from animals in two $^{239}PuO_2$ exposure groups, approximately 4 yr after exposure. One group had an initial deep lung deposition of ∿ 1000 nCi and a pronounced lymphocytopenia (lymphocyte count ∿ 30% of normal). The second exposure group received an initial deep lung burden of ∿ 100 nCi and had a lymphocyte count ∿ 60% of normal.

In 12 control animals, 30% ± 5% of the isolated lymphocytes bound anticanine immunoglobulin antibodies (Table 28.9). In the 1000-nCi group, the lymphocytes of 10 dogs were analyzed and 17% ± 6% bound the labeled antibody. In the 100-nCi group, eight dogs were examined and 26% ± 5% bound this antibody. This last result was not statistically significant. However, there was an apparent difference in the distribution of binding of anti-immunoglobulin antibodies to the surface of isolated lymphocytes obtained from exposed and control groups, with exposed animals showing a less uniform distribution of anti-immunoglobulin binding sites on their surfaces compared with controls.

TABLE 28.9. Effects of Inhaled $^{239}PuO_2$ on Peripheral Lymphocyte Populations

INITIAL DEEP LUNG DEPOSITION, nCi	NUMBER OF ANIMALS	% LYMPHOCYTES BINDING FLUORESCENT-LABELED ANTIBODY	P VALUE
CONTROLS	12	30% ± 5%[a]	
100	8	26% ± 6%	< 0.1
1000	10	17% ± 6%	< 0.01

[a] MEAN ± STD DEVIATION

Since B cells are the lymphocytes associated with immunoglobulin synthesis and are measured with this assay, these data suggest that there may be an alteration of the immune system of exposed animals as a result of the reduced number and altered membrane characteristics of these cells. Studies are underway to investigate the response of $^{239}PuO_2$-exposed animals to T-cell- and B-cell-related antigens, as well as studies for defining the T-cell population by spontaneous rosette assay using human red blood cells (see article by H. A. Ragan in this Annual Report).

HEMATOLOGIC EFFECTS OF $^{239}PuO_2$ IN RATS

Investigators:

H. A. Ragan

Technical Assistance:

E. F. Blanton, E. T. Edmerson, S. L. English, K. H. Debban, M. C. Perkins and M. J. Pipes

Rats exposed to approximately 200 nCi deep lung deposition of $^{239}PuO_2$ developed a mild, transient lymphopenia 4 weeks later. A trend to concurrent neutrophilia was evident along with a significant increase in lung weights.

Numerous studies in this laboratory have shown that beagles exposed to $^{239}PuO_2$ by inhalation developed a sustained, dose-related, selective lymphopenia.

In attempts to develop the rat as a model to study the pathogenesis of lymphopenia and the subsequent effects on immune competence and pulmonary neoplasia, a group of rats was exposed to approximately 1 μCi $^{239}PuO_2$ (Annual Report, 1975). A significant lymphopenia was present 4 weeks later but because of the high dose level, marked respiratory insufficiency developed along with severe weight loss and death in less than 90 days. Even though severely stressed, it appeared that lymphocyte concentrations were recovering to normal values by 60 days postexposure.

To further evaluate the hematologic effects of $^{239}PuO_2$ in rats, a group was exposed at 70 days of age to produce a retained lung dose of approximately 200 nCi. A group of litter mates was sham-exposed to serve as controls. Blood samples were obtained periodically from the tail vein; the rats were then killed and tissues selected for radioanalyses. Rats with lung burdens less than 50 nCi were not considered in the statistical evaluations. With the exception of one rat, all lung burdens were less than 300 nCi.

Only at 4 weeks postexposure was a significant lymphopenia evident in the exposed rats (Table 28.10), at which time a significant neutrophilia was also evident. Although neutrophil values remained elevated at subsequent sample periods, they were not significantly different from control values (Table 28.10). The most consistent finding was an increase in lung weights of the exposed rats (Table 28.10). At all time periods, greater than 95% of the body burden of plutonium was in the lungs. There was no significant effect on body weights or thymus weights except in one rat, which was in severe respiratory distress, was emaciated, had a marked leukocytosis, and a thymus weight only 25% that of the group mean. However, the total lung burden in this animal was comparable to that of others killed at the same period.

The hematologic results of this study, and of the one reported on last year, indicate that the rat is probably not a good model in which to attempt correlations of lymphopenia, immune competence, and subsequent development of pulmonary neoplasms.

TABLE 28.10. Lung Weights and Leukocyte Evaluations in Rats Following Inhalation of $^{239}PuO_2$ (Mean +SD)

GROUP	POST EXPOSURE, wks	n	LUNG WEIGHT, g	LUNG BURDEN, nCi	LEUKOCYTES, $x10^3$ µl	NEUTROPHILS, $x10^3$ µl	LYMPHOCYTES, $x10^3$ µl
CONTROL	2	10	1.08 ± 0.10	----	7.5 ± 1.8	0.73 ± 0.40	6.69 ± 1.79
EXPOSED		9	1.19 ± 0.14	174 ± 68	7.8 ± 1.2	0.94 ± 0.41	6.71 ± 1.31
CONTROL	4	10	1.20 ± 0.09	----	8.0 ± 1.2	0.65 ± 0.26	7.10 ± 1.07
EXPOSED		9	1.45 ± 0.24[a]	198 ± 76	7.4 ± 1.6	0.94 ± 0.32[c]	6.03 ± 1.32[d]
CONTROL	8	10	1.17 ± 0.12	----	9.7 ± 1.2	0.97 ± 0.30	8.55 ± 1.34
EXPOSED		7	1.47 ± 0.26[b]	185 ± 121	10.3 ± 2.7	1.76 ± 1.48	8.33 ± 2.13
CONTROL	12	10	1.25 ± 0.16	----	9.8 ± 2.7	0.67 ± 0.36	8.67 ± 2.3
EXPOSED		7	1.55 ± 0.12[b]	100 ± 32	11.1 ± 1.3	1.33 ± 1.23	9.36 ± 1.02

[a] $P < 0.025$ TWO-TAIL t TEST
[b] $P < 0.01$ TWO-TAIL t TEST
[c] $P < 0.025$ ONE-TAIL t TEST
[d] $P < 0.05$ ONE-TAIL t TEST

AN IMPROVED GRADIENT FOR ISOLATION OF DOG LYMPHOCYTES AND SUBSEQUENT QUANTITATION OF T-CELL ROSETTES

Investigator:
H. A. Ragan
Technical Assistance:
K. Debban

Preparation of an improved density gradient for isolation of dog lymphocytes is discussed. About 68% of the lymphocytes from a sample of blood were recovered using this gradient, compared to approximately 50% recovery from the gradient used previously. Cytochemical staining indicated the gradient does not selectively remove a subpopulation of lymphocytes. A greater percent of lymphocytes capable of forming E rosettes with human blood was found in plutonium-exposed than in control dogs.

The Annual Report for 1975 described the isolation of lymphocytes from peripheral blood of dogs by use of a commercial density gradient with physical characteristics optimized for human blood. Recovery of dog lymphocytes with this preparation was approximately 50%.

To improve this recovery, various modifications were made by altering the density and osmolality of the gradient. The final preparation used was as follows:

Ficoll (6.1% in distilled water)	86 ml
Hypaque 75	14 ml
NaCl	0.05 g

This gradient results in a density of 1.064 and osmolality of 304 mOsm. Recovery of lymphocytes with this gradient was approximately 68% (Table 28.11). The cells recovered included some monocytes, eosinophils, and a few platelets, but was devoid of erythrocytes or neutrophil contamination. Viability of the isolated lymphocytes was >95% as determined by the trypan blue dye-exclusion method.

It is important to determine that any separation procedure does not selectively eliminate a subpopulation of lymphocytes from the total whole-blood population. As one evaluation for this, nucleoli in lymphocytes from whole blood, and those recovered from the gradient, were quantitated using a cytochemical method. The results, shown in Table 28.12, indicate that the distribution of lymphocytes containing various numbers of nucleoli is the same from isolated lymphocytes as from peripheral blood. In addition, it is also the same in control dogs and those with mean ^{239}Pu lung burdens of approximately 1.0 μCi.

In the continuing evaluation of immune competence in dogs exposed to plutonium by inhalation, the number of non-complement-dependent E-rosette-forming lymphocytes (T cells) was quantitated using human erythrocytes. The percent of such lymphocytes was significantly greater ($P < 0.01$) in dogs with ^{239}Pu lung burdens of approximately 1.0 μCi than in age-related controls (Table 28.13). Such a finding would be consistent with a relative increase in T cells due to a decrease in B cells in lymphocytopenic dogs following the inhalation of plutonium. Another study in this Annual Report details additional immonologic investigations in which a reduction of B lymphocytes was found in these dogs.

TABLE 28.11. Percent of Lymphocytes Recovered from Blood of Control Dogs and Those with ^{239}Pu Lung Burdens of ∿ 1.0 μCi, Using a Density Gradient Method (Mean ± SD)

GROUP	N	% RECOVERY
CONTROL	20	67.5 ± 13.3
EXPOSED	16	67.1 ± 16.1

TABLE 28.13. Lymphocytes From Control Dogs and Those With Lung Burdens of ∿ 1.0 μCi ^{239}Pu Forming Noncomplement-Dependent Rosettes With Human Erythrocytes (Mean + SD)

GROUP	N	%	P
CONTROL	20	16.0 ± 6.9	
EXPOSED	16	27.9 ± 9.6	< 0.01

TABLE 28.12. Cytochemical Comparison of Azure-C-Stained Nucleoli in Whole Blood Lymphocytes and Gradient-Separated Lymphocytes of Control Dogs and Those With Lung Burdens of ∿ 1.0 μCi ^{239}Pu (Mean ± SD)

			NUCLEOLI (%)				
GROUP	PREPARATION	N	4	3	2	1	0
CONTROL		20					
	WHOLE BLOOD		1.0 ± 1.1	3.1 ± 1.8	12.1 ± 3.4	70.9 ± 5.9	12.9 ± 5.6
	ISOLATED		1.2 ± 1.3	3.5 ± 1.9	11.6 ± 4.0	69.5 ± 7.5	14.2 ± 5.5
EXPOSED		16					
	WHOLE BLOOD		1.0 ± 0.5	4.8 ± 2.9	14.6 ± 4.2	66.8 ± 10.4	13.4 ± 8.6
	ISOLATED		1.2 ± 0.9	4.8 ± 2.7	12.8 ± 5.3	68.0 ± 7.8	13.3 ± 7.9

• METAL-MEMBRANE INTERACTIONS

Person in Charge: R. P. Schneider

The ionic forms of most toxic metals penetrate cell membranes slowly and it seems likely that their primary effects are exerted at the membrane level. Information on the interaction of metals with defined membrane functions may therefore be expected to aid in predicting potential effects of trace metals derived from fossil-fuel combustion. Since changes in membranes are on the cell surfaces, these should be detectable in intact cells, and may therefore be useful for biochemical and immunobiological assessment of early effects.

Functions of cell membranes which may be linked to possible mechanisms of trace metal pathogenesis, including carcinogenesis, are being investigated. In its present stage, the research is attempting to define the role of membranes in regulating cellular synthetic activity and cell division and to study membrane alterations which accompany cell transformation to the neoplastic state.

Membranes may be directly involved in regulation of cell growth and division by sensing cell-cell contact and relaying this information to the nucleus. We are examining the role of the membrane in these processes using cultured glial (brain) cells, which simultaneously stop cell division and synthesize a specific protein (S-100 protein).

Control of cell activity and division is, to a large extent, dependent on the transmission of information contained in external impermeant signal molecules through the cell membrane to the nucleus. The induction of exocellular protease synthesis by external protein inducers in Neurospora crassa is being studied as a model system.

The envelope of RNA tumor viruses is derived, in part, from the host-cell membrane. The ATPase of avian myeloblastosis virus is being used as a marker for studying the origin of virus envelope proteins and the extent of viral control over host-cell membrane composition and organization. Understanding of this control should increase the ability to distinguish cancer cells from normal ones.

CHARACTERIZATION OF THE ATPASE OF AVIAN MYELOBLASTOSIS VIRUS

Investigator:
R. P. Schneider
Technical Assistance:
L. M. Butcher

The ATPase of avian myeloblastosis virus is used as a marker to study alterations of the host-cell membrane caused by tumor virus infection and the incorporation of host membrane proteins into virus during maturation. The enzyme, which is presumably derived from the host-cell membrane, remains attached to the virus envelope during detergent treatment which releases 25% of the envelope protein. This suggests that it is an integral component of the envelope matrix. Particles which contain the ATPase, phospholipid and at least nine other proteins have been isolated from cholate-treated virus. The enzyme activity is totally lost when the complex is disassociated; hence purification to a single protein has been impossible to date. If the ATPase is a single polypeptide, it constitutes about 1% of the viral protein.

One of the major problems confronting cancer diagnosis and treatment is the difficulty in biochemically distinguishing between cancer and normal cells. Several changes in the membrane resulting from transformation of cells by tumor viruses have been observed, e.g., increased glucose transport, alterations in the sugar content of glycolipids and glycoproteins, changes in lipid composition, and the appearance of new antigens. Type C tumor virus maturation includes the acquisition of a lipoprotein envelope during budding through the host cell membrane and, not surprisingly, virus glycoproteins have been immunologically identified in host-cell membranes. It seems unlikely, however, that all of the observed changes are the result of addition of virus precursor polypeptides to the cells, since the genome of the viruses is large enough to code for only 200,000-300,000 daltons of polypeptide. The viruses, then, appear to have the ability to alter the organization or regulation of synthesis (or both) of cell membrane polypeptides. An understanding of this control and the budding process will provide a more rational basis for the study of tumor virus-induced changes in the composition of host-cell membranes. The ATP-hydrolyzing enzyme (ATPase) of avian myeloblastosis virus (AMV) is a promising model for the study of virus control of host membrane composition. The virus envelope contains an ATPase which is presumably derived from the host-cell membrane, but which has a specific activity about 10-fold higher than that of any known cellular membrane preparation of ATPase.

In earlier efforts, we characterized the viral enzyme and found it to be distinct from other membrane-bound ATPases of animal cells. We determined some of the conditions for stabilization and loss of this activity. This year, purification of the ATPase from virus was our major goal. Although we have

been unsuccessful in reaching this goal, the attempts have provided information about the organization of the enzyme within the virus. Last year it was reported that the enzyme in intact virus was inhibited by proteases and that it required phospholipid for activity, suggesting that the ATPase is located in the virus envelope with at least a portion of it exposed to the exterior surface. We have also shown that disruption of the virus in 1% cholate followed by dialysis and separation by centrifugation permits isolation of particles which contain ATPase activity and several proteins.

We have varied the conditions used for disrupting the virus so that we might obtain a more selective release of the enzyme and thus a more pure preparation. When the treatment with 1% cholate is limited to 0.5 hr, the virion is only partially disrupted. The protein and ATPase profile of the sucrose density centrifugation of this preparation shows that all of the activity and 75% of the protein bands in 31% sucrose (Figure 29.1).

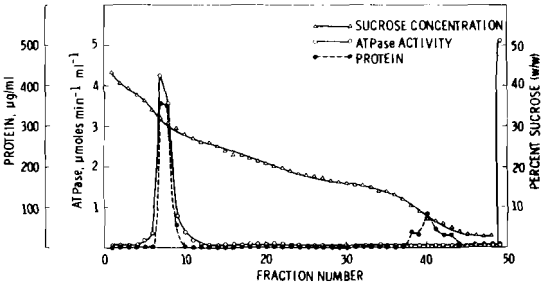

FIGURE 29.1. Profile of a Sucrose Density Gradient of Purified AMV Treated With 1% Cholate for 30 Min Followed by Dilution to 0.1% and Dialysis. The gradients were centrifuged at 250,000 X g for 16 hr.

Since intact virus, which contains the dense cores, bands at 36% sucrose, the major peak represents essentially intact envelope minus 25% of the protein which was solubilized and found at the top of the gradient. Under conditions in which 25% of the more loosely attached material (presumably glycoprotein spikes) is removed from the envelope, the ATPase remains firmly attached to the envelope. As suggested by its phospholipid requirement, the enzyme must be an integral component of the envelope structure.

Increasing the exposure of AMV to 1% cholate at 0° for 1 hr results in solubilization of 80-90% of the envelope protein (Figure 29.2). The solubility of this protein is demonstrated by the fact that it remains in the supernatant (above the sucrose) after centrifugation at 250,000 x g

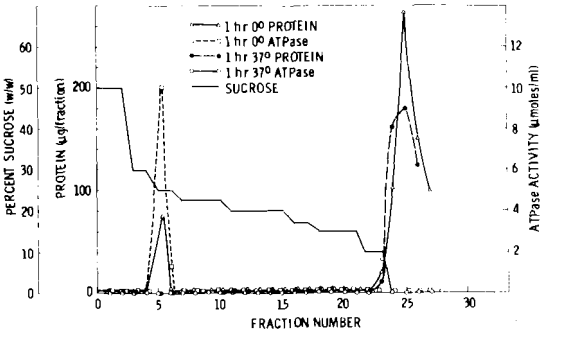

FIGURE 29.2. Profile of a Sucrose Density Gradient of AMV Treated With 1% Cholate for 1 Hr at 0° and 37°. The samples were centrifuged for 2 hr at 250,000 X g.

for 2 hr. As with the dialyzed samples described in last year's report, the ATPase activity was associated with particles which constitute 10-20% of the virus protein. Although the ATPase-containing complexes can be prepared more quickly in this way than with the dialysis technique, the yield of enzyme is generally higher and the enzyme activity is more stable with the latter method. We have attempted to solubilize the enzyme in order to facilitate isolation of the enzyme in pure form. When virus suspensions are treated with 1% cholate for 1 hr at 37° and subsequently centrifuged, all of the virus protein is soluble. As is shown in Figure 29.2, all of the protein of virus treated in this way remained in the supernatant, i.e., above the sucrose gradient. All of the viral ATPase activity, however, was destroyed by this treatment. In general, all combinations of temperature and detergent concentration which completely solubilize the virus protein also irreversibly destroy the ATPase activity. Thus, we have defined the conditions required for isolating virus envelopes which are 75% intact, as well as 75% and 100% solubilized. Both the duration and the temperature of exposure to detergent are critical variables controlling disassociation of the envelope.

Table 29.1 summarizes the data of several experiments which investigated the dissociation of the ATPase from AMV. As is shown in Table 29.1, the recovery of ATPase activity after dialysis of cholate-treated AMV varied over a range of 19% (2b) to 77% (1b), with an average of about 40%. The specific activity of the ATPase bands recovered from sucrose density gradients (1c and 2c) of the two dialysates (1b and 2b), however, were the same. Since the ratio of ATPase activity to protein is constant in the bands, even though it varied by a factor of four in the dialysate prior to centrifugation, the bands must contain only one kind of particle.

TABLE 29.1. Separation of ATPase From AMV

EXPERIMENT		PREPARATION[a]	ATPase ACTIVITY μmoles min^{-1}	ATPase RECOVERY (%)	PROTEIN (mg)	SPECIFIC ACTIVITY (μmoles mg^{-1} min^{-1})
1	a)	PURIFIED VIRUS	378	--	18.3	20.6
	b)	EXTRACT VIRUS, 1% CHOLATE + DPL, DIALYSIS	291	77	19.2	15.1
	c)	CENTRIFUGATION	112	29	2.6	43.8
	d)	EXTRACT ATPase (1C) - 1% CHOLATE FOR 2 hr, CENTRIFUGATION	114	29	1.05	108.6
2	a)	PURIFIED VIRUS	190	--	--	--
	b)	EXTRACT VIRUS 1% CHOLATE + DPL, DIALYSIS	36.5	19	5.04	7.2
	c)	CENTRIFUGATION	37.8	20	0.8	47.2
3	a)	PURIFIED VIRUS	69	--	--	--
	b)	EXTRACT VIRUS, 1% CHOLATE THEN CENTRIFUGATION	6	9	0.160	37.5
4	a)	PURIFIED VIRUS	151	--	6.39	23.6
	b)	EXTRACT VIRUS, 1% CHOLATE + DPL FOR 2 hr THEN CENTRIFUGATION, EXTRACT ATPase 2 hr IN 1% CHOLATE, CENTRIFUGATION IN 1% CHOLATE	37.5	24	0.42	89.0

[a] WHEN DPL (DIPALMITOYL LECITHIN) WAS PRESENT ITS CONCENTRATION WAS 4 mg/ml. ALL CENTRIFUGED PREPARATIONS WERE COLLECTED AS BANDS FROM SUCROSE DENSITY GRADIENTS. ALL EXPOSURE TO CHOLATE WERE AT 0°.

When the ATPase particles recovered from dialysed samples were incubated in 1% cholate for 2 hr, then centrifuged through a sucrose gradient containing 1% cholate, all of the activity was recovered as a band (Table 29.1, 1d) with the loss of more than one-half of the protein. The enzyme is apparently resistant to the cholate because it is stabilized by the DPL during dialysis. This experiment demonstrates that the ATPase particle is stable in 1% cholate and is not the result of reassembly of solubilized proteins caused by loss of the detergent during dialysis.

This stability is further shown by experiments in which virus was treated with 1% cholate (with or without DPL) for 1 to 2 hr (Figure 29.2 and Table 29.1, 3b) and centrifuged on sucrose gradient without dialysis. The material recovered from bands of these gradients had a specific activity which was about the same as that of dialysed virus extracts. As with the dialyzed preparations, treatment of this banded material with 1% cholate and subsequent centrifugation increased the specific activity of the ATPase about two-fold.

Preliminary study of the isolated enzyme particles was made with polyacrylamide gel electrophoresis in the presence of sodium dodecyl sulfate. This technique, which fractionates proteins on the basis of their molecular weight, shows that the particles of highest specific activity (Table 29.1, 1d) contain seven major and three minor protein components. The particles are enriched in six of the major proteins relative to the whole virus and lack all of the major structural proteins of the virus core. They comprise about 6% of the total virus proteins and each of the six major bands is about 10-15% of the protein in the particle. It follows, then, that the ATPase is about 1% of the virus protein and the specific activity of the pure enzyme in native form must be about 2 mmoles mg^{-1} min^{-1} or about 40 times higher than that of any known membrane ATPase.

The stability of the ATPase particle suggests that it is present in the cell membrane and that the intact package is transferred to the virus during budding. We intend to test this hypothesis by purifying host-cell membranes, extracting these membranes with cholate, and comparing polyacrylamide gels of the extracted particles to those extracted from virus.

SIMPLIFIED METHOD FOR THE PURIFICATION OF *N. CRASSA* EXOCELLULAR ALKALINE PROTEASE

Investigators:

J. S. Price and H. Drucker

Technical Assistance:

L. C. Neil

A simple method for purification of N. crassa exocellular alkaline protease has been developed, involving one ammonium sulfate fractionation and chromatography on carboxymethylsephadex. The technique results in a 125-fold purification of enzyme with the same specific activity as that reported previously for crystallized enzyme.

Previous studies (Annual Report, 1973) resulted in a purification scheme for N. crassa exocellular alkaline protease requiring four steps, including two chromatographic resolutions of enzyme. This procedure was laborious, took long periods of time, and was not applicable to the preparation of large quantities of the enzyme. Within the last year we have developed a purification method which allows manipulation of large quantities of culture filtrate and protein resulting in purification of usable amounts of this enzyme.

Table 29.2 summarizes the procedure. N. crassa exocellular filtrate was concentrated approximately five-fold by ultrafiltration through hollow filter cartridge. The concentrate was then subjected to ammonium sulfate fractionation [0.6 g solid $(NH_4)_2SO_4$ added/ml concentrate], the precipitate resuspended in 0.01 M histidine-HCl buffer, pH 6.15 + 0.001 M $CaCl_2$ (buffer), exhaustively dialyzed against buffer [$(NH_4)_2SO_4$ + fraction, Table 29.2] and placed on a 2.5 x 35-cm column of CM-52 Sephadex. The column was then washed exhaustively with

TABLE 29.2. Preparation of N. crassa Exocellular Protease

	PREPARATION OF N. crassa EXOCELLULAR PROTEASE						
	VOLUME	PROTEIN, mg/ml	SPECIFIC ACTIVITY, Pu/mg	TOTAL PROTEIN, mg	TOTAL ENZYME ACTIVITY, UNITS	YIELD, %	FOLD PURIFICATION
EXOCELLULAR FILTRATE FRACTION	000	4.87	2.00	83,700	167,000	100	1
$(NH_4)_2SO_4$ FRACTION	77	11.5	65.1	885	57,000	34	32.5
CM-52 CHROMATOGRAP-	30	1.0	250	30	7,500	4.5	125

buffer until all protein not adsorbed to the resin was eluted. A linear gradient of 0-0.2 M KCl in buffer was then applied to the column and a peak of protein and enzyme activity eluted. The column was then stripped with 0.5 M KCl, resulting in a small protein peak.

Fractions 165-175 resulting from CM-52 chromatography were concentrated by ultrafiltration. These enzymes, of specific activity identical to that of enzymes prepared by previous methods, were fully inhibited by diisopropylfluorophosphate or phenylmethylsulfonylfluoride, but not by o-phenanthroline or EDTA, suggesting that it is an alkaline protease activity. It reacted, immunologically, with antiserum directed against alkaline protease prepared by the previous method, with full identity. Sedimentation-velocity analyses in the ultracentrifuge showed one sedimenting peak, suggesting, as did immunoanalyses, a homogenous protein preparation.

Antibody to this purified enzyme will be used to purify an activity that appears to be an intracellular zymogen of this exocellular alkaline protease. We will then compare the properties of this intracellular enzyme to those determined for exocellular enzyme. By so doing, we hope to demonstrate the feasibility of our proposed model for regulation of synthesis of exocellular protease.

PROTEIN SUBSTRATES AND AMINO ACID POOLS IN *NEUROSPORA CRASSA*

Investigators:

J. S. Price and H. Drucker

Technical Assistance:

L. C. Neil

Amino acid pools in N. crassa were measured as a function of carbon starvation and growth on synthetic amino acid mixtures during the course of protease induction under various regimes of starvation and with four different protein substrates. The data suggest a strong correlation between amino acid pool size and qualitative nature and induction of exocellular protease. This implies some degree of coordinate regulation for enzymes of amino acid metabolism and the process of exocellular protease biosynthesis.

The biosynthesis of exocellular proteases by N. crassa is a process controlled both by induction and repression. In the absence of an adequate source of carbon (C), nitrogen (N), or sulfur (S), a protein substrate serves as inducer of exocellular protease and thus, by its degradation, as a source of the limiting nutrilite. The presence of substrate-level concentrations of materials containing readily metabolized C, N, or S will repress the synthesis of exocellular protease, with extent and type of repression dependent upon both the chemical structure of the repressor and its concentration in the milieu.

When protein serves as sole source of C, N, or S, it would appear likely that certain of the amino acids derivable from the protein would serve as repressors. That is, a certain concentration of some given amino acids might signal to the cell that adequate supplies of C, N, or S have been released by the action of exocellular protease on external protein substrate, and thus synthesis of these enzymes can be terminated. If this were the case, two phenomena would be expected:

1) Amino acids added to cells would repress protease biosynthesis, with

extent of repression contingent upon nature of culture condition (whether protein serves as sole source of C, N, or S) and structure and concentration of the added amino acid.

2) Cells induced to make exocellular protease would tend to "pool" repressor amino acids, with the nature of the pooled amino acid, again, contingent upon culture conditions.

We found, some time ago, that added amino acids would repress protease biosynthesis, with extent and nature of repression dependent upon culture conditions and structure and concentration of amino acids (Table 29.3). In the sulfur-deprived case, this is most obvious: only the S-containing amino acids (cystine, cysteine, and methionine) repress protease biosynthesis. However, under conditions of C-starvation, these last amino acids and ten others would repress exocellular enzyme production. In point of fact, with the exception of arginine, all the amino acids repressing under conditions of S- or N-deprivation are repressors under conditions of C-starvation.

The apparent specificity of repression under conditions of N- or S-deprivation was not reflected in the nature of amino acid pools accumulating under conditions where protein served as sole source of N, S, or C. Rather, the amino acids which accumulated in the cells with, in almost all cases, kinetics of accumulation consonant with the kinetics of protease induction/secretion, were those that repressed protease biosynthesis under conditions of C-starvation (Table 29.3). In terms of accumulation and kinetics of accumulation, these ten or so amino acids were distinct from the other amino acids measured, which either remained constant in level throughout protease induction or decreased in level to some final value upon induction.

It would thus appear that pools of repressing amino acids do accumulate in N. crassa but, unlike the situation when amino acids are added to cultures, the same amino acids accumulate regardless of culture milieu.

This last observation could be caused by two "artifacts". It is possible that intracellular protein turnover, known to occur under conditions of starvation in almost all biota, results in these pools. In this case, conditions of starvation, resulting in hydrolysis of intracellular protein to amino acids and derived metabolites, cause the observed accumulation of amino acids. Conversely, the amino acid pools observed might be solely a function of the kinetics of amino acid transport and accumulation, with protein substrate the direct source of the amino acid pools. That is, digestion of exocellular protein by exocellular protease results in a group of amino acids and derived metabolites which are transported into the cell and thus accumulate. The specificity of the transport systems and their rates of action thus control the intracellular amino acid pools.

To examine these possibilities, amino acid pools were measured in cells starved for a C and energy source (no protein substrate) and in cells given an amino acid

TABLE 29.3. Amino Acid Repressors of Protease Biosynthesis and Amino Acid Pool Accumulation

AMINO ACIDS[a] EFFECTING REPRESSION	AMINO ACIDS[b] ACCUMULATING TO >3X; INDUCTION UPON N-STARVATION	AMINO ACIDS[b] ACCUMULATING TO >3X; INDUCTION UPON C-STARVATION	AMINO ACIDS ACCUMULATING TO >3X; INDUCTION UPON S-STARVATION
ARGININE (N)	HISTIDINE	HISTIDINE	HISTIDINE
CYSTINE (C, S)	LEUCINE	ISOLEUCINE	ISOLEUCINE
HISTIDINE (C)	LYSINE	LEUCINE	LEUCINE
ISOLEUCINE (C)	METHIONINE	LYSINE	LYSINE
LEUCINE (C)	PHENYLALANINE	PHENYLALANINE	METHIONINE
LYSINE (C)	THREONINE	PROLINE	PHENYLALANINE
METHIONINE (S, C)	TYROSINE	THREONINE	SERINE
PHENYLALANINE (C)	VALINE	SERINE	THREONINE
TRYPTOPHAN (N, C)		TYROSINE	TYROSINE
THREONINE (N, C)		VALINE	VALINE
SERINE (N, C)			
VALINE (C)			

[a] LETTER IN PARENTHESES REFERS TO CONDITIONS UNDER WHICH GIVEN AMINO ACID REPRESSES

N: ADDED TO CULTURE WHERE PROTEIN IS NITROGEN SOURCE
C: ADDED TO CULTURE WHERE PROTEIN IS CARBON AND ENERGY SOURCE
S: ADDED TO CULTURE WHERE PROTEIN IS SULFUR SOURCE

[b] ACCUMULATION REFERS TO FOLD INCREASE OVER CELLS GROWN IN COMPLETE MEDIUM, NO SUBSTITUTE.

mixture equivalent in composition to that of the protein substrate bovine serum albumin (BSA). A limited number of amino acids accumulated under either regime of culture (Table 29.4). Qualitatively, it is obvious that amino acid pool accumulation is not the same under these conditions as it is under conditions of protease induction (compare Tables 29.3 and 29.4). Further, the kinetics of amino acid accumulation under both these test conditions was not at all similar to the kinetics of exocellular protease biosynthesis.

TABLE 29.4. Amino Acid Pools in C-Starved Cells and in Cells Grown on an Amino Acid Mixture

AMINO ACIDS[a] ACCUMULATING TO >3X; C-STARVED	AMINO ACIDS[a] ACCUMULATING TO >3X; GROWN ON AMINO ACID MIXTURE
HISTIDINE	HISTIDINE
SERINE	METHIONINE
	PROLINE
	SERINE

[a]ACCUMULATION REFERS TO FOLD INCREASE OVER CELLS GROWN ON GLUCOSE AS SOLE CARBON ENERGY SOURCE

Amino acid pools in protease-induced cells of N. crassa therefore do not appear to be solely a function of intracellular protein turnover nor of transport rates for an amino acid mixture.

One might consider, as a third possibility, that these intracellular amino acid pools arise in rather direct fashion from specific protein substrates. That is, they reflect the extent of hydrolysis of a given protein by N. crassa exocellular proteases and thus the amino acid composition of the protein. If this is the case, then amino acid pools in N. crassa induced for protease biosynthesis should, in some measure, reflect the amino acid composition of protein inducer.

To examine this possibility, amino acid pools in N. crassa were measured under conditions where four proteins, differing widely in amino acid compositions (Table 29.5), were used as inducers of exocellular protease. Regardless of the amino acid composition of the substrate proteins, essentially the same amino acids were accumulated; again, in almost all cases, with kinetics consonant with exocellular protease induction (Table 29.6). Three of these proteins (BSA, myoglobin, gelatin) are good inducers of exocellular protease and reasonably good sources of carbon and energy for growth. The fourth protein source employed (N. crassa soluble extracted protein) is not as good an inducer as the other materials (effects approximately 1/2 the previous induction rate of exoenzyme synthesis) and does not support growth as well (less than 25% of growth rate of the other protein substrates). This may account for the differences in pool sizes and rates of accumulation observed during culture on this substrate relative to the others.

Our results in total suggest that there is some form of linkage between amino acid metabolism in N. crassa and induction of exocellular protease under conditions of nutrilite deprivation. It would appear that the pooled amino acids arise, either from intracellular protein/ amino acid or protein substrate/released amino acid by way of a controlled process of amino acid metabolism; the nature of this process is contingent not only upon nutrilite deprivation but upon synthesis of exocellular protease.

TABLE 29.5. Amino Acid Composition of Protein Substrate

AMINO ACID	GELATIN g/100 g protein	BOVINE SERUM ALBUMIN g/100 g protein	MYOGLOBIN g/100 g protein
ALANINE	4.2	4.6	5.7
ARGININE	7.4	5.3	2.7
ASPARTIC	5.6	9.1	9.2
CYSTEINE	--	5.5	0
GLUTAMIC	9.5	15.2	17.3
GLYCINE	23.0	1.0	6.3
HISTIDINE	0.7	3.4	8.2
ISOLEUCINE	1.4	2.3	5.0
LEUCINE	2.8	9.6	12.2
OH-LYSINE + LYSINE	4.6	10.9	16.1
METHIONINE	0.7	0.8	2.5
PHENYLALANINE	1.8	5.6	6.2
OH-PROLINE + PROLINE	25.5	4.0	4.0
SERINE	3.5	3.3	4.6
THREONINE	1.8	5.0	2.9
TRYPTOPHAN	n.d.	0.5	3.6
TYROSINE	0.2	4.6	2.4
VALINE	2.2	5.1	5.3
ASPARAGINE	n.d.		
GLUTAMINE	n.d		

TABLE 29.6. Amino Acid Pool Accumulation as a Function of Protein Substrate: Carbon-Starved Cells

PROTEIN INDUCER:[a] BOVINE SERUM ALBUMIN (BSA). AMINO ACIDS ACCUMULATING >3X	PROTEIN INDUCER:[a] MYOGLOBIN. AMINO ACIDS ACCUMULATING >3X	PROTEIN INDUCER:[a] GELATIN. AMINO ACIDS ACCUMULATING >3X	PROTEIN INDUCER:[b] N. crassa SOLUBLE EXTRACT. AMINO ACIDS ACCUMULATING >3X
HISTIDINE	GLYCINE	ASPARTIC	ARGININE
ISOLEUCINE	HISTIDINE	GLYCINE	GLYCINE
LEUCINE	ISOLEUCINE	HISTIDINE	HISTIDINE
LYSINE	LEUCINE	ISOLEUCINE	LYSINE
PHENYLALANINE	LYSINE	LEUCINE	SERINE
PROLINE	PHENYLALANINE	LYSINE	THREONINE
THREONINE	PROLINE	PHENYLALANINE	
SERINE	SERINE	PROLINE	
TYROSINE	THREONINE	SERINE	
VALINE	TYROSINE	VALINE	
	VALINE		

[a] ACCUMULATION REFERS TO FOLD INCREASE OVER CELLS GROWN ON GLUCOSE AS SOLE CARBON-ENERGY SOURCE

[b] CELLS GROWN ON N. crassa PROTEIN HAD ISOLEUCINE PROLINE, TYROSINE ACCUMULATE >2X; POOLS WERE NOT AT SATURATION AT TERMINATION OF EXPERIMENT

DENSITY-DEPENDENT GROWTH REGULATION AND S-100 PROTEIN SYNTHESIS IN THE RAT GLIAL CELL STRAIN C6 AND SUBLINES

Investigators:
R. G. Rupp, L. S. Winn, W. R. Wiley, and
J. E. Morris

The relationships between density-dependent growth regulation and the cellular accumulation of a brain-specific protein, S-100, was examined in a clonal glial cell culture, C6. The temporal accumulation of S-100 was examined in dense and sparse resting-cell cultures of the parental line C6 and two subcell lines. The data obtained for C6 showed that S-100 is present in exponentially growing cells and that the concentration of S-100 per cell decreases until the exponential phase of growth is concluded, at which time a net accumulation of S-100 per cell occurs. The accumulation of S-100 in sparse and dense cultures was the same qualitatively and quantitatively. Two sublines of C6 isolated by a negative selection procedure grew to 2.5-fold lower saturation densities than the parent cell line, C6. The subcell line accumulated insignificant levels of S-100 in all phases of growth. We conclude from these studies that the synthesis and/or accumulation of S-100 protein may not be inextricably linked to density-dependent inhibition as indicated in previous publications on the subject.

The clonal rat glial cell strain, C6, has been reported to accumulate the brain-specific S-100 protein as cells progress from low density to high density in monolayer cultures. The implication of these studies is that synthesis and/or accumulation of S-100 is inextricably linked to density-dependent growth regulation. We investigated this phenomenon in an attempt to determine whether synthesis and accumulation of S-100 protein by C6 cells is dependent upon cell-cell contact, a condition which prevails at high cell densities, or whether synthesis is associated with the presence or absence of essential constituents in the growth medium. Specifically, we investigated the accumulation of S-100 in C6 cells growing under conditions of nutritional deficiency and sufficiency. We also examined S-100 synthesis in subcell lines of C6 which grow to lower saturation densities than the parental strain.

We reported previously (1975 Annual Report) that C6 cells attain lower cell densities when grown under conditions of infrequent medium changes than cells grown under nutritionally sufficient conditions. It has been suggested that high cell densities (cell-cell contact) arrest cells in G_1 (G_0) (Pfeiffer et al., J. Cell Physiol. 75:329) and that cells arrested in G_1 by cell-cell contact are responsible for the synthesis of S-100 protein. If the synthesis of S-100 is specifically linked to cell-cell contact, the cultures which are arrested in G_1 at lower cell densities due to less frequent medium changes should synthesize less S-100 than cultures with daily changes. Further, to corroborate the hypothesis that S-100 synthesis is inextricably

linked to cell density (cell-cell contact), the variant sublines which grow to 2.5-3.5 lower saturation densities (14-1 and 6-1) should show fewer cell-cell contacts and, consequently, decreased S-100 accumulation.

We tested these hypotheses by examining the temporal synthesis of S-100 by C6 cells growing under conditions with frequent changes in medium (every 24 hr) and in cells growing under conditions in which the growth medium was changed at 96-hr intervals. Similar studies were conducted with the cloned sub-cell lines (6-1 and 14-1). Table 29.7 summarizes the growth properties of the C6 parental line and the sublines 6-1 and 14-1 under these nutritional conditions of growth.

TABLE 29.7. Growth Properties of Rat Glial Cell Line C6 and Sublines Under Nutritionally Replete and Deficient Conditions

	MEDIUM CHANGE, 24-hr INTERVALS		MEDIUM CHANGE, 96-hr INTERVALS	
CELL LINE	SATURATION DENSITY (cells/cm^2 x 10^6)	DOUBLING TIME (hr)	SATURATION DENSITY (cells/cm^2 x 10^6)	DOUBLING TIME (hr)
C6	2.4	18	0.93	24
Fdu 14-1	0.93	19	0.53	> 25
Fdu 6-1	0.79	19	0.25	36

With slightly increased doubling time, C6 cells attain a > 2.5-fold higher density when the medium is changed at 24-hr intervals compared to 96-hr intervals (Table 29.7). Similar results are shown for the two sublines. It should be noted that increasing the frequency of medium changes to more than one per 24 hr did not increase the saturation densities for either the parental or subcell lines.

The double antibody radioimmunoassay described in the next report was used to measure the accumulation of S-100 in the three cell lines growing under nutritional conditions described in Table 29.7. The data shown in Figure 29.3 depict the changes in S-100 accumulation in parental C6 cells. Under nutritionally replete conditions, the concentration of S-100 protein per culture bottle increased in parallel with the increase in cell number during the exponential phase of growth. However, the concentration of S-100 per cell decreased until the cells reached a phase of decreased growth and/or high cell densities. At this point a net accumulation of S-100 protein per cell began.

Cells growing under nutritionally deficient conditions grew to levels 2.6-fold lower than cells grown under nutritionally replete conditions, while the accumulation of S-100 per cell was comparable. It should be noted that in the nutritionally deprived cells there was a slow but continuous increase in cell number. The implication of this data is that cells grown under nutritionally deficient conditions grew to lower saturation densities, yet the accumulation of S-100 is similar to cells growing to high cell densities (greater cell-cell contact). Thus, the data suggest that any condition of growth which results in the cessation of cell growth (entry of cells into G_1 phase of the cell cycle) will result in the initiation of S-100 accumulation.

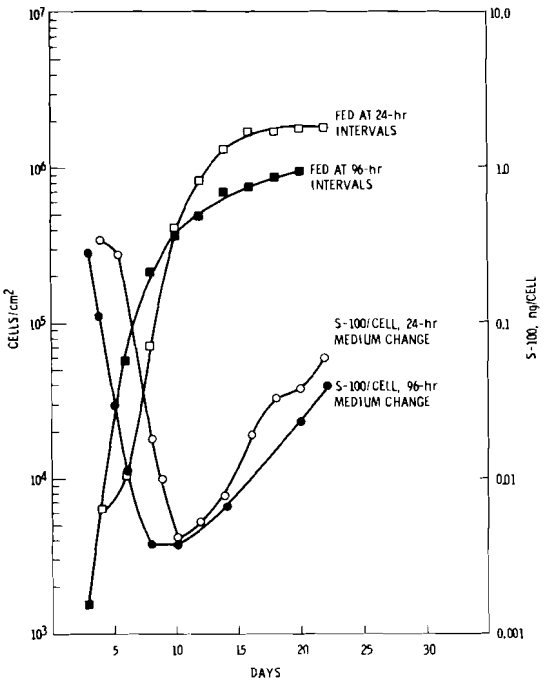

FIGURE 29.3. Growth and Accumulation of S-100 Protein in C6 Cultures With 24-Hr and 96-Hr Changes in Growth Medium. Cells were grown in 75-cm^2 bottles. Cells were removed from the surface of the bottles and counted in a Coulter counter. S-100 was determined by solubilization of cells in NP-40, a nonionic detergent, and the radioimmune assay described in the following report was used to determine S-100 protein per cell.

The temporal accumulation of S-100 in the subcell lines 6-1 and 14-1 was examined in the manner described for the parental strain. Figure 29.4 shows that under nutritionally sufficient conditions there is little or no synthesis of S-100 protein. Similar results were obtained for nutritionally deficient conditions. We do not know how the two sublines are able to maintain low saturation densities; however, assuming that the cells are blocked in the G_1 phase of the growth cycle, this condition is not sufficient to

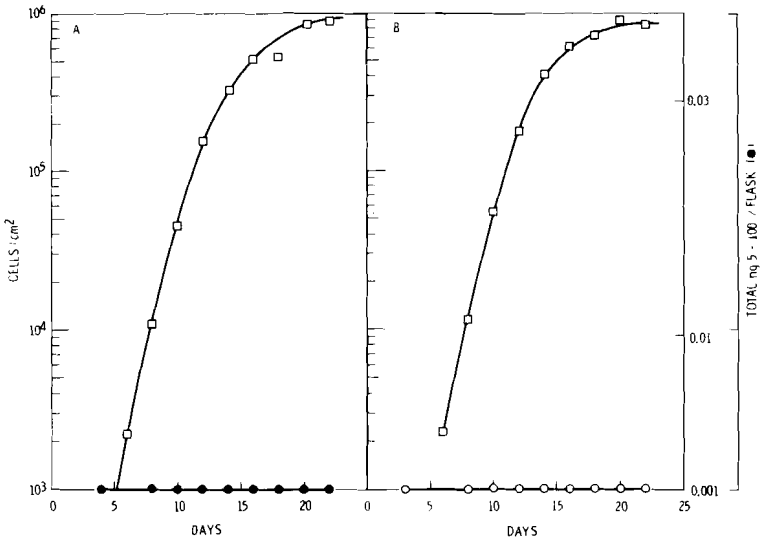

FIGURE 29.4A and B. Growth and Accumulation of S-100 Protein in Subcell Lines 14-1, 6-1 With 24-Hr Changes in Culture Medium. Cells were grown and assayed as described for Figure 29.3. S-100 protein is recorded in ng/flask. The amounts of S-100/flask in these studies are at the lower limits of the assay system and are probably not significant.

initiate S-100 synthesis in the subcell lines. The background levels of S-100 shown in Figure 29.4 are at the lower levels of detection for S-100 per flask and are therefore not significant.

There are several distinct explanations to account for the inability of 6-1 and 14-1 to accumulate S-100. Paramount among the options is that the C6 parental culture is a mixed-cell culture and that we have selected for a minor cell line which does not synthesize S-100 protein. It is also possible that S-100 is excreted into the medium by the subcell lines. This possibility is being examined. We are also examining 14 other morphologically distinguishable subclones which grow to lower saturation densities than the parental C6 line for their ability to synthesize S-100 protein. Considerable evidence has been accumulated which suggests that all of the subcell lines are of neural origin.

We conclude from our preliminary data that the initiation of S-100 synthesis and cell-cell contact may not be inextricably linked; i.e., culture milieu favors the initiation of S-100 synthesis as well as high cell densities. In the next year we plan to examine cell surface changes and cyclic nucleotide metabolism in cells actively synthesizing S-100. We will also investigate whether the regulation of S-100 accumulation occurs at the level of translation or transcription as a prerequisite to the determination of the metabolic signals involved in the process. Such studies are expected to provide data which will permit us to ultimately identify extracellular factors controlling cell growth and consequently S-100 synthesis.

RADIOIMMUNE ASSAYS FOR S-100 PROTEIN

Investigators:
J. E. Morris, L. S. Winn, and W. R. Wiley

A double-antibody radioimmune assay was developed for quantitating S-100 protein in tissue and tissue culture preparations. The sensitivity of the assay was in the low nanogram range.

A sensitive assay method for measuring S-100 protein in tissue culture cells and in tissues of neural origin was required for our investigations of the role of S-100 protein in the physiology and molecular biology of cells. The double-antibody assay developed involves the incubation of ^{125}I-labeled S-100 protein and the unknown with goat anti-S-100, precipitation of the complex with horse anti-goat IgG, and measurement of the radioactivity precipitated. The amount of S-100 in the unknown sample is ascertained from the decrease in specific activity of the ^{125}I-tagged antigen as exhibited in the presence of the nonradioactive unknown.

The goat anti-S-100 was prepared by injection of the S-100 protein (10 μg) linked to methylated bovine serum albumin and emulsified with an equal quantity of Freund's complete adjuvant. Three monthly injections were given before a suitable antibody titer was achieved. The anti-goat IgG was prepared by immunization of a horse with an initial injection of 1 mg of goat IgG emulsified in Freund's complete adjuvant. This was followed by a booster of 10 μg at 1.5 mo.

Radioiodination of S-100 was performed with the ^{125}I-labeled Bolton-Hunter reagent (iodinated N-hydroxysuccinimide ester of p-hydroxyphenylpropionic acid). A specific activity of approximately 30,000 dpm per ng of S-100 protein was obtained. Initial attempts to iodinate S-100 protein using the chloramine-T procedure were unsuccessful because of alteration induced in the protein.

A summary of the assay protocol is shown in Figure 29.5. The 10-μl solution of S-100·^{125}I contained 3 μg of the antigen and was incubated with 100 μl of sample to be assayed and 50 μl of goat anti-S-100, overnight at 4°C. Horse anti-goat IgG was added and the incubation continued for 4 hr at 4°C. The precipitate was packed and a 100-μl aliquot of the supernatant counted. The amount of S-100 protein in an unknown sample was ascertained from the decrease in binding of the radiotagged antigen in the presence of the unknown by reference to a standard curve prepared with known amounts of S-100 protein (Figure 29.6).

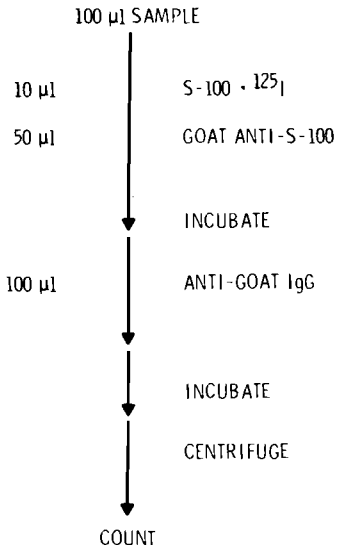

FIGURE 29.5. Summary of the Assay Protocol

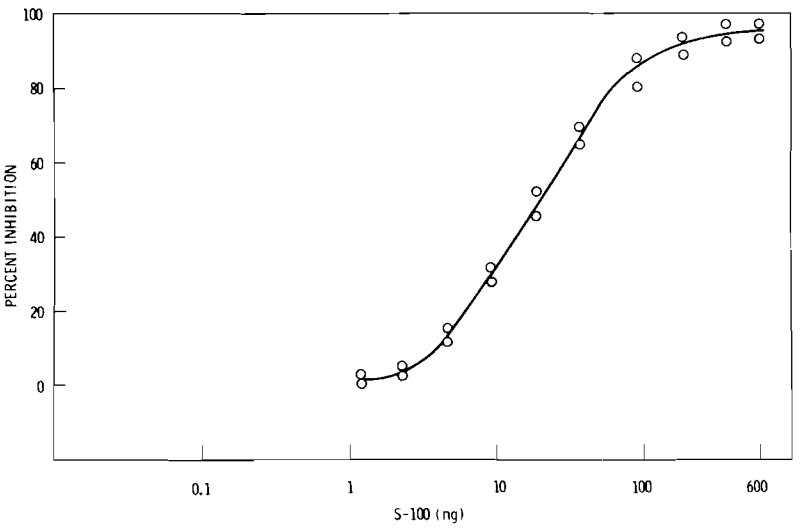

FIGURE 29.6. Standard Inhibition Curve Obtained by the Addition of Unlabeled S-100 to a Constant Amount of S-100·125I

• FACTORS INFLUENCING CROSS-PLACENTAL TRANSFER AND TERATOGENICITY OF METALLIC POLLUTANTS

Person in Charge: P. L. Hackett

This project seeks to define the specific influences of factors affecting the cross-placental transfer of heavy metals and their distribution throughout the fetoplacental unit as a function of time after exposure. These data will define the tissues at risk and provide a quantitative estimate of dose. As such, they will provide a rational basis on which to interpret and interrelate the results of teratologic studies.

The precise design of studies to be performed with specific pollutants will vary with the amount and credibility of the information presently available, or that which may become available during the course of the study. In general, however, cross-placental transfer and distribution will be evaluated at four different gestational ages selected to represent stages in the continuum of embryonic and placental development. The intravenous, oral, and inhalation routes of administration, which will provide differences in the rate at which the metals are presented to the placenta, as well as possible differences in their chemical binding in blood, will be compared. Since metabolism may be influenced by the mass administered, a low dose level, as well as one in the teratogenic range, will be studied.

This project will provide some of the toxicity data required to assess the teratogenic hazard of heavy metal pollutants. More important, it will provide the distribution and retention data required to integrate the results of past and future studies on these materials and to more readily extrapolate them to the practical situation. Initial studies are being performed with lead, which is known to be fetotoxic and teratogenic. Subsequent studies will investigate arsenic, cadmium, and selenium, which have been shown to be embryocidal and/or teratogenic, as well as nickel, which has yielded equivocal results, and vanadium, which apparently has not been evaluated.

CROSS-PLACENTAL TRANSFER AND EMBRYOTOXICITY OF LEAD IN RATS

Investigators:

P. L. Hackett and M. R. Sikov

Technical Assistance:

J. O. Hess, M. J. Kujawa, M. M. Conger, R. F. Meyers, and L. D. Montgomery

The kinetics of lead distribution in the fetoplacental unit was studied during the 30-hr period following intravenous administration of 0, 5, and 25 mg $Pb(NO_3)_2$/kg to pregnant rats at 9 and 15 days of gestation. Subsequent evaluation of 20-day fetuses showed that the highest dose level produced teratisms or mortality, depending on the time of administration.

Administration of lead to pregnant animals at specific gestation times causes embryonic death and resorption, as well as characteristic developmental abnormalities in the near-term fetus. To determine the genesis of these lesions we have studied lead metabolism and its effects in the fetoplacental unit (FPU) immediately following administration, to provide correlations with fetal development and viability in late gestation.

Aqueous solutions of 0, 5, or 25 mg $Pb(NO_3)_2$/kg, containing freshly-separated ^{210}Pb tracer, were injected into the tail vein of female rats (Hilltop Wistar) of timed pregnancies, on 9 (early organogenesis) or 15 (early histogenesis) days of gestation (dg). Lead kinetics were determined in FPUs from five females at each of five intervals during the ensuing 30-hr period. Concentrations were also measured and fetal development and mortality were evaluated at 20 dg. Radiolead concentrations were measured in selected fetal tissues by determining the 47 KeV gamma emission of ^{210}Pb using a scintillation counter after secular equilibrium had been established. Other fetuses were used for study of morphologic change and autoradiographic distribution.

Hemorrhage was observed within the uterus between implantation sites and within the extraembryonic coelom of the egg cylinder as early as 6 hr postinjection of 25 mg/kg at 9 dg. By 20 dg, fetuses from this treatment group exhibited stunting and characteristic external malformations such as gastroschisis and a urorectocaudal syndrome which included absent limbs or tails and hind-limb fusion. Severe ossification defects were also evident. When 25 mg/kg was administered at 15 dg, small hemorrhagic spots were present in the midmesoencephalon of the fetal brain at the earliest observation period, and hemorrhage in the central nervous system was a consistent finding by 24 hr postinjection.

Early mortality in the 9-dg egg cylinders was not studied because of the difficulty in determining viability, but approximately 50% fetal mortality was observed at the high lead level by 20 dg. About 25% of the fetuses were dead by 24 hr postinjection of 25 mg/kg at 15 dg and all were dead by 20 dg.

The concentrations of lead (% dose/g) in 9-dg and 15-dg FPUs (Figure 30.1) were largely independent of the administered lead dose. The exception, the significantly lower values at 24 and 30 hr for the 9 dg-5 mg level, may be due to differences in specific activity. The fact that the curve for the 25-mg/kg level did not also display this trend (i.e., fall below the 5-mg/kg curve) may be evidence for early toxic events. Initial concentrations were somewhat higher in the 9-dg egg cylinder than in the 15-day FPU and apparent clearance was more rapid. This difference is not due to growth, since both units increase in weight about 1.5-fold during the 30-hr interval.

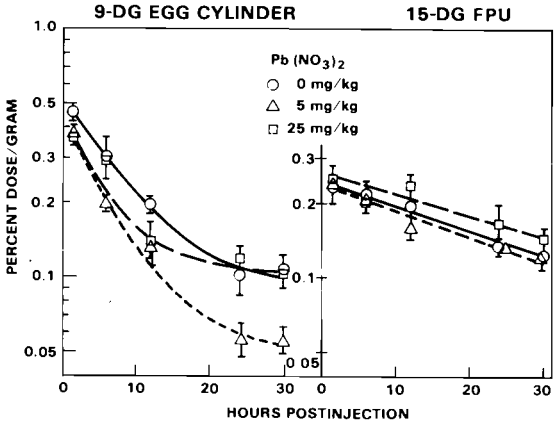

FIGURE 30.1. Percentage of Administered Dose Per Gram in Fetoplacental Units From Dams Injected at 9 and 15 Days Gestation

These data, re-expressed in terms of absolute amounts of lead, (Figure 30.2) remain relatively constant throughout the sampling period for 15-dg fetuses but decrease somewhat, indicating clearance, in the 9-dg egg cylinder. Nevertheless, initial values are proportional, i.e., the FPU value from the higher dose level is five times the lower dose and 15-dg FPU values are ten times 9-dg levels, as are the unit weights. Despite this clearance, the lead content of the FPUs at 20 days following injection at 9 dg is the same

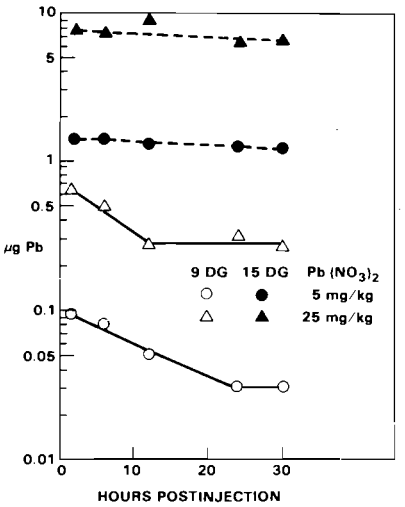

FIGURE 30.2. Micrograms of Lead in Fetoplacental Units of Dams Injected With $Pb(NO_3)_2$ at 9 and 15 Days Gestation

as the initial content of the 9-dg egg cylinder. This undoubtedly reflects translocation from maternal lead sources with deposition in the rapidly growing fetus.

The initial concentrations (% dose/g) in the placenta and membranes are higher than that of the 15-dg fetus and the shapes of the retention curves are different (Figure 30.3). Peak fetal concentrations are not obtained until about 6 hr postinjection as lead is being cleared from the placenta. Comparison of placental values again shows the effect of lower specific activity at the 5 mg/kg dose level, but the high dose curve resembles that of the tracer level. In the fetus the relationship is similar but the positions of the curves are reversed. Accordingly, if the 30-hr partition within the FPU at tracer levels is considered, the fetus contains 32% of the total FPU burden, while the lead-exposed fetuses contain 55% of the total. This suggests that the amount of carrier lead influences lead partition and, perhaps, cross-placental transfer. The change in distribution at 25 mg/kg is thought to reflect the toxic action at this dose.

These results demonstrate that embryotoxicity is evident soon after injection and can be correlated with a rapid intake of lead into the fetoplacental unit. They also confirm and help to explain earlier reports of embryolethality and malformations observed near term.

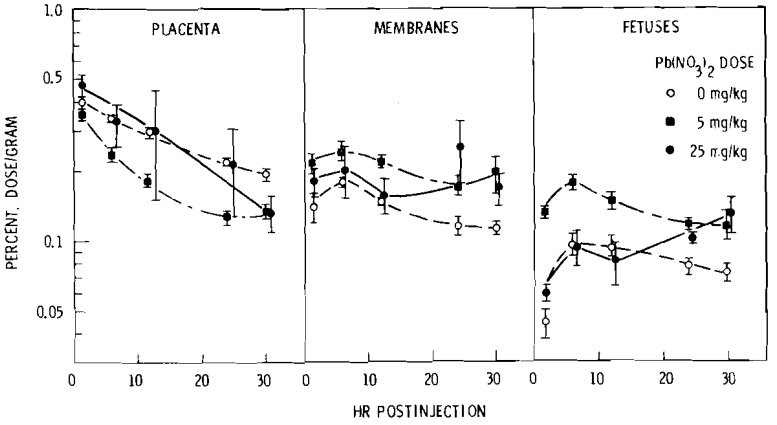

FIGURE 30.3. Percentage of Administered Dose in Fetoplacental Components From Dams Injected at 15 Days Gestation

LEAD TOXICITY IN PREGNANT RATS

Investigators:

P. L. Hackett and M. R. Sikov

Technical Assistance:

J. O. Hess, M. J. Kujawa, M. J. Conger, R. F. Meyers, and L. D. Montgomery

Lead in pregnant rats was rapidly cleared from blood with immediate uptake into major organ systems (skeleton, kidney, and liver). This was accompanied by early hemolysis and hematuria as well as gross kidney damage and hemorrhage of the gastrointestinal tract. Skeletal content increased over an 11-day period, during which time about 90% of the lead was removed from kidneys and liver. Distribution and retention were affected by lead dose level.

Lead retention and distribution have been well-documented in adult rats but there are few data on the metabolism of lead in pregnant animals. The present study was an effort to relate lead kinetics in pregnant rats to subsequent effects in the dam and the conceptus.

Pregnant rats were injected on gestation day 9 with aqueous solutions containing constant levels of tracer ^{210}Pb (specific activity: 17 µg Pb/mCi) and stable $Pb(NO_3)_2$ levels of 0, 5 and 25 mg/kg. Five animals from each dose level were sacrified at 1.5, 6, 12, 24 and 30 hr, and at 11 days post-injection, and Pb concentrations were determined by measuring the 47 KeV gamma emission of ^{210}Pb.

Ten percent of the rats injected with the highest dose level (25 mg/kg) died within 48 hr. There was immediate and severe hematuria at this dose level with a decrease in hematocrit from 41 to 35% within 1-1/2 hr. From 75 to 90% of the injected dose was cleared from the blood

before the first sampling at 90 min. Whole blood retention curves (Figure 30.4) varied significantly with dose level for reasons which are apparent from the erythrocyte and plasma curves (Figure 30.4). Binding of lead by erythrocytes was sharply reduced at the higher lead doses, due to lead-reduced hemolysis, which is also reflected in the plasma levels.

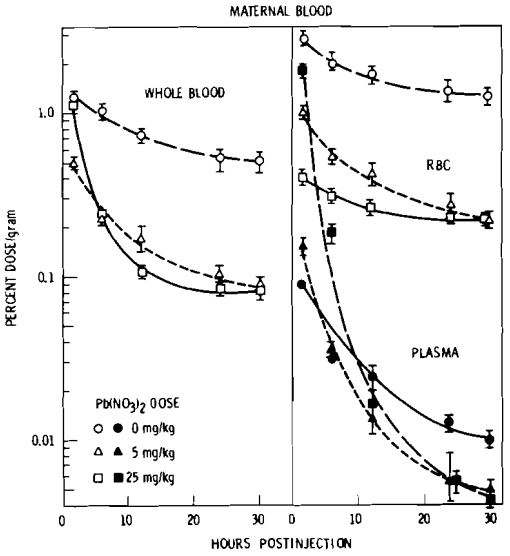

FIGURE 30.4. Percentage of Pb Dose Per Gram in Maternal Blood, Plasma and Red Blood Cells

Gastrointestinal hemorrhage was observed in 12% of the rats at 5 mg and in 80% at 25 mg/kg. This was most frequently at the ileocecal junction; gastric hemorrhage was less common. From 6 to 15% of the dose was found in the GI tract 1.5 hr after administration, and the concentrations peaked at still higher values at 6 hr (Figure 30.5). The excretion route was dose-dependent, renal clearance predominating in the animals receiving the tracer ^{210}Pb (17% of the dose at 30 hr). Only 6% of the dose had been excreted in the urine by the lead-loaded animals by 30 hr, but higher percentages of the dose were observed in the gastrointestinal tract of these rats. Gross kidney damage was apparent at 24 hr postinjection

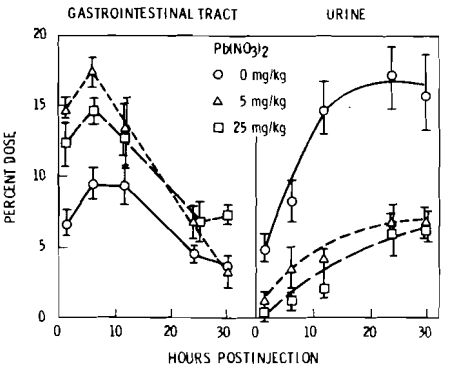

FIGURE 30.5. Percentage of Administered Pb Dose Appearing in the Gastrointestinal Tract and Urine up to 30 Hours Postinjection

in some of the animals receiving the high dose level.

The skeleton showed the greatest avidity for lead, the burden increasing by about 10% during the sampling period to attain a value of 40-50% of the administered dose on the 20th day of gestation (Figure 30.6). Urinary ^{210}Pb excretion was lower in the rats which received stable lead than in those which received only the tracer (Figure 30.5). In contrast, these rats retained a greater fraction of the ^{210}Pb in the kidney. Rats receiving 25 mg/kg exhibited the highest hepatic values, probably due to hepatic clearance of lead-induced erythrocyte hemolysates. In the interval between 30 hr and 11 days postinjection the liver and kidneys lost about 90% of their deposited lead. The mobilization of these lead stores may be the main source of lead translocated to the maternal skeleton and fetoplacental unit during this period.

Data obtained in these experiments will be compared with values from various gestation times and from nongravid animals in order to determine the effect of pregnancy or of maternal-fetal relationships on metabolism and biological consequences of metal deposition.

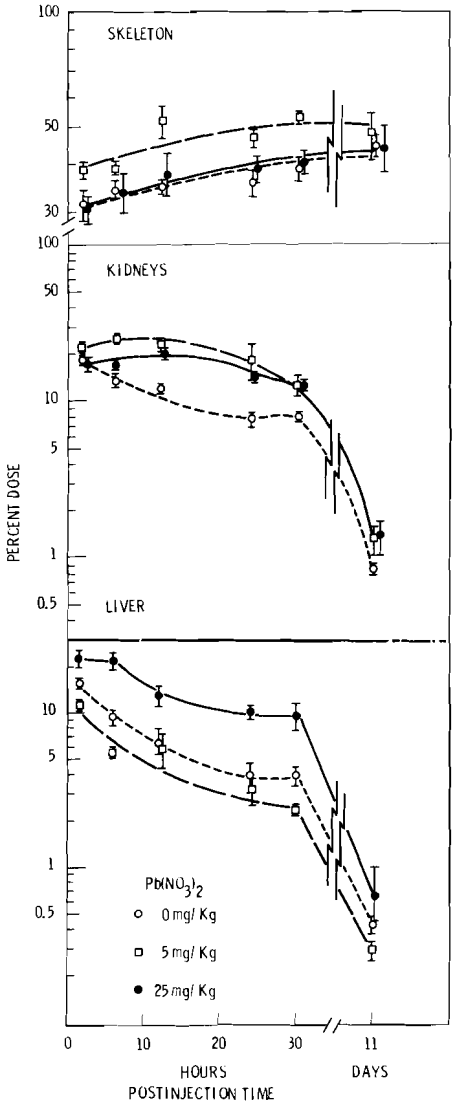

FIGURE 30.6. Percentage of the Pb Dose Deposited in the Maternal Skeleton, Kidney and Liver

• GENETIC EFFECTS FROM ELECTRIC FIELDS AT THE CHROMOSOMAL LEVEL OF *DROSOPHILA*

Person in Charge: F. P. Hungate

This project was initiated in FY 1976 to examine the possibility that electric fields induce changes in the genetic mechanism of cells. Such an examination of potential effect is dictated by the increased general environmental awareness and the recognition that the United States is rapidly evolving toward increased dependence on energy delivered in the form of electricity. Thus, more frequent exposures of workers and the public to higher electric fields will occur unless there are demonstrable reasons to curb such fields. While there is little evidence of biological damage from electromagnetic fields (other than from current flow), it is prudent to examine the possibility for such damage. The genetic system, fundamental to all living organisms, comprises large molecular species potentially subject to the forces exerted in electromagnetic fields, and is a logical subject for a study of possible effects.

An analysis of electromagnetic effects has been made relevant to a projected US Navy Communication System (Project Sanguine), involving exposures of life forms to fields no greater than are common in US homes. In these studies, involving only low field strengths, no genetic effects were identified. In contrast, our study employs extremely high fields to determine whether effects can be detected at any field strength, with the assumption that demonstration of a particular effect must precede any evaluation of the relevance of that effect to exposures of workers in the electric utility industry or the general public.

The study is initially directed toward evaluation of genetic changes induced by DC fields, then moves to a similar evaluation of effects from AC fields. Data for mutation frequencies in several bacterial strains and in the fruit fly, Drosophila, following exposure to DC fields have been obtained and are now being examined for an indication of their statistical significance.

ARE MUTATIONS INDUCED BY ELECTRIC FIELDS?

Investigators:

F. P. Hungate, R. L. Richardson, and M. F. Gillis

Technical Assistance:

M. P. Fujihara

This report summarizes progress made during the first year in a study of the mutagenicity of electric fields. Several bacterial strains and the fruit fly, Drosophila, have been studied for evidence of mutagenicity following exposure to DC fields up to 10 kV/cm. Initial data suggest a mutagenic response following exposure of dividing cell systems in the higher-strength fields but the present data are not sufficiently consistent to relate effect to dose.

This report describes results from tests with static (DC) fields. Future work with alternating (60 Hz AC) fields will complement the present studies.

The field was produced by applying a voltage to two flat, horizontal, parallel, circular copper electrodes 25 cm in diameter, the edges of which were rolled away from the space between the plates to reduce edge field strength and the possibility of corona (Figure 31.1). Electrode separation was maintained with lucite spacer rings 20 cm in diameter, 0.3 cm thick and of variable height (maximum 6 cm). By connecting several such electrode pairs in parallel, using spacers of differing heights, several field strengths could be produced simultaneously. In most experiments, 2-cm and 6-cm spacers were used, giving a threefold difference in field strengths. Each exposure "chamber" was supplied sterile humidified air through small plastic tubes inserted into holes in the spacers.

Early experiments used a Von Hipot Tester, model C-1, capable of producing 100 kV DC. Most experiments used an

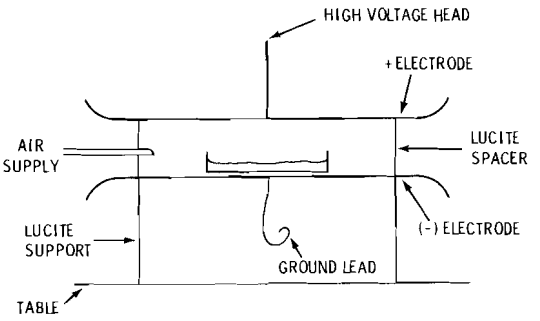

FIGURE 31.1. Exposure System

Associated Research DC Model 5270 power supply capable of 45 kV DC. There was no visible or audible corona, no detectable odor of ozone, and the power supply microammeters indicated that leakage currents were less than 0.1 μA. The field in the exposure region (unperturbed) was calculated by dividing the voltage by the electrode spacing.

All controls were enclosed in identical exposure chambers with zero voltage on the

electrodes. Their air supply was in parallel with the experimental groups.

Three types of genetic systems were used: The Muller-5 test for induction of sex-linked lethals in Drosophila, Ames' histidine auxotroph→prototroph system in Salmonella, and a more general test of induction of resistance to tetracycline in the MAV strain of Photobacterium fisheri. All exposures were performed at ambient temperature (22-24°C), using 10-cm plastic petri plates with tops removed.

Drosophila males of the Canton-S strain were exposed as adults or in the early pupal stage and subsequently mated with virgin Muller-5 females. The F_1 offspring were pair mated and the offspring examined for evidence of sex-linked lethals.

To evaluate the possibility of a synergistic effect of ionizing radiation and the electric field, adult flies were placed in one of two exposure chambers, 1 meter from a ^{60}Co gamma source. One chamber was connected to the high voltage while flies in the other served as controls. Following activation of the electric field (6 kV/2 cm) the gamma source was raised for 6 min to give 1500 rads and the electric field was maintained for an additional 2 hr. At the same time an additional pair of exposure chambers was placed outside the gamma field, one electrically activated and the other not activated.

Salmonella strains used were TA-100 and 1535, which mutate primarily by base pair substitution, and TA-98 and 1537, which mutate primarily by frameshift. Standardized cultures in log growth phase were prepared and 20-ml aliquots were placed in sterile plastic petri dishes for exposed and control cultures. Growth in the field and in control cultures was allowed without shaking for 16-18 hr, with approximately four cell doublings. Following exposure, the cells were washed and plated on agar plates containing minimal medium. The number of colonies on the minimal plates grown at 37° was determined 3 days later, each colony representing a mutant. Aliquots of the primary suspensions were plated on medium containing histidine to evaluate the total number of cells in the suspension. Control cultures were treated similarly and concurrently with the exposed cultures. The MAV strain was tested in a similar manner, except that the initial shake cultures were grown at 25° in medium containing high salt, and mutants were detected by their ability to grow on solid medium containing 2.5 μg tetracycline/ml.

Irrelevant and undesirable static electrical effects occurred with high fields: polarization of the flies produced distinct erection of their wings at 1.5 kV/cm; when in direct contact with the metal electrode, the flies accumulated free charge and experienced an electrostatic force toward the opposite electrode. At > 2 kV/cm, this force is sufficient to pull them off one electrode and transport them rapidly to the other, where they accumulate a charge of the opposite sign and the process is repeated, the flies bouncing rapidly between the plates. If the flies remain on a petri dish (nonconducting) or on the food in it, free charge is not accumulated and this phenomenon does not occur. The flies are still polarized by the field, however, and act as small dipoles. Thus, they can stick to each other and form chains which align with the field, an extreme situation being the formation of a chain which reaches from one electrode to another. Current flow through the chain kills the flies instantly, of course, but the polarized chain of carcasses remains.

There was no evidence from a preliminary study that a DC field augmented the frequency of sex-linked lethals in mature sperm over that produced by 1500 rads of gamma radiation. The data obtained are shown below.

Exposure	Mutation Frequency %
Control (no gamma, no DC field)	0.6 (2 mutants/333)
Gamma only	5.3 (10 mutants/189)
Gamma + 3 kV/cm	3.6 (9/248)
DC field only (3 kV/cm)	0.6 (2/313)

Drosophila adult males exposed for 13 days to 1 kV/cm were mated with virgin Muller-5 females and the F_1 offspring then individually mated, with subsequent inspection of the F_2 generation of mutations. These flies showed a 3% mutation frequency (4/139) while the controls gave a 1% frequency (1/94). A similar series at 3 kV/cm failed early in the test due to bridging of the space between the electrodes with flies.

Since exposure of mid and early pupal stages to ionizing radiation leads to higher mutation frequencies, pupae 0-48 hr and 48-72 hr post-pupation were exposed for 48 hr to 3 and 0.75 kV/cm with appropriate matings. The results are shown below.

Pupal Age at Start of Exposure (hr)	Mutation Frequency		
	3 kV/cm	0.75 kV/cm	0 kV/cm
48 - 72	1/110	2/139	0/102
0 - 48	8/288	0/209	2/216

Salmonella strains TA-100 (mutation by base substitution) and TA-98 (mutation by frameshift) have been extensively studied, with TA-100 showing a consistently increased mutation frequency following exposure to DC fields in excess of 7 kV/cm. Substantial variation in the data prevents any extrapolation to lower field strengths at this time.

Data from strain TA-98 fail to indicate any evidence of mutation effects with voltages up to 10 kV/cm, suggesting that misreading in the -C-G-C-G-sequence, by which TA-98 primarily reverts, does not occur.

Mutation to tetracycline resistance in the genetically undefined MAV strain of Photobacterium fisheri has consistently occurred with DC voltages up to 7.5 kV/cm. The data have not yet been statistically analyzed, so it is not possible to infer the nature of the relationship between effect and field strength.

It is absolutely essential that these data be considered preliminary and subject to further evaluation based on continued experimentation. A conducting body placed in a DC electric field will, in a very short time, have zero field in its interior. Thus, it is difficult to comprehend how even the extremely large DC fields used in these experiments can influence genetic material in a living cell. Other sources of effect which we must consider and investigate include insensible ozone, mechanical stresses due to electrostatic forces, alteration of air ion distribution or concentration, air ion current, contamination of air by electrically leached constituents from materials in the field, "local corona" and ozone production at the surface of the subject due to field enhancement by the subject and time-varying "ripple" voltage on the power supply output, to name a few. We believe we have eliminated ambient ozone with the flowing air system; total air ion currents are not detectible (less than 0.1 μA), and ripple voltage is very small (less than 2% of the applied DC voltage). Ripple is an important artifact, since alternating electric fields produce current densities in conducting bodies which are proportional to the frequency of the field, and the small ripple on typical power supplies may have very high-frequency components (not, however, observed on the oscilloscope used to characterize this field). Transient currents produced by turning the field on and off are easily minimized by changing the voltage slowly.

Studies with alternating fields are planned. We also plan to repeat some of the tests reported here using series-connected batteries as a source of voltage, thereby eliminating completely the possibility of ripple.

APPENDIX

DOSE-EFFECT STUDIES WITH INHALED PLUTONIUM IN BEAGLES

On the following pages data are presented on selected parameters relative to the current life-span dose-effect studies with inhaled $^{239}PuO_2$, $^{238}PuO_2$, and ^{239}Pu nitrate in beagles. Information is presented on the estimated initial alveolar deposition based on external thorax counts at 14 and 30 days postexposure and on estimated lung weights, assuming lung weights of 0.011 X body weight at the time of exposure. Information is also provided on the current interpretation of the most prominent clinical-pathological features associated with the death of animals. The data represent the information presently available. Certain values and diagnoses may be updated as new information becomes available. The data are presented as reference for scientists who desire to follow in detail the progress of these experiments.

DOSE-EFFECT STUDIES WITH INHALED PU-239 OXIDE IN BEAGLES

DOSE GROUP	DOG NUMBER	SEX	INITIAL ALVEOLAR DEPOSITION: NCI	NCI/G LUNG	NCI/KG	INHALATION EXPOSURE: WEIGHT (KG)	AGE* (MO)	DATE	DATE OF DEATH	MONTHS SINCE INHALATION: 09/30/76	DEATH	COMMENTS ON DEAD DOGS
CONTROL	775	F	0	0.00	0.00					87.1*		
CONTROL	766	M	0	0.00	0.00					87.5*		
CONTROL	755	M	0	0.00	0.00					87.9*		
CONTROL	749	F	0	0.00	0.00					87.9*		
CONTROL	740	F	0	0.00	0.00					89.2*		
CONTROL	738	F	0	0.00	0.00					89.2*		
CONTROL	861	M	0	0.00	0.00					81.1*		
CONTROL	846	M	0	0.00	0.00					81.8*		
CONTROL	811	F	0	0.00	0.00					82.2*		
CONTROL	801	M	0	0.00	0.00					83.3*		
CONTROL	800	F	0	0.00	0.00					83.3*		
CONTROL	792	M	0	0.00	0.00				04/28/76		79.5*	ORAL TUMOR
CONTROL	789	M	0	0.00	0.00					86.1*		
CONTROL	785	M	0	0.00	0.00					86.4*		
CONTROL	903	F	0	0.00	0.00					74.6*		
CONTROL	885	F	0	0.00	0.00					76.9*		
CONTROL	882	M	0	0.00	0.00					77.5*		
CONTROL	878	M	0	0.00	0.00					77.7*		
CONTROL	872	F	0	0.00	0.00					79.6*		
CONTROL	868	F	0	0.00	0.00					79.7*		
CONTROL SACRIFICE	724	M	0	0.00	0.00					90.0*		
CONTROL SACRIFICE	703	M	0	0.00	0.00					90.5*		
CONTROL SACRIFICE	701	F	0	0.00	0.00					90.5*		
D-1 LOWEST	762	M	0	0.00	0.00	11.5	19.3	01/19/71		68.8		
D-1 LOWEST	754	M	0	0.00	0.00	13.0	19.5	01/19/71		68.8		
D-1 LOWEST	865	F	0	0.00	0.00	9.0	17.8	07/06/71		62.9		
D-1 LOWEST	854	M	0	0.00	0.00	13.0	18.2	07/06/71		62.9		
D-1 LOWEST	847	M	0	0.00	0.00	13.0	18.5	07/06/71		62.9		
D-1 LOWEST	907	F	0	0.00	0.00	11.5	15.9	11/10/71		58.7		
D-1 LOWEST	886	F	0	0.00	0.00	10.5	18.2	11/10/71		58.7		
D-1 LOWEST	879	M	0	0.00	0.00	14.5	17.9	10/07/71		59.8		
D-1 LOWEST	904	F	1	0.01	0.07	10.0	15.9	11/10/71		58.7		
D-1 LOWEST	849	F	1	0.01	0.10	10.0	21.3	10/07/71	10/26/72		12.6	SACRIFICED
D-1 LOWEST	825	F	1	0.01	0.12	11.5	18.1	06/08/71		63.8		
D-1 LOWEST	900	M	3	0.02	0.22	13.0	16.0	11/10/71		58.7		
D-1 LOWEST	833	F	2	0.02	0.24	8.5	16.5	04/26/71		65.2		
D-1 LOWEST	899	F	4	0.03	0.31	11.5	16.0	11/10/71		58.7		
D-1 LOWEST	870	F	4	0.03	0.32	12.0	16.9	07/06/71		62.9		
D-1 LOWEST	867	M	5	0.04	0.41	11.5	17.8	07/06/71		62.9		
D-1 LOWEST	891	M	6	0.04	0.41	14.0	16.0	11/10/71		58.7		
D-1 LOWEST	853	M	8	0.05	0.51	15.0	21.3	10/07/71		59.8		
D-1 LOWEST	875	M	8	0.05	0.54	14.0	16.8	07/06/71		62.9		
D-1 LOWEST	350	F	5	0.05	0.59	8.5	21.3	10/07/71		59.8		

* INDICATES AGE IN MONTHS SINCE BIRTH, ALL OTHER AGES ARE IN MONTHS SINCE EXPOSURE

DOSE-EFFECT STUDIES WITH INHALED PU-239 OXIDE IN BEAGLES

DOSE GROUP	DOG NUMBER	SEX	INITIAL ALVEOLAR DEPOSITION: NCI	NCI/G LUNG	NCI/KG	INHALATION EXPOSURE: WEIGHT (KG)	AGE* (MO)	DATE	DATE OF DEATH	MONTHS SINCE INHALATION: 09/30/76	DEATH	COMMENTS ON DEAD DOGS
D-1 LOWEST	893	M	9	0.06	0.61	14.8	14.9	10/07/71		59.8		
D-1 LOWEST	786	M	8	0.06	0.62	13.0	18.7	02/09/71		67.7		
D-1 LOWEST	776	F	6	0.06	0.63	9.5	19.1	01/19/71		68.4		
D-1 LOWEST	807	F	8	0.07	0.73	11.0	14.6	02/09/71		67.7		
D-1 LOWEST	841	F	6	0.07	0.75	8.0	17.7	06/08/71		63.8		
D-1 LOWEST	903	M	9	0.07	0.77	11.0	15.9	11/10/71		58.7		
D-2 LOW	774	M	10	0.07	0.74	13.5	20.2	03/04/71		66.9		
D-2 LOW	767	M	10	0.08	0.83	12.0	18.2	12/21/70		69.3		
D-2 LOW	843	M	10	0.08	0.83	12.5	18.6	07/06/71		62.9		
D-2 LOW	920	M	11	0.08	0.92	12.0	16.0	06/08/72	07/07/72		1.0	SACRIFICED
D-2 LOW	871	M	13	0.09	0.96	13.5	16.9	07/06/71		62.9		
D-2 LOW	863	M	13	0.09	1.00	13.0	17.3	06/08/71		63.8		
D-2 LOW	874	M	16	0.11	1.24	13.0	16.8	07/06/71		62.9		
D-2 LOW	845	F	19	0.15	1.63	11.5	17.6	06/08/71		63.8		
D-2 LOW	758	M	22	0.15	1.69	13.0	19.5	01/19/71		68.4		
D-2 LOW	785	F	14	0.16	1.75	8.0	19.5	01/19/71		68.4		
D-2 LOW	798	F	16	0.16	1.78	9.0	15.6	12/09/71	08/29/74		42.6	SACRIFICED
D-2 LOW	836	F	19	0.16	1.81	10.5	19.1	07/06/71		62.9		
D-2 LOW	831	F	21	0.18	2.00	10.5	17.9	06/08/71		63.8		
D-2 LOW	881	F	19	0.19	2.09	9.0	17.7	10/07/71		59.8		
D-2 LOW	796	F	24	0.22	2.00	10.0	18.2	01/19/71		68.4		
D-2 LOW	859	M	35	0.22	2.41	14.5	18.2	07/06/71		62.9		
D-2 LOW	876	F	19	0.23	2.51	7.5	17.9	10/07/71		59.8		
D-2 LOW	757	M	36	0.23	2.57	14.0	18.5	12/21/70		69.3		
D-2 LOW	806	F	26	0.25	2.74	9.5	15.3	03/04/71		66.9		
D-2 LOW	814	F	32	0.28	3.05	10.5	15.1	03/04/71		66.9		
D-2 LOW	877	F	31	0.29	3.24	10.5	17.9	10/07/71		59.8		
D-2 LOW	763	F	28	0.33	3.50	8.0	18.2	12/21/70		69.3		
D-2 LOW	802	M	30	0.33	3.64	11.0	18.1	04/26/71		65.2		
D-3 MED-LOW	781	F	43	3.43	4.17	11.5	17.3	12/21/70		69.3		
D-3 MED-LOW	771	F	44	3.40	4.40	10.0	19.2	01/20/71		68.3		
D-3 MED-LOW	796	M	62	0.42	4.59	13.5	19.5	03/04/71		66.9		
D-3 MED-LOW	783	F	62	0.42	4.59	13.5	19.1	02/10/71		67.6		
D-3 MED-LOW	752	M	62	0.43	4.77	13.0	18.6	12/21/70		69.3		
D-3 MED-LOW	834	M	65	0.44	4.81	13.5	16.8	04/26/71		65.2		
D-3 MED-LOW	883	M	63	0.44	4.85	13.0	17.7	10/07/71		59.8		
D-3 MED-LOW	838	M	56	1.46	5.09	11.0	17.8	06/08/71		63.8		
D-3 MED-LOW	779	M	74	0.46	5.10	14.5	20.2	03/04/71		66.9		
D-3 MED-LOW	815	M	68	0.52	5.67	12.0	16.8	04/26/71	05/22/73		24.9	SACRIFICED
D-3 MED-LOW	795	F	58	0.52	5.68	9.5	15.0	01/20/71		68.3		
D-3 MED-LOW	851	F	53	0.58	5.89	9.0	21.3	10/07/71		59.8		
D-3 MED-LOW	913	M	70	0.58	6.04	11.5	16.0	06/08/72	07/06/72		0.9	SACRIFICED
D-3 MED-LOW	830	F	67	0.68	7.44	9.0	17.8	06/08/71		63.8		

* INDICATES AGE IN MONTHS SINCE BIRTH, ALL OTHER AGES ARE IN MONTHS SINCE EXPOSURE

DOSE-EFFECT STUDIES WITH INHALED PU-239 OXIDE IN BEAGLES

DOSE GROUP	DOG NUMBER	SEX	INITIAL ALVEOLAR DEPOSITION: NCI	NCI/G LUNG	NCI/KG	INHALATION EXPOSURE: WEIGHT (KG)	AGE* (MO)	DATE	DATE OF DEATH	MONTHS SINCE INHALATION: 09/30/76	DEATH	COMMENTS ON DEAD DOGS
D-3 MED-LOW	797	F	85	0.70	7.73	11.0	16.4	03/04/71		66.9		
D-3 MED-LOW	888	F	75	0.72	7.94	9.5	21.3	10/07/71		59.8		
D-3 MED-LOW	827	F	89	0.81	8.90	10.0	16.7	04/26/71		65.2		
D-3 MED-LOW	697	M	140	0.85	9.33	15.0	19.5	10/30/70		71.0		
D-3 MED-LOW	750	M	118	0.93	10.26	11.5	19.6	01/20/71		68.3		
D-3 MED-LOW	888	M	123	1.12	12.30	10.0	17.8	10/08/71		59.8		
D-3 MED-LOW	884	F	135	1.23	13.50	10.0	17.6	06/09/71		63.8		
D-3 MED-LOW	905	F	127	1.40	15.88	8.0	15.9	11/10/71		58.7		
D-4 MEDIUM	809	F	151	1.25	13.73	11.0	15.3	03/04/71		66.9		
D-4 MEDIUM	866	M	200	1.35	14.81	13.5	17.4	07/06/71		62.9		
D-4 MEDIUM	764	F	158	1.37	15.05	10.5	18.2	12/21/70		69.3		
D-4 MEDIUM	835	F	163	1.48	16.30	10.0	16.4	04/26/71		65.2		
D-4 MEDIUM	839	F	189	1.49	16.43	11.5	16.3	04/26/71		65.2		
D-4 MEDIUM	814	F	140	1.50	16.47	8.5	15.1	03/04/71		66.9		
D-4 MEDIUM	836	M	256	1.66	18.29	14.0	17.8	06/08/71		63.8		
D-4 MEDIUM	819	F	163	1.74	19.18	8.5	18.2	06/08/71		63.8		
D-4 MEDIUM	888	M	274	1.78	19.57	14.0	17.1	10/08/71		59.8		
D-4 MEDIUM	824	F	227	1.79	19.74	11.5	18.1	06/08/71		63.8		
D-4 MEDIUM	860	M	254	1.85	20.32	12.5	17.3	06/09/71		63.8		
D-4 MEDIUM	833	F	248	2.37	26.11	9.5	16.5	04/26/71		65.2		
D-4 MEDIUM	810	F	302	2.39	26.26	11.5	15.3	03/04/71		66.9		
D-4 MEDIUM	798	M	404	2.60	28.65	15.5	17.7	03/08/71		66.9		
D-4 MEDIUM	854	M	465	2.64	29.06	16.0	21.3	10/08/71		59.8		
D-4 MEDIUM	879	M	298	2.71	29.80	10.0	68.0	10/09/70	10/16/70		0.2	SACRIFICED
D-4 MEDIUM	803	F	270	2.73	30.00	9.0	14.6	02/10/71		67.6		
D-4 MEDIUM	805	F	257	3.12	34.27	7.5	18.5	06/08/71		63.8		
D-4 MEDIUM	812	M	438	3.19	35.04	12.5	17.1	04/26/71		65.2		
D-4 MEDIUM	857	M	486	3.40	37.38	13.0	17.3	06/08/71		63.8		
D-4 MEDIUM	893	M	494	3.59	39.52	12.5	16.0	11/10/71		58.7		
D-4 MEDIUM	816	M	398	3.62	39.80	10.0	16.8	04/26/71	05/11/71		0.5	SACRIFICED
D-4 MEDIUM	777	M	546	3.97	43.68	12.5	20.2	03/04/71		66.9		
D-4 MEDIUM	803	M	547	4.32	47.57	11.5	16.1	04/26/71		65.2		
D-5 MED-HI	787	M	651	4.73	52.08	12.5	19.5	03/04/71		66.9		
D-5 MED-HI	880	F	703	4.92	54.08	13.0	17.7	06/08/71		63.8		
D-5 MED-HI	727	M	733	5.33	58.64	12.5	18.8	10/26/70		71.2		
D-5 MED-HI	898	F	711	5.39	59.25	12.0	16.0	11/10/71		58.7		
D-5 MED-HI	759	M	809	6.13	67.42	12.0	18.3	12/21/70	06/02/75		53.4	LUNG TUMOR
D-5 MED-HI	864	F	801	6.42	72.82	11.0	17.4	07/07/71		62.8		
D-5 MED-HI	900	M	747	6.70	73.70	10.0	15.9	11/10/71		58.7		
D-5 MED-HI	734	M	914	6.92	76.17	12.0	19.2	11/10/70	04/01/71		4.7	SACRIFICED
D-5 MED-HI	856	F	918	7.08	77.90	10.5	18.2	07/07/71		62.8		
D-5 MED-HI	837	M	1283	8.04	88.48	14.5	18.8	07/07/71		62.8		
D-5 MED-HI	863	F	950	8.48	93.33	10.5	17.4	07/07/71		62.8		

* INDICATES AGE IN MONTHS SINCE BIRTH, ALL OTHER AGES ARE IN MONTHS SINCE EXPOSURE

DOSE-EFFECT STUDIES WITH INHALED PU-239 OXIDE IN BEAGLES

DOSE GROUP	DOG NUMBER	SEX	INITIAL ALVEOLAR DEPOSITION NCI	NCI/G LUNG	NCI/KG	INHALATION EXPOSURE WEIGHT (KG)	AGE* (MO)	DATE	DATE OF DEATH	MONTHS SINCE INHALATION 09/30/76	MONTHS SINCE INHALATION DEATH	COMMENTS ON DEAD DOGS
D-5 MED-HT	820	F	887	8.56	94.11	9.0	18.2	06/08/71		63.8		
D-5 MED-HT	852	F	1187	9.38	103.22	11.5	21.3	10/08/71		59.8		
D-5 MED-HT	880	F	880	9.55	105.00	8.0	17.8	10/08/71		59.8		
D-5 MED-HT	889	F	1089	9.90	108.90	10.0	16.0	11/10/71		58.7		
D-5 MED-HT	783	M	1394	10.14	111.52	12.5	18.9	02/09/71	12/03/75		57.8	LUNG TUMOR
D-5 MED-HT	800	M	1344	10.18	112.00	12.0	20.5	07/07/71	08/18/74		37.4	LUNG TUMOR RESPIRATORY INSUFFICIENCY
D-5 MED-HT	873	M	1767	10.71	117.80	15.0	16.8	07/07/71	09/03/76		61.9	LUNG TUMOR
D-5 MED-HT	760	M	1378	10.89	119.93	11.5	19.3	01/20/71	08/15/73		30.8	RESPIRATORY INSUFFICIENCY
D-5 MED-HT	796	F	1319	11.41	125.52	10.5	15.6	02/09/71	09/17/75		55.2	LUNG TUMOR
D-5 MED-HT	761	M	1460	12.07	132.73	11.0	19.3	01/20/71		68.3		
D-5 MED-HT	709	M	1726	12.55	138.08	12.5	19.6	11/10/70	03/31/71		4.6	SACRIFICED
D-5 MED-HT	773	M	1896	14.99	164.87	11.5	19.8	02/09/71	06/26/75		52.5	LUNG TUMOR
D-5 MED-HT	702	F	1692	15.29	168.20	10.0	19.8	11/10/70	03/31/71		4.6	SACRIFICED
D-5 MED-HT	739	F	1511	17.17	188.88	8.0	18.5	11/10/70	04/01/71		4.7	SACRIFICED
D-6 HIGH	787	F	7476	97.09	1068.00	7.0	19.6	01/20/71	01/13/72		11.8	RESPIRATORY INSUFFICIENCY
D-6 HIGH	911	M	10267	103.76	1141.36	12.5	15.9	11/10/71	10/12/72		11.1	RESPIRATORY INSUFFICIENCY
D-6 HIGH	753	F	2488	23.83	257.68	9.5	18.5	12/21/70		69.3		
D-6 HIGH	817	M	3164	23.97	263.67	12.0	19.2	07/07/71	03/26/73		20.6	RESPIRATORY INSUFFICIENCY
D-6 HIGH	823	M	3515	24.59	270.38	13.0	19.1	07/07/71	09/13/73		26.3	RESPIRATORY INSUFFICIENCY
D-6 HIGH	890	F	3101	31.32	344.56	9.0	16.0	11/10/71	06/13/74		31.1	RESPIRATORY INSUFFICIENCY
D-6 HIGH	835	F	3880	33.25	365.71	10.5	75.5	11/05/70	11/12/70		0.2	SACRIFICED
D-6 HIGH	913	M	8000	35.64	392.00	12.5	17.4	07/19/72	08/19/72		1.0	SACRIFICED
D-6 HIGH	906	F	6632	63.46	698.11	9.5	15.9	11/10/71	11/22/72		12.4	RESPIRATORY INSUFFICIENCY
D-6 HIGH	896	F	5515	66.85	735.33	7.5	16.0	11/10/71	02/12/73		15.1	RESPIRATORY INSUFFICIENCY

* INDICATES AGE IN MONTHS SINCE BIRTH, ALL OTHER AGES ARE IN MONTHS SINCE EXPOSURE

DOSE-EFFECT STUDIES WITH INHALED PU-238 OXIDE IN BEAGLES

DOSE GROUP	DOG NUMBER	SEX	INITIAL ALVEOLAR DEPOSITION: NCI	NCI/G LUNG	NCI/KG	INHALATION EXPOSURE: WEIGHT (KG)	AGE* (MO)	DATE	DATE OF DEATH	MONTHS SINCE INHALATION: 09/30/76	DEATH	COMMENTS ON DEAD DOGS
CONTROL	978	M	0	0.00	0.00					64.6*		
CONTROL	949	F	0	0.00	0.00					64.7*		
CONTROL	939	M	0	0.00	0.00					64.9*		
CONTROL	1061	F	0	0.00	0.00					61.0*		
CONTROL	1054	F	0	0.00	0.00					61.1*		
CONTROL	1045	M	0	0.00	0.00					61.4*		
CONTROL	1038	M	0	0.00	0.00					61.4*		
CONTROL	1024	M	0	0.00	0.00					63.5*		
CONTROL	1007	F	0	0.00	0.00					64.0*		
CONTROL	1005	M	0	0.00	0.00					64.0*		
CONTROL	996	F	0	0.00	0.00					64.0*		
CONTROL	990	F	0	0.00	0.00					64.2*		
CONTROL	1225	F	0	0.00	0.00					47.9*		
CONTROL	1209	M	0	0.00	0.00					48.7*		
CONTROL	1197	M	0	0.00	0.00					49.0*		
CONTROL	1186	F	0	0.00	0.00					49.5*		
CONTROL	1116	F	0	0.00	0.00					56.1*		
CONTROL	1112	M	0	0.00	0.00					56.4*		
CONTROL	1097	F	0	0.00	0.00					56.6*		
CONTROL	1093	M	0	0.00	0.00					57.3*		
CONTROL SACRIFICE	966	M	0	0.00	0.00					64.6*		
CONTROL SACRIFICE	1087	M	0	0.00	0.00					57.5*		
CONTROL SACRIFICE	1014	F	0	0.00	0.00					63.9*		
CONTROL SACRIFICE	1011	F	0	0.00	0.00					63.9*		
CONTROL SACRIFICE	1228	M	0	0.00	0.00					47.9*		
CONTROL SACRIFICE	1227	M	0	0.00	0.00					47.9*		
CONTROL SACRIFICE	1223	F	0	0.00	0.00				05/15/75		31.9*	SACRIFICED
CONTROL SACRIFICE	1118	M	0	0.00	0.00				01/13/76		47.5*	SACRIFICED
D-1 LOWEST	1064	M	0	0.00	0.00	14.5	16.7	01/18/73		44.4		
D-1 LOWEST	1055	M	0	0.00	0.00	13.0	16.8	01/18/73		44.4		
D-1 LOWEST	1044	F	0	0.00	0.00	11.5	17.0	01/18/73		44.4		
D-1 LOWEST	1039	M	0	0.00	0.00	11.0	17.0	01/18/73		44.4		
D-1 LOWEST	1027	F	0	0.00	0.00	12.5	19.2	01/18/73		44.4		
D-1 LOWEST	1003	M	0	0.00	0.00	14.0	19.6	01/18/73		44.4		
D-1 LOWEST	998	M	0	0.00	0.00	10.5	19.6	01/18/73		44.4		
D-1 LOWEST	1230	M	0	0.00	0.00	12.5	18.4	04/19/74		29.4		
D-1 LOWEST	1215	M	0	0.00	0.00	15.5	19.3	04/18/74		29.4		
D-1 LOWEST	1194	F	0	0.00	0.00	10.5	19.8	04/18/74		29.4		
D-1 LOWEST	1165	F	0	0.00	0.00	10.0	16.4	05/31/73		40.0		
D-1 LOWEST	951	M	?	0.01	0.14	14.0	19.3	12/19/72		45.4		
D-1 LOWEST	1008	M	?	0.01	0.15	13.5	19.6	01/18/73		44.4		
D-1 LOWEST	1193	F	?	0.01	0.16	12.5	19.8	04/18/74		29.4		
D-1 LOWEST	1095	F	?	0.02	0.19	10.5	16.6	05/31/73		40.0		

* INDICATES AGE IN MONTHS SINCE BIRTH, ALL OTHER AGES ARE IN MONTHS SINCE EXPOSURE

DOSE-EFFECT STUDIES WITH INHALED PU-238 OXIDE IN BEAGLES

DOSE GROUP	DOG NUMBER	SEX	INITIAL ALVEOLAR DEPOSITION NCI	NCI/G LUNG	NCI/KG	INHALATION EXPOSURE WEIGHT (KG)	AGE* (MO)	DATE	DATE OF DEATH	MONTHS SINCE INHALATION 09/30/76	MONTHS SINCE INHALATION DEATH	COMMENTS ON DEAD DOGS
D-1 LOWEST	959	M	3	0.02	0.22	13.5	19.2	12/19/72		45.4		
D-1 LOWEST	1060	F	2	0.02	0.24	8.5	18.1	05/31/73		40.0		
D-1 LOWEST	921	F	3	0.03	0.31	10.0	19.5	11/30/72	12/27/72		0.9	SACRIFICED
D-1 LOWEST	989	F	3	0.03	0.32	9.5	18.8	12/19/72		45.4		
D-1 LOWEST	923	F	3	0.03	0.35	8.5	19.5	11/30/72	01/26/73		1.9	SACRIFICED
D-1 LOWEST	925	M	5	0.04	0.40	12.5	19.5	11/30/72	02/27/73		2.9	SACRIFICED
D-1 LOWEST	1204	M	6	0.04	0.43	14.0	17.7	02/26/74		31.1		
D-1 LOWEST	993	F	6	0.04	0.46	13.0	18.8	12/19/72		45.4		
D-1 LOWEST	1106	F	5	0.05	0.50	10.0	16.4	05/31/73		40.0		
D-1 LOWEST	970	F	6	0.05	0.55	11.0	19.2	12/19/72		45.4		
D-2 LOW	1065	F	6	0.05	0.60	10.0	18.3	05/31/73		40.0		
D-2 LOW	1083	M	11	0.06	0.69	16.0	18.0	05/31/73		40.0		
D-2 LOW	1183	M	11	0.06	0.71	15.5	16.4	02/26/74		31.1		
D-2 LOW	1081	M	13	0.07	0.74	17.5	17.5	05/31/73		40.0		
D-2 LOW	1090	F	10	0.10	1.05	9.5	17.3	05/31/73		40.0		
D-2 LOW	1222	M	15	0.10	1.11	13.5	19.0	04/18/74		29.4		
D-2 LOW	999	F	11	0.11	1.16	9.5	18.7	12/19/72		45.4		
D-2 LOW	1220	M	16	0.11	1.23	13.0	16.8	02/26/74		31.1		
D-2 LOW	971	F	13	0.11	1.24	10.5	19.2	12/19/72		45.4		
D-2 LOW	1074	M	22	0.11	1.26	17.5	18.1	05/31/73		40.0		
D-2 LOW	1219	M	17	0.12	1.36	12.5	19.3	04/18/74	05/12/75		12.8	SACRIFICED
D-2 LOW	1038	F	16	0.13	1.45	11.0	18.2	02/22/73		43.2		
D-2 LOW	955	M	17	0.14	1.55	11.0	19.2	12/19/72		45.4		
D-2 LOW	1216	M	23	0.16	1.77	13.0	19.0	04/09/74		29.7		
D-2 LOW	1033	M	17	0.17	1.89	9.0	19.1	02/22/73		43.2		
D-2 LOW	1060	F	22	0.18	2.00	11.0	17.8	02/22/73		43.2		
D-2 LOW	981	M	30	0.22	2.40	12.5	19.0	12/19/72		45.4		
D-2 LOW	1074	F	29	0.22	2.42	12.0	18.0	05/31/73		40.0		
D-2 LOW	1050	F	22	0.22	2.44	9.0	18.1	02/22/73		43.2		
D-2 LOW	1046	M	27	0.22	2.45	11.0	18.1	02/22/73		43.2		
D-2 LOW	1207	F	22	0.24	2.59	8.5	17.6	02/26/74		31.1		
D-2 LOW	1196	F	28	0.25	2.80	10.0	17.9	02/26/74		31.1		
D-2 LOW	1180	M	38	0.26	2.91	13.5	20.0	04/18/74		29.4		
D-2 LOW	930	M	38	0.27	2.92	13.0	19.2	11/30/72	12/28/72		0.9	SACRIFICED
D-3 MED-LOW	1066	M	54	0.31	3.38	16.0	18.3	05/31/73		40.0		
D-3 MED-LOW	1089	F	41	0.31	3.42	12.0	17.3	05/31/73		40.0		
D-3 MED-LOW	972	F	40	0.33	3.64	11.0	19.2	12/19/72		45.4		
D-3 MED-LOW	1410	M	54	0.34	3.72	14.5	18.5	03/04/75		18.9		
D-3 MED-LOW	1313	M	58	0.34	3.74	15.5	18.5	03/04/75		18.9		
D-3 MED-LOW	1311	M	54	0.36	4.00	13.5	18.5	03/04/75		18.9		
D-3 MED-LOW	1219	F	46	0.40	4.38	10.5	19.0	04/18/74		29.4		
D-3 MED-LOW	1317	M	72	0.41	4.50	16.0	18.1	03/04/75		18.9		
D-3 MED-LOW	1158	M	73	0.43	4.71	15.5	17.7	11/06/73		34.8		

* INDICATES AGE IN MONTHS SINCE BIRTH, ALL OTHER AGES ARE IN MONTHS SINCE EXPOSURE

DOSE-EFFECT STUDIES WITH INHALED PU-238 OXIDE IN BEAGLES

DOSE GROUP	DOG NUMBER	SEX	INITIAL ALVEOLAR DEPOSITION: NCI	NCI/G LUNG	NCI/KG	INHALATION EXPOSURE: WEIGHT (KG)	AGE* (MO)	DATE	DATE OF DEATH	MONTHS SINCE INHALATION: 09/30/76	DEATH	COMMENTS ON DEAD DOGS
D-3 MED-LOW	1165	M	76	0.43	4.75	16.0	17.3	11/06/73		34.8		
D-3 MED-LOW	1309	M	60	0.44	4.80	12.5	18.5	03/04/75		18.9		
D-3 MED-LOW	1318	M	67	0.45	4.96	13.5	18.1	03/04/75	03/08/76		12.2	SACRIFICED
D-3 MED-LOW	929	F	41	0.50	5.47	7.5	19.2	11/30/72	01/25/73		1.8	SACRIFICED
D-3 MED-LOW	1316	M	84	0.53	5.79	14.5	18.1	03/04/75		18.9		
D-3 MED-LOW	960	M	68	0.54	5.91	11.5	19.2	12/19/72		45.4		
D-3 MED-LOW	1190	F	71	0.54	5.92	12.0	18.1	02/26/74		31.1		
D-3 MED-LOW	1072	M	98	0.54	5.94	16.5	18.1	05/31/73		40.0		
D-3 MED-LOW	926	M	75	0.55	6.00	12.5	19.5	11/30/72	02/28/73		3.0	SACRIFICED
D-3 MED-LOW	1315	M	90	0.55	6.00	15.0	18.1	03/04/75		18.9		
D-3 MED-LOW	982	M	76	0.58	6.33	12.0	19.0	12/19/72		45.4		
D-3 MED-LOW	1040	M	84	0.64	7.00	12.0	18.2	02/22/73		43.2		
D-3 MED-LOW	1059	F	71	0.65	7.10	10.0	17.8	02/22/73		43.2		
D-3 MED-LOW	1319	M	99	0.67	7.33	13.5	18.1	03/04/75	03/09/76		12.2	SACRIFICED
D-3 MED-LOW	1108	F	84	0.69	7.64	11.0	16.4	05/31/73		40.0		
D-3 MED-LOW	1056	M	97	0.71	7.76	12.5	17.9	02/22/73		43.2		
D-3 MED-LOW	1000	F	70	0.71	7.78	9.0	18.7	12/19/72		45.4		
D-3 MED-LOW	1000	M	116	0.73	8.00	14.5	19.6	01/18/73		44.4		
D-3 MED-LOW	1026	M	116	0.78	8.59	13.5	19.2	01/18/73		44.4		
D-3 MED-LOW	1043	F	98	0.89	9.80	10.0	18.1	02/22/73		43.2		
D-3 MED-LOW	1031	F	76	0.92	10.13	7.5	19.1	02/22/73		43.2		
D-3 MED-LOW	1212	F	111	1.12	12.33	9.0	17.6	02/26/74		31.1		
D-4 MEDIUM	1176	M	129	0.87	9.56	13.5	16.6	11/06/73		34.8		
D-4 MEDIUM	1221	F	124	1.13	12.40	10.0	19.0	04/18/74		29.4		
D-4 MEDIUM	1195	M	228	1.38	15.20	15.0	18.1	02/26/74		31.1		
D-4 MEDIUM	1032	M	162	1.40	15.43	10.5	16.3	11/30/72	12/08/72		0.3	SACRIFICED
D-4 MEDIUM	1053	F	148	1.42	15.58	9.5	17.9	02/22/73		43.2		
D-4 MEDIUM	997	M	203	1.60	17.65	11.5	19.6	01/18/73		44.4		
D-4 MEDIUM	991	F	198	1.76	19.40	10.0	18.8	12/19/72		45.4		
D-4 MEDIUM	1177	M	262	1.76	19.41	13.5	16.6	11/06/73		34.8		
D-4 MEDIUM	932	F	216	1.79	19.64	11.0	19.1	11/30/72	01/25/73		1.8	SACRIFICED
D-4 MEDIUM	1103	F	260	1.89	20.80	12.5	16.5	05/31/73		40.0		
D-4 MEDIUM	973	F	271	2.20	24.64	11.0	19.2	12/19/72		45.4		
D-4 MEDIUM	931	F	289	2.39	26.27	11.0	19.1	11/30/72	12/28/72		0.9	SACRIFICED
D-4 MEDIUM	1091	F	243	2.60	28.59	8.5	17.3	05/31/73		40.0		
D-4 MEDIUM	1114	M	430	2.70	29.66	14.5	16.4	05/31/73		40.0		
D-4 MEDIUM	1062	M	435	2.93	32.22	13.5	17.8	02/22/73		43.2		
D-4 MEDIUM	934	M	454	3.06	33.63	13.5	19.1	11/30/72	03/01/73		3.0	SACRIFICED
D-4 MEDIUM	1081	M	501	3.07	33.81	16.0	18.0	05/31/73		40.0		
D-4 MEDIUM	1030	F	340	3.25	35.79	9.5	19.1	02/22/73		43.2		
D-4 MEDIUM	952	F	365	3.49	38.42	9.5	19.2	12/19/72		45.4		
D-4 MEDIUM	1193	M	539	3.50	38.50	14.0	17.9	02/26/74		31.1		
D-4 MEDIUM	1166	M	673	4.08	44.87	15.0	17.3	11/06/73		34.8		

* INDICATES AGE IN MONTHS SINCE BIRTH, ALL OTHER AGES ARE IN MONTHS SINCE EXPOSURE

DOSE-EFFECT STUDIES WITH INHALED PU-238 OXIDE IN BEAGLES

DOSE GROUP	DOG NUMBER	SEX	INITIAL ALVEOLAR DEPOSITION NCI	NCI/G LUNG	NCI/ KG	INHALATION EXPOSURE WEIGHT (KG)	AGE* (MO)	DATE	DATE OF DEATH	MONTHS SINCE INHALATION 09/30/76	DEATH	COMMENTS ON DEAD DOGS
D-4 MEDIUM	1220	F	518	4.28	47.09	11.0	19.0	04/18/74		29.4		
D-4 MEDIUM	992	F	555	4.59	50.45	11.0	18.8	12/19/72		45.4		
D-4 MEDIUM	983	M	617	4.67	51.42	12.0	19.0	12/19/72		45.4		
D-5 MED-HI	1191	F	591	4.30	47.28	12.5	19.8	04/18/74		29.4		
D-5 MED-HI	1157	M	700	4.71	51.85	13.5	17.7	11/06/73		34.8		
D-5 MED-HI	1035	F	571	5.46	60.11	9.5	18.2	02/22/73		43.2		
D-5 MED-HI	1192	F	754	6.23	68.55	11.0	18.1	02/26/74		31.1		
D-5 MED-HI	1140	M	1014	6.58	72.43	14.0	18.2	11/06/73		34.8		
D-5 MED-HI	1071	M	1269	6.79	74.65	17.0	18.1	05/31/73		40.0		
D-5 MED-HI	1173	M	1023	7.75	85.25	12.0	17.3	11/06/73		34.8		
D-5 MED-HI	1174	M	1125	8.52	93.75	12.0	16.6	11/06/73		34.8		
D-5 MED-HI	1047	M	900	8.41	94.74	9.5	18.1	02/22/73		43.2		
D-5 MED-HI	1109	F	1119	8.85	97.30	11.5	16.4	05/31/73		40.0		
D-5 MED-HI	1160	F	1344	9.77	107.52	12.5	17.3	11/06/73		34.8		
D-5 MED-HI	1211	M	1764	11.06	121.66	14.5	17.6	02/26/74		31.1		
D-5 MED-HI	1096	F	1476	12.20	134.18	11.0	16.0	05/11/73		40.7		
D-5 MED-HI	1214	F	1710	12.95	142.50	12.0	17.3	02/26/74		31.1		
D-5 MED-HI	1092	M	1848	13.44	147.84	12.5	17.3	05/31/73		40.0		
D-5 MED-HI	1027	M	2148	13.95	153.43	14.0	19.2	01/18/73		44.4		
D-5 MED-HI	1115	F	1885	14.90	163.91	11.5	16.1	05/31/73		40.0		
D-5 MED-HI	971	F	1718	15.62	171.80	10.0	20.2	01/18/73		44.4		
D-5 MED-HI	1079	M	2620	15.88	174.67	15.0	18.0	05/31/73		40.0		
D-5 MED-HI	1053	F	1907	16.51	181.62	10.5	17.8	02/22/73		43.2		
D-6 HIGH	1002	M	2907	18.88	207.64	14.0	19.6	01/18/73		44.4		
D-6 HIGH	1057	M	3116	20.98	230.81	13.5	17.9	02/22/73		43.2		
D-6 HIGH	1009	M	3630	26.40	290.40	12.5	19.6	01/18/73		44.4		
D-6 HIGH	1042	F	2959	28.32	311.47	9.5	18.1	02/22/73		43.2		
D-6 HIGH	994	F	3453	31.39	345.30	10.0	19.6	01/18/73	07/04/76		41.5	PROCESSING
D-6 HIGH	1006	F	3810	31.40	346.36	11.0	19.6	01/18/73		44.4		
D-6 HIGH	975	F	3968	36.07	396.80	10.0	20.2	01/18/73		44.4		
D-6 HIGH	1037	M	4954	44.13	485.40	10.0	18.2	02/22/73		43.2		
D-6 HIGH	1144	M	7691	53.78	591.62	13.0	18.2	11/06/73		34.8		
D-6 HIGH	1025	M	8479	57.10	628.07	13.5	19.2	01/18/73		44.4		
D-6 HIGH	1064	M	9453	63.66	700.22	13.5	16.7	01/18/73		44.4		
D-6 HIGH	1162	F	6959	70.29	773.22	9.0	17.3	11/06/73		34.8		
D-6 HIGH	1175	F	6201	75.16	826.80	7.5	16.6	11/06/73		34.8		

* INDICATES AGE IN MONTHS SINCE BIRTH, ALL OTHER AGES ARE IN MONTHS SINCE EXPOSURE

LOW LEVEL PU-239 NITRATE INHALATION STUDIES

DOSE GROUP	DOG NUMBER	SEX	INITIAL ALVEOLAR DEPOSITION NCI	NCI/G LUNG	NCI/KG	INHALATION EXPOSURE WEIGHT (KG)	AGE* (MO)	DATE	DATE OF DEATH	MONTHS SINCE INHALATION 09/30/76	DEATH	COMMENTS ON DEAD DOGS
CONTROL	1543	M	0	0.00	0.00					22.9*		
CONTROL	1528	F	0	0.00	0.00					23.1*		
CONTROL	1526	M	0	0.00	0.00					23.6*		
CONTROL	1525	M	0	0.00	0.00					23.6*		
CONTROL	1516	F	0	0.00	0.00					23.9*		
CONTROL	1509	M	0	0.00	0.00					24.1*		
CONTROL	1483	F	0	0.00	0.00					24.9*		
CONTROL	1455	F	0	0.00	0.00					25.9*		
CONTROL	1450	F	0	0.00	0.00					26.3*		
CONTROL	1425	M	0	0.00	0.00					26.5*		
CONTROL	1418	M	0	0.00	0.00					26.5*		
CONTROL	1409	M	0	0.00	0.00					26.8*		
CONTROL	1405	M	0	0.00	0.00					26.9*		
CONTROL	1393	M	0	0.00	0.00					27.3*		
CONTROL	1388	M	0	0.00	0.00					27.3*		
CONTROL	1376	F	0	0.00	0.00					27.5*		
CONTROL	1365	M	0	0.00	0.00					28.6*		
CONTROL	1356	M	0	0.00	0.00					28.7*		
VEHICLE	1542	M	0	0.00	0.00	12.0	20.8	07/27/76		2.1		
VEHICLE	1531	F	0	0.00	0.00	9.0	20.9	07/27/76		2.1		
VEHICLE	1524	M	0	0.00	0.00	12.0	21.5	07/27/76		2.1		
VEHICLE	1514	M	0	0.00	0.00	14.0	20.9	06/23/76		3.3		
VEHICLE	1504	F	0	0.00	0.00	10.0	20.9	06/23/76		3.3		
VEHICLE	1491	F	0	0.00	0.00	8.5	21.6	06/23/76		3.3		
VEHICLE	1457	F	0	0.00	0.00	12.0	20.6	04/22/76		5.3		
VEHICLE	1421	M	0	0.00	0.00	13.0	23.3	06/23/76		3.3		
VEHICLE	1412	F	0	0.00	0.00	9.0	19.0	02/13/76		7.6		
VEHICLE	1406	M	0	0.00	0.00	15.0	21.6	04/22/76		5.3		
VEHICLE	1392	M	0	0.00	0.00	12.5	22.0	04/22/76		5.3		
VEHICLE	1381	F	0	0.00	0.00	8.5	19.8	02/13/76		7.6		
VEHICLE	1361	M	0	0.00	0.00	15.0	21.0	02/13/76		7.6		
D-1 LOWEST	1515	M	1	0.01	0.07	13.5	19.8	05/20/76		4.4		
D-1 LOWEST	1507	M	1	0.01	0.07	14.5	19.8	05/20/76		4.4		
D-1 LOWEST	1519	M	1	0.01	0.08	12.5	19.5	05/20/76		4.4		
D-1 LOWEST	1501	M	1	0.01	0.08	12.5	20.4	05/20/76		4.4		
D-1 LOWEST	1487	F	1	0.01	0.08	13.0	20.5	05/20/76		4.4		
D-1 LOWEST	1465	F	1	0.01	0.08	12.5	21.0	05/20/76		4.4		
D-1 LOWEST	1416	M	1	0.01	0.08	12.0	22.1	05/20/76		4.4		
D-1 LOWEST	1470	F	1	0.01	0.10	10.5	21.0	05/20/76		4.4		
D-1 LOWEST	1458	F	1	0.01	0.10	10.0	21.5	05/20/76		4.4		
D-1 LOWEST	1489	F	1	0.01	0.12	8.5	20.5	05/20/76		4.4		
D-1 LOWEST	1339	F	2	0.02	0.22	9.0	17.5	10/16/75	11/13/75		0.9	SACRIFICED
D-1 LOWEST	1335	M	5	0.04	0.43	11.5	18.0	10/16/75	11/13/75		0.9	SACRIFICED

* INDICATES AGE IN MONTHS SINCE BIRTH, ALL OTHER AGES ARE IN MONTHS SINCE EXPOSURE

LOW LEVEL Pu-239 NITRATE INHALATION STUDIES

DOSE GROUP	DOG NUMBER	SEX	INITIAL ALVEOLAR DEPOSITION: NCI	NCI/G LUNG	NCI/KG	INHALATION EXPOSURE: WEIGHT (KG)	AGE* (MO)	DATE	DATE OF DEATH	MONTHS SINCE INHALATION: 09/30/76	DEATH	COMMENTS ON DEAD DOGS
D-1 LOWEST	1351	M	7	0.06	0.64	11.0	17.2	10/16/75	11/13/75		0.9	SACRIFICED
D-2 LOW	1517	M	1	0.01	0.08	12.0	19.8	05/20/76		4.4		
D-2 LOW	1520	M	1	0.01	0.10	10.5	19.5	05/20/76		4.4		
D-2 LOW	1415	M	2	0.02	0.17	11.5	22.2	05/20/76		4.4		
D-2 LOW	1465	F	5	0.03	0.37	13.5	21.0	05/20/76		4.4		
D-2 LOW	1423	M	10	0.06	0.91	11.0	22.1	05/20/76		4.4		
D-2 LOW	1417	M	11	0.08	0.92	12.0	22.1	05/20/76		4.4		
D-2 LOW	1563	F	9	0.09	1.00	9.0	19.8	05/20/76		4.4		
D-2 LOW	1472	F	10	0.10	1.05	9.5	21.0	05/20/76		4.4		
D-2 LOW	1484	F	11	0.10	1.10	10.0	20.5	05/20/76		4.4		
D-2 LOW	1498	F	16	0.15	1.60	10.0	20.5	05/20/76		4.4		
D-3 MED-LOW	1336	M	20	0.13	1.48	13.5	18.0	10/16/75	11/13/75		0.9	SACRIFICED
D-3 MED-LOW	1341	F	18	0.16	1.71	10.5	17.2	10/16/75	11/13/75		0.9	SACRIFICED
D-3 MED-LOW	1395	M	54	0.21	2.34	14.5	22.0	04/20/76		5.4		
D-3 MED-LOW	1433	M	26	0.23	2.48	10.5	21.9	04/20/76	05/04/76		0.5	SACRIFICED
D-3 MED-LOW	1405	F	33	0.23	2.54	13.0	21.0	04/20/76	05/05/76		0.5	SACRIFICED
D-3 MED-LOW	1413	F	29	0.24	2.64	11.0	18.2	01/20/76		8.3		
D-3 MED-LOW	1390	M	42	0.29	3.23	13.0	21.9	04/20/76	05/04/76		0.5	SACRIFICED
D-3 MED-LOW	1391	M	53	0.30	3.31	16.0	21.9	04/20/76		5.4		
D-3 MED-LOW	1541	M	54	0.31	3.38	16.0	20.7	07/22/76		2.3		
D-3 MED-LOW	1459	M	50	0.32	3.57	14.0	20.2	01/20/76	01/23/76		0.1	SACRIFICED
D-3 MED-LOW	1529	F	43	0.37	4.10	10.5	20.8	07/22/76		2.3		
D-3 MED-LOW	1434	F	41	0.37	4.16	10.0	17.2	10/16/75	11/14/75		1.0	SACRIFICED
D-3 MED-LOW	1375	F	50	0.40	4.35	11.5	19.1	01/20/76	01/23/76		0.1	SACRIFICED
D-3 MED-LOW	1434	F	52	0.41	4.52	11.5	21.0	04/20/76		5.4		
D-3 MED-LOW	1380	M	62	0.42	4.59	13.5	19.1	01/20/76		8.3		
D-3 MED-LOW	1406	F	53	0.42	4.67	10.5	21.0	04/20/76		5.4		
D-3 MED-LOW	1531	M	65	0.45	5.00	13.0	20.7	07/22/76		2.3		
D-3 MED-LOW	1523	F	55	0.45	5.00	11.0	21.3	07/22/76		2.3		
D-3 MED-LOW	1407	F	50	0.51	5.56	9.0	18.5	01/20/76	01/23/76		0.1	SACRIFICED
D-3 MED-LOW	1427	F	57	0.61	6.70	10.0	21.1	04/20/76		5.4		
D-3 MED-LOW	1522	F	78	0.71	7.80	10.0	21.3	07/22/76		2.3		
D-3 MED-LOW	1382	M	84	0.73	8.00	10.5	20.2	01/20/76		8.3		
D-3 MED-LOW	1454	F	60	0.78	8.57	7.0	20.5	04/20/76		5.4		
D-3 MED-LOW	1530	F	72	0.82	9.00	8.0	20.8	07/22/76		2.3		
D-3 MED-LOW	1423	F	97	1.10	12.13	8.0	18.1	01/20/76		8.3		
D-4 MEDIUM	1404	M	252	1.43	15.75	16.0	21.5	04/20/76		5.4		
D-4 MEDIUM	1521	F	205	1.62	17.83	11.5	21.3	07/22/76		2.3		
D-4 MEDIUM	1470	M	273	1.65	18.20	15.0	19.1	01/20/76		8.3		
D-4 MEDIUM	1362	M	245	1.77	19.48	13.5	20.2	01/20/76		8.3		
D-4 MEDIUM	1535	M	294	2.14	23.52	12.5	20.8	07/22/76		2.3		
D-4 MEDIUM	1395	M	364	2.21	24.27	15.0	19.0	01/20/76		8.3		
D-4 MEDIUM	1411	F	228	2.59	28.50	8.0	18.2	01/20/76		8.3		

* INDICATES AGE IN MONTHS SINCE BIRTH, ALL OTHER AGES ARE IN MONTHS SINCE EXPOSURE

LOW LEVEL PU-239 NITRATE INHALATION STUDIES

DOSE GROUP	DOG NUMBER	SEX	INITIAL ALVEOLAR DEPOSITION NCI	NCI/G LUNG	NCI/ KG	INHALATION EXPOSURE WEIGHT (KG)	AGE* (MO)	DATE	DATE OF DEATH	MONTHS SINCE INHALATION 09/30/76	DEATH	COMMENTS ON DEAD DOGS
D-4 MEDIUM	1408	F	323	2.94	32.30	10.0	18.5	01/20/76		8.3		
D-4 MEDIUM	1535	F	344	3.13	34.40	10.0	20.7	07/22/76		2.3		
D-4 MEDIUM	1364	M	453	3.17	34.85	13.0	20.2	01/20/76		8.3		
D-4 MEDIUM	1428	F	373	3.23	35.52	10.5	21.1	04/20/76		5.4		
D-4 MEDIUM	1446	F	348	3.33	36.63	9.5	21.0	04/20/76		5.4		
D-4 MEDIUM	1387	F	339	4.40	48.43	7.0	19.0	01/20/76		8.3		
D-5 MED-HI	1329	F	395	3.59	39.50	10.0	18.0	10/16/75	11/14/75		1.0	SACRIFICED
D-5 MED-HI	1346	M	649	4.37	48.07	13.5	17.2	10/16/75	11/14/75		1.0	SACRIFICED
D-5 MED-HI	1347	F	681	6.88	75.67	9.0	17.2	10/16/75	11/14/75		1.0	SACRIFICED
D-5 MED-HI	1429	M	1376	9.62	105.85	13.0	23.2	06/23/76		3.3		
D-5 MED-HI	1512	M	2400	14.55	160.00	15.0	20.9	06/23/76		3.3		
D-5 MED-HI	1419	M	1559	14.92	164.11	9.5	23.3	06/23/76		3.3		
D-5 MED-HI	1498	F	2009	16.60	182.64	11.0	21.5	06/23/76		3.3		
D-5 MED-HI	1506	M	2645	17.18	188.93	14.0	20.9	06/23/76		3.3		
D-5 MED-HI	1502	F	3008	21.03	231.38	13.0	20.9	06/23/76		3.3		
D-5 MED-HI	1485	F	2320	21.09	232.00	10.0	21.7	06/23/76		3.3		
D-5 MED-HI	1471	F	2508	21.71	238.86	10.5	22.1	06/23/76		3.3		
D-5 MED-HI	1492	F	2463	24.88	273.67	9.0	21.6	06/23/76		3.3		
D-5 MED-HI	1459	F	2645	26.72	293.89	9.0	22.6	06/23/76		3.3		
D-6 HIGH	1518	M	3550	29.34	322.73	11.0	20.6	06/23/76		3.3		
D-6 HIGH	1420	M	3840	30.36	333.91	11.5	23.3	06/23/76		3.3		
D-6 HIGH	1517	F	5186	52.38	576.22	9.0	20.6	06/23/76		3.3		
D-6 HIGH	1510	F	6969	55.09	606.00	11.5	20.9	06/23/76		3.3		
D-6 HIGH	1424	M	7680	69.82	768.00	10.0	23.2	06/23/76		3.3		

* INDICATES AGE IN MONTHS SINCE BIRTH, ALL OTHER AGES ARE IN MONTHS SINCE EXPOSURE

PUBLICATIONS AND PRESENTATIONS

1976 BIOLOGY DEPARTMENT PUBLICATIONS

Reprints may be requested from the author at the address shown below[a], except for those articles marked with an asterisk, which are no longer available.

*Bair, W. J. 1976. Description of the hot particle issue and concluding comments. Radiat. Res. 67:582-583. (Abstract)

Bair, W. J. and J. M. Thomas. 1976. Prediction of the health effects of inhaled transuranium elements from experimental animal data, pp. 569-585. In: Transuranium Nuclides in the Environment, IAEA, Vienna.

Bair, W. J. 1976. Recent animal studies on the deposition, retention and translocation of plutonium and other transuranic compounds, pp. 51-97. In: Diagnosis and Treatment of Incorporated Radionuclides, IAEA, Vienna.

*Bair, W. J., Chairman of the Writing Committee. 1976. Health Effects of Alpha-Emitting Particles in the Respiratory Tract. Report of Ad Hoc Committee on "Hot Particles" of the Advisory Committee on the Biological Effects of Ionizing Radiation, National Academy of Sciences/National Research Council, Washington, D.C.

*Ballou, J. E. (Ed.). 1976. Radiation and the Lymphatic System. 14th Annual Hanford Biology Symposium, Battelle, Pacific Northwest Laboratories, Richland, WA. (CONF-740930). NTIS, Springfield, VA.

*Ballou, J. E., G. E. Dagle, K. E. McDonald, and R. L. Buschbom. 1975. Influence of inhaled Ca-DTPA on the long-term effects of inhaled Pu nitrate. Health Phys. 29:921. (Abstract)

*Ballou, J. E. 1975. Effect of ventilation variables on breath thoron output, pp. 520-526. In: Noble Gases, R. E. Stanley and A. A. Moghissi (eds.). (CONF-730915). NTIS, Springfield, VA.

*Beamer, J. L., J. M. Malin, G. W. R. Endres, F. T. Cross, and M. F. Sullivan. 1976. Ureteral dosimetry of swine exposed to intracervical irradiation. Radiat. Res. 67:558. (Abstract)

*Bistline, R. W., J. L. Lebel, and G. E. Dagle. 1976. Translocation dynamics of $Pu(NO_3)_4$ and PuO_2 from puncture wounds to lymph nodes and major organs of beagles, pp. 10-18. In: Radiation and the Lymphatic System, J. E. Ballou (ed.). (CONF-740930) NTIS, Springfield, VA.

Cataldo, D. A., E. L. Klepper, and D. K. Craig. 1976. Fate of plutonium intercepted by leaf surfaces: leachability and translocation to seed and root tissues, pp. 291-301. In: Transuranium Nuclides in the Environment, IAEA, Vienna.

Craig, D. K., J. F. Park, and J. L. Ryan. 1976. Effect of physicochemical properties on metabolism of transuranium oxide inhaled by beagle dogs, pp. 429-445. In: Aerosole in Naturwissenschaft, Medizin und Technik Chemie der Umweltaerosole, V. Bohlau and H. Straubel (eds.). Annual Congress, 1975 of (GAF) Gesellschaft fur Aersol-forschung, e.V., Bad Soden, W. Germany.

*Craig, D. K., B. L. Klepper, and R. L. Buschbom. 1976. Deposition of various plutonium-compound aerosols onto plant foliage at very low wind velocities, pp. 244-263. In: Atmosphere-Surface Exchange of Particulate and Gaseous Pollutants 1974, R. J. Engelmann and G. A. Sehmel (eds.). (CONF-740921). NTIS, Springfield, VA.

Craig, D. K., W. C. Cannon, R. E. Filipy, G. J. Powers, and P. J. Dionne. 1976. SNS Source Term Evaluation Program, BNWL-1971, Battelle-Northwest, Richland, WA.

*Craig, D. K., J. R. Decker, and R. L. Buschbom. 1975. Disposition of highly toxic radioactive aerosol inhaled by beagle dogs. Health Phys. 29:919. (Abstract)

*Dagle, G. E., J. E. Lund, and J. F. Park. 1976. Pulmonary lesions induced by inhaled plutonium in beagles, pp. 161-168. In: The Health Effects of Plutonium & Radium, W. S. S. Jee (ed.). The J. W. Press, Salt Lake City, UT.

*Dagle, G. E. and J. F. Park. 1976. Plutonium-induced lymphadenitis in beagles, pp. 239-245. In: Radiation and the Lymphatic System, J. E. Ballou (ed.). (CONF-740930). NTIS, Springfield, VA.

*Frazier, M. E., L. P. Mallavia, and F. Akiya. 1976. DNA polymerase activity in tissues from miniature swine chronically exposed to ^{90}Sr. Radiat. Res. 67:530. (Abstract)

*Frazier, M. E., J. F. Park, W. S. S. Jee, and G. Taylor. 1976. RNA-instructed DNA polymerase activity in radiation-induced osteosarcomas, pp. 707-716. In: The Health Effects of Plutonium & Radium, W. S. S. Jee (ed.). The J. W. Press, Salt Lake City, UT.

[a] Battelle, Pacific Northwest Laboratory, P.O. Box 999, Richland, WA 99352

*Frazier, M. E., J. E. Lund, and R. H. Busch. 1976. In vitro interactions of lymphocytes and cultured cells from beagles with plutonium-induced bone tumors, pp. 197-202. In: Radiation and the Lymphatic System, J. E. Ballou (ed.). (CONF-740930). NTIS, Springfield, VA.

*Gruber, H. 1976. X-ray and proton-induced ultrastructural changes in Chlamydomonas reinhardi. Radiat. Res. 67:565. (Abstract)

*Hampton, J. C., H. Drucker, L. C. Neil, and J. T. Cresto. 1976. Intracellular localization of ^{35}S-WR2721 in mice. Radiat. Res. 67:640-641. (Abstract)

*Hungate, F. P., W. F. Riemath, L. R. Bunnell, and M. F. Gillis. 1976. Chronic blood irradiation: a new approach, pp. 149-152. In: Radiation and the Lymphatic System, J. E. Ballou (ed.). (CONF-740930). NTIS, Springfield, VA.

Klepper, B. and D. K. Craig. 1976. Deposition of airborne particulates onto plant leaves. J. Environ. Qual. 4:495-499.

*Lebel, J. L., R. W. Bistline, J. A. Schallberger, G. E. Dagle, and L. S. Gomez. 1976. Studies of plutonium and the lymphatic system: six years of progress at Colorado State University, pp. 2-9. In: Radiation and the Lymphatic System, J. E. Ballou (ed.). (CONF-740930). NTIS, Springfield, VA.

*Mahlum, D. D. and M. R. Sikov. 1976. Alteration of ^{239}Pu metabolism by pregnancy and lactation. Radiat. Res. 67:520. (Abstract)

*Mahlum, D. D., M. R. Sikov, and F. P. Hungate. 1976. Influence of temporal distribution of alpha dose in bone tumor incidence, pp. 49-56. In: The Health Effects of Plutonium & Radium, W. S. S. Jee (ed.). The J. W. Press, Salt Lake City, UT.

Mahlum, D. D. 1976. Biomagnetic effects: A consideration in fusion reactor development, BNWL-1973, Battelle-Northwest, Richland, WA.

*Palmer, R. F., B. O. Stuart, and R. E. Filipy. 1975. Biological effects of daily inhalation of radon and its short-lived daughters in experimental animals, pp. 507-519. In: Noble Gases, R. E. Stanley and A. A. Moghissi (eds.). (CONF-730915). NTIS, Springfield, VA.

Park, J. F., J. E. Lund, H. A. Ragan, P. L. Hackett, and M. E. Frazier. 1976. Bone tumors induced by inhalation of $^{238}PuO_2$ in dogs, pp. 17-35. In: Recent Results in Cancer Research, Vol. 54, E. Grundmann (ed.). Springer-Verlag, Berlin, Heidelberg.

Phalen, R. F., W. C. Cannon, and D. Esparza. 1976. Comparison of impaction, centrifugal separation and electron microscopy for sizing cigarette smoke, pp. 731-737. In: Fine Particles Aerosol Generation, Measurement, Sampling, and Analysis, B. Y. H. Liu (ed.). Academic Press, NY.

Ragan, H. A., P. L. Hackett, and G. E. Dagle. 1976. Acute myelomonocytic leukemia manifested as myelophthisic anemia in a dog. J. Am. Vet. Med. Assoc. 169:421-425.

*Ragan, H. A., J. F. Park, R. J. Olson, and R. L. Buschbom. 1976. Lymphocytopenia induced in beagle dogs by inhalation of $^{239}PuO_2$, pp. 100-105. In: Radiation and the Lymphatic System, J. E. Ballou (ed.). (CONF-740930). NTIS, Springfield, VA.

*Ragan, H. A. 1976. Effects of chronic cigarette smoking on platelet function and coagulation in beagles, p. 205. In: Abstracts for the 19th Annual Meeting of the American Society of Hematology, Charles B. Slack, Inc., Thorofore, NJ. (Abstract)

Sanders, C. L., G. E. Dagle, W. C. Cannon, D. K. Craig, G. J. Powers, and D. M. Meier. 1976. Inhalation carcinogenesis of high-fired $^{239}PuO_2$ in rats. Radiat. Res. 68:349-360.

*Sanders, C. L. 1976. Health implications of plutonium: inhalation carcinogenesis in rodents, p. 128. In: Proc. APHA 103rd Meeting, Chicago, Nov. 16-20, 1975. American Public Health Association, Washington, D.C. (Abstract)

*Sanders, C. L. 1976. Effects of transuranics on pulmonary lymph nodes of rodents, pp. 225-229. In: Radiation and the Lymphatic System, J. E. Ballou (ed.). (CONF-740930). NTIS, Springfield, VA.

Schaffner, T., J. Herring, H. Gerber, and H. Cottier. 1976. Bursa of Fabricius: uptake of radioactive particles and radiotoxic "sealing" of bursal follicles, pp. 33-39. In: Immune Reactivity of Lymphocytes, M. Feldman and A. Globerson (eds.). Plenum Pub. Corp., NY.

*Sikov, M. R., W. C. Cannon, and D. D. Mahlum. 1976. Comparison of the deposition and retention of inhaled $^{239}PuO_2$ in newborn and adult rats. Radiat. Res. 67:578. (Abstract)

Sikov, M. R., B. P. Hildebrand, and J. D. Stearns. 1976. Effects of exposure of the nine-day rat embryo to ultrasound, pp. 529-530. In: Ultrasound in Medicine, Vol. 2, D. White and R. Barnes (eds.). Plenum Pub. Corp., NY.

*Sikov, M. R. and D. D. Mahlum. 1976. Influence of age and physicochemical form on the effects of ^{239}Pu on the skeleton of the rat, pp. 33-48. In: The Health Effects of Plutonium & Radium, W. S. S. Jee (ed.). The J. W. Press, Salt Lake City, UT.

Smith, V. H., J. E. Ballou, J. E. Lund, G. E. Dagle, H. A. Ragan, R. H. Busch, P. L. Hackett, and D. H. Willard. 1976. Aspects of inhaled DTPA toxicity in the rat, hamster and beagle dog and treatment effectiveness for excorporation of plutonium from the rat, pp. 517-530. In: Diagnosis and Treatment of Incorporated Radionuclides. (CONF-751205) IAEA, Vienna.

*Smith, V. H., H. A. Ragan, J. E. Lund, P. L. Hackett, and D. H. Willard. 1975. The toxicity of inhaled Ca-DTPA in the beagle dog. Health Phys. 29:920-921. (Abstract)

Stuart, B. O. 1976. Selection of animal models for evaluation and inhalation hazards in man, pp. 268-288. In: Air Pollution and the Lung: Proceedings of the Twentieth Annual OHOLD Biological Conference, E. F. Ahararonson, A. Ben-David, M. A. Klingberg (eds.). John Wiley & Sons, New York.

*Sullivan, M. F. 1976. The hazard of ingested radionuclides to the newborn. Radiat. Res. 67:519-520. (Abstract)

*Swinth, K. L., J. F. Park, G. L. Voelz, and J. H. Ewins. 1976. In vivo detection of plutonium in the tracheobronchial lymph nodes with a fiber-optic coupled scintillator, pp. 59-66. In: Radiation and the Lymphatic System, J. E. Ballou (ed.). (CONF-740930). NTIS, Springfield, VA.

*Thompson, R. C. 1976. Plutonium-implications for man and his environment (Part of Panel Discussion), pp. 629-632. In: Transuranium Nuclides in the Environment, IAEA, Vienna.

Thompson, R. C. 1976. Biology of the Transuranium Elements - An Indexed Bibliography, BNWL-2056, Battelle-Northwest, Richland, WA.

Tombropoulos, E. G. and J. G. Hadley. 1976. Lipid synthesis by perfused lung. Lipids 11:491-497.

Viola, M. V., M. Frazier, P. H. Wiernik, K. B. McCredie, and S. Spiegelman. 1976. Reverse transcriptase in leukocytes of leukemic patients in remission. N. Engl. J. Med. 294:75-80.

1976 BIOLOGY DEPARTMENT PRESENTATIONS

Allen, M. D. A method for vaporizing mixed oxide fast reactor fuels for animal inhalation studies. Seminar, Civil Engineering Department, University of Washington, Seattle, WA, October 1, 1976.

Bair, W. J. Plutonium toxicology. Seminar, ERDA Nevada Operations Office staff and consultants, Las Vegas, NV, February 11, 1976.

Bair, W. J. Description of the hot particle issue and concluding comments. 24th Annual Radiation Research Society Meeting, San Francisco, CA, June 27 - July 2, 1976.

Ballou, J. E. and R. A. Gies. The excretion and early disposition of inhaled transuranic nitrates in rats. Health Physics Society Meeting, San Francisco, CA, June 27 - July 2, 1976.

Beamer, J. L., M. J. Malin, G. W. R. Endress, F. T Cross, and M. F. Sullivan. Ureteral dosimetry of swine exposed to intracervical irradiation. 24th Annual Radiation Research Society Meeting, San Francisco, CA, June 27 - July 2, 1976.

Craig, D. K., W. C. Cannon, M. D. Allen, and W. T. Kaune. New techniques for the continuous generation of vaporization-condensation aerosols from refractory materials. Ninth Aerosol Technology Meeting, Battelle-Columbus, Columbus, OH, October 21-22, 1976.

Dagle, G. E. Classification of pulmonary neoplasms. Canine Pathology Colloquium, Estes Park, CO, August 16-17, 1976.

Dagle, G. E., R. E. Filipy, R. R. Adee, and B. O. Stuart. Morphogenesis of pulmonary hyalinosis in dogs. American College of Veterinary Pathologists Meeting, Miami, FL, December 4, 1976.

Frazier, M. E. Evidence for RNA tumor virus in leukemic miniature swine. Seminar and Advanced Virology Lecture, University of Montana, Missoula, MT, May 25, 1976.

Frazier, M. E., L. P. Mallavia, and F. Akiya. DNA polymerase activity in tissues from miniature swine chronically exposed to ^{90}Sr. 24th Annual Radiation Research Society Meeting, San Francisco, CA, June 27 - July 2, 1976.

Gruber, H. X-ray and proton-induced ultrastructural changes in Chlamydomonas reinhardi. 24th Annual Radiation Research Society Meeting, San Francisco, CA, June 27 - July 2, 1976.

Hackett, P. L. and M. R. Sikov. Cross-placental transfer and embryotoxicity of lead in rats. Annual Meeting of the Society for Experimental Biology and Medicine, Portland, OR, October 30, 1976.

Hampton, J. C., H. Drucker, L. C. Neil, and J. T. Cresto. Intracellular localization of ^{35}S-WR2721 in mice. 24th Annual Radiation Research Society Meeting, San Francisco, CA, June 27 - July 2, 1976.

Hungate, F. P. Chronic blood irradiation: A new approach. Seminar, Mol Laboratory, Belgium and the Radiobiological Institute, Ryswijk, The Netherlands.

Mahlum, D. D. and M. R. Sikov. Alteration of ^{239}Pu metabolism by pregnancy and lactation. 24th Annual Radiation Research Society Meeting, San Francisco, CA, June 27 - July 2, 1976.

Park, J. F. Animal exposure methods for evaluating carcinogenicity of inhaled pollutants. Symposium on Inhalation Toxicology: Carcinogenic Testing Facilities and Test Design, Atlanta, GA, May 16-21, 1976.

Ragan, H. A., C. R. Watson, and J. F. Park. Hematologic data handling and analyses in life-span studies with beagles. American Society of Veterinary Clinical Pathologists Meeting, Cincinnati, OH, July 18-19, 1976.

Ragan, H. A. Effects of chronic cigarette smoking on platelet functions and coagulation in beagles. American Society of Hematology Meeting, Boston, MA, December 4-7, 1976.

Sanders, C. L. Inhalation carcinogenesis of transuranics. Seminar, IRTI, Albuquerque, NM, January 5-8, 1976.

Sanders, C. L. Inhalation carcinogenesis from transuranic oxides. Seminar, Biology Department, Battelle-Northwest, Richland, WA, January 20, 1976.

Sanders, C. L. Transuranic pulmonary carcinogenesis. Seminar, Harvard University, Cambridge, MA, May 19, 1976.

Sanders, C. L. and G. E. Dagle. Inhalation toxicology of $^{244}CmO_2$. Health Physics Society Meeting, San Francisco, CA, June 27 - July 2, 1976.

Sanders, C. L., R. R. Adee, K. Rhoads, and R. M. Madison. Life history of plutonium dioxide in the lung: From macrophage to carcinoma. 16th Annual Hanford Biology Symposium, Battelle-Northwest, Richland, WA, September 27-29, 1976.

Sikov, M. R., W. C. Cannon, and D. D. Mahlum. Comparison of the deposition and retention of inhaled $^{239}PuO_2$ in newborn and adult rats. 24th Annual Radiation Research Society Meeting, San Francisco, CA, June 27 - July 2, 1976.

Sikov, M. R. Embryotoxicity of ultrasound exposure at nine days gestation in the rat. Poster Presentation at 24th Annual Radiation Research Society Meeting, San Francisco, CA, June 27 - July 2, 1976.

Smith, V. H. Chelation therapy and late effects. Late Effects Colloquium, San Francisco, CA, June 27, 1976.

Stuart, B. O. Studies of the chronic inhalation of diesel engine exhaust. Seminar, University of Rochester, School of Medicine and Dentistry, Rochester, NY, July 22, 1976.

Stuart, B. O. Inhalation hazards generated by nuclear and fossil fuel energy technologies. Seminar, Massachusetts Institute of Technology, Cambridge, MA, October 25, 1976.

Sullivan, M. F., J. L. Beamer, and T. D. Mahony. The response of normal tissues to an intracavitary exposure to californium-252. International Symposium on Californium-252 Utilization, Brussels, Belgium, April 22-24, 1976.

Sullivan, M. F. The hazard of ingested radionuclides to the newborn. 24th Annual Radiation Research Society Meeting, San Francisco, CA, June 27 - July 2, 1976.

Sullivan, M. F., J. L. Beamer, T. D. Mahony, F. T. Cross, J. E. Lund, and G. W. R. Endres. The long-term effects of an intracavitary treatment with californium-252 on normal tissues. IAEA Symposium on Radiobiological Research Needed for the Improvement of Radiotherapy. Vienna, Austria, November 22-26, 1976.

Sullivan, M. F. Has the Hanford minipig provided information useful to the radiotherapist needing an implantable neutron source? Seminar, Biology Department, Battelle-Northwest, Richland, WA, December 14, 1976.

Veal, J. T. Technique for assay of nicotine and cotinine in blood and urine. Seminar, Illinois Institute of Technical Research Chicago, IL, July 20, 1976.

Wierman, E. L. and V. G. Horstman. Techniques for reducing newborn mortality rates in a beagle breeding colony. 27th Annual Session of the American Association for Laboratory Animal Science, Houston, TX, November 7-12, 1976.

Wildung, R. E. and H. Drucker. The relationship of microbial processes to the fate of transuranic elements in soil. Nevada Applied Ecology Group Symposium on the Dynamics of Transuranics in Terrestrial and Aquatic Environments, Gatlinburg, TN, October 5-7, 1976.

Wildung, R. E., H. Drucker, T. R. Garland, and R. A. Pelroy. Transformation of trace metals by soil microorganisms. ASA, CSSA, and SSSA Annual Meetings, Houston, TX, November 28 - December 3, 1976.

ORGANIZATION CHARTS

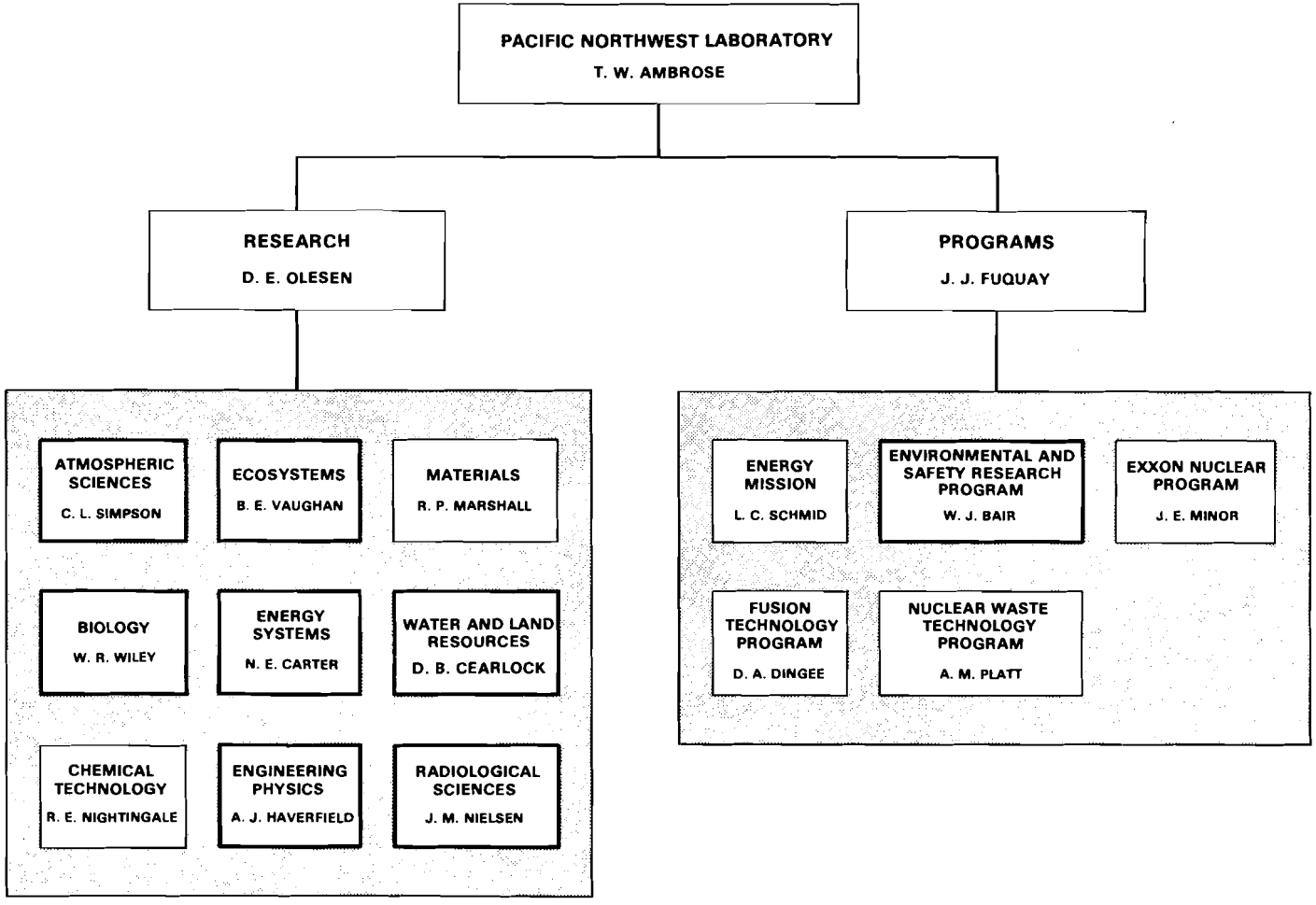
PACIFIC NORTHWEST LABORATORY
T. W. AMBROSE
RESEARCH
D. E. OLESEN
PROGRAMS
J. J. FUQUAY
ATMOSPHERIC SCIENCES
C. L. SIMPSON
ECOSYSTEMS
B. E. VAUGHAN
MATERIALS
R. P. MARSHALL
BIOLOGY
W. R. WILEY
ENERGY SYSTEMS
N. E. CARTER
WATER AND LAND RESOURCES
D. B. CEARLOCK
CHEMICAL TECHNOLOGY
R. E. NIGHTINGALE
ENGINEERING PHYSICS
A. J. HAVERFIELD
RADIOLOGICAL SCIENCES
J. M. NIELSEN
ENERGY MISSION
L. C. SCHMID
ENVIRONMENTAL AND SAFETY RESEARCH PROGRAM
W. J. BAIR
EXXON NUCLEAR PROGRAM
J. E. MINOR
FUSION TECHNOLOGY PROGRAM
D. A. DINGEE
NUCLEAR WASTE TECHNOLOGY PROGRAM
A. M. PLATT

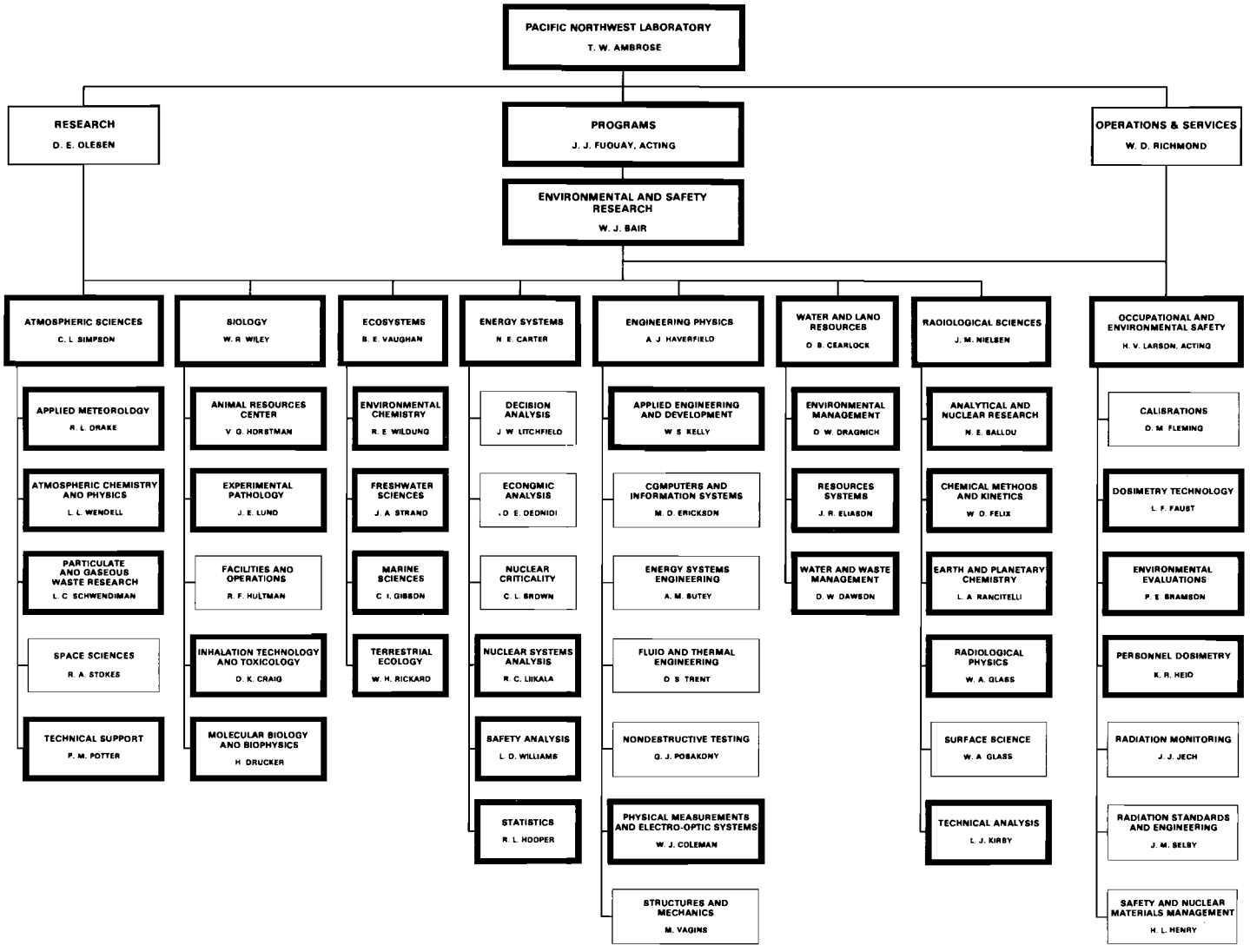
PACIFIC NORTHWEST LABORATORY
T. W. AMBROSE
RESEARCH
D. E. OLESEN
PROGRAMS
J. J. FUQUAY, ACTING
OPERATIONS & SERVICES
W. D. RICHMOND
ENVIRONMENTAL AND SAFETY RESEARCH
W. J. BAIR
ATMOSPHERIC SCIENCES
C. L. SIMPSON
APPLIED METEOROLOGY
R. L. DRAKE
ATMOSPHERIC CHEMISTRY AND PHYSICS
L. L. WENDELL
PARTICULATE AND GASEOUS WASTE RESEARCH
L. C. SCHWENDIMAN
SPACE SCIENCES
R. A. STOKES
TECHNICAL SUPPORT
P. M. POTTER
BIOLOGY
W. R. WILEY
ANIMAL RESOURCES CENTER
V. Q. HORSTMAN
EXPERIMENTAL PATHOLOGY
J. E. LUND
FACILITIES AND OPERATIONS
R. F. HULTMAN
INHALATION TECHNOLOGY AND TOXICOLOGY
D. K. CRAIG
MOLECULAR BIOLOGY AND BIOPHYSICS
H. DRUCKER
ECOSYSTEMS
B. E. VAUGHAN
ENVIRONMENTAL CHEMISTRY
R. E. WILDUNG
FRESHWATER SCIENCES
J. A. STRAND
MARINE SCIENCES
C. I. GIBSON
TERRESTRIAL ECOLOGY
W. H. RICKARD
ENERGY SYSTEMS
N. E. CARTER
DECISION ANALYSIS
J. W. LITCHFIELD
ECONOMIC ANALYSIS
D. E. DEONIDI
NUCLEAR CRITICALITY
C. L. BROWN
NUCLEAR SYSTEMS ANALYSIS
R. C. LIIKALA
SAFETY ANALYSIS
L. D. WILLIAMS
STATISTICS
R. L. HOOPER
ENGINEERING PHYSICS
A. J. HAVERFIELD
APPLIED ENGINEERING AND DEVELOPMENT
W. S. KELLY
COMPUTERS AND INFORMATION SYSTEMS
M. O. ERICKSON
ENERGY SYSTEMS ENGINEERING
A. M. BUTEY
FLUID AND THERMAL ENGINEERING
D. S. TRENT
NONDESTRUCTIVE TESTING
Q. J. POSAKONY
PHYSICAL MEASUREMENTS AND ELECTRO-OPTIC SYSTEMS
W. J. COLEMAN
STRUCTURES AND MECHANICS
M. VAGINS
WATER AND LAND RESOURCES
D. B. CEARLOCK
ENVIRONMENTAL MANAGEMENT
D. W. DRAGNICH
RESOURCES SYSTEMS
J. R. ELIASON
WATER AND WASTE MANAGEMENT
D. W. DAWSON
RADIOLOGICAL SCIENCES
J. M. NIELSEN
ANALYTICAL AND NUCLEAR RESEARCH
N. E. BALLOU
CHEMICAL METHODS AND KINETICS
W. D. FELIX
EARTH AND PLANETARY CHEMISTRY
L. A. RANCITELLI
RADIOLOGICAL PHYSICS
W. A. GLASS
SURFACE SCIENCE
W. A. GLASS
TECHNICAL ANALYSIS
L. J. KIRBY
OCCUPATIONAL AND ENVIRONMENTAL SAFETY
H. V. LARSON, ACTING
CALIBRATIONS
D. M. FLEMING
DOSIMETRY TECHNOLOGY
L. F. FAUST
ENVIRONMENTAL EVALUATIONS
P. E. BRAMSON
PERSONNEL DOSIMETRY
K. R. HEID
RADIATION MONITORING
J. J. JECH
RADIATION STANDARDS AND ENGINEERING
J. M. SELBY
SAFETY AND NUCLEAR MATERIALS MANAGEMENT
H. L. HENRY

1976

BIOLOGY DEPARTMENT STAFF

William R. Wiley, Ph.D. - Manager
Marguerite S. Stack - Secretary

James F. Park, D.V.M. - Associate Manager
Judith A. Rising - Clerk
David G. Ryden - Jr. Technician (1)

Murlin F. Gillis, M.S., D.V.M. - Manager, Project Development
Frank P. Hungate, Ph.D. - Education and Training Coordinator

Roy C. Thompson, Ph.D. - Sr. Staff Scientist, ERDA Health and Safety Research Coordinator
Judith A. Rising - Clerk
Debbie L. Atkin - Clerk
Patricia M. Bresina - Clerk
Joanne E. Olsen - Technical Typist

Ray F. Hultman - Senior Specialist - Facilities Manager
Russell D. Tucker - Specialist II
Gertrude G. Haggard - Clerk
Andrew S. Bates - Jr. Technician (2,3)
Kenneth K. Baugh - Technician (4)
Nell P. Couch - Receptionist
Debra A. Evans - Clerk (4)
Linda L. Kemp - Receptionist (2)
Elizabeth J. Kinney - Jr. Technician (2,3)
Linda K. Lane - Clerk
Catherine M. Praino - Receptionist (2,3)
Patricia R. Saucier - Clerk (1)
Sharon K. Shepard - Clerk
Jean I. Tegner - Clerk (1,4)
Bruce E. Wilson - Jr. Technician (2,3)

LIBRARY

Elizabeth H. Groff (Technical Services Department) - Librarian (3)
Harry George (Technical Services Department) - Librarian
Zona G. Wright (Technical Services Department) - Clerk

TECHNICAL EDITOR

Dvara L. Felton, B.A. (Communications Department) - Technical Editor

BUSINESS AND OPERATIONS

Terry D. Blankenship, B.A. (Finance Department) - Financial Specialist (4)
Kathy S. Mikols, B.S., M.B.A. (Finance Department) - Financial Specialist
Roger A. Pollari, B.A. (Finance Department) - Financial Specialist
Ruth E. Palmer (Finance Department) - Clerk

RADIONUCLIDE COUNTING FACILITY

Arthur C. Case, B.A. (Radiological Sciences Department)

BIOMETRICS CENTER

Professional Staff

Jessie L. Burns, B.A. (Systems Dept.)
Ray L. Buschbom, M.A. (Systems Dept.)
Pam Doctor, Ph.D. (Systems Dept.)
Ethel S. Gilbert, Ph.D. (Systems Dept.)
V. Maitland Lee, A.B. (Systems Dept.)
Judy A. Mahaffey, M.S. (Systems Dept.)
Don L. Stevens, Ph.D. (Systems Dept.)
John R. Tadlock, A.B. (Systems Dept.)
John M. Thomas, Ph.D. (Ecosystems Dept.)
Paul E. Tucker, B.A. (Systems Dept.)
Charles R. Watson, Ph.D. (Systems Dept.)

Technical Staff

Kim A. Bainard (Systems Dept.) (5)
Marjorie I. Cochran (Ecosystems Dept.)
Kathie Eschbach (Systems Dept.) (2)
James M. McIntyre (Systems Dept.) (2)
Lorrie McVey (Systems Dept.) (2)
Sarah L. Owzarski, B.A. (Systems Dept.)
Jacqueline C. Wallace (Systems Dept.)

Northwest College and University Association for Science Fellows (NORCUS)

Mary A. Hill, B.A.
University of Puget Sound
Tacoma, Washington

---

(1) Cooperative Office Education Program (COE)
(2) Hourly
(3) Terminated
(4) Transferred to another Department
(5) Inquiry Into Science Program (IIS)

EXPERIMENTAL PATHOLOGY SECTION

John E. Lund, D.V.M., Ph.D., A.C.V.P. - Manager
Harvey A. Ragan, D.V.M. - Associate Manager
Jeanette F. Hunt - Secretary
Judith M. Proud - Clerk
Judith E. Beck - Clerk (1)

Professional Staff

Gerald E. Dagle, D.V.M., Ph.D., A.C.V.P.
Ronald E. Filipy, Ph.D.
Michael J. Free, Ph.D.
Robin M. Madison, A.A., A.S.C.P., H.T.
Keith E. McDonald
Roger A. Renne, D.V.M., A.C.V.P.
Linda G. Smith, M.S.
Gary M. Zwicker, D.V.M., Ph.D., A.C.V.P.

Technical Staff

Kathryn H. Debban, B.S., A.S.C.P., M.T. (1)
Karla M. Dragoo
Eugenia T. Edmerson
Sandra L. English, B.S., A.S.C.P., M.T.
Carole A. Fankhauser (2,3)
Victor T. Faubert
Catherine M. Ferguson (3)
Robert F. Flores
Kelly L. Furner (2,3)
Franna S. Gerber, A.T.
Linda S. Gorham, A.A.
Donna M. Jeske
Sherri L. Krum
William W. Laegreid (1)
Barbara G. Moore
Michele E. Moser (2)
Martha C. Perkins
Marcia J. Pipes, B.S., A.S.C.P., M.T.
Roger B. Samples, B.S.
Sandra L. Schively (2)
Janet R. Smith (1)
Judy K. Sweeney, B.A. (1)
Bonnie B. Thompson

Consultants

W. W. Carlton, D.V.M., Ph.D., A.C.V.P.
Purdue University
West Lafayette, Indiana

S. Nielsen, D.V.M., Ph.D., A.C.V.P.
University of Connecticut
Storrs, Connecticut

S. S. Schmidt, M.D.
Private Practice
Eureka, California

Northwest College and University Association for Science Fellows (NORCUS)

Carol E. McNinch
Ft. Wright College
Spokane, Washington

(1) Hourly
(2) Inquiry Into Science Program (IIS)
(3) Terminated

INHALATION TECHNOLOGY AND TOXICOLOGY SECTION

Douglas K. Craig, Ph.D. - Manager
Bruce O. Stuart, Ph.D. - Associate Manager
Virginia J. Choate - Secretary (1)
Linda C. Wood - Secretary
Barbara J. Cole, B.A. - Clerk
Mona G. Edwards - Clerk
Dorothy I. McDonald - Secretary (2)
Elizabeth A. Sellers - Clerk (3,1)

Professional Staff

Michael D. Allen, M.S.
Floyd D. Andrew, Ph.D.
John E. Ballou, Ph.D.
James L. Beamer, B.S.
Frederick G. Burton, Ph.D.
William C. Cannon, Ph.D.
Dennis L. Catt
John R. Decker, B.S., E.E.
A. Jay Gandolfi, Ph.D.
John C. Gaven
Patricia L. Hackett, Ph.D.
John P. Herring, A.A.
Dennis L. Hjeresen, B.S.
Hisamasa Joshima, Ph.D. (4,2)
Richard A. Jaffe, Ph.D.
Manuel T. Karagianes, D.V.M.
William T. Kaune, Ph.D.
Susan M. Loscutoff, Ph.D.
Dennis D. Mahlum, Ph.D.
Owen R. Moss, Ph.D.
Ray F. Palmer, M.S.
Daniel W. Phelps, Ph.D.
Richard D. Phillips, Ph.D.
Gerald J. Powers
Melvin R. Sikov, Ph.D.
Herbert E. Stevens
Jack T. Veal, Ph.D. (2)
Alfred P. Wehner, Dr. Med. Dent.
Donald H. Willard, M.S.
Karen Zawlocki, B.S. (7,1)

Technical Staff

Juanita S. Barnett
Louisa J. Beal (2)
Edwin F. Blanton
James K. Briant, B.S.
James H. Chandon, B.S.
A. Jacqueline Clary
Gayle L. Collins, B.S.
Mary J. Conger, A.A.
Henry S. DeFord, B.S.
Alan W. Endres (5,2)
Craig R. Endres (6)
Martha F. England, B.A. (6)
Benjamin R. Garrity
Richard A. Gies, B.A.
Juan A. Gonzales (2)
Julie L. Gurtison
Edward J. Guthrie (6)
Kathleen R. Hanson, B.S.
Linda F. Haug, B.S.
Joan O. Hess
David I. Hilton, B.S.
Daniel W. Hole
Darlene H. Hunter
Sheria G. Irby (2)
Gerald D. Irwin
Debora L. Jeffs
Bruce W. Killand, B.S.
Edward G. Kuffel, A.A.
Mary J. Kujawa, B.S. (2)
James R. Laidler (5)
Lyn L. Lang
Stanley J. Lepka (2)
Laurie J. Lucke (2)
Karla J. Mapstead, B.S.
Sybil McCormack
Judy S. Meyer (2)
Michael C. Miller
Edward M. Milliman
Larry D. Montgomery, B.A.
Ramona L. Music, B.S.
R. Faye Myers, B.S.

Technical Staff (continued)

Linda C. Orem, Vet. Tech.
Leonard R. Peters
Carl R. Petty
Gordon R. Preecs, B.S. (2)
Patricia J. Raney, B.S.
Charles T. Resch (5)
Randahl D. Roadifer (6,2)
Dennis H. Roberts (5)
Keith W. Roberts (5,2)
Karen E. Rodriguez
Ernest J. Rossignol
Janet A. Russell (2)
Lawrence D. Sackmann
Patricia L. Savignac, B.S. (6)
Dan R. Sheen (5)
Randi L. Sheldon, B.A.
Christine A. Shields, B.S.
Wilbur Skinner
James W. Sloot
Jean D. Stearns
Douglas A. Teats
K. C. Upton (2)
Dale C. Wardell (2)
Janet L. Warren (6,2)
Gary L. Webb
Karyn D. Wiemers, B.S.
Michael D. Wonacott (5)

Consultants

C. C. Diemond, B.S.
4840 S. W. Fairhaven Lane
Portland, Oregon

D. C. England, Ph.D.
Oregon State University
Corvallis, Oregon

Arthur Furst, Ph.D.
University of San Francisco
San Francisco, California

A. W. Guy, Ph.D.
Bio-Electromagnetics Research Labs
University of Washington
Seattle, Washington

R. L. Hamlin, D.V.M., Ph.D.
Ohio State University
1900 Coffey Road
Columbus, Ohio

W. A. Lewis, Ph.D.
1081 W. Washington Avenue
Sunnyvale, California

M. Lodmell, D.D.S.
Walla Walla Medical Center
Walla Walla, Washington

R. H. Lovely, Ph.D.
University of Washington
Seattle, Washington

Consultants (continued)

H. A. Menkes, M. D.
John Hopkins Hospital
Baltimore, Maryland

D. K. Merkeley, M.D.
Laboratory of Clinical Medicine
Seattle, Washington

G. Saccomanno, M.D.
St. Mary's Hospital
Grand Junction, Colorado

R. L. Van Citters, M.D.
University of Washington
Seattle, Washington

Paul F. Winkleman
Rt. 1, Box 534
Beaverton, Oregon

Northwest College and University Association for Science Fellows (NORCUS)

James L. Daniel
Whitman College
Walla Walla, Washington

---

(1) Transferred to another Department
(2) Terminated
(3) Cooperative Office Education Program (COE)
(4) Visiting Scientist from the National Institute of Radiological Sciences, Chiba-shi, Japan
(5) Inquiry Into Science Program (IIS)
(6) Hourly
(7) Science and Engineering Program (S&E)

MOLECULAR BIOLOGY AND BIOPHYSICS SECTION

Harvey Drucker, Ph.D. - Manager
Richard P. Schneider, Ph.D. - Associate Manager
R. Maxine Faubion - Secretary (1)
Marilyn J. Love - Typist (2,1)
Mary Lou Rusin - Secretary
Rhonda L. Smith - Secretary

Professional Staff

Roy R. Adee, B.S.
Thomas K. Andrews, B.A.
Marvin E. Frazier, Ph.D.
M. Paul Fujihara
James C. Hampton, Ph.D.
Frank P. Hungate, Ph.D.
Philip T. Johns, Ph.D. (1)
Paul E. Kolenbrander (5,1)
Beatrice J. McClanahan, Ph.D.
James E. Morris, Ph.D.
Richard A. Pelroy, Ph.D.
Jeffrey S. Price, Ph.D. (3,1)
Alfred V. Robinson, M.S.
Randall G. Rupp, Ph.D. (3,1)
Charles L. Sanders, Ph.D.
William D. Schulz (5,1)
Victor H. Smith, Ph.D.
Maurice F. Sullivan, Ph.D.
Laura S. Winn

Technical Staff

Joseph A. Anderson (4)
Julie M. Baker (2,1)
Susanne I. Baker
Kenton D. Bricker (4,1)
Vicky G. Bushaw, B.S.
Lucille M. Butcher
Allen W. Conklin, B.S.
James T. Cresto, B.A.
Alma L. Crosby
Jeanne C. Engstrom (2,1)
Marc W. Franco, B.S. (2,1)
Rose A. Gelman, M.S.
Tonia M. Graham, B.S.
Marilyn J. Hooper (2)
Fenya T. Kashergen, B.S.
Todd W. McVey (4)
Doris M. Meier
R. Scott Moore, B.S.
Louise C. Neil
Sandra A. Newman, A.A. (2)
Kathleen A. Poston, B.A. (1)
Kathleen Rhoads, M.S. (2)
Victoria M. Rothwell (1)
Patricia S. Ruemmler (2)
Marlo J. Sandvig (2,1)
Wilhelmina Van Krieken (1)
Clotis White

Consultants

T. D. Mahony, M. D.
Medical Arts Building
Richland, Washington

R. T. Schimke, M.D.
Stanford University
Stanford, California

R. N. Ushijima, Ph.D.
University of Montana
Missoula, Montana

Northwest College and University Association for Science Fellows (NORCUS)

Fredrick I. Akiya, M.S.
University of Montana
Missoula, Montana

Theresa L. Felton, M.S.
Oregon State University
Corvallis, Oregon

Bernadette L. Huard
Washington State University
Pullman, Washington

Barbara Mayer
University of Puget Sound
Tacoma, Washington

Debra A. Moon
Washington State University
Pullman, Washington

Stanley R. Strankman
Pacific Lutheran University
Tacoma, Washington

---

(1) Terminated
(2) Hourly
(3) Battelle Institute Fellow
(4) Inquiry Into Science Program (IIS)
(5) National Science Foundation

ANIMAL RESOURCES CENTER

V. Glenn Horstman, B.S. - Manager
Carol A. Hanf - Clerk
Elna May Akre - Clerk (1)

Supervisory Staff

M. Gilbert Brown
Roy F. Howard
Stephen E. Rowe, D.V.M.
Vall D. Tyler
Edward L. Wierman

Technical Staff

Steven S. Bailie
Sharon M. Baze
Richard L. Brooks
Deborah R. Bryant
Ronald D. Burdett, A.A.
Dee A. Butler (3)
Thomas M. Carney
Harriet C. Colwell, B.S. (1)
Roderick M. Coutee (1)
Victor L. Dedmond (1)
John C. Drewrey, B.S.
Gary R. Ell
Reinhold P. Emineth
Paul L. Evans, Jr.
Kathleen L. Friday, A.S.
David E. Friedrichs
Myron M. Hankins
Otis L. Jackson
Donald O. Jenkins
Troy A. Johnson
Robert C. Joyce
Thomas R. Kasari, B.S. (4,1)
Thomas C. Kinnas
Dan G. Martinez
Carol D. Matsumura (4,1)
Kelli K. McCauley (4,1)
Glen L. Miller
Barbara J. Northern (1)
Albert J. Orem
Wallace B. Peterson
Patrick D. Pierce
Jen M. Ranta, M.S. (4,1)
Rodolpho Rodriguez (2,1)
Philip A. Saenz (1)
Kenneth L. Scherbarth
Richard M. Schumacher (4,1)
Robert P. Schumacher
Roger L. Sheley (4,1)
Betty C. Shipp (3)
Donald C. Snyder
Norva L. Tate (1)
Glen L. Thompson (4,1)
Freddie L. Wallace
Terence J. Weber (4,1)
Mary A. Whittle
Bradley U. Zunker

---

(1) Terminated
(2) Training Orientation Placement Program (TOPP)
(3) Transferred to Another Department
(4) Hourly

GENERAL SERVICES
CRAFT AND OPERATION SERVICES DEPARTMENT

Power Operator - Steve C. Gillihan
Richard F. Heinemeyer
Herman H. Hunnicutt
Howard L. Meyer
V. Eugene Regimbal

Robert H. Berndt - Foreman
John W. Cunningham - Foreman (1)
John D. Hughes - Foreman
Gene E. Schmitt - Foreman

Carpenter - Russ D. Combs
Harry D. Longwell

Electrical - Miguel Pineda, Jr.
George W. Sharp
H. Duane Steele
C. Jim Sullivan

Millwright - Lawrence F. Conley
Richard W. Hormel
E. Gene Larson

Instruments - George G. Alexander
James L. Young
Lou E. Ziege

Pipefitters - Roy C. Dunn
Clyde T. Ford
John J. Gore
Richard E. Helland
Ed Tamez, Jr.

Serviceman - Earl G. Leggett

Janitors - Kenneth K. Baugh
Betty M. Faris
Anton Fleckenstein
Maxine D. Herrington
Sophia B. Mattern
Nick J. Merrill
Frank J. Vargas

RADIATION MONITORING
OCCUPATIONAL AND ENVIRONMENTAL SAFETY DEPARTMENT

Supervisor - Manford W. Leale
Eugene D. McFall (1)

Radiation Monitors - Bev Allen (2)
Larry L. Belt
Howard W. Dains
Dale D. Dickinson
John D. Harrison (3)
Claude D. Hooker (4)
Karen Kenyon (3)
Mike McCoy (3)
David L. Merrill
Oscar R. Mulhern (4)
Ronald C. Schrotke (4)
William P. Walsh (4)

---

(1) Transferred to another Department
(2) Terminated
(3) Temporary in 331 Building
(4) Worked during strike

AUTHOR INDEX

DISTRIBUTION

No. of Copies

OFFSITE

1 ERDA Chicago Patent Group
9800 So. Cass Avenue
Argonne, Illinois 60439

A. A. Churm

63 ERDA Office of the Assistant Administrator for Environment and Safety
Washington, D.C. 20545

W. R. Albers
T. M. Albert (3)
R. W. Barber
N. F. Barr
M. A. Bell
W. G. Belter
W. A. Brobst
A. L. Brooks
W. W. Burr, Jr.
C. E. Carter (4)
J. A. Coleman
R. D. Cooper
L. J. Deal
G. G. Duda
C. W. Edington
H. G. Fish
H. Glauberman
G. Hagey
E. B. Harvey
H. Hollister
H. R. Holt
R. M. Jimeson
W. J. Little, Jr. (3)
J. L. Liverman (2)
E. K. Loop
J. N. Maddox
J. R. Maher
R. P. Malloch
M. L. Minthorn
W. E. Mott (2)
J. Nash
D. E. Patterson
W. H. Pennington (3)
R. Rabson
D. M. Ross
A. A. Schoen
M. Schulman
G. Shippard
N. F. Simpson
D. Smith
H. P. Smith
G. E. Stapleton
J. B. Stromberg
J. Swinebroad
E. J. Vallario
B. W. Wachholz

No. of Copies

H. R. Wasson
W. W. Weyzen
J. C. Whitnah
W. H. Wisecup
R. W. Wood
C. I. York
F. R. Zintz

2 ERDA Division of Nuclear Research and Application, Space Applications
Washington, D.C. 20545

G. P. Dix
T. J. Dobry

198 ERDA Technical Information Center

ONSITE ERDA Richfield Operations Office

9
P. F. X. Dunigan
P. G. Holsted
J. L. Landon
W. Lei
H. E. Ransom
P. R. Rhodes
F. R. Standerfer
M. W. Tiernan
J. D. White

1 Atlantic Richfield Hanford Company

V. A. Uresk

4 Battelle Memorial Institute

R. S. Paul (4)

4 Battelle - Seattle

G. W. Duncan
J. L. Hebert
S. M. Nealey
J. E. Rasmussen

1 Douglas United Nuclear, Inc.

DUN File

3 Hanford Environmental Health

B. Breitenstein
P. A. Fuqua
W. D. Norwood

No. of Copies

1 U. S. Testing

W. V. Baumgartner

344 Battelle-Northwest

R. R. Adee
M. D. Allen
T. W. Ambrose
F. D. Andrews
T. K. Andrews
W. J. Bair (20)
J. E. Ballou
J. L. Beamer
M. G. Brown
F. G. Burton
W. C. Cannon
N. E. Carter
D. L. Catt
D. B. Cearlock
J. P. Corley
D. K. Craig
G. E. Dagle
G. M. Dalen
J. R. Decker
D. A. Dingee
P. J. Dionne
H. Drucker
C. E. Elderkin
S. J. Farmer
R. E. Filipy
J. W. Finnigan
R. F. Foster
J. C. Fox
M. E. Frazier
M. J. Free
M. P. Fujihara
J. J. Fuquay
A. J. Gandolfi
J. C. Gaven
M. F. Gillis
W. A. Glass
P. L. Hackett
J. C. Hampton
A. J. Haverfield
K. R. Heid
J. P. Herring
D. L. Hessel
D. L. Hjeresen
V. G. Horstman
R. F. Howard
F. P. Hungate
R. A. Jaffe
M. T. Karagianes
W. T. Kaune
L. J. Kirby

No. of Copies

H. V. Larson
S. M. Loscutoff
J. E. Lund
R. M. Madison
D. D. Mahlum
S. Marks
R. P. Marshall
B. J. McClanahan
K. E. McDonald
J. E. Morris
O. R. Moss
J. M. Nielsen
R. E. Nightingale
D. E. Olesen
R. F. Palmer
J. F. Park
H. M. Parker
R. A. Pelroy
R. W. Perkins
D. W. Phelps
R. D. Phillips
A. M. Platt
G. J. Powers
L. L. Rader
H. A. Ragan
R. A. Renne
W. D. Richmond
A. V. Robinson
W. C. Roesch
S. E. Rowe
C. L. Sanders
L. C. Schmid
R. P. Schneider
L. C. Schwendiman
M. R. Sikov
C. L. Simpson
L. G. Smith
V. H. Smith
H. E. Stevens
R. W. Stewart
B. O. Stuart
M. F. Sullivan
K. L. Swinth
W. L. Templeton
R. C. Thompson
V. D. Tyler
C. M. Unruh
B. E. Vaughan (7)
A. P. Wehner
E. L. Wierman
W. R. Wiley (200)
D. H. Willard
L. S. Winn
G. M. Zwicker
Biology Library (2)
Technical Information Files (5)
Technical Publications (4)